34314

National Library of Canada | Bibliothèque nationale du Canada

CANADIAN THESES ON MICROFICHE | THÈSES CANADIENNES SUR MICROFICHE

NAME OF AUTHOR/*NOM DE L'AUTEUR* STEWART JAY COHEN

TITLE OF THESIS/*TITRE DE LA THÈSE* LAND USE CHANGE ON MICRO-CLIMATE IN CENTRAL ALBERTA : AN ENERGY BALANCE STUDY

UNIVERSITY/*UNIVERSITÉ* U. OF ALBERTA

DEGREE FOR WHICH THESIS WAS PRESENTED/*GRADE POUR LEQUEL CETTE THÈSE FUT PRÉSENTÉE* M. Sc.

YEAR THIS DEGREE CONFERRED/*ANNÉE D'OBTENTION DE CE GRADE* 1977

NAME OF SUPERVISOR/*NOM DU DIRECTEUR DE THÈSE* S. I. SMITH

Permission is hereby granted to the NATIONAL LIBRARY OF CANADA to microfilm this thesis and to lend or sell copies of the film.

The author reserves other publication rights, and neither the thesis nor extensive extracts from it may be printed or otherwise reproduced without the author's written permission.

L'autorisation est, par la présente, accordée à la BIBLIOTHÈQUE NATIONALE DU CANADA de microfilmer cette thèse et de prêter ou de vendre des exemplaires du film.

L'auteur se réserve les autres droits de publication; ni la thèse ni de longs extraits de celle-ci ne doivent être imprimés ou autrement reproduits sans l'autorisation écrite de l'auteur.

DATED/*DATÉ* May 17, 1977 SIGNED/*SIGNÉ* Stewart Cohen

PERMANENT ADDRESS/*RÉSIDENCE FIXÉ* 5885 CENTENNIAL #98
MONTREAL, QUE. H4W 1T2
CANADA

NL-91 (3-74)

National Library of Canada

Cataloguing Branch
Canadian Theses Division

Ottawa, Canada
K1A 0N4

Bibliothèque nationale du Canada

Direction du catalogage
Division des thèses canadiennes

NOTICE

The quality of this microfiche is heavily dependent upon the quality of the original thesis submitted for microfilming. Every effort has been made to ensure the highest quality of reproduction possible.

If pages are missing, contact the university which granted the degree.

Some pages may have indistinct print especially if the original pages were typed with a poor typewriter ribbon or if the university sent us a poor photocopy.

Previously copyrighted materials (journal articles, published tests, etc.) are not filmed.

Reproduction in full or in part of this film is governed by the Canadian Copyright Act, R.S.C. 1970, c. C-30. Please read the authorization forms which accompany this thesis.

THIS DISSERTATION
HAS BEEN MICROFILMED
EXACTLY AS RECEIVED

AVIS

La qualité de cette microfiche dépend grandement de la qualité de la thèse soumise au microfilmage. Nous avons tout fait pour assurer une qualité supérieure de reproduction.

S'il manque des pages, veuillez communiquer avec l'université qui a conféré le grade.

La qualité d'impression de certaines pages peut laisser à désirer, surtout si les pages originales ont été dactylographiées à l'aide d'un ruban usé ou si l'université nous a fait parvenir une photocopie de mauvaise qualité.

Les documents qui font déjà l'objet d'un droit d'auteur (articles de revue, examens publiés, etc.) ne sont pas microfilmés.

La reproduction, même partielle, de ce microfilm est soumise à la Loi canadienne sur le droit d'auteur, SRC 1970, c. C-30. Veuillez prendre connaissance des formules d'autorisation qui accompagnent cette thèse.

LA THÈSE A ÉTÉ
MICROFILMÉE TELLE QUE
NOUS L'AVONS REÇUE

THE UNIVERSITY OF ALBERTA

LAND USE CHANGE ON MICRO-CLIMATE IN CENTRAL ALBERTA; AN ENERGY BALANCE STUDY.

BY

© STEWART JAY COHEN

A THESIS

SUBMITTED TO THE FACULTY OF GRADUATE STUDIES AND RESEARCH IN PARTIAL FULFILMENT OF THE REQUIREMENTS FOR THE DEGREE OF

MASTER OF SCIENCE

DEPARTMENT OF GEOGRAPHY

EDMONTON, ALBERTA

FALL, 1977

THE UNIVERSITY OF ALBERTA

FACULTY OF GRADUATE STUDIES AND RESEARCH

The undersigned certify that they have read, and recommended to the Faculty of Graduate Studies and Research, for acceptance, a thesis entitled Land Use Change on Micro-Climate in Central Alberta: An Energy Balance Study submitted by Stewart Jay Cohen in partial fulfilment of the requirements for the degree of Master of Science.

.....
Supervisor

.....

.....

DATE: 16th May 1977

ABSTRACT

Effects or rural land-use change on micro-climate in Central Alberta are investigated by comparing the energy balances of six differently vegetated small plots. The plots are located at the University of Alberta Agricultural Research Station at Ellerslie, 10 km south of Edmonton.

The six surfaces are trembling aspen (Populus tremuloides Michx.), white spruce (Picea glauca Voss), western snowberry (S. occidentalis), barley, fallow, and short grass. All plant species are common locally. The plots are situated in close proximity to one another, on a relatively flat plain, thereby negating the effects of varied topographic exposure, soil type, and timing of weather events on energy balance differences calculated among them. Any significant variation in net radiation, soil heat flux, sensible heat flux, or latent heat flux, can be traced to the influences of the landscape and vegetation surfaces themselves.

Statistical analysis of the results reveals significant differences in net radiation, sensible heat flux, and soil heat flux. There is no significant difference in latent heat flux between the plots, despite wide variations in soil moisture content. Poplar has the highest net radiation values, while barley and grass record the lowest. The remaining surfaces are ranked between these.

The major factors influencing the energy balance differences during the growing season are albedo, canopy

structure, snow accumulation, and growth characteristics. Short period variation in the observed differences reflects phenological differences among the six surfaces. Variations in the plots' soil and air temperatures are a consequence of the aforementioned.

Results are considered in relation to possible effects of rural land-use change on Central Alberta microclimate. It is concluded that a change from farmland to woodlots will result in a decrease in albedo, and soil and surface temperatures, and an increase in canopy level air temperatures. Soil moisture levels will decline with increasing tree density, while an increase will occur if shelterbelts, low density woodlots, or shrub woodlots are used. Numerous small woodlots will result in an increase in sensible heat advection from surrounding farmland, depending on the woodlots' moisture supply.

If present land use trends continue, and woodlots are replaced by farmland, albedo will increase, soil and surface temperatures will increase, while canopy level air temperatures will decrease. As a result, local convective activity may be enhanced, while soil moisture levels will decline, depending on the use of shelterbelts and/or snow fences.

Differences between these and published results with respect to sensible and latent heat fluxes under woodlots, are due in large part to low soil moisture

levels generally existing at Ellerslie. Suggestions for future research should emphasize closer examination of soil moisture and snow accumulation under wooded plots, canopy level air temperature, wind, water consumption of weed infested fallow vs tilled fallow, and surface reactions under unlimited or controlled soil moisture.

ACKNOWLEDGEMENTS

I would like to thank Prof. S. I. Smith for acting as my supervisor, and Profs. K. D. Hage and J. A. Toogood for serving on my thesis committee.

The instrumentation required for measuring solar and net radiation, albedo, soil heat flux, air temperature, and relative humidity was obtained through Prof. Hage and Mr. Bob Weatherburn of the Meteorology Division. The soil moisture equipment was obtained from the Soil Science Department and the Alberta Research Council. My thanks to Prof. Toogood, Dr. A. Maclean, and Mr. H. H. Rix for their efforts. The net pyrradiometers, soil heat flux plates and some of the data logging equipment were provided by grants from the Water Resources Research Program of Inland Waters Directorate of Environment Canada.

The research site at the University of Alberta Research Station at Ellerslie was made available through the Soil Science Department, while the large poplar forest site was utilized with the permission of the Plant Science Department. My thanks to Mr. John Taylor, manager of the Ellerslie Farm for his assistance.

Soil moisture measurements during August were accomplished by Mr. Rolf Hopkinson. Soil temperature data were made available through Prof. Toogood. Additional material and field assistance were provided on

several occasions by Prof. Hage, Prof. Toogood, Mr. Weatherburn, Mr. Taylor, Mr. Bruce Fielhaber of the Soil Science Department, Dr. J. Honsaker of the Geography Department, Miss Iris Rosman, Miss Patti Demco, and my dear brother Mr. Michael Cohen.

Computer time, and financial support were provided by the Department of Geography.

My sincere thanks to Mr. Alexander Strembitsky for computer assistance; to Mr. Michael Cohen for taking some of the photographs; to the cartography section of the Geography Department for advice and material assistance; to the photography section of the department for reproducing the figures and photos; to my friend Miss Susie Feher for typing the first draft of chapters II and III; and to Mrs. Susan McKeen and Miss Darlene McIntosh for typing the final draft.

Finally, I would like to thank my friends at Pembina Hall and Theta Chi Fraternity, and my family in Montreal, for their support and encouragement throughout the study.

TABLE OF CONTENTS

CHAPTER		PAGE
I	INTRODUCTION	1
II	LITERATURE REVIEW	6
	2.1 Introduction	6
	2.2 Radiation Balance	6
	2.2.1 Basic Physical Laws	6
	2.2.2 Radiation Balance Equation . . .	7
	2.2.3 Recent Work--Vegetation Transmission, Regression Analysis, and Variations in Albedo	16
	2.3 Energy Balance	21
	2.3.1 Energy Balance Equation . . .	21
	2.3.2 The Case for the Water Budget Approach	25
	2.4 Effects of Land Use Change on Micro- and Macro-Climate	32
	2.4.1 Albedo and Energy Balance . .	32
	2.4.2 The Hydrologic Cycle	41
III	INSTRUMENTATION AND EXPERIMENTAL PROCEDURE . .	46
	3.1 Introduction	46
	3.2 The Site	46
	3.2.1 General Characteristics . . .	46
	3.2.2 Experimental Plots	52
	3.3 Instrumentation	60
	3.3.1 Radiation	60

PAGE

3.3.2 Soil Heat Flux 66

3.3.3 Soil Moisture, Bulk Density, Organic Matter 66

3.3.4 Temperature and Relative Humidity 72

3.3.5 Precipitation and Evaporation 72

3.3.6 Deployment of Equipment . . . 78

3.3.7 Supplementary Measurements . . 80

IV GENERAL CLIMATE AND FIELD OBSERVATIONS 82

4.1 Introduction 82

4.2 Twelve Year Mean Climate Observations . 82

4.2.1 Air Temperature 82

4.2.2 Precipitation 83

4.2.3 Sunshine 85

4.2.4 Soil Temperature 86

4.2.5 Pan Evaporation 94

4.2.6 Relative Humidity 96

4.2.7 Overall Assessment 96

4.3 June, 1975 - April, 1976 100

4.4 Climate and Field Conditions: April - October, 1976 106

4.4.1 April - May 106

4.4.2 June 129

4.4.3 July 131

4.4.4 August 133

PAGE

4.4.5 September - October 135

4.4.6 Summary 140

V RESULTS AND ANALYSIS 142

5.1 Introduction 152

5.2 Radiation Balance 142

5.2.1 Albedo and Global Solar Radiation 142

5.2.2 Net Radiation--Diurnal Variations 145

5.2.3 Net Radiation--Weekly Totals 163

5.2.4 Radiation Balance 174

5.2.5 Errors and Preliminary Analysis 179

5.3 Energy Balance 184

5.3.1 LE 184

5.3.2 Gs 195

5.3.3 H 204

5.3.4 Bowen Ratio 209

5.3.5 Errors and Preliminary Analysis 214

5.4 Statistical Analysis of Energy Balance 223

5.4.1 Analysis Procedure 223

5.4.2 Results 227

5.5 Implications and Results on Central Alberta Climate 247

5.5.1 Introduction 247

PAGE

5.5.2 Potential Micro-Scale Effects 248

5.5.3 Potential Macro-Scale Effects 256

VI SUMMARY AND CONCLUSIONS 258a

6.1 Summary of Findings 258

6.2 Conclusions and Recommendations 260

* * *

BIBLIOGRAPHY 264

APPENDIX I Calibrations 270

APPENDIX II Ellerslie (Q+q) Measurements; Digital Counts vs Strip Chart Analysis 272

LIST OF TABLES

Table	Description	Page
2.1	Albedos of Various Surfaces	11
2.2	Soil Heat Flux for Different Surfaces	34
2.3	Changes of Heat Budget After Conversion from Forest to Agricultural Use	39
3.1	Ellerslie Site Descriptions	58
3.2	Bulk Density -- Porosity	73
3.3	Organic Matter	75
4.1	Mean Soil Temperatures, January, 1970 - June, 1973	88
4.2	Winter and Summer Mean Air and Soil Temperatures for G Plot	93
4.3a	Weekly Mean Temperature and Relative Humidity	97
4.3b	Regression of Mean Weekly Temperature and RH.	99
4.4	1975 - 1976 Soil Temperatures	104
4.5	Gravimetric Soil Moisture	107
4.6	Dew Formation in September	136
5.1	Albedo	144
5.2	Equation (2.6): $Rn = a(Q+q) + b$	164
5.3	Regression Slopes and Intercepts to be Used in Eq. (5.2): $Rn\ (rotated) = a\{Rn\ (G\ plot)\} + b$	166

Table	Description	Page
5.4	Mean Daily Rn	170
5.5	Radiation Balance	175
5.6	G Plot, Ellerslie vs Stony Plain-- Rn, (Q+q).	182
5.7	Mean Daily LE	188
5.8	Regression of $\overline{LE}$ and LE/Rn	194
5.9	Regression Slopes and Intercepts to be Used in Eq. (5.3): Gs (rotated) = a{Gs (G plot)} + b	197
5.10	Mean Daily Gs	201
5.11	Mean Daily H	205
5.12	Bowen Ratio	210
5.13	Procedure for Soil Moisture Calculations .	215
5.14	Energy Balance	218
5.15	Mean Energy Balance	222
5.16	T Test Results	230
5.17	Correlation Test Results	236

LIST OF FIGURES

Figure	Description	Page
3.1	Location of Study Area	47
3.2	Ellerslie Site	49
3.3	Annual March of the Heat Balance	
	a. Barnaul	51
	b. Grossevichi	51
4.1	Mean Monthly Precipitation	84
4.2	Mean Monthly Sunshine urs	84
4.3	Mean 20 cm Soil Temperatures	87
4.4	Mean 100 cm Soil Temperatures	91
4.5	Evaporation--Class A Pan	95
4.6	20 cm. Soil Temperatures: July, 1975 - October, 1976	102
4.7	100 cm. Soil Temperatures: July, 1975 - October, 1976	103
4.8	Weekly Temperature and Precipitation . . .	109
4.9	Soil Moisture: 0.1 m.	111
4.10	Soil Moisture: 0.2 m.	115
4.11	Soil Moisture: 0.5 m.	119
4.12	Soil Moisture: 0.8 m.	123
4.13	Soil Moisture: 1.0 m.	127
	Figs. 5.1 - 5.12: Diurnal Variations of Rn and Gs	
5.1	June 19, 1976	148
5.2	October 2, 1976	149
5.3	June 30, 1976	151
5.4	September 26, 1976	152

Figure	Description	Page
5.5	May 31, 1976	154
5.6	July 24, 1976	155
5.7	May 27, 1976	156
5.8	July 4, 1976	157
5.9	September 17, 1976	158
5.10	June 2, 1976	169
5.11	July 18, 1976	161
5.12	September 18, 1976	162
5.13	Mean Daily Rn	172
5.14	ΔPW	185
5.15	Cumulative ΔPW	187
5.16	Mean Daily LE	190
5.17	LE/Rn	193
5.18	Mean Daily Gs	203
5.19	Mean Daily H	207
5.20	Bowen Ratio	212
5.21	Histograms	224

LIST OF PLATES

Plate	Description	Page
3.1a	Deciduous Plot (PS)	53
3.1b	Inside PS Plot	54
3.2	Coniferous Plot (S)	54
3.3	Shrub Plot (W)	55
3.4	Barley (B) and Fallow (F) Plots (May, 1976)	55
3.5	Grass Plot (G)	56
3.6	Poplar Forest (P)	57
3.7	Ellerslie Small Plots (July, 1976)	59
3.8	Eppley Pyranometer	62
3.9	Albedo and Net Radiation Measurements	63
3.10	Albedo Measurements Above Deciduous Plot	63
3.11	Instrument Tower at S Plot	64
3.12a	Albedo Recorder	65
3.12b	Digital Counter	65
3.13	Air Pump With Silica Gel Drying Agent	67
3.14	Automatic Recording of Net Radiation and Soil Heat Flux	68
3.15	Soil Heat Flux Disk (Rotated)	68
3.16	Surface Moisture Probe and Scalar in Use at F Plot	70
3.17	Standard Count Apparatus for Surface Probe	70

Plate	Description	Page
3.18	Depth Moisture Probe with Scalar in Use at F Plot	71
3.19	Maximum-Minimum Temperature and Relative Humidity Measurements at G Plot	76
3.20	Thermohygrograph and Maximum-Minimum Thermometer in Screen at PS Plot	77
3.21	Evaporation Pan (Foreground) and Rain Gauge	79
3.22	Large Barley Field	81
3.23	Albedo and Net Radiation Instruments on Large Barley Field	81

LIST OF SYMBOLS

Units and Conversions

T	= °K - 273 = (5/9) (°F - 32) = °C
cc	= cm^3
cm m^{-1}	= cm water m^{-1} soil
g, gm	= gram
Kg	= kilogram = 1000 gm
mv	= millivolt
Wm^{-2}	= watts per square metre; 1 langley = 697.3 Wm^{-2} = 1 cal cm^{-2}; 1000 Wm^{-2} = KWm^{-2}
μ	= micron = 10^{-4} cm
∞	= infinity

Physical

c	= speed of light, cm sec^{-1}
Cp	= specific heat of air at constant pressure = 0.24 cal $gm^{-1}deg^{-1}$
Db	= bulk density, g/cc
de	= vapour pressure gradient within layer of z thickness
dT/dZ, dT/dz	= temperature gradient within layer of z or Z thickness
E	= quantity of water evaporated, gm cm^{-2}
ET	= evapotranspiration, cm
exp	= exponential (2.7182)

Gs	= soil heat flux, Wm^{-2}
H	= sensible heat flux, Wm^{-2}
I	= flux intensity after passage through a medium, Wm^{-2}
Io	= initial flux intensity, Wm^{-2}
K	= thermal conductivity
Kh	= coefficient of turbulent (or sensible heat) exchange, cm^2sec^{-1}
Kv	= coefficient of latent exchange, cm^2sec^{-1}
L	= latent heat of vapourization, cal gm^{-1}
LE	= latent heat flux, Wm^{-2}
Ln	= net longwave radiation, Wm^{-2}
M	= miscellaneous exchanges, Wm^{-2}
m	= extinction coefficient of the medium
POR	= porosity, %
Q	= direct beam solar radiation, Wm^{-2}
q	= sky diffuse radiation, Wm^{-2}
(Q+q)	= global solar radiation, Wm^{-2}
R	= pressure, mb
RH.	= relative humidity, %
Rn	= net balance of all-wave radiation (net radiation), Wm^{-2}
V	= energy stored within a crop canopy
Y	= photosynthesis, Wm^{-2}
Z,z	= thickness of layer, cm or m

λ = wavelength, cm or μ

β = Bowen Ratio = H/LE

ΔPW = change in volume of water stored in the soil

ϵ = emissivity = 1.0 for a black body

ϵr = ratio of mole weights of moist air to dry air

ρa = density of air = 1.13×10^{-3} gm cm^{-3}

σ = Stefan-Bolzman constant = 5.67×10^{-5} erg cm^{-2} sec^{-1} K^{-4}

ν = frequency, cycles sec^{-1}

α = surface albedo

αh = molecular diffusivity of air for heat = 0.16 - 0.24 cm^2 sec^{-2}

Plot Names

B = barley plot

F = fallow plot

G = grass plot

LB = large barley field

P = large poplar forest

P1 = site 1 in P

P2 = site 2 in P

P3 = site 3 in P

PS = poplar plot

S = spruce plot

W = shrub plot

Statistical

a	= regression slope
b	= regression intercept
N,n	= number of cases
r	= correlation
r^2	= variance
SD	= standard deviation
S.E.	= standard error
SIG.	= level of significance
x	= x axis parameter in equation of the line
y	= y axis parameter in equation of the line
ø	= not significant

CHAPTER I

INTRODUCTION

Climate is changing on a global scale, and this idea has been generally accepted for many years. However, climate on a micro-scale is also undergoing change, and this can be traced (at least in part) to the influence of man. Although the effects of industrial and urban areas on micro-climate have been widely recognized, man also affects his environment when the rural landscape is altered. By transforming forests into agricultural or pasture lands, and by stripping the vegetation in advance of mineral exploration and extraction activities, man has changed the rural micro-climate. This indirectly affects the watershed as well, since water yield and timing are dependent on the watershed's vegetation cover.

Recent micro-climatological investigations of different rural land uses have become quite extensive. Some of the research has concentrated on global and net radiation and albedo (Monteith and Szeicz, 1961; Stanhill et al., 1966; Federer, 1968, 1971; Impens et al., 1970; Glover, 1972). Others have examined the flux parameters of the energy balance, i.e. net radiation, sensible heat, soil heat and evaporation (or latent heat), and subsequently, potential and actual evapotranspiration (Fritschen, 1966; Rosenberg, 1969b; Davies, 1972; Dilley and Shepherd, 1972; Priestly and Taylor, 1972; Blad and Rosenberg, 1974).

While the above studies have many implications for both agriculture and watershed management, they are essentially examining static unique conditions. The energy balance of a beanfield in Southern Ontario cannot be compared to that of alfalfa in the Great Plains because of the unique situation existing at each of the two locations. Southern Ontario is a moist region, while the Great Plains are drier, and experience strong sensible heat advection during summer. Their respective soils have different structures and different moisture capacities. The surface topography and exposure of the plants may vary. There are latitudinal differences in radiation intensity and daylength. Most important of all, particular weather events (eg rain) will not occur on these surfaces simultaneously, so the stresses they experience will be of unequal magnitude. Even studies comparing different natural vegetation covers in the same general location (Federer, 1968) suffer from the problem of unequal exposure to climatic elements, differences in soil conditions, and diversity of plant communities. Muller's (1971) study of solar radiation in different coniferous stands also exposed this problem of comparison between different regions. Data from other studies could not be directly comparable because investigations had been carried out over a wide range of solar climates and because of largely unsatisfactory measures of stand

biomass which directly produce attenuation of the solar beam downward through the tree crowns. Another factor was differences in soil moisture, and the inability to separate evapotranspiration from drainage during moist periods (Satterlund, 1972).

The word "static" was previously used to describe the above mentioned studies. This is due to the fact that the land use is constant throughout the research. With the many land use changes that have taken place in the past, there must have been changes in the micro-climate of these locations. Jeffrey (1964) has illustrated several micro-climate changes that are caused by removal of forest cover. Muller (1966) showed that the abandonment of farms in New York State, and the subsequent plant succession and reforestation of these lands, had affected the water yield of nearby watersheds. In a review of recent research in watershed management, Leaf (1975) has indicated several micro-climate changes that can occur due to certain cutting patterns and practices, and reforestation.

So, it can be concluded that land use change will affect micro-climate to some degree. Consequently, the change in micro-climate has some influence on various human endeavours such as agriculture, forestry, and land use planning. But research into the effects of land use change on micro-climate have produced more questions than

answers. Jeffrey (1964) lamented that "so little is confidently known of vegetation-water-climate interactions that a comprehensive list of research avenues could be almost infinite." He included, among a list of priorities, an urgent need for research into albedo and energy exchange, and how they are affected by different species, stand density, and structure. Baumgartner (1965) stated that energy balance studies of different plant covers were important since they could be used to predict the effects of different plant cover treatments. More recently, Satterlund (1972) echoed the need for more research on the effects of different plant species on energy balance.

Additional uncertainties exist when trying to appraise the potential effects of altering the ratio of heating of the surface and of evaporation (the Bowen Ratio), especially if human activities, such as deforestation and irrigation, are involved (Study of Man's Impact on Climate--SMIC, 1971).

Obviously, the need exists for research into the energy balance of different types of vegetation covers experiencing the same outside stresses. Under natural conditions, it is hard to imagine finding a pure coniferous stand, a pure deciduous stand, agricultural crops or other plant covers sharing the same location, soil, and exposure. If this situation was common, comparison

of the effects of different vegetation covers on the energy balance could be accomplished easily, since all outside factors could be considered constant, hence isolating the effects of the vegetation from those of weather, soil, and topography.

A unique and very suitable research site was available at the U. of Alberta climatological station at Ellerslie. This site was utilized for the purpose of investigating and quantifying gross differences in energy balance between the various forest, agricultural, grass, and fallow covers that are maintained at the station. Since topographic conditions and prevailing weather were identical for each plot, the differences in sensible and latent heat (evaporative) fluxes are directly comparable to one another. Thus, the potential effects of rural land use change on micro-climate, and subsequently, soil temperature and moisture, are examined.

CHAPTER II

LITERATURE REVIEW

2.1 Introduction

The following chapter includes a brief review of the background theory to be employed in this study. The energy and water balance equations basic to much of climatological research have been in use ever since instrumentation and techniques were available to measure or derive their components. Besides examining these and related methods, this chapter deals with previous attempts at deriving individual components. Finally, there is a review of previous studies on the effects of land use change on micro-climate. Such studies may or may not have employed the methodology implied above.

2.2 Radiation Balance

2.2.1 Basic Physical Laws

Physics has provided climatology with several fundamental laws on electromagnetic radiation. Wavelength is given by

$$\lambda = c/\nu \qquad (2.1)$$

λ = wavelength (cm.)

c = speed of light (cm sec^{-1})

ν = frequency (cycles sec^{-1})

The wavelength of maximum emission is related to the absolute temperature of the radiating body by Wien's Displacement Law:

$$\lambda \text{ max} = \frac{2.898 \times 10^{-1} \text{ cm } ^\circ\text{K}}{T} \qquad (2.2)$$

T = temperature (°K)

These two equations yield both the wavelength and speed of radiation being emitted from the sun and the earth. From eq. (2.2), it is found that the earth's maximum emissions are at much longer wavelengths than the sun's because of the earth's lower surface temperature.

The flux intensity of the radiation (I), is a function of the fourth power of its absolute temperature, as given by the Stefan-Bolzman Law:

$$I = \varepsilon \sigma T^4 \qquad (2.3)$$

ε = emissivity, which for a black body = 1.0

$\sigma = 5.67 \times 10^{-5}$ erg cm^2 sec^{-1} °K^{-4}

Eq. (2.3) is important when considering the relationship between the longwave radiation balance and surface temperature.

2.2.2 Radiation Balance Equation

The radiation balance at the earth's surface is expressed as follows:

$$Rn = (Q+q)(1-\alpha) + Ln \quad (2.4)$$ where

Rn = net balance of all-wave radiation)(Wm^{-2})

Q+q = global solar radiation (Wm^{-2})

α = surface albedo

Ln = net longwave radiation (Wm^{-2})

This applies if both the atmosphere and the earth's surface are considered.

Global solar radiation is made up of two components, direct-beam solar radiation (Q), and sky diffuse radiation (q). Of the solar radiation incident on the top of the atmosphere, an average of 22% reaches the earth's surface as diffuse, and 31% as direct-beam solar radiation (Sellers, 1965). Cloud cover affects the ratio of direct to diffuse by proportionately increasing the diffuse component and reducing the direct component. The former is almost independent of solar elevation. However, since complete diffusion of light can be attained in nature only with a low overcast cloud cover and very low sun altitudes, measurements on most cloudy days will include some direct-beam radiation.

Beer's Law describes the reduction of flux density as an exponential function of the depth of the homogeneous

absorbing medium:

$$I = Io \exp^{-mx} \qquad (2.5)$$

Io = initial flux intensity (Wm^{-2})

I = flux intensity after passage through a depth X of the medium (Wm^{-2})

m = extinction coefficient of the medium

The extinction coefficient depends on the quantities and characteristics of the major absorbing and scattering materials within the medium, such as gases, water droplets, dust, or other suspended material. The situation is further complicated if the medium is a plant canopy, since its architecture is rarely completely homogeneous. Besides this, the variation of species and their seasonal changes (such as the shedding of leaves by deciduous hardwoods) affect the canopy's geometry, and thus, the radiation balance of that surface.

Changing weather conditions must also be considered when examining the radiation input available at different locations within a plant canopy. On cloudy days, the higher diffuse component of incoming radiation is instrumental in creating a higher ratio of below canopy/above canopy radiation (Cohen, 1975). The absolute value of

radiative energy reaching a forest floor may not vary significantly from cloudy to clear days (since the higher ratios occur during periods of lower energy input), thereby creating a daily radiation input that is much less variable than that of an open field. An open field has no overhead canopy cover that can intercept much of the direct beam component. Obviously, this must affect the longwave and energy balances as well.

Surface albedo (α) represents the fraction of incoming radiation reflected by the earth's surface upward into the atmosphere. Monteith (1959) showed that most agricultural crops which completely shade the ground have a mean albedo of 0.26, while most grass surfaces have an only slightly lower albedo of 0.25. Both values showed remarkable consistency throughout the growing season. There will be some variation over the course of a clear day with a high direct-beam component, due to the roughness of the ground and canopy surfaces, the changes in sun angles, and the presence or absence of moisture.

Albedo values for a variety of natural surfaces are shown in Table 2.1. In general, vegetative surfaces have higher albedos than bare ground. Albedo of forests (especially needleleaf forest) is, in most cases, slightly lower than both surfaces. Budyko (1974, p. 13) explains that this phenomenon is probably a result of better conditions of absorption within the limits of deep vegetation

TABLE 2.1

ALBEDOS OF VARIOUS SURFACES

Surface	Albedo	Comment	Author
grass	0.23	solar elevation = 60°	Monteith and Szeicz (1961)
grass	0.28	solar elevation = 20°	Monteith and Szeicz (1961)
grass	0.26	daily mean	Monteith and Szeicz (1961)
agricultural crops	0.26		Monteith (1959)
grass	0.25	constant throughout the season	Monteith (1959), Davies and Buttimor (1969)
short grass	0.22-0.33		Angström (1925)
short grass	0.14-0.37		Kalitin quoted by Monteith (1959)
short grass	0.22-0.50		Blackwell quoted by Roach (1955)
meadows	0.15-0.25		Budyko (1958)
short grass	0.211	3 year mean, clear days	Polavarapu (1970)
short grass	0.214	3 year mean, all days	Polavarapu (1970)
short grass	0.20-0.24	monthly means	Polavarapu (1970)

TABLE 2.1 (con't.)

forest and grassland	0.146	airborne measurements (50 - 55°N)	Kung et al. (1964)
forest and grassland	0.148	airborne measurements (45 - 50°N)	Kung et al. (1964)
pine	0.12	above canopy measurements	Stanhill et al. (1966)
pine	0.13	above canopy measurements	Davies and Buttimor (1969)
needleleaf forest	0.14	mid-summer, temperatures >10°C	Budyko (1974)
maple-beech	0.19	above canopy measurements	Budyko (1958)
oak forest	0.18	above canopy measurements	Angström (1925), Stanhill et al. (1966)
deciduous forest	0.15-0.20	above canopy measurements	Budyko (1958)
oak, pine	0.03-0.06	airborne measurements	Kimball and Hand*
oak, pine	0.04-0.10	airborne measurements	Towsey and Hurlbut*
oak, pine	0.03-0.05	airborne measurements	Luckiesh*

TABLE 2.1 (con't.)

beech tree	0.19		Rouse (1965)
maple tree	0.19		Rouse (1965)
orange orchard	0.17	above canopy measurements	Stanhill et al. (1966)
bare soil	0.16-0.19		Monteith and Szeicz (1961)
bare soil	0.17	mean	Monteith and Szeicz (1961)
bare ground - dry	0.18		Monteith (1959)
bare ground - wet	0.11	moisture content = 35% dry weight	Monteith (1959)

*These studies are quoted by Rouse (1965).

cover, where there is an increased probability that solar radiation fluxes having penetrated the vegetation will be absorbed after their first reflection from elements of the vegetation. However, forests show marked albedo differences between species, and this could be a result of stand height and density, or reflectivity of individual leaves and needles.[1]

Although moisture content and solar elevation are major factors in albedo variance, prevailing weather is not, as the difference between mean albedo values of clear days and all days is negligible (Polavarapu, 1970). Albedo measurements taken just above the canopy give significantly higher values than airborne measurements, because of atmospheric attenuation of the reflection component, hence, the above canopy measurements are considered to be more pertinent on a microscale (Rouse, 1965).

Since α is the reflective component of global solar radiation, then $(1 - \alpha)$ is considered the absorbable component, which makes up the largest proportion of the net radiation balance. This is contained in the short wavelengths from 0.15 - 4.0 microns.

The net longwave component, unlike the shortwave radiation, is readily absorbed in the atmosphere at all

---

[1] A detailed review of albedo for various coniferous species can be found in a review by Jarvis et al. (1976).

but a narrow band of wavelengths, 8.5 - 11.0 microns, usually referred to as the atmospheric window. Longwave flux emissions can be related to temperature by eq. (2.3). The sun is assumed to be a black body ($\varepsilon = 1.0$), that is, one which absorbs and emits all the radiation falling upon its surface. Most of the earth's natural surfaces are considered grey bodies with emissivities somewhat less than 1.0. Most forests and grasses, for example, have an emissivity of 0.90 (individual leaves may be higher), while values for most bare soil surfaces range from 0.89 - 0.98 depending on moisture content (Sellers, 1965).

Longwave energy emitted and absorbed by the atmosphere without clouds present is, in general, determined by the presence of water vapour and carbon dioxide, and much less on ozone. The atmosphere actually emits longwave radiation both to the earth's surface and to space, but the downward flux usually originates in a lower and warmer atmosphere than does the upward flux, so the atmosphere will emit more energy to the earth's surface than to space. Therefore the longwave balance will usually be negative, and this, combined with the shortwave balance (which is positive during the day and zero at night) creates a net all-wave balance which is positive during the day and negative at night, depending on the sun's elevation and the degree of cloudiness. From this, it is

evident that radiation incident at the surface will also be affected by location, topography, and time of year, despite the fact that the sun emits radiation at a constant rate of approximately 1,359.74 $Wm^{-2}min^{-1}$ (1.95 ly min^{-1}). Lambert's Cosine Law defines the radiation emitted as varying with the cosine of the angle between the normal to a surface and the direction of radiation. Therefore, an inclined surface oriented towards the sun will receive greater radiation intensity from the sun, and this has a large effect on the micro-climate of that surface.

As α values for most agricultural crops are relatively constant (when there is full canopy coverage), so are the values of Rn. Freely transpiring vegetation does not have large differences in surface temperature. Therefore, if crops are in similar environmental conditions, small differences in longwave emission would result (Monteith, 1959). However, a change in albedo can be expected to change the surface temperature, its longwave emission, and its net radiation.

2.2.3 Recent Work--Vegetation Transmission, Regression Analysis, and Variations in Albedo

Several recent studies have focused on the effects of vegetation on the radiation balance. There were different objectives available for workers to pursue. Little work had previously been done on radiation distribution

in forests, and there were several unanswered questions. The spatial variation of direct, diffuse, and net radiation within plant canopies was unknown, and researchers desired to find this out in order to determine how much instrumentation would be necessary to measure the energy available within the total plant area for snowmelt, evaporation, evapotranspiration, and photosynthesis. Other questions were: What was causing the spatial variation of radiation within the same plant canopy? Could this spatial variation be approximated statistically? How much of this radiation was being reflected? Was there a temporal variation? Could water stress be a factor in net radiation or albedo? Also, since global radiation measurements were more readily available than net radiation data, could global be used to predict net?

Within the last decade, there have been attempts to resolve these questions. Anderson (1970) examined the spatial variation of solar radiation within forest and crop canopies at Madingly Wood, England. She found that while the fraction of diffuse radiation was not much affected by weather and showed little spatial variation, the fraction of direct beam radiation transmitted varied as solar altitude changed. There was also considerable spatial and day to day variation because of local variation of canopy structure and cloud duration. Reifsnyder et al. (1971) found that this extreme spatial variation

necessitated the use of 10 instruments to determine a full day average value under a pine canopy at New Haven, Conn., and many times that number would be required to estimate instantaneous radiation. For hardwoods, though, only one is needed for a full day average. Apparently, the different canopy structures of hardwoods and conifers yield different direct beam radiation profiles within them. While an exponential-extinction law similar to Beer's Law appeared to fit the coniferous canopy, a constant-ratio law sufficed for hardwoods. Therefore, while the coniferous cover was acting as a uniformly scattering medium, the hardwood canopy acted more like a layer of horizontally flat leaves. Since the extinction coefficient of Beer's Law is a constant characterizing the optical opacity of the canopy, the difference in canopy structure is all important. This became a factor in the difference in instrument requirements for each canopy.

Federer (1968) had found a range of 0.03 in the spatial variation of albedos in hardwoods, while for several vegetation covers, including conifers and herbaceous plants, the range was 0.13. The surface temperature range for hardwoods was 1 - 5°C, while a larger range, 5 - 11°C, existed for the other covers. These two factors were seen as the main cause of spatial variation in net radiation, which was 20.92 $Wm^{-2}min^{-1}$ (0.03 ly min^{-1}) for hardwoods, and 76.70 $Wm^{-2}min^{-1}$ (0.11 ly min^{-1}) for the other covers except

in winter. However, a more controversial conclusion arrived at was that one or two measurements of net radiation within each cover type were sufficient for calculating mean net radiation values, if the instrument was placed high enough to see the crowns of a number of trees. Reifsnyder et al. had disagreed, and Impens et al. (1970) later found that during sunny conditions with a high direct beam component, extreme values were generally much more frequent than mean values in several crop canopies. This suggested that the determination of mean net radiation by few measurements may be grossly inadequate. They concluded that several dozen instruments might be needed to determine even 12 hour totals of net radiation with reasonable accuracy.

Besides this spatial variation, temporal variations of a diurnal and seasonal nature, were found for albedo. This variation is important because of its implications for net radiation. Kalma and Badham (1972) found that seasonal changes in the albedo of grasses were very likely due to changes in the surface characteristics of the vegetation. On a diurnal scale, however, a general increase was observed with increasing zenith angle, and this must be due to the fact that natural surfaces are not perfect diffusers, and specular reflection becomes more important at lower sun elevations. This situation would only occur under periods with a high direct beam component as opposed

to diffuse. Under overcast conditions, the evenness of the light would not allow the different vegetation properties to assert their respective influences on albedo.

Another factor that appeared to affect albedo was water stress. Kalma and Badham (1972) found that wetting of the underlying soil caused a decrease in albedo, while under periods of water stress, an increase in albedo occurred, leading to a decrea in surface temperature (Kalma, 1972). Similar results were obtained by Glover (1972), although his findings were partially based on visual observation. However, he used regression analysis of net vs. global radiation to determine the albedo change between stressed and unstressed vegetation, and found an increase of 0.12 during the water stress period.

Regression analysis was, by this time, widely used to estimate net radiation from global, because of its simplicity, and the resulting high correlations. This linear relationship can be expressed as follows:

$$Rn = a(Q+q)+b \qquad (2.6)$$

a = slope
b = intercept

The slope and intercept terms are components of the equation of the line. Eq. (2.6) is generally applied to grass or crop surfaces, to day-time net radiation, and to the snow-free season. Accuracy is acceptable, although there may be problems with the intercept due to lack of data near the origin (sunrise and sunset periods when global is

near zero, and Rn is often negative). This error can be reduced, however, by applying daily or hourly radiation values.

Attempts had previously been made to improve eq. (2.6), the most noteworthy being the heating coefficient (Monteith and Szeicz, 1962). Idso (1968) claimed that this was invalid because it considered net longwave radiation loss to be a linear function of net radiation, which is a physically unrealistic assumption. Gay (1971) went further, when he stated that (Q+q) was being autocorrelated, and that regression analysis was producing useless results. However, other studies such as Glover's, continued to use eq. (2.6) because it was fulfilling its purpose. Albedo could be inserted into the regression model to produce different regression slopes, hence, different results for net radiation, because of the variation in global radiation absorption of different surfaces.

2.3 Energy Balance

2.3.1 Energy Balance Equation

The energy balance at the earth's surface is expressed as follows:

$$Rn = H+LE+Gs+Y+M \qquad (2.7)$$

H = sensible heat flux (Wm^{-2})

L = latent heat of vapourization (cal. gm^{-1})

E = quantity of water evaporated ($gm\ cm^{-2}$)

Gs= soil heat flux (Wm^{-2})

Y = photosynthesis (Wm^{-2})

M = miscellaneous exchanges (Wm^{-2})

The L and E terms combine to make up the flux of latent heat (units are cal cm^{-2} which are converted to Wm^{-2}). M includes energy exchanges which are due to metabolic activity and the storage of heat in the plant tissue or the volume of the canopy.

Eq. (2.7) is an approximate term and does not include effects of snowmelt, which would affect the right side of the equation by about 6,970 $Wm^{-2}\ day^{-1}$, heat transfer by precipitation, which would affect Gs, wind effects, which are an energy source and would be included on the left side of the equation, and other biological influences such as oxidation of substances (e.g. by fire). Also, since the sum of Y and M terms is usually smaller than the experimental error in measurement of the major components, these are generally ignored so that

$$Rn = H+LE+Gs \qquad (2.8)$$

adequately describes the energy budget of the earth's surface (Rosenberg, 1974).

At night, with no shortwave radiation available, Rn equals Ln, which is usually negative since the earth is radiating more heat than it receives from cloud transmissions. Therefore,

$$Ln = H+LE+Gs \qquad (2.9)$$

The four components of eq. (2.8) can be directly measured or calculated from other parameters, such as temperature and vapour pressure (Sellers, 1965). Rn and Gs can be directly measured. H is calculated using the following equation:

$$H = 60\ \rho_a C_p\ \alpha h\ dT/dZ \qquad (2.10)$$

ρ_a = density of air (1.13×10^{-3} gm cm^{-3})

C_p = specific heat of air at constant pressure (0.24 cal gm^{-1} deg^{-1})

αh = molecular diffusivity of air for heat ($0.16-0.24$ cm^2 sec^{-2})

dT/dZ = temperature gradient within layer of Z thickness

This applies from the surface to the top of the laminar sublayer. Above that, the airflow becomes turbulent and αh is replaced by Kh, the coefficient of turbulent exchange, which may vary from near zero to 10,000 $cm^2 sec^{-1}$. E can then be calculated as the residual term of the energy balance equation. On the other hand, E can be measured using lysimeters, atmometers (porous ceramic or porous paper evaporating surfaces connected to a water reservoir), or evaporation pans. In that case, results for H can be determined as the residual term of the equation.

"Evapotranspiration"(ET) is used to describe the total process of water transfer into the atmosphere from water and vegetated land surfaces. Soil evaporation (as well as evaporation of intercepted rainwater) and plant transpiration occur simultaneously in nature, and since the two terms cannot be distinguished easily, their combined effects are lumped into this term. ET can be estimated hydrologically, using a form of water balance equation:

$$\text{rainfall} + \text{irrigation} - \text{runoff} - \Delta PW - \text{percolation} = ET \qquad (2.11)$$

where ΔPW is the change in volume of water stored in the soil during some specified time period. There are problems with this because of measurement difficulties, as well as theoretical difficulties with percolation and ΔPW. However,

due to the climate and soil conditions of Central Alberta, runoff and percolation can be neglected. The local runoff hazard is low, due to the low precipitation and generally flat topography. Also, during the growing season, the soils of this area normally contain much less moisture than their moisture holding capacity. Therefore, the chances of deep percolation are also negligible (Verma, 1968). Since there is no irrigation here, eq. (2.11) becomes

$$\text{rainfall} - \Delta PW = ET \qquad (2.12)$$

2.3.2 The Case for the Water Budget Approach

In order to complete the calculations for the energy balance, either H or LE had to be determined by whatever means available. Eq. (2.10) would be very difficult to use because of the Kh term, which is extremely variable. The temperature gradient, while easy to measure, would not be valid in this situation because of the characteristics of the field site to be used in this study. The plots range in area from 85 - 500 m^2, and with such a small fetch, advective effects will be prominent for any temperature measurement taken above the plot surface. Therefore, the LE term will be calculated while H becomes the residual in eq. (2.7).

It now becomes necessary to decide the manner in which LE can be approached. Only the water balance (or water budget) method has been described so far, but there are many others, including the Bowen Ratio, the resistance approach, and the Penman and van Bavel combination methods.

The Penman method involves the use of several empirical constants, but also requires knowledge of vapour pressures, sunshine duration, α , Rn, wind speed, and mean air temperature. The van Bavel method depends on the estimation of surface roughness. The resistance approach requires knowledge of air and leaf stomatal resistances, since these have profound influence on sensible heat transport and leaf transpiration respectively. This is an analogy of Ohm's Law, since the latent flux is being regarded as a potential difference (in this case, T and vapour pressure gradients) divided by a resistance (Davies, 1972).

Other methods, including the aerodynamic approach and the eddy correlation technique, have been hindered by instrumentation difficulties. An example of this is McBean's (1968) study of turbulent fluxes within a forest. Results of some recent studies appear to favor the Bowen Ratio, because the resistance approach has not been perfected yet, the Penman combination method has been shown to seriously underestimate water loss under conditions of strong sensible heat advection, and the Van Bavel method was very sensitive to windiness (Rosenberg, 1969a, 1969b, Rose et al., 1972). It

thus becomes appropriate at this time to briefly examine the Bowen Ratio.

Given the energy balance equation (eq. 2.7), and assuming soil moisture is not a limiting factor, so that Gs can be neglected since it constitutes only a small fraction of Rn, H and LE can be expressed as functions of the exchange coefficients Kh (for sensible heat) and Kv (for latent heat) respectively:

$$H = -Cp\ \rho_a\ Kh\ (dT/dZ) \qquad (2.13)$$

$$LE = \frac{-\rho a\ L\varepsilon r}{R}\ Kv(de/dZ) \qquad (2.14)$$

R = pressure (mb)

εr = ratio of mole weights of moist air to dry air

de/dZ = vapour pressure gradient within layer of Z thickness

ρa = density of air

Other symbols have been previously defined. Subsequently, the Bowen Ratio (β) can be calculated thus:

$$\beta = \frac{H}{LE} = \frac{RCp}{L\varepsilon}\ (dT/de) \qquad (2.15)$$

Also; $$\beta = \frac{H}{LE} = \frac{Rn - LE - Gs}{LE} \quad \text{or,} \quad LE = \frac{Rn - Gs}{1 + \beta} \qquad (2.16)$$

An important assumption in simplifying the equation is Kh = Kv.

β can vary between $+\alpha$ for a dry surface (LE = 0) to -1 for an evaporating wet surface for which all the energy necessary for evaporation is supplied by convection. In other words, there is no net radiation gain so that H = -LE, and energy is directed towards the surface. β may be very close to zero when LE is at a maximum, and LE = Rn-G. In the case of sensible heat advection, β is greater than or equal to 1, and LE is greater than Rn-Gs.

Fritschen (1966) used the Bowen Ratio method on six different irrigated crops, and found that ET rates were 1.0-1.8 times that of Rn, indicating that large amounts of energy were being extracted from the air mass. He found the Bowen Ratio to be good for short period observations, and one of the few methods that would yield valid results when crops were subjected to heavy and frequent irrigation, or where high water tables were present. Denmead and McIlroy (1970) compared evaporation calculated from the Bowen Ratio to lysimeter measurements and found the results to be accurate within ± 0.1 mm hr^{-1}. They also confirmed that the assumption of equality between the eddy diffusivities of heat and water vapour, upon which the Ratio calculations could be simplified, was valid (at least over the range of instabilities examined in the study).

Fuchs and Tanner (1970) found a way to reduce the effect of a potential measurement error on the Ratio. Apparently, wet and dry-bulb temperature measurement

errors were found to be directly proportional to the Ratio. The smaller the temperature gradient between the two measurement levels, the greater the potential error, which would become infinity at isothermy. If the temperature of the two air streams would be equalized, using differential psychrometers, the measurement error would become independent of the calculated Ratio.

Rouse and Wilson (1972) actually used the Bowen Ratio as the standard with which to compare another method's accuracy. This was somewhat premature, although it probably did not affect the conclusions they drew on the usefulness of the method examined, that being the water budget approach. It was found that this was reasonably accurate for long term periods, but could not give good daily estimates of ET, due to unavoidable large potential errors in measuring soil moisture. The use of neutron scattering devices was found to be more accurate than the gravimetric method, but on a day to day basis, this could not be relied upon for soil moisture measurements.

Meanwhile, Dilley and Shepherd (1972) tried using a formula of the combination type, and the class A evaporation pan. These were compared with lysimeters, and both of them correlated well for estimating evaporation over irrigated grass and soil. Over a more variable and water sensitive surface, such as potatoes, correlations were somewhat lower, but still satisfactory. However, there was high

local advection, and considering Rosenberg's findings (1969a, 1969b), and the local situation with respect to the siting of lysimeters, these correlations must be considered suspect. Davies (1972) also used the combination model for actual evaporation calculations over a non-irrigated beanfield. He found that the equilibrium evaporation results were closer to actual evaporation than to potential evaporation.[1] Since advection was not occurring at the site, the results can be considered valid.

In a study examining non-steady-state conditions, when advection is prominent, Rose et al. (1972) found that the rate of energy stored within a crop canopy (V) was important in this situation. It was irregular in character, and often as large as Gs. Therefore, it may not be justifiable to neglect this in the energy balance equation. This could affect not only the combination model, bu the Bowen Ratio as well.

Blad and Rosenberg (1974), like Rouse and Wilson, had used the Bowen Ratio as a field standard, but it was first calibrated against a lysimeter, and underestimation of ET by about 20% was found during advective periods. This is in agreement with Rose's and Rosenberg's findings. It

---

[1] Equilibrium and potential evaporation are special cases, requiring modification of the combination model. The equilibrium case occurs if the evaporating surface is located downwind from a long fetch over a moist surface. However, if the air next to the surface is saturated, this becomes the potential case (Davies, 1972).

was suggested that under these conditions, the heat and water vapour eddy diffusivities were not equal, and as previously mentioned, their equality is a factor in simplifying the calculations of the Ratio. Adjusting the ratio of these eddies to a value favouring the heat eddy would be sufficient to correct the observed underestimation. Obviously, these eddies would require further study, and until that time, the Bowen Ratio could not be considered a "universal" standard with which to compare other methods. That role is still occupied by the lysimeter.

It becomes apparent that the Bowen Ratio will suffer from the same problem as the other approaches--advective effects caused by the small fetch of the plots at the field site. Due to the unavailability of an instrument as large and expensive as a lysimeter (and at least seven would have been necessary), the water budget becomes the most feasible method available. It is not significantly affected by the size of the plots, and equipment is available for the frequent soil moisture measurements that the method requires. The H/LE (or β) values however, can be used for analysis purposes, since they allow for quick comparisons of energy utilization to be made between surfaces. β values will be calculated from the final results for H and LE.

2.4 Effects of Land Use Change on Micro- and Macro-Climate

2.4.1 Albedo and Energy Balance

Stemming from previous discussion of items of the energy budget and the factors influencing it, one can now appreciate the significance of the effect of a land use change on the various items. A brief return to Table 2.1 reveals that deforestation of deciduous trees in favour of agriculture or pasture may increase albedo as much as 10-14% because of greater bare soil exposure, while larger increases would occur if the original cover was coniferous.[1] Similar increases occur for revegetation of bare ground with grass. Deciduous reforestation of a bare area (as well as the reverse process) would have little short term effect on albedo. However, if the soil was to remain bare for long, and become a desert with a very dry surface crust, its albedo would sharply increase (SMIC, 1971; Satterlund, 1972).

A higher albedo will reduce the absorbable component of eq. (2.4), thereby reducing the amount of energy available for heating the surface or for evapotranspiration. If the reverse land use change occurred, the resulting lower albedo would theoretically yield a higher surface temperature,

---

[1] One example is Denmead's (1969) study of wheat and pine. He found that wheat's higher albedo led to lower Rn values because of greater exposure of bare ground in the wheat field. Unfortunately, the two sites were not examined simultaneously.

depending on the soil moisture supply and other soil characteristics. It is important to note that the ground's surface layer acts as a heat reservoir--absorbing part of the excess heat of midday and summer, and returning it during the night and winter to the atmosphere. This storage lessens temperature extremes and acts as a climatic stabilizer, but of more short term importance is its ability to radiate heat quickly. This creates steep atmospheric lapse rates, which can easily lead to convection and heavy turbulence. So it is not surprising to find that higher values for H and lower LE values are common for bare soil (Satterlund, 1972). Meanwhile, vegetated surfaces with their lower radiation absorption rates (due to higher albedo) and better insulating qualities, show lower heat emissions and greater storage. This creates a stable lapse rate, and at night, inversions are more likely to occur over this surface, than over bare soil. Baumgartner's (1965) findings would seem to support this view. He compared the energy balances of several different surfaces in Germany, and found that bare soil had the highest soil heat flux rate. (Table 2.2). However, bare soil has the smallest Gs/Rn ratio, which could indicate that a land use change will not result in a linear change in either soil heat flux, or the other parameters of the energy balance.

Another aspect of land use change is plant species and stand density. Dilley and Shepherd (1972) cite seasonal

TABLE 2.2

SOIL HEAT FLUX FOR DIFFERENT SURFACES

	conifer forest	tall grass	grain	short grass	bare soil
% Rn reaching surface	7	9	20	55	100
% used as soil heat	4	5	10	15	23
% used as latent heat of evaporation	3	4	10	40	77

Adapted from Baumgartner (1965).

change in crop structure, change in species combination, as well as plant physiology, surface geometry, and local environment as factors in land use effects on climate. Fritschen (1966) claimed that higher stand density leads to higher LE/Rn ratios because the reduced bare soil exposure provides greater insulation. This view was confirmed by Satterlund (1972). However, Timmons et al (1966) found that corn evapotranspiration rates were not significantly affected by stand density, though it was noted that higher stands usually (but not always) had the highest evapotranspiration rates. The water budget approach was used in the Timmons study, with a sufficiently long time span employed between soil moisture measurements.

In a review of recent literature on coniferous forests, Jarvis et al (1976) confirmed Dilley and Shepherd's views, citing cloud cover and canopy wetness as two important local environment factors. For most sites, irrespective of species, the daytime β of a dry canopy varied from 0.1 to 1.5, and when the canopy was wet with rain or dew, between -0.7 and 0.4. However, certain locations show much larger values, exceeding those for field crops, and in some cases by a very large margin. It has been found that β values depend particularly on the stomatal resistance, but also on the general climatic and local weather conditions at the site. For continental climates such as Ellerslie's, higher β values are expected, as opposed to oceanic sites.

Jarvis et al. also quote values for LE/Rn at Fetteresso, U.K. When the canopy was wet, values were close to unity, since most of the water was used for evaporation, but under dry conditions, values ranged from 0.25 to 0.5. The authors conclude that the evaporation from dry foliage is only about 5% of that from wet foliage exposed to the same weather because the diffusion resistance of the canopy is much greater than that for air under dry conditions.

Rauner's (1976) review of studies involving deciduous forests reveals that LE dominates the picture, especially during the second part of summer. During this period, small forests less than a kilometer in diameter create an "oasis" effect which reduces H to zero or even to stable negative quantities. In other words, the surrounding countryside supplies the forest with heat. This is also common in irrigated lands, and around springs and other moist areas under dry weather and in arid regions. Even in humid areas when Rn is low, advected sensible heat may contribute appreciably to evapotranspiration (Satterlund, 1972). For larger forests, this effect is rather weak. However, a similar effect can still occur if warm dry winds prevail over larger wet areas, even for a short time period. The chinook has been shown to affect a white spruce - fir forest at Marmot Creek, Alberta, in this manner (Storr et al., quoted by Wilson, 1974).

Seasonal change in vegetation structure affects values in deciduous forests. During early spring as leaves appear, β changes drastically from near unity to near zero, and maintains this level until defoliation in autumn. Rauner also states that deciduous forests seem able to use soil water very effectively. The structure of their heat balance depends less on soil water than herbaceous vegetation or crops under comparable conditions.

Recent grassland studies were reviewed by Ripley and Redmann (1976). At Matador, Saskatchewan, a 1971 experiment revealed that β values approached unity during late summer, but this was more due to lower Rn and LE values, since H was fairly steady. LE/Rn was 0.7 in late July and 0.5 in August, with Gs accounting for about 7% of Rn. Apparently, a large part of the decrease in LE was due to increasing transpiration and transpiring leaf area (mainly the result of water stress and high leaf temperatures). The remainder was attributed to the decrease in evaporation from the soil due to the drying of the upper layers. Despite the fact that much of the total root biomass is above 30 cm, the steadying of β near unity during drought conditions in late August indicates that the vegetation was able to use soil water from lower depths. Another explanation put forward by the authors is that stomatal closure and perhaps internal plant and soil resistances would limit evaporation during much of the day during the evaporative

demand period of late July and early August. These effects would be reduced in the cooler month of September and evaporation might continue through the midday period.

Energy balance changes can act as indicators of alterations of other climate parameters. Fritschen (1966) concluded that higher LE/Rn ratios indicated warmer air temperatures, while lower ratios indicated higher atmospheric vapour pressure. Higher ratios, especially those greater than 1.0, indicate that energy is being extracted from the air mass by the plants. On that basis, Fritschen's experimental results indicated to him that broad leaf plants use more water than grasses. He attributed this to their rougher and more rigid surface structure which would allow greater energy extraction from the air mass in the form of sensible heat.

Table 2.3 illustrates a theoretical change in energy balance if forest is converted to agricultural use. This assumes an incoming shortwave radiation intensity of 125 Wm^{-2}, and an outgoing infrared radiation level of 50 Wm^{-2}. It is interesting to notice the difference between wet and dry arable surfaces. Apparently, the first priority of energy use is to evaporate water, hence a low β value. Once ET is satisfied, the remainder of the energy is used to heat the surface, and β increases.

Natural grassland, which is found in semi-arid and prairie regions had the highest β value, but this is still

TABLE 2.3

CHANGES OF HEAT BUDGET AFTER CONVERSION FROM FOREST TO AGRICULTURAL USE

	α assumed as representative	β	$Rn(Wm^{-2})$	$H(Wm^{-2})$	$LE(Wm^{-2})$	ET (mm/month)
coniferous forest	0.12	0.50	60	20	40	41
deciduous forest	0.18	0.33	53	13	39	40
arable land, wet	0.20	0.19	50	8	42	43
arable land, dry	0.20	0.41	50	15	35	36
grassland	0.20	0.67	50	20	30	31

Source: adapted from SMIC (1971), p. 173.

Numbers are rounded.

well below typical desert values of 2.0 - 6.0 or higher. Coniferous forests have higher sensible heat values than deciduous, due to its lower albedo. This will probably mean warmer temperatures during high radiation periods. During periods of low radiation, the surface's emissivity and insulating qualities determine temperature levels.

Many scientists believe that the energy balances created by widespread deforestation could be enough to significantly alter circulation patterns, especially in tropical areas (SMIC, 1971). In the mid-latitudes, especially the prairie regions which are only slightly wetter than deserts, Bowen Ratios become very important indicators of climate trends. If β is greater than 1.0, it indicates very high sensible heat levels, low availability of moisture, and a warm continental arid climate.

At the present time, little replacement of temperate forests by arable lands is in progress. Indeed, there are many marginal farm areas that have seen a return to forest cover, such as the Piedmont area of Georgia (Brender, 1974), Central Manitoba (White, 1975), and Northern New York (Muller, 1966). However, urban expansion and mining exploration may create a very different trend, with its own unique effects on climate.

2.4.2 The Hydrologic Cycle

Land use change alters the surface cover, and so, has a profound effect on the various components of the hydrologic cycle. But many of the changes are not obvious, and in the final analysis, it is difficult to conclude whether there will be an increase in water yield, or a decrease, without first considering a wide range of factors.

Deforestation is a fairly drastic land use change, whether conifers or deciduous trees were the original cover. So the question is asked--what changes will occur if an area's forest cover is removed? To answer that, each hydrologic component, as well as the area's forest cover must be considered. Air temperature, wind, and absolute humidity are affected, too, and since these factors influence evapotranspiration, they are discussed here.

In general, deforestation results in increased low-level (low altitude) maximum temperatures of from 1 - 5°C in the warm season and from 1 - 2°C in the cold season. The warm season temperature change is dependent on forest type. In addition, minimum temperatures decrease 1 - 4°C in all seasons. Therefore, a 1 - 9°C greater temperature range is produced on a monthly and annual basis (Changnon, 1972).

Absolute humidity at and near the surface is reduced 2 - 25%, depending on cover, forest type, and the new land use type. The amount of moisture added to the atmosphere by evapotranspiration is lessened, but since

low level winds in deforested areas are increased 2 - 4 times, a greater rate of evaporation (and more wind erosion) from the soil occurs, partially offsetting the reduced evapotranspiration. It has been suggested, that increase in drought frequency and a general drying of the climate in eastern Europe have been due largely to deforestation and to poor surface water management, which together led to a lowering of the soil moisture. Other controversial questions concerning land use and climate include deforestation's effect on rainfall production in the Mediterranean, and climate changes in semi-arid regions caused by cultivation of previously undisturbed grasslands (Changnon, 1972). These are macro-scale phenomena, and are beyond the scope of this study, but they are worth mentioning because they illustrate the potential magnitude of the problem.

The components of the hydrologic cycle include interception, throughfall, infiltration, runoff, and evapotranspiration. If deforestation occurs, interception losses will be reduced and throughfall will increase. If the area is on a slope, this would affect surface runoff and erosion. However, the new vegetation will be different in density and foliage arrangement so as to reduce the effects of wind while it is becoming established. These "replacement plants" may transmit or reflect more radiant energy from leaf surfaces, or transfer absorbed heat to surroundings more effectively, so that less is used in transpiration. Also,

they may have a shorter period of soil moisture use or a shallower or perhaps, less efficient root system, and thus extract less water from soil storage (Jeffrey, 1964).

On the other hand, not all grasses have shallower root systems than trees or shrubs. Grass species vary from one to the other, just as do trees. Comparisons must be made--species vs species--for the kinds of sites under consideration. For example, the conifers have not been shown to use either more or less water than hardwood trees, with similar rooting depths (Jeffrey, 1964; Satterlund, 1972). Trees and shrubs g[illegible]ong stream banks and in areas of high water tables [illegible]en shown to use large amounts of water. Transp[illegible] varies with age too, increasing up to a certain age, levelling off, and then decreasing (Jeffrey, 1964).

Infiltration will be greatly affected by age, stand density, and human activity. High infiltration rates occur in dense, old, and undisturbed stands. Highest rates occur in undisturbed forest while lowest rates occur in overgrazed pastures and in cropped fields. Rates will increase if the area is reforested, thereby reducing runoff. Consequently, streamflow leaving the drainage basin will be reduced (Muller, 1966).

Time of year will be a factor when comparing the water use of different tree species in the same location. Satterlund (1972), stated that the seasonal pattern of

soil moisture removal is different for aspen and spruce in Colorado, or red pine and oak in Michigan, to name two examples.

Despite the effects different plant species may cause, there is still one basic similarity among them--their presence on the surface and their roots below. If the soil is bared, only a very shallow depth is dried since there is less energy available to transfer deep into the soil (depending on albedo and H values), as well as the lack of roots to cause water uptake (Satterlund, 1972; Muller, 1966). Farmers in prairie and semi-arid environments often use fallow rotations (dry farming) as a water conservation practice because of this fact.

Having examined each of the separate components, one finds that there are both positive and negative feedbacks from each when a land use change occurs. What is the net result of these feedbacks? Muller's (1966) study of abandoned New York State farmland which has returned to natural overgrown pasture, deciduous forest cover, or coniferous plantations, reveals a decrease in water yield. Both in winter and summer, radiative energy and moisture are more readily available for evapotranspiration in these land uses. During winter, greater snow evaporation occurs in snow-covered crowns of conifers, because of favourable daytime radiation balance. In summer, deciduous and coniferous trees absorb more radiation than open and overgrown

areas. Also, differential rates of evaporation and transpiration during moisture deficits, and greater infiltration rates, will increase evapotranspiration loss and decrease water yield from the overgrown and forest covers. The greatest changes occurred when conifers were planted, as water yields decreased by up to 24.4 cm yr^{-1}. Muller had to qualify his conclusions, however, since subsequent water balance and multiple regression tests were significantly affected by estimates of precipitation income and water yield outgo which may have been unrepresentative of watershed-wide conditions. Mean monthly temperatures from an open base station were used for evapotranspiration calculations, and with reforestation, rain gauge exposure changed. Therefore, it was admitted that land use change may not have been the exclusive factor.

Taking these factors into account, this study will use mean weekly temperatures from all different cover sites when making evapotranspiration calculations. The open station data will be used for open area sites such as fallow and shrub, while data are available for the individual spruce and poplar plots. Only 1 rain gauge is used at the site, but since the plots are all within 500 metres of the rain gauge, significant variation is not expected. Also, as previously mentioned, runoff and percolation can be neglected under the local conditions studied.

CHAPTER III

INSTRUMENTATION AND EXPERIMENTAL PROCEDURE

3.1 Introduction

The following presents a description of the field site and test plots to be examined during the course of this study. A detailed account of the type of instrumentation used, and its deployment, is included. Calibrations are listed in Appendix I. A detailed chronicle of the biological changes observed on each plot from April - October, 1976, is found in Chapter IV.

3.2 The Site

3.2.1 General Characteristics

The site chosen for the investigation is the University of Alberta Farm at Ellerslie, Alberta (lat. 53° 25' N, long. 113° 33' W), about 15 km south of Edmonton's city core (Fig. 3.1). Located in the transition zone between the Boreal and Prairie regions, the natural vegetation here is mostly trembling aspen (Populus tremuloides Michx.) and white spruce (Picea glauca Voss). However, a large portion of the area is under pasture and mixed grain cultivation with barley being the most popular grain crop.

FIG. 3.1: LOCATION OF STUDY AREA

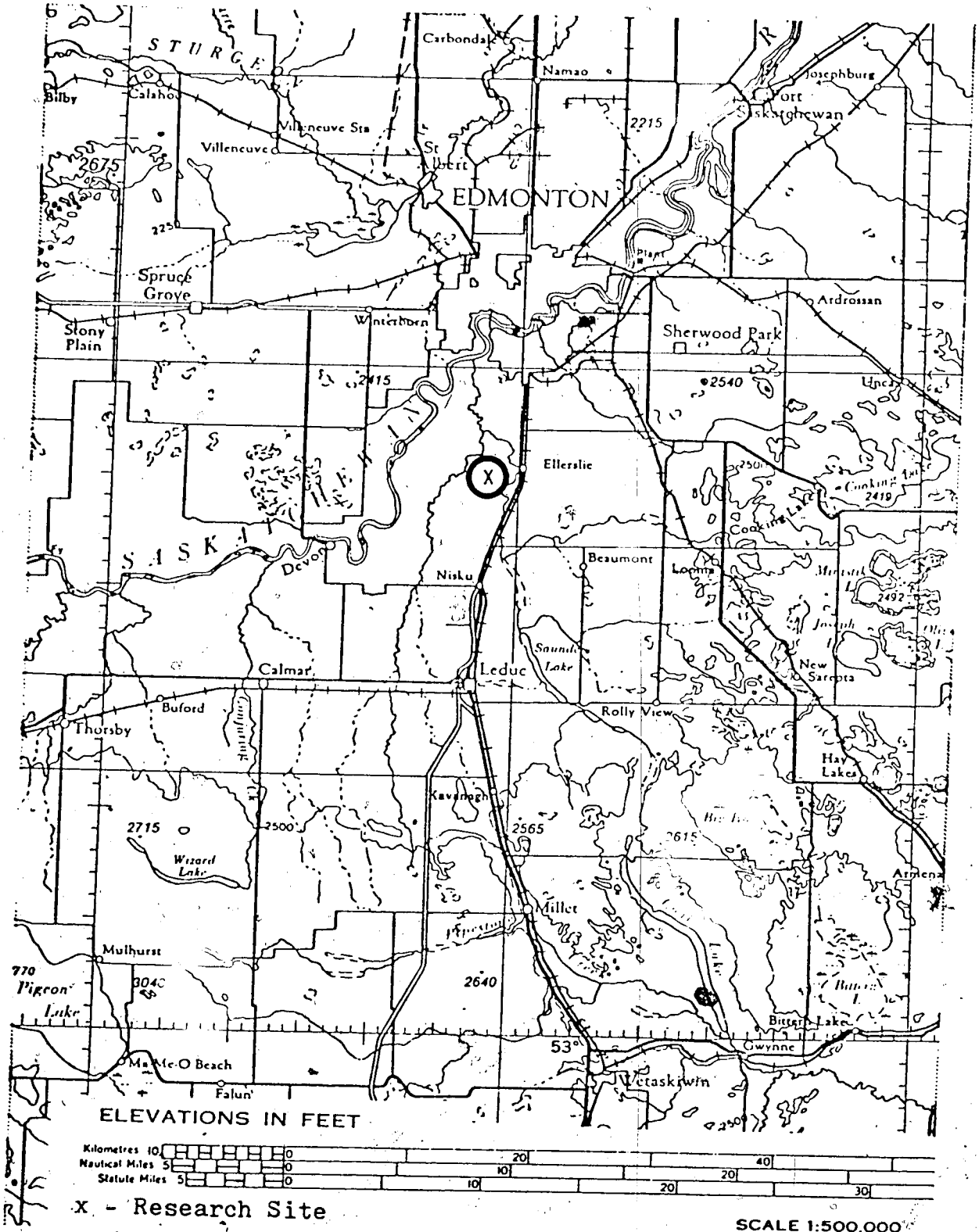

X - Research Site

SOURCE: Canada, Dept. of E., M., and R., N. T. S. No. 83 S. E.

The area is underlain by shale, siltstone, and sandstone deposits from the upper Cretaceous period. Ground moraines, creek channels, and prairie mounds are evidence of previous glacial activity. Topography at Ellerslie is fairly level with slopes rarely exceeding 2% (Fig. 3.2), except at river and creek channels. The experimental plots are on a NNW facing slope of about 1%.

A cool continental climate exists here (Dfc on the Köppen system) with a mean summer temperature of 13°C, and mean summer precipitation of 30 cm. The average growing season is 165 days, commencing April 25 and ending October 6. However, only 90 days are frost-free. June and July are the wettest months, but rainfall is generally low in intensity and well distributed throughout the growing season. There is a comparatively low variability in growing season precipitation here. Average variability is 20 - 25% from the mean, whereas elsewhere in Alberta, especially in the northwest and south, this variation exceeds 35% (Weir, 1971). There are about 110 - 120 days with precipitation per year, mostly during summer. Mean annual soil moisture deficit is 10 cm and mean annual potential evapotranspiration is 51 cm, 5 cm greater than mean annual precipitation. Annual bright sunshine hours slightly exceed 2200.

The annual march of the components of the energy balance for the continental mid-latitudes shows differences

FIG. 3.2: ELLERSLIE SITE

0 200 400 ft.
0 61 122 m.

N

CONTOUR INTERVAL = 3ft.
= 0.91m.

ABOVE LOWEST POINT

SOURCE: SOIL SCIENCE DEPT., U. OF ALBERTA

in time of maximum flux intensity. A sample curve (Barnaul, U.S.S.R.) shown in fig. 3.3a illustrates a large time difference between LE and Rn maxima, which, in this case, is close to 6 weeks. The maximum outgo of heat for evaporation can be observed earlier or later than the maximum in Rn, depending on the annual march of precipitation and the associated change in soil moisture. If the LE maximum precedes the Rn maximum, then the H maximum is commonly observed after the Rn peak, and vice versa. For climates with wet summers, heavy cloudiness in summer reduces the Rn maximum (Fig. 3.3b). The LE max. occurs in August, while the winter period shows a curve similar to Fig. 3.3a (Budyko, 1974). Although this curve is more typical of a mid-latitude summer monsoon climate, there are similarities in annual precipitation distribution and latitude between Grossevichi and Ellerslie. Ellerslie's annual curve for any particular year could be similar to either of the above two figures, depending on summer precipitation levels.

Soil climate is moderately cold cryoboreal. Mean annual soil temperature is 2 - 8°C, 120 - 220 days are above 5°C, there is a short thermal period of less than 60 days with temperatures above 15°C, and there is a mild summer. Soil moisture regime is subhumid, with a 5 - 10 cm water deficit during the growing season (Fremlin, 1974).

FIG. 3.3: ANNUAL MARCH OF HEAT BALANCE

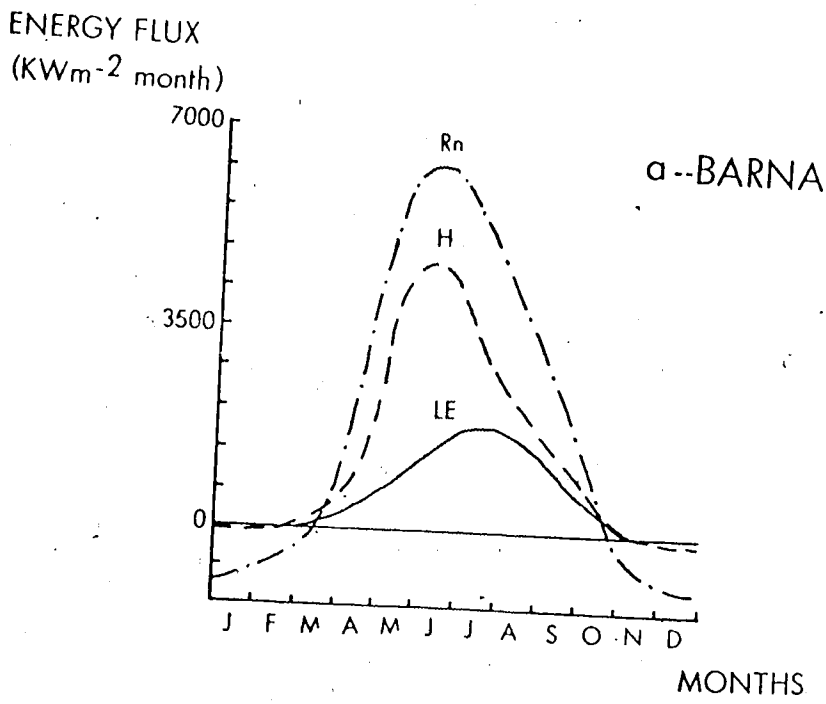

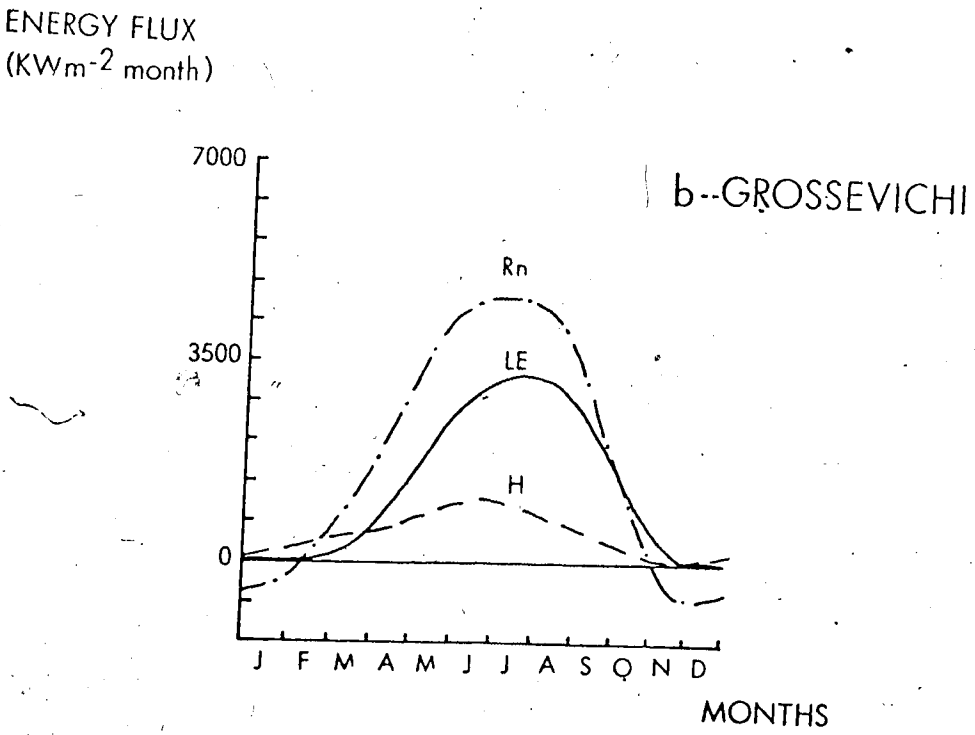

SOURCE: ADAPTED FROM BUDYKO (1974) -- FIGS. 61 + 62

Soil types in the small plot area are Malmo clay loam and Ponoka loam. Malmo clay loam is developed from lacustrine parent material, generally underlain by till at depths varying from 51 - 102 cm below the surface. The upper horizons of the profile (Ap, Ah), are black (10 YR. 2/1 - 3/1) with a clay loam texture and coarse granular structure. Ponoka loam is coarser in texture, with a parent material of stratified silts and very fine sand clay loam. Till generally occurs at depths varying from 38 - 102 cm below the surface. The Ap and Ah horizons are of similar colour, but the texture is loam rather than clay loam (Pawluk, 1964).

3.2.2 Experimental Plots

Six small plots and one forest site were employed during the study (Fig. 3.2). A deciduous plot (PS), 330 m^2 in area, consists of poplar trees approximately 6 metres high (Plate 3.1a and 3.1b). South of it is a coniferous plot (S) approximately the same area (Plate 3.2). White spruce is the tree species occupying it. Trees are 4 - 6 m high and form a very dense canopy. A shrub plot (W), 150 m^2 consists of western snowberry less than 1 m high, tall grasses, and some weeds, including Hawk's beard (genus Hieracium) and Canada thistle (Carduus arvensis) (Plate 3.3). Barley (B) and fallow plots (F), 85 m^2 each, are the only ones which suffer seasonal human

Plate 3.1a. Deciduous plot (PS). The screen is visible on the left.

Plate 3.1b. Inside PS plot. From left to right: screen, soil moisture access tube (at author's feet), tower.

Plate 3.2. Coniferous plot (S). The tower is visible at the center.

Plate 3.3. Shrub plot (W).

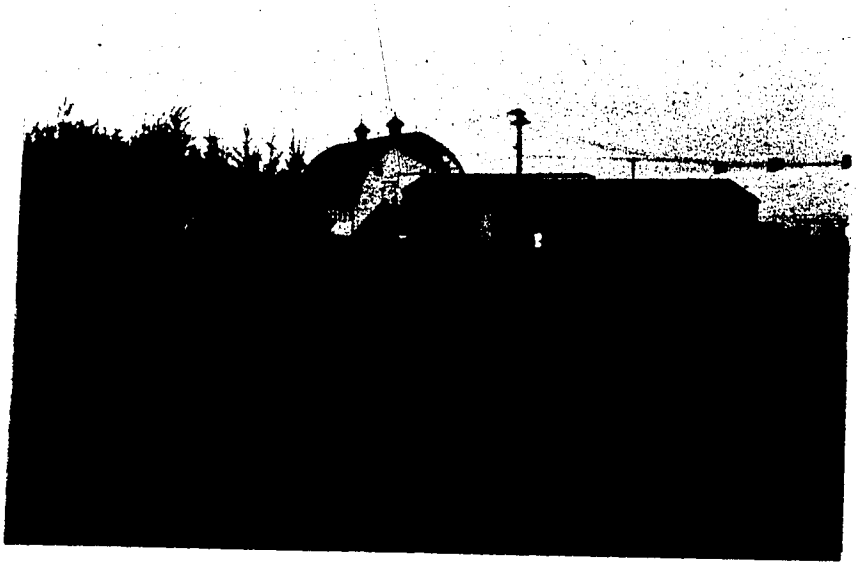

Plate 3.4. Barley (B) and fallow (F) plots (May, 1976). Barley stubble (background) was cut and the plot was seeded one week after the photo was taken.

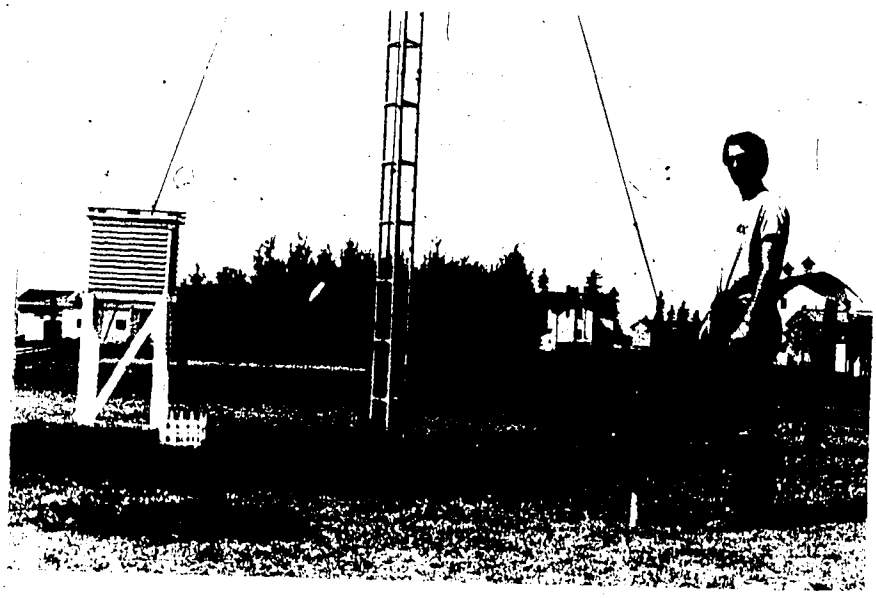

Plate 3.5. Grass plot (G). This is the meteorological installation.

Plate 3.6. Poplar forest (P).

TABLE 3.1

ELLERSLIE SITE DESCRIPTIONS

Plot Name	Symbol	Area (m^2)	Height (m)	Plant Type
Deciduous	PS	330	6	Poplar (Trembling Aspen)
Coniferous	S	330	4-5	White Spruce
Shrub	W	1 0	1	Western snowberry, tall grass, weeds
Barley	B	85	1	Active barley crop
Fallow	F	85	0-1	Periodic weed cover
Grass	G	500	0.1	Short grass
Poplar forest	P	5000	14-18	Aspen

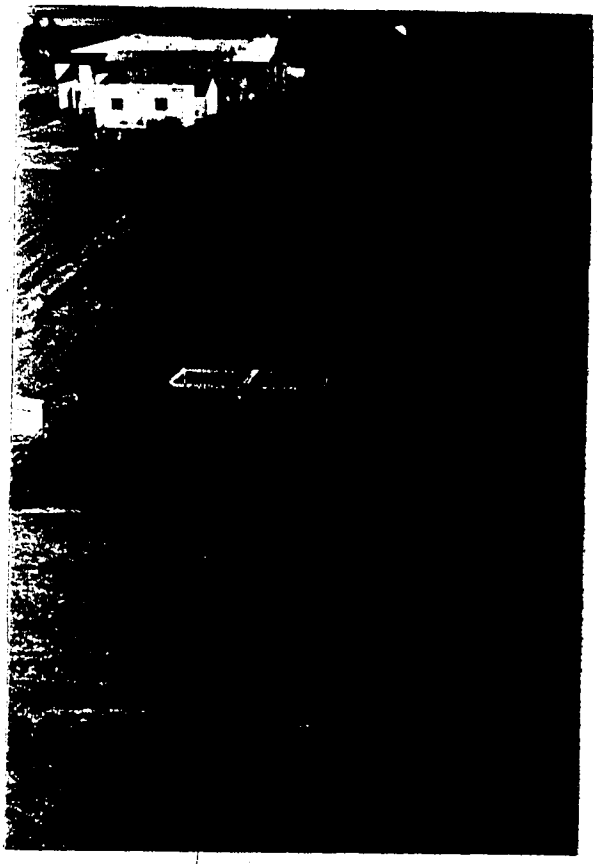

Plate 3.7. Ellerslie small plots (July, 1976). From top to bottom: PS, S, W, B (with radiation equipment) and F (with heavy weed cover).

attention. Stubble from the previous barley crop was removed in spring 1976 and the plot was re-seeded, creating a continuous cover slightly less than 1 m high by June. The neighbouring plot (F) was kept fallow throughout the experiment, although periodic weeding was necessary since common weeds such as Ball Mustard (genus Brassica) and Stinkweed (Datura stramonium) invaded the plot (Plate 3.4) A short grass cover (G) was maintained as part of a well-serviced meteorological installation south of the fallow plot (Plate 3.5) The actual measurement area was approximately 25 m from F plot. Distances between the other small plots ranged from 5 - 13 m.

In addition to these sites, a nearby poplar forest site (P) was used on a limited scale. The site is located approximately 300 m west of the small plots, and consists of poplars 14 - 18 metres high (Plate 3.6). This forest area is much older and larger than the small plots, and has a denser cover than the small poplar site. Table 3.1 summarizes the above descriptions, and includes the plot symbols to be used throughout the text. Plate 3.7 shows an overview of five of the small plots.

3.3 Instrumentation

3.3.1 Radiation

Global solar radiation was measured with an Eppley

pyranometer (Plate 3.8), sensitive to shortwave radiation in the range 0.3 - 3.5 μ. The sensor is constructed with a circular multi-junction copper-constantan thermopile with temperature compensation, housed in 2 optical glass domes. It has an approximate sensitivity of 9 microvolts per Wm^{-2}. Reflected solar radiation (albedo) was measured with a second Eppley pyranometer, held inverted approximately 1 metre above the ground surface for G, B, F, and W plots, (Plate 3.9). For PS and S plots, the pyranometer was attached to the top rung of an instrument tower (Plates 3.10 - 11). The resulting voltage reading was recorded in an electrically powered Leeds and Northrup strip chart recorder (Plate 3.12a). Digital counters were used for both daily global and albedo measurements (Plate 3.12b). These provided daily voltage totals. The albedo recorder was housed in a white shelter located next to the plot being measured, while the global Honeywell recorder housed in the lab building.

Net radiation in the range of 0.3 - 60.0 μ was measured with two CSIRO net pyrradiometers. The sensing element is similar to that of the pyranometer, but since it is housed in plastic hemispheric domes, the longer waves are permitted to strike the sensor directly. The plastic hemispheres cover both sides of the element (Plate 3.9), so that incoming and outgoing radiation are measured simultaneously. The domes were kept inflated by an air pump

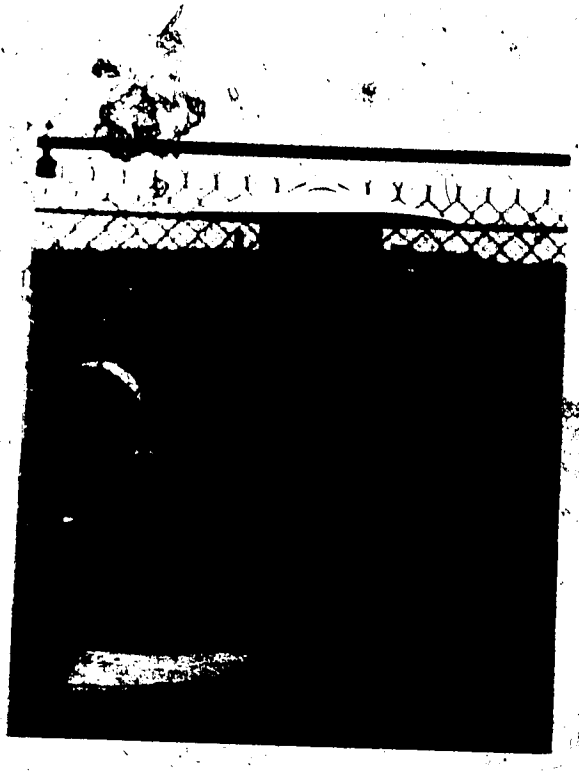

Plate 3.8. Eppley pyranometer.

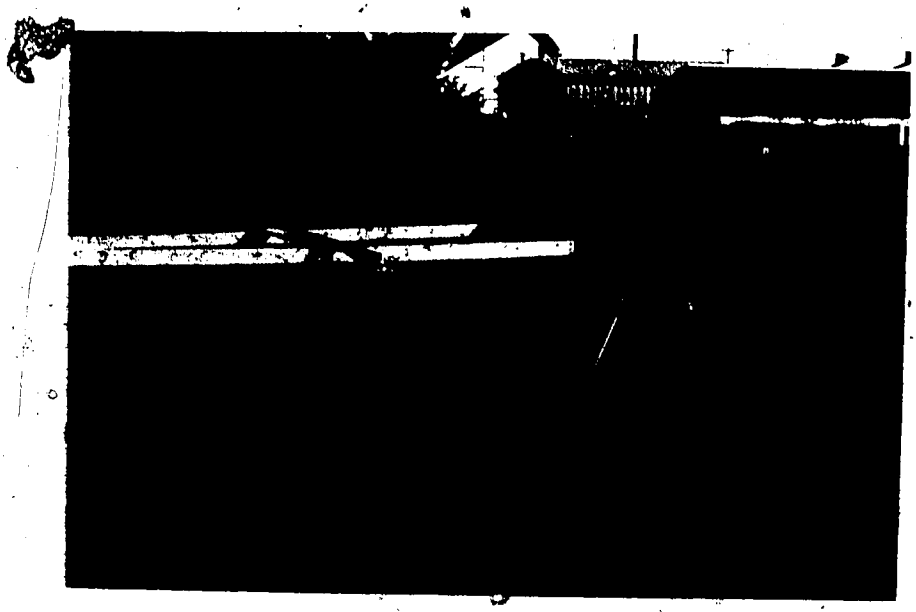

Plate 3.9 Albedo and net radiation measurements.

Plate 3.10. Albedo measurement above deciduous plot.

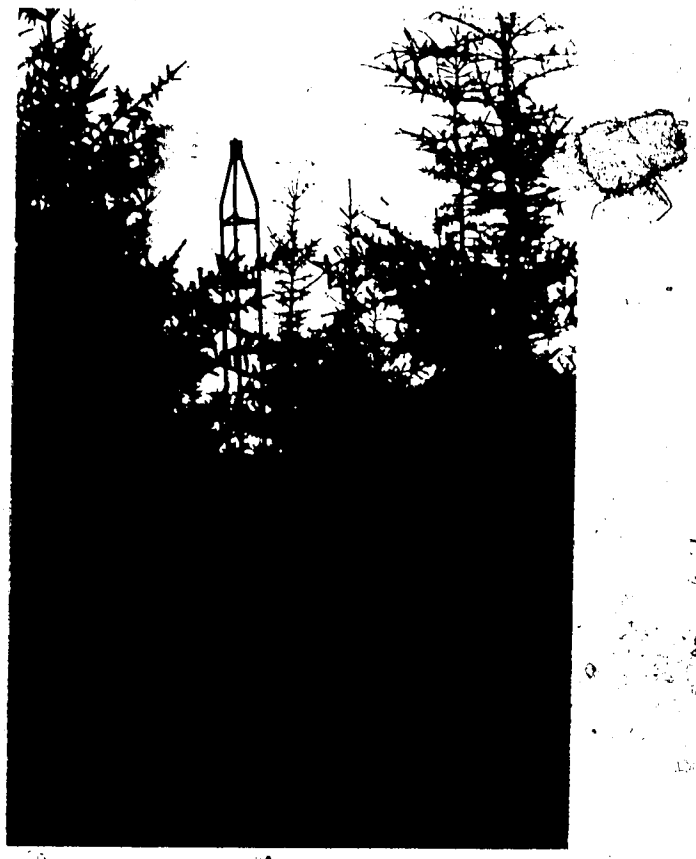

Plate 3.11. Instrument tower at S plot.

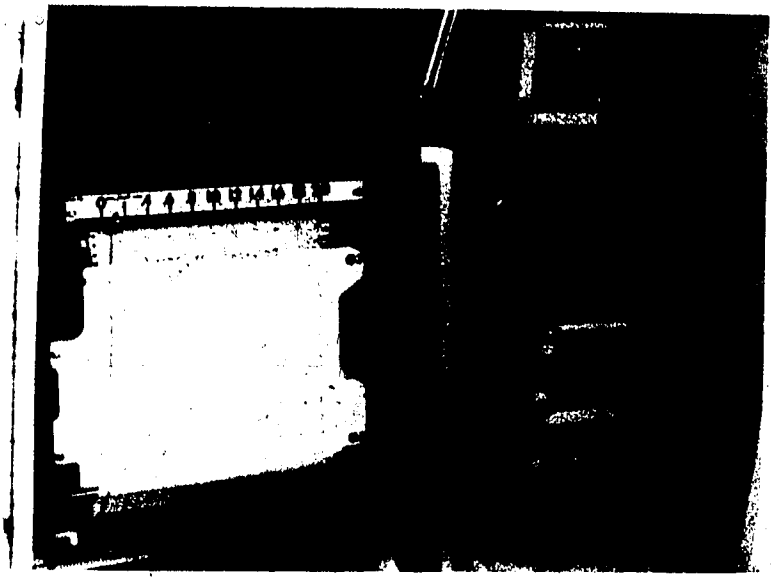

Plate 3.12a. Albedo recorder.

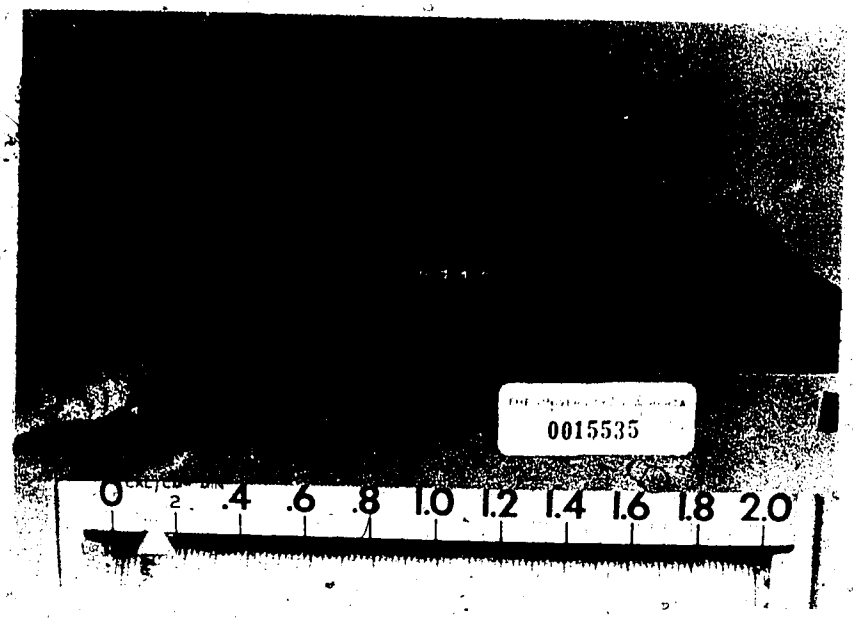

Plate 3.12b. Digital counter.

that allowed a flow of dry air to be continuously maintained. Silica gel was used as a drying agent (Plate 3.13). The resulting net all-wave balance was recorded on a Rustrak battery-operated strip chart recorder (Plate 3.14), housed in a white shelter similar to the aforementioned.

3.3.2 Soil Heat Flux

Soil heat flux was measured with a soil heat flux disk, similar to the one used by Fuchs and Tanner (1968). The disk is circular and quite small, and is inserted between 1 and 3 cm below the soil surface (Plate 3.15). The upper and lower surfaces of the disk attain a temperature difference which is proportional to the soil heat flux. This temperature difference is sensed by a thermopile similar to those used for radiation measurements. The output was recorded on the same type of battery-powered recorder used for the net radiation output (Plate 3.14).

3.3.3 Soil Moisture, Bulk Density, Organic Matter

Surface soil moisture was measured with a Nuclear Chicago surface moisture probe. The probe has a Radium-Beryllium source which emits fast neutrons into a hemispherical volume of soil. When the neutrons are

Plate 3.13. Air pump with silica gel drying agent (right).

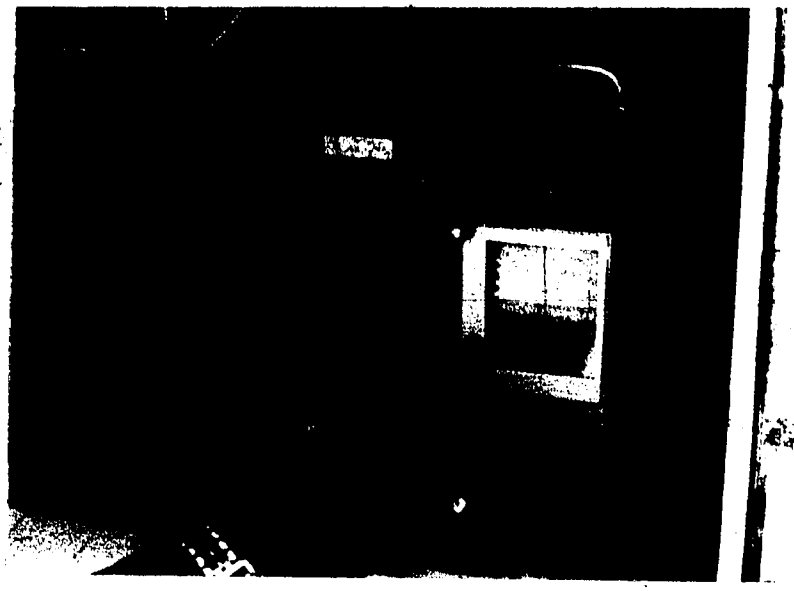

Plate 3.14. Automatic recording of net radiation and soil heat flux.

Plate 3.15. Soil heat flux disk (rotated). The coin is a quarter.

sufficiently slowed by the hydrogen nuclei in soil moisture, the detectors will produce a pulse which is counted by the scalar (Plate 3.16). The number of counts per unit time (in this case, one minute) was divided by the standard count, which was accomplished using a granite block and paraffin standard (Plate 3.17). These were taken before and after each set of readings. The resulting ratios were converted to percent volume of soil moisture by calibrating the probe against gravimetric measurements taken in April. Bulk density measurements of the soil allowed percent volume to be converted to cm water m^{-1} soil, thereby facilitating data use in the water balance equation.

Soil moisture at 0.2, 0.5, 0.8 and 1.0 metres was measured with a Nuclear Chicago depth moisture probe (Plate 3.18), It has a source similar to the surface probe. Data were calculated by using the "ratio method" as above, with Alberta Research Council calibration standards being employed rather than gravimetric samples. One access tube for each small plot, and three for the forest plot were installed at the end of April, 1976. Measurements of surface and depth moisture levels were made each week from May 2 - October 7, 1976.

Bulk density (Db) samples were collected with a Bull Core Sampler in June. The oven dry weight of the core samples was related to the core volumes to calculate dry density. Subsequently, porosity was calculated as follows:

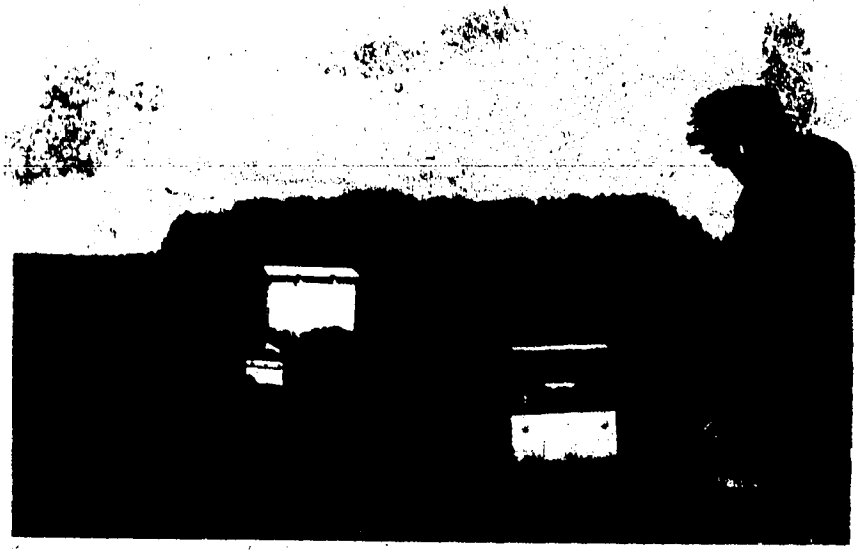

Plate 3.16. Surface moisture probe and scalar in use at F plot.

Plate 3.17. Standard count apparatus for surface probe. The probe is sitting in the paraffin which is placed on the granite block.

Plate 3.18. Depth moisture probe with scalar in use at F plot.

$$POR\% = \left(1 - \frac{Db}{2.65\ g/cc}\right) \times 100 \qquad (3.1)$$

The constant is the assumed particle density of soil. For surface horizons, this was lowered to 2.55g/cc. Results are listed in Table 3.2

Percent organic matter content was determined by ignition at 450°C. Results are listed in Table 3.3.

3.3.4 Temperature and Relative Humidity

Maximum and minimum temperatures were measured with Taylor or Casella max-min. thermometers. These were placed in Stevenson screens, which were installed approximately [illegible] meters above the ground in PS, S, and P plots in May. Data for the other sites were provided by equipment in operation at the Department's meteorological installation, which doubled as G site (Plate 3.19).

Relative humidity at PS, S, and P plots was measured with Negretti and Zambra or Casella thermohygrographs, located in the same screens as the thermometers. (Plates 3.20, 3.1b). Wet and dry bulb thermometers were used for the open site measurements (Plate 3.19).

3.3.5 Precipitation and Evaporation

Precipitation was measured with a standard rain gauge located at the meteorological installation. Open

TABLE 3.2

BULK DENSITY

($g/cc = 10^3 kg/m^3$)

Plot Depth		F	PS	P2
0.1 m	2 - 5 in.	1.04	0.93	1.46
0.3	11 - 14	1.25	1.35	1.48
0.6	23 - 26	1.66	1.58	1.54
0.9	35 - 38	1.70	1.60	1.48
1.1	41 - 44	1.66		

TABLE 3.2 (con't.)

POROSITY

(%)

Plot Depth		F	PS	P2
0.1 m	2 - 5 in.	59	64	43
0.3	11 - 14	53	49	44
0.6	23 - 26	38	40	42
0.9	35 - 38	36	38	44
1.1	41 - 44	37		

TABLE 3.3

ORGANIC MATTER

(%)

Plot Depth		P1	P2	P3	PS	S	W	B	F	G
0.15 m.	0.5 ft.	69.4*	72.5*	6.1	12.2	12.3	11.9	12.0	12.3	12.2
0.30	1	43.8*	11.1	10.3	8.5	11.3	10.3	9.0	6.2	7.7
0.61	2	9.3	6.0	5.6	3.1	3.0	3.2	7.9	4.5	11.7
0.91	3	6.5	3.9	3.3	2.7	N/A	3.0	6.8	3.2	1.9
1.22	4	3.8	2.6	2.6	2.9	N/A	2.3	5.2	1.9	2.3

* The high values for P1 and P2 indicate the existence of peat layers.

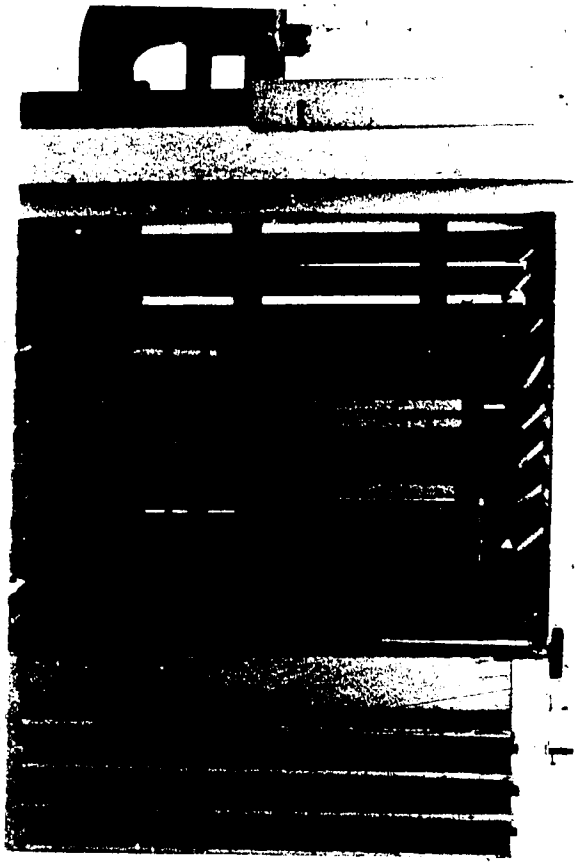

Plate 3.19. Maximum and minimum temperature and relative humidity measurements at G plot (the meteorological installation).

Plate 3.20. Thermohygrograph and maximum-minimum thermometer in screen at PS plot.

air evaporation was measured using a Class A evaporation pan (Plate 3.21).

3.3.6 Deployment of Equipment

One net pyrradiometer and one soil heat flux disk were installed at G plot on May 22, 1976. These remained stationary throughout the measurement period, and so became the base station. The pyranometer (global) was also stationary. The other three radiation instruments were rotated among PS, S, W, B, and F plots. During the May - July period, the net pyrradiometer and albedo instruments were moved twice weekly as a precaution against creating too large a time gap between readings for any individual plot. During August, this was changed to weekly. The soil heat flux disk was rotated weekly due to the sensitivity of the instrument.

Surface soil moisture was measured within 24 hours of previous precipitation from May 22 - July 11, 1976. For the remainder of the program, surface readings followed the same schedule as the depth readings.

Relative humidity was measured at 0900 hrs. MST. Spot measurements were effected at G plot, while points were taken from the thermohygrograph charts. These chart readings are probably not very accurate due to calibration difficulties. The data will be reviewed briefly in Chapter IV.

Plate 3.21. Evaporation pan (foreground) and rain gauge.

3.3.7 Supplementary Measurements

Additional data were obtained from a neighbouring large barley field, September 5 - 10, 1976 (Plate 3.22). The barley had reached maturity, and had very few weeds. Net radiation, albedo, and soil heat flux were measured continuously (Plate 3.23). Surface soil moisture was measured September 5 and 10. Concurrent moisture data were obtained at B and G plots, and at a grass area midway between B plot and the large barley field.

Plate 3.22. Large barley field. P site is at the upper left. Instruments and recorder shelters are on the right.

Plate 3.23. Albedo and net radiation instruments on large barley field. PS and S plots are on the right. The lab building is on the left.

CHAPTER IV

GENERAL CLIMATE AND FIELD OBSERVATIONS

4.1 Introduction

This chapter deals with general climate and field conditions obtained before and during the field program. Climate parameters to be discussed are air and soil temperatures, precipitation, evaporation, and sunshine hours. Current trends are compared with previous data collected over the past 12 years at Ellerslie. Changes in soil moisture and vegetation characteristics during the growing season are described.

Soil temperature data comparisons are for the four year period 1970 - 1973 instead of the 12 year period. This is due to the relatively incomplete stage of the tree plots' canopy development before 1970, and the lack of data for 1974.

Relative humidity is briefly discussed in Section 4.2.6. Data comparisons are for the study period only.

4.2 Twelve Year Mean Climate Conditions

4.2.1 Air Temperature

Mean annual air temperature for Ellerslie was 1.4°C. Monthly values ranged from -17.7°C in January to 16°C in July. Mean monthly values below 0°C have been

recorded from November to March (Fig. 4.1), and individual negative monthly values have occurred twice during April. Seasonal change appeared to be fairly regular, although deviations could be seen in March and September, both of which appeared slightly cooler than might have been anticipated.

Winter monthly means were highly variable. December had recorded values of -5.5°C and -21.3°C, while extremes for March were 0.7°C and -11.5°C. During the summer months, however, temperatures were more consistent. July, for example, had recorded extreme values of 14.0°C and 17.7°C.

Since the available data cover a short time period, winter mean monthly temperatures should only serve as rough approximations, rather than useful mean values. Due to the wide range of individual values, a larger sample size is required before means can be calculated with confidence. Summer mean monthly temperatures are more reliable, however, because their ranges of individual values are small.

4.2.2 Precipitation

Definite wet and dry seasons are evident in the mean monthly precipitation curve (Fig. 4.1). Mean annual precipitation was 454.7 mm, but 53% occurred during the June - August period, with an additional 16% recorded during the "shoulder" months of May and September. Monthly

FIG. 4.1: MONTHLY TEMPERATURE AND PRECIPITATION

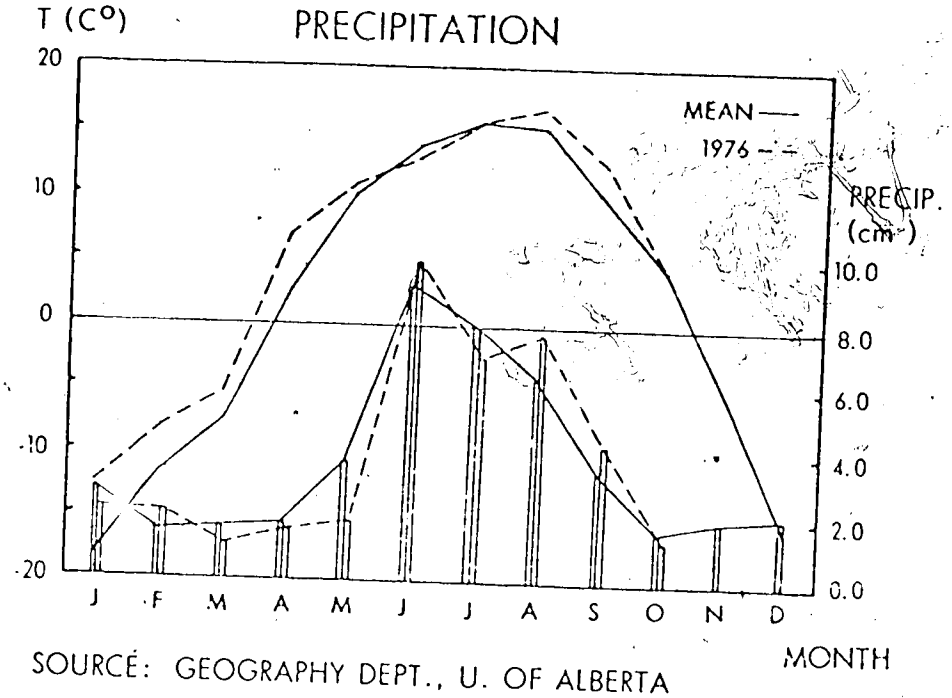

SOURCE: GEOGRAPHY DEPT., U. OF ALBERTA

FIG. 4.2: MONTHLY SUNSHINE HOURS

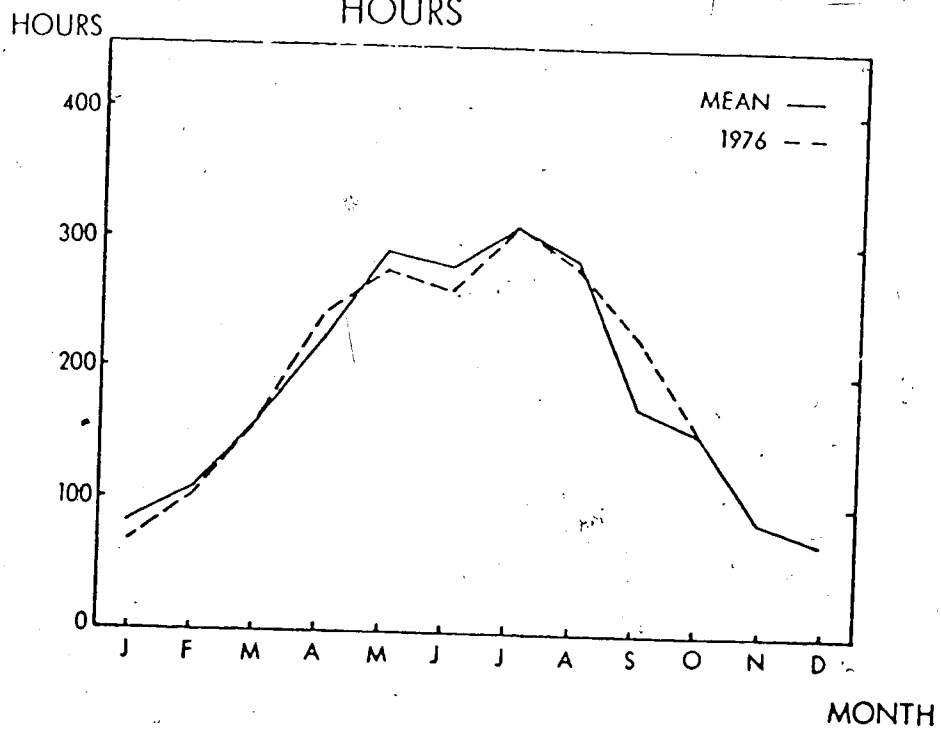

SOURCE: GEOGRAPHY DEPT., U. OF ALBERTA

values varied considerably from year to year, especially during summer. February, the driest month, averaged 16.4 mm, and recorded extreme values of 2.6 mm and 34.3 mm Extreme values for the wettest month, June, were 23.5 mm and 176.4 mm Longer records are therefore required before true monthly means can be obtained, but the data are sufficient to serve as rough approximations with which data for 1976 may be compared.

4.2.3 Sunshine

Mean monthly sunshine hours varied from 72.1 hours in December to 310.7 hours in July. The most striking feature of the sunshine hours distribution curve (Fig. 4.2) was the comparatively low value for June, which, as the month of greatest daylength, would be expected to exceed values for July, May and August. The cause for this decline becomes readily apparent upon examining the precipitation distribution. High precipitation values also appear to affect September's sunshine input, when compared to October's; October's values were higher 5 out of 12 years.

As with the aforementioned parameters, mean sunshine values varied considerably from year to year. Extreme values for December were 50.2 and 92.3 hours, while for July, they were 247.1 and 348.7 hours. However, June's position with respect to July was fairly consistent, since

it had the lower value 10 out of 12 years. For May and August, there was more variability, as June exceeded their totals 5 and 4 times respectively. Although there is some variability in mean monthly sunshine hours, the rankings of the months are more consistent (May and October are exceptions), and make a reasonably valid basis for comparison with 1976 values.

4.2.4 Soil Temperatures

20 cm soil temperatures at G plot were warmest overall, especially during summer (Fig. 4.3), with an annual mean of 6.2°C (Table 4.1). S is coldest at 5.1°C, due to cooler conditions in spring and fall. B and F were much colder than the other plots during winter, with B recording a temperature of -5.9°C in January. It is interesting to notice one common feature for the plots, namely that during the transition periods between hot and cold seasons (spring and fall), the plots reacted almost homogeneously, while during periods of consistent heating and cooling (summer and winter), their monthly mean temperatures diverged. For example, mean monthly temperature differences of 5.4°C and 3.0°C occurred in January and July respectively, but during May and October, the ranges of values between the plots were only 1.5°C and 1.2°C respectively. This indicates both the influence

FIG. 4.3: MEAN 20 cm SOIL TEMPERATURES
JAN. 1970-JUNE 1973

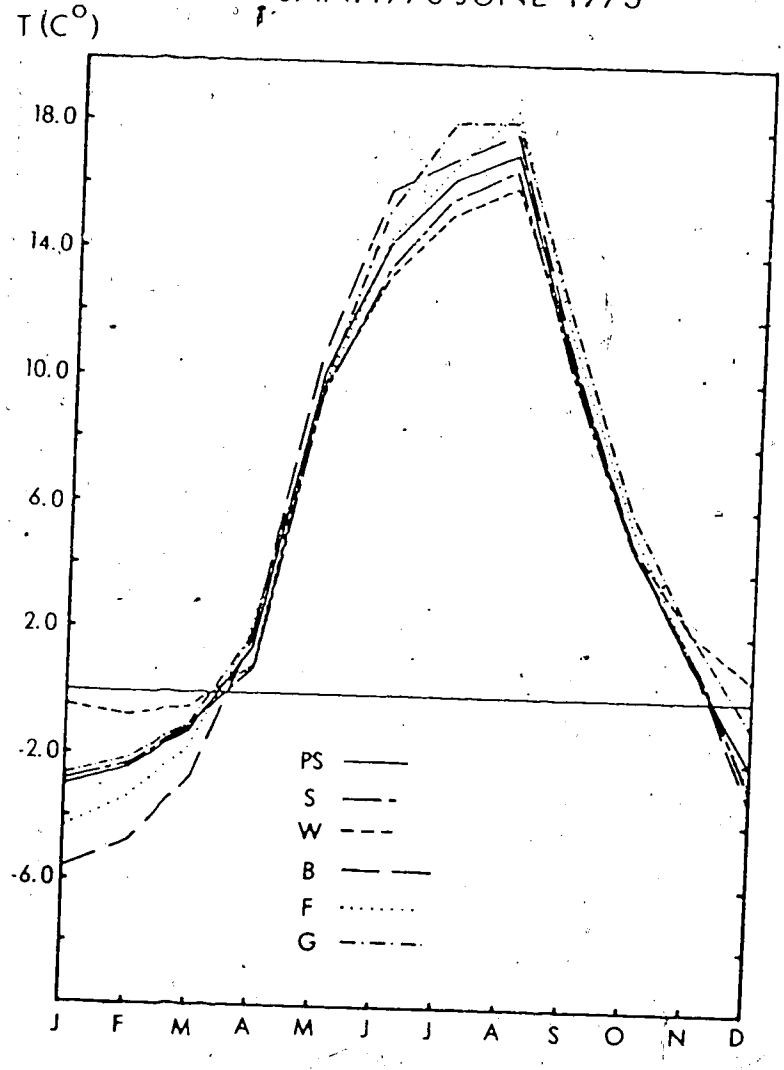

SOURCE: SOIL SCIENCE DEPT., U. OF ALBERTA

TABLE 4.1

MEAN SOIL TEMPERATURES (°C)

January, 1970 - June, 1973

	20 cm						100 cm					
	PS	S	W	B	F	G	PS	S	W	B	F	G
J.	-3.07	-2.96	[illegible]	-5.86	-4.51	-2.86	0.35	0.50	1.83	0.33	0.04	0.87
F.	-2.53	-2.[illegible]6	0.8[illegible]	-4.87	-3.50	-2.31	-0.14	0.22	1.17	-0.71	-0.68	0.17
M.	-1.19	-1.24	-0.49	-2.71	-1.96	-1.19	-0.07	0.25	1.01	-0.64	-0.50	0.01
A.	0.89	0.65	0.78	1.39	1.19	1.53	0.36	0.61	1.04	0.17	0.04	0.33
M.	9.89	8.96	9.58	10.50	9.21	9.46	4.07	3.97	5.11	4.07	2.83	4.54
J.	14.32	13.36	13.14	15.82	14.42	15.22	9.05	8.75	9.29	9.43	9.04	10.05
J.	16.05	15.64	15.13	16.87	16.54	18.05	11.54	11.41	11.46	12.02	12.15	13.00
A.	16.95	16.68	15.98	17.76	[illegible]8.61	18.24	12.80	12.85	12.63	14.15	14.46	14.59
S.	10.04	9.85	10.17	10.74	11.20	11.59	10.85	10.94	10.92	11.41	12.33	12.31

TABLE 4.1 (con't.)

	20 cm						100 cm					
	PS	S	W	B	F	G	PS	S	W	B	F	G
O.	4.78	4.65	5.02	4.61	5.15	5.83	7.22	7.54	7.33	7.78	7.98	8.11
N.	0.81	1.02	1.98	0.81	0.69	1.98	4.30	4.72	4.83	5.04	4.44	5.28
D.	-2.18	-2.91	0.46	-3.04	-2.74	-1.11	1.70	2.00	3.02	2.44	1.61	2.54
Mean	5.40	5.11	5.87	5.17	5.36	6.20	5.17	5.31	5.80	5.46	5.31	5.98
Rank	3	6	2	5	4	1	6	4	2	3	4	1

Source: Adapted from Soil Science Department records, U. of Alberta.

of changing general weather conditions on the micro-climate of each plot, and the ability of each surface cover to modify its own micro-climate during periods of more stable weather. In other words, these covers can exert some influence on their 20 cm soil temperatures if general weather conditions remain relatively stable for a prolonged time period, such as 2 - 3 months.

These mean values, however, were calculated from only 3 1/2 years of records, and cannot be considered long term means. It is more difficult to examine soil temperatures than air temperatures over a short period because of the influence of general weather conditions, overlying cover, and the soil itself, especially its moisture level, which may not be the same from one year to the next. However, as with other parameters, the months maintained similar ranks during the entire period. The exceptions are July vs. August and December vs. January. These are respectively the periods of maximum and minimum temperatures. This is an indication that the time of occurrence of annual extreme values is not consistent.

At 100 cm, the influence of general weather and surface conditions on soil temperatures is somewhat reduced, and the seasonal changes are less pronounced than at the shallower depths. Mean values below freezing occurred only on F, B, and PS plots (Fig. 4.4), while G and S plots recorde brief periods of below 0°C temperatures.

FIG. 4.4: MEAN 100 cm. SOIL TEMPERATURES
JAN. 1970-JUNE 1973

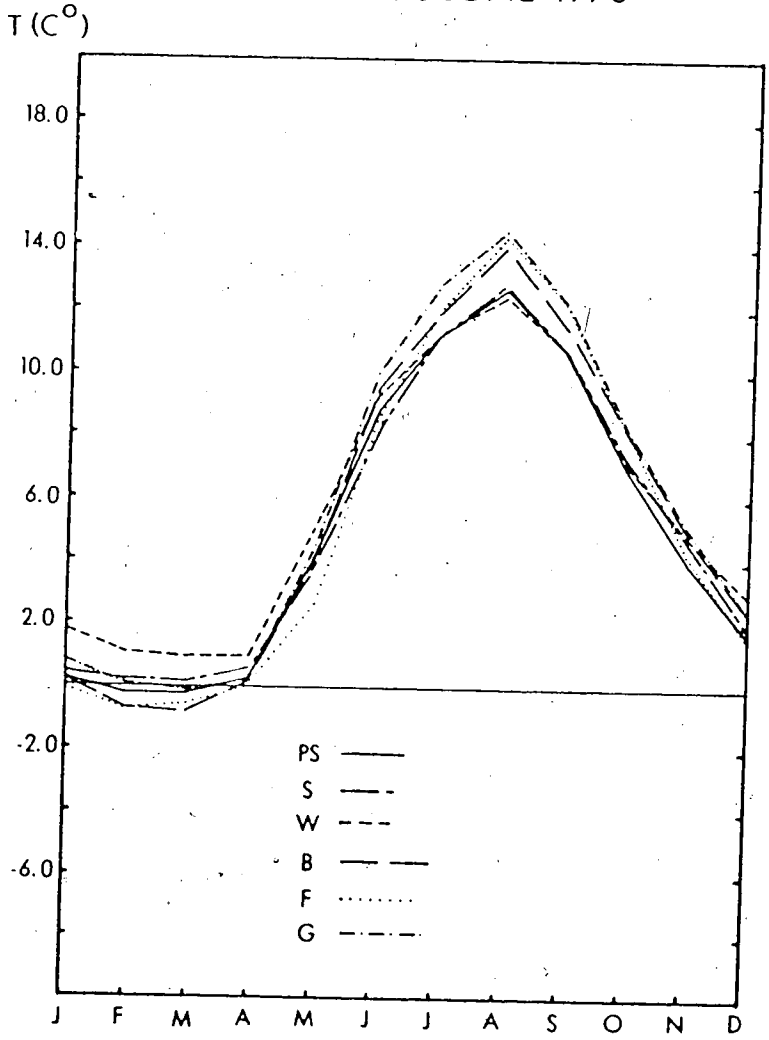

SOURCE: SOIL SCIENCE DEPT., U. OF ALBERTA

W has yet to record freezing temperatures at this depth. As with the 20 cm curve, the 100 cm curve showed some divergence of values during winter and summer. However, major variations could also be seen in May, while April appeared to show a reduction in temperature range. Annual means varied from 5.2°C for PS to 6.0° C for G (Table 4.1), resulting from much warmer monthly values for G during late summer and much of autumn.

The time of occurrence of annual maxima and minima at the 100 cm depth was more consistent than at shallower depths. At Ellerslie, the months were August and February, respectively, with the exception of W and G plots, where the minimum occurred in March. In fact, monthly ranks were more consistent here than at 20 cm for all 6 plots. This curve also reflects the time lag that commonly exists between surface weather events and their resulting effects at depth.

One may note that mean annual soil temperatures exceeded mean annual air temperatures by more than 4°C. It is apparent that the cause of this divergence was the winter situation, and the insulating qualities of the overlying snow and vegetation cover on the soil. Means calculated for G (used since air temperatures were recorded over G) during the November - March and May - September periods are shown in Table 4.2, along with mean air temperatures for these periods. The difference

TABLE 4.2

WINTER AND SUMMER MEAN AIR AND SOIL TEMPERATURES FOR G PLOT

	Air	20 cm.	100 cm
Nov. - March	-11.73°C	-1.10°C	1.77°C
May - Sept.	13.45°C	14.52°C	10.90°C

in winter temperatures was greater than 10°C at these depths, and it is anticipated that similar conditions exist within the tree plots as well.

Although it will be difficult to make valid comparisons between the above means and 1975 - 1976 values, the monthly rankings and time of minimum and maximum temperatures can be used as guides for later commentary.

4.2.5 Pan Evaporation

A 6 year mean was calculated from data for 1969, 1971 - 73, and 1975 - 76 data. There are data missing for May, 1972 and 1975, June, 1975, and September, 1971 and 1972, and no readings were ever taken during April or October. At best, these data provide a very rough first approximation, rather than a usable mean, so only a cursory examination will be given.

May recorded the highest monthly mean value, 6.39 mm/day (Fig 4.5). Steadily declining values occurred during the remainder of the summer. This could be indicative of more humid conditions during summer, while September would show lower values because of its cooler temperatures.

FIG. 4.5: EVAPORATION
CLASS 'A' PAN

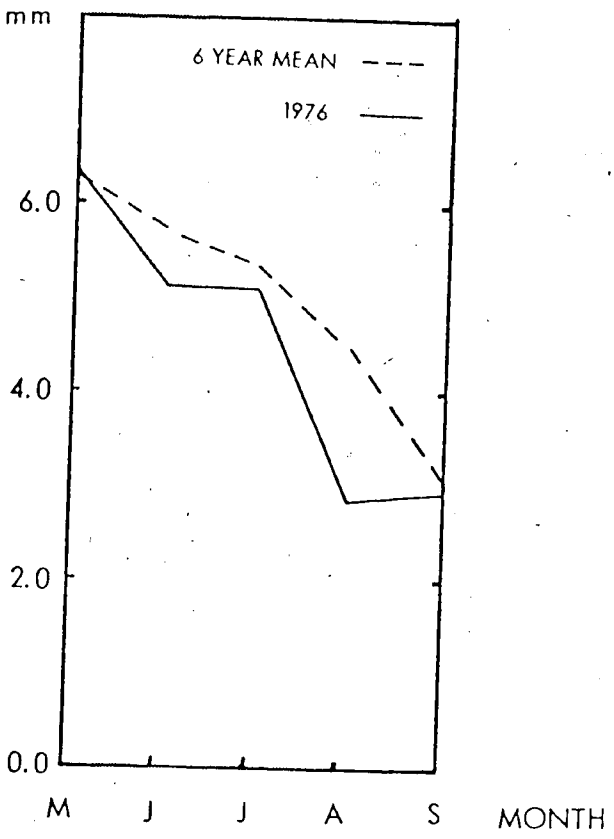

SOURCE: GEOGRAPHY DEPT., U. OF ALBERTA

4.2.6 Relative Humidity

Weekly mean values for relative humidity are listed in Table 4.3a. Regression values (Table 4.3b) for temperature are listed for comparative purposes and will be discussed later. Relative humidity values for PS, S, and P are probably not very accurate, but they can be compared to one another on the basis of thermohygrograph calibrations (Appendix 1) effected after termination of the field program. Since correlations and standard errors are similar, it can be assumed that the calibrations reflect the instrument error with reasonable accuracy. Although the magnitude of the error is uncertain, the direction (positive or negative) is consistent.

The slopes and intercepts indicate that PS is the most humid, and P, the least humid plot. There is a large spread in slope values, indicating that relative humidity differences between the three can be substantial. Since the temperature slopes do not vary in the same manner, temperature alone cannot account for these differences. Therefore, stand structure and density, and their effects on evapotranspiration, should be considered as important factors.

4.2.7 Overall Assessment

The 12 year Ellerslie records indicate a climate

TABLE 4.3a

WEEKLY MEAN TEMPERATURE (°C)

AND R.H. (%)

	G		PS		S		P	
DATE	T	RH	T	RH	T	RH	T	RH
5/19	12.6	41.7	10.6	54.9	11.1	49.4	-	-
26	13.1	58.3	11.6	61.0	12.4	51.0	12.7	46.3
6/	12.0	53.9	11.3	51.7	12.1	47.0	12.2	43.7
9	11.6	63.4	11.1	64.4	12.1	63.6	11.6	49.4
16	13.9	64.0	13.2	62.4	14.1	62.0	13.7	49.9
23	13.9	61.9	13.4	60.1	14.3	56.4	13.9	46.0
30	12.1	79.7	11.6	76.4	12.1	64.9	12.0	57.0
7/7	16.4	60.6	15.7	60.3	16.4	51.7	16.0	51.6
14	17.1	72.4	16.3	71.1	17.6	64.1	16.8	61.3
21	16.9	75.1	16.2	60.0	17.6	61.6	16.9	50.0
28	15.6	55.4	15.1	56.3	16.4	53.6	15.9	50.0
8/4	17.4	83.3	16.6	80.4	17.2	72.3	17.0	64.1
11	17.9	79.4	17.0*	81.4	18.0*	70.8	17.5*	62.1

TABLE 4.3a (con't.)

	G		PS		S		P	
	T	RH	T	RH	T	RH	T	RH
8/18	18.7	69.6	18.2	72.0	18.5	60.4	18.4	53.6
25	15.3	74.4	14.3*	74.3	15.3*	60.5	15.3*	54.0
9/1	13.9	74.3	13.1*	76.4	14.6*	63.5	14.2*	55.9
8	12.0	75.6	11.2*	66.7	11.7*	60.0	11.9	54.7
15	11.5	76.4	11.1	73.3	11.1	70.7	11.3	60.1
22	13.1	77.1	12.6	70.9	12.6	69.0	12.2	62.1
29	13.4	80.7	12.9	73.6	13.2	77.3	13.4	59.1
10/6	7.0	66.0	6.6	64.0	6.7	65.0	7.3	55.6

* Estimate partially based on thermohygrograph data.

TABLE 4.3b

REGRESSION OF MEAN WEEKLY

TEMPERATURE (°C) AND RH. (%)

Plots	Slope	Intercept	S.E.	r	r^2	SIG	N
			Temperature				
G vs PS	0.99	-0.6	0.4	0.99	0.98	0.00001	21
G vs S	1.06	-0.9	0.5	0.99	0.97	0.00001	21
G vs P	0.96	0.4	0.3	0.99	0.99	0.00001	20
			RH.				
G vs PS	0.69	19.7	4.4	0.86	0.75	0.00001	21
G vs S	0.64	17.7	4.3	0.85	0.73	0.00001	21
G vs P	0.56	15.3	3.3	0.84	0.71	0.00001	20

of cold dry winters and mild moist summers, with rapid transition periods. High summer precipitation is further reflected in the low values for sunshine hours in June, and for pan evaporation in middle and late summer.

Soil temperature records indicate that consistent differences between the plots have already developed, with values diverging in winter and summer, while surface covers appear to have little effect during the transition months of spring and fall.

4.3 June, 1975 - April, 1976

The 11 month period preceding the start of the field program was warmer and drier than the mean conditions described above. Ten months had below mean precipitation, especially the September - November period and the months of January and March, all of which recorded values rarely exceeding 65% of the 12 year mean. It was the second driest September on record (4.4 mm) at the station, and the winter precipitation as a whole (November - March) was 20% below normal.

Temperatures were close to normal during the summer, but were consistently above the mean from November - April. January and April both recorded new monthly absolute maximum values. Sunshine hours were close to normal, except for November, which exceeded mean values by 50%. Evaporation

data were incomplete, but showed mean conditions for July, and below mean for August and September. Soil temperature extremes were recorded in July for all 6 plots at 20 cm depth (Fig. 4.6). However, as a result of the mild winter, minimum values were reached in December, except on the S plot which recorded its lowest monthly temperature in January. S plot was by far the coldest, and was the last one to thaw during spring. This was also true at 100 cm (Fig. 4.7). The difference between S and the warmest summer plots, G and F, exceeded 5°C at times, while during winter, S was more than 2°C colder than W at 100 cm, and 5°C colder at 20 cm.

) cm depth temperature extremes were reached during August and March for most plots. Although W and B had their maxima in July, the time difference is not considered significant, since their values were only marginally above August values. The colder conditions for March as opposed to February, were probably a consequence of the dry winter, which reduced the snow cover, and so allowed the winter cold to penetrate to greater depths.

Mean values for the period reveal that G and S plots were warmest and coldest respectively (Table 4.4). This is quite similar to mean conditions. Although PS remained much colder than the open plots, PS plot's 100 cm mean temperatures were somewhat higher than S because of milder winter temperatures. Snow cover was probably a factor,

FIG. 4.6: 20 cm SOIL TEMPERATURES
JUNE 1975-SEPT. 1976

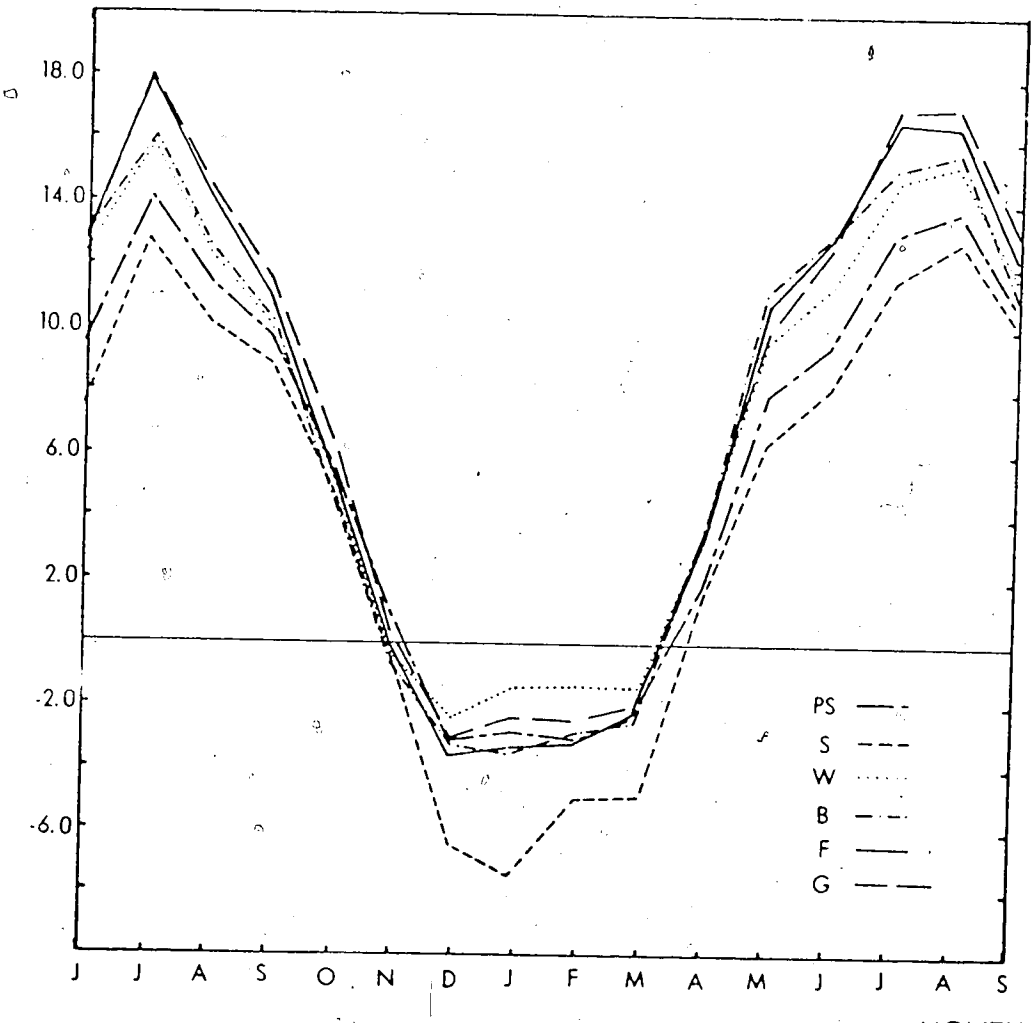

SOURCE: SOIL SCIENCE DEPT., U. OF ALBERTA

FIG. 4.7: 100 cm SOIL TEMPERATURES
JUNE 1975-SEPT. 1976

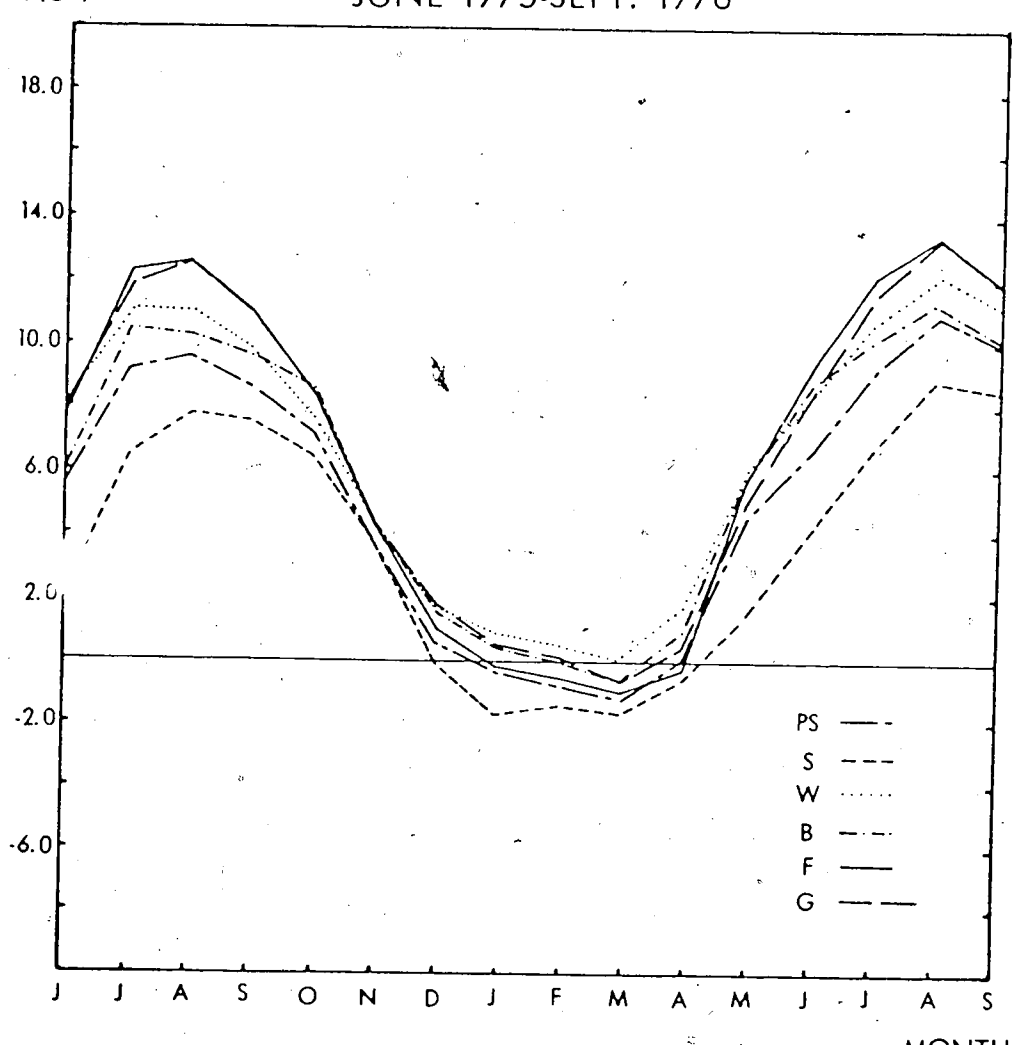

SOURCE: SOIL SCIENCE DEPT., U. OF ALBERTA

TABLE 4.4

1975 - 1976 SOIL TEMPERATURES (°C)

	20 cm						100 cm					
	PS	S	W	B	F	G	PS	S	W	B	F	G
1975												
J.	9.55	7.55	12.44	13.00	13.05	12.67	5.61	1.94	8.05	6.11	7.67	7.72
J.	14.11	12.83	15.72	16.00	17.78	17.89	9.22	6.39	11.22	10.39	12.17	11.94
A.	11.33	10.22	12.39	12.50	14.71	14.55	9.61	7.78	11.11	10.33	12.50	12.44
S.	9.72	8.89	9.83	10.22	11.11	11.72	8.72	7.55	9.78	9.61	10.89	10.94
O.	5.83	5.06	5.28	4.78	5.56	6.44	7.11	6.55	7.67	7.67	8.44	8.61
N.	0.50	-0.11	-0.28	-0.72	0.00	0.39	3.72	3.78	4.11	4.22	4.44	4.72
D.	-3.11	-6.44	-2.44	-3.33	-3.61	-2.61	0.56	-0.11	1.39	1.50	1.06	1.67
1976												
J.	-2.83	-7.50	-1.72	-3.56	-3.39	-2.33	-0.50	-1.67	0.78	0.39	-0.28	0.50
F.	-2.94	-4.94	-1.28	-2.89	-3.17	-2.44	-0.89	-1.50	0.50	0.00	-0.56	0.00
M.	-2.39	-4.89	-1.33	-2.44	-2.39	-2.11	-1.11	-1.72	0.11	-0.50	-0.94	-0.50
*A.	1.83	1.56	3.28	3.33	2.89	3.44	0.17	-0.61	1.67	0.89	-0.28	0.44

* end of 11 month period.

TABLE 4.4 (con't.)

	20 cm						100 cm.					
1976	PS	S	W	B	F	G	PS	S	W	B	F	G
M.	7.89	6.39	9.67	11.22	10.89	10.00	4.50	1.39	6.00	5.94	5.67	5.06
J.	9.50	8.05	11.44	13.11	13.05	12.67	6.78	4.28	8.39	8.83	9.44	8.33
J.	13.05	11.78	14.72	15.22	16.61	16.94	9.22	6.94	10.83	10.33	12.33	11.67
A.	13.89	12.94	15.22	15.67	16.39	17.16	11.00	9.05	12.22	11.55	13.50	13.28
S.	10.67	10.17	11.50	11.05	12.11	12.83	10.05	8.72	11.22	10.39	12.00	12.00
11 month mean	3.78	2.02	4.72	4.26	4.72	5.24	3.84	2.58	5.13	4.60	5.01	5.32
11 month rank	5	6	2	4	2	1	5	6	2	4	3	1
summer mean	11.00	9.89	12.51	13.26	13.81	13.92	8.31	6.08	9.73	9.41	10.59	10.07
summer rank	5	6	4	3	2	1	5	6	3	4	1	2

Source: Soil Science Department, U. of Alberta

since the open hardwood canopy would allow more snow to reach the surface than the dense closed canopy of spruce, especially during a dry winter. F and G recorded highest summer temperatures at both depths, while W was the warmest winter plot. This is similar to previous years.

As the 1976 growing season approached, conditions were ripe for early planting. Soils were dry at the surface, snow cover had disappeared early, and buds had already formed on the poplars by April.

4.4 Climate and Field Conditions: April - October, 1976[1]

4.4.1 April - May

April recorded above mean monthly temperatures and sunshine hours, and normal precipitation values (Figs. 4.1 and 4.2). B plot was covered with last year's stubble. F plot was invaded by stinkweed (Datura stramonium), and there were weeds on W as well. Leaves began to appear on PS, P, and W, while G was still a yellow colour. Soil samples collected April 28 - 29 and examined gravimetrically for soil moisture, revealed extremely dry surface conditions under PS, S, and F plots, while P and W were quite moist at this level (Table 4.5). At depth, F had higher moisture contents than all the other plots, thereby

[1] All mean values discussed herein refer to those described in Section 4.2.

TABLE 4.5

GRAVIMETRIC SOIL MOISTURE

(% oven-dry weight)

April 28-29, 1976

	P1	P2	P3	PS	S	W	B	F	G
.1 m.	214*	230*	39	35	13	43	34	30	36
.2	86*	29	38	32	16	37	31	26	31
.5	27	30	28	17	13	21	27	19	20
.8	26	25	24	18	-	19	23	18	20
1.0	25	28	26	24	-	26	22	28	24

* The high values for P1 and P2 indicate the existence of peat layers.

providing an illustration of the usefullness of a fallow rotation for conserving soil water. PS had the lowest recorded values, but if data for S plot had been available below 0.5 m, it would probably have shown similar conditions, since this was the case at shallower depths.

The field program started in May, so data were available on air temperatures and soil moisture content for each plot. Temperatures recorded over G plot were used for the other open plots (W, B, and F), while the forested plots had their own screens. Open air temperatures were slightly above normal while sunshine hours were below normal. Weekly mean temperatures were calculated for P, PS, S, and G plots commencing on the 13th (Fig. 4.8, Table 4.3a), and they reveal a wide variation. PS was 2°C colder than G on the 19th, and the other plots were cooler by at least 0.5°C. Leaf cover on P and PS plots was complete by the third week. B plot was cultivated during the second week, and was then seeded. By May 27, sprouts as high as 8 cm had appeared. F plot was tilled and weeded while G was still somewhat yellow, with some dandelions (Taraxocum Dens-leonis) present.

Soil temperatures were below 0°C for S and F at 100 cm in April (Fig. 4.7). By May, all soils were thawed, but S was still registering a chilly 1.4°C at 100 cm, and 6.4°C at 20 cm. W and B were warmest at 100 cm, while B and F had high temperatures at the shallower depth. The

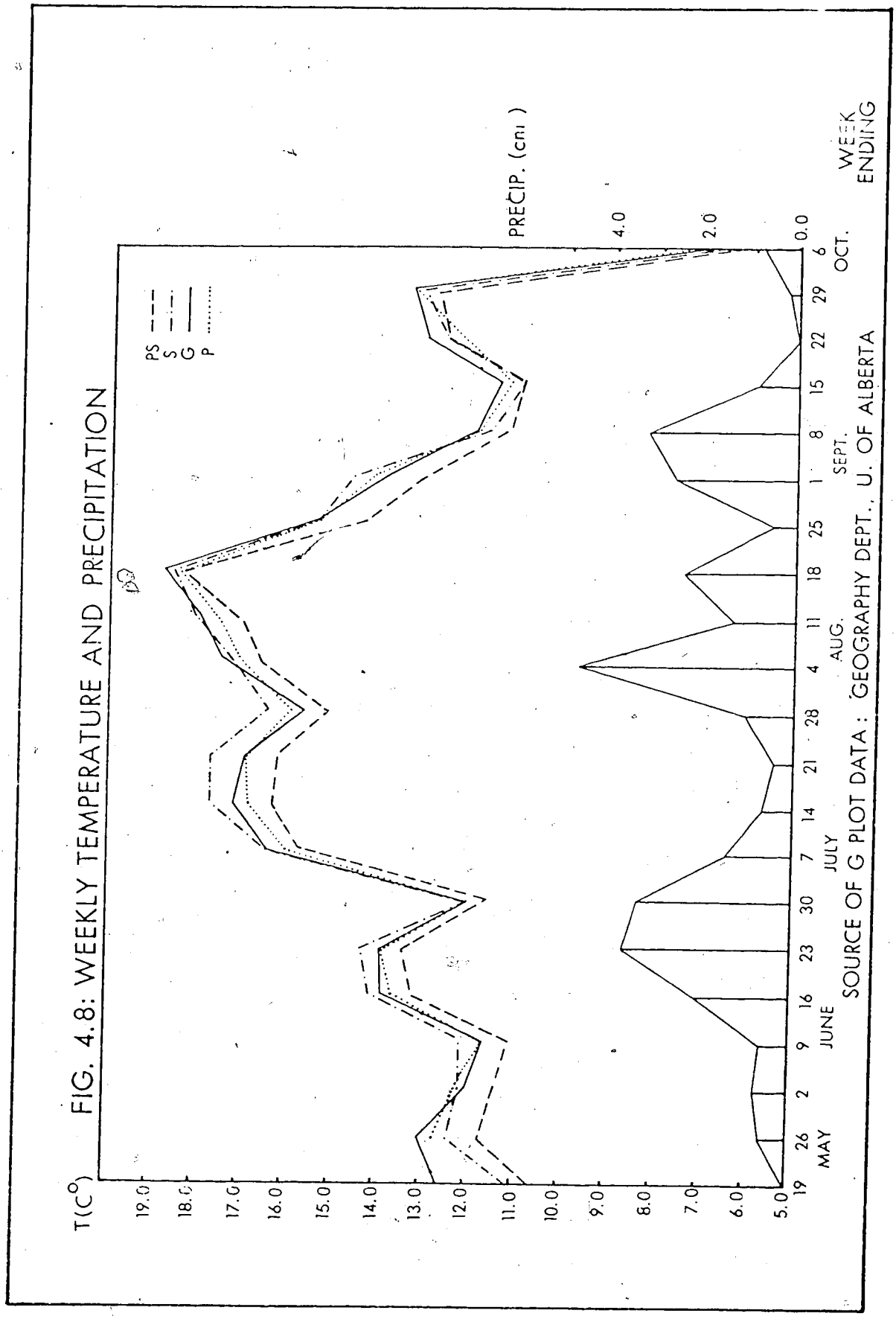
FIG. 4.8: WEEKLY TEMPERATURE AND PRECIPITATION
T(C°)
PRECIP. (cm)
PS
S
G
P
19.0
18.0
17.0
16.0
15.0
14.0
13.0
12.0
11.0
10.0
9.0
8.0
7.0
6.0
5.0
4.0
2.0
0.0
19 26 2 9 16 23 30 7 14 21 28 4 11 18 25 1 8 15 22 29 6
MAY
JUNE
JULY
AUG.
SEPT.
OCT.
WEEK ENDING
SOURCE OF G PLOT DATA : GEOGRAPHY DEPT., U. OF ALBERTA

only unusual aspect about this period is B's 100 cm temperature being higher than that for G, especially since their winter temperatures were similar.

Soil moisture levels for 0.1 m (Fig. 4.9) fluctuated drastically in response to rainfall and time of moisture measurement, but showed a general decrease during the first 3 weeks of May. This trend was reversed towards the end of the month due to increased rainfall. A general downward trend was apparent for all plots at 0.2 m, which is probably the best depth at which to examine week to week changes in moisture content (Fig. 4.10). Data for 0.5 m (Fig. 4.11) seem to indicate a lag time that is somewhat longer than at 0.2 m, but well within the time frame that this study covered. May values at this level showed a downward trend for P2, P3, W, and PS, while the other plots remained relatively stationary. These results are probably a consequence of the dry weather which occurred in April and early May. 0.8 m and 1.0 m (Figs. 4.12 and 4.13 respectively) generally showed little fluctuation, and were obviously not altered by short-term weather events.

There was little change in the plots' ranks during the period. The 3 P plots and W showed highest moisture contents at 0.1 m, with values ranging from 35 - 45 cm water m^{-1} soil (cm m^{-1}). S was definitely the driest at 23 cm m^{-1}. The order was similar at 0.2 m, but G was wetter than PS, B, and F, and almost as wet as W. Moisture

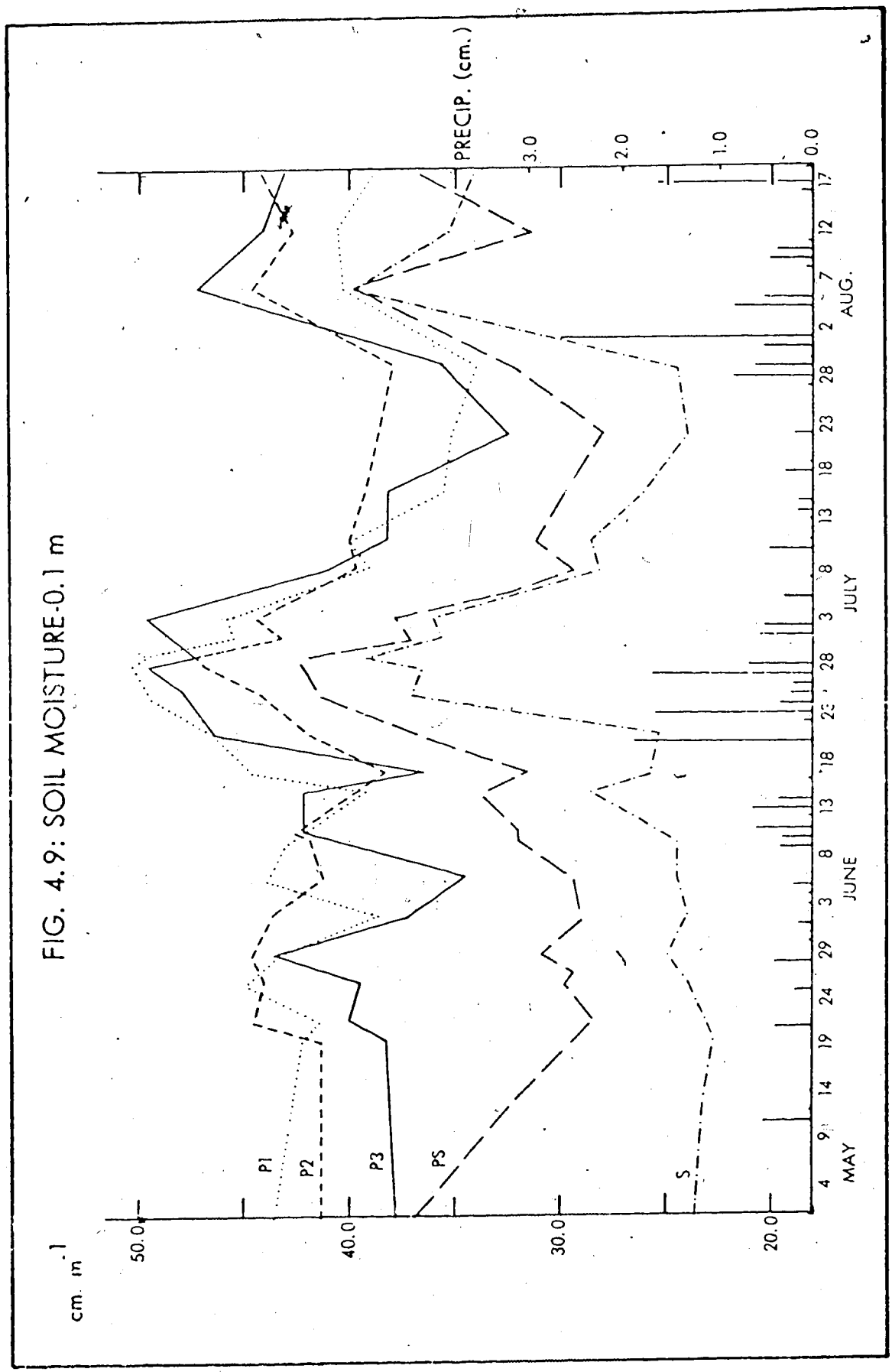

FIG. 4.9: SOIL MOISTURE-0.1 m

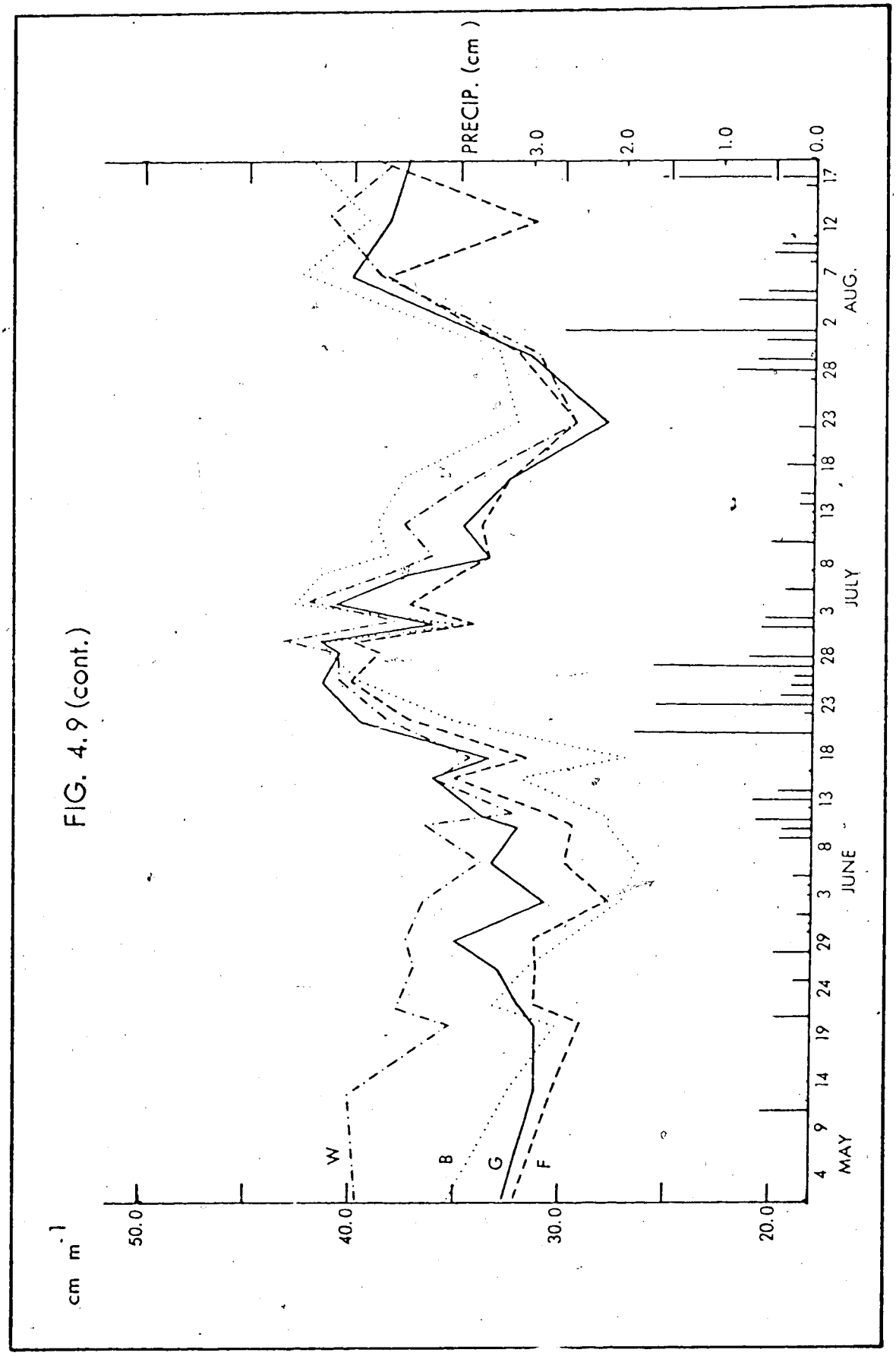
PRECIP. (cm)
3.0
2.0
1.0
0.0
cm m⁻¹
50.0
40.0
30.0
20.0
W
B
G
F
4 9 14 19 24 29 3 8 13 18 23 28 3 8 13 18 23 28 2 7 12 17
MAY
JUNE
JULY
AUG.

FIG. 4.9 (cont.)

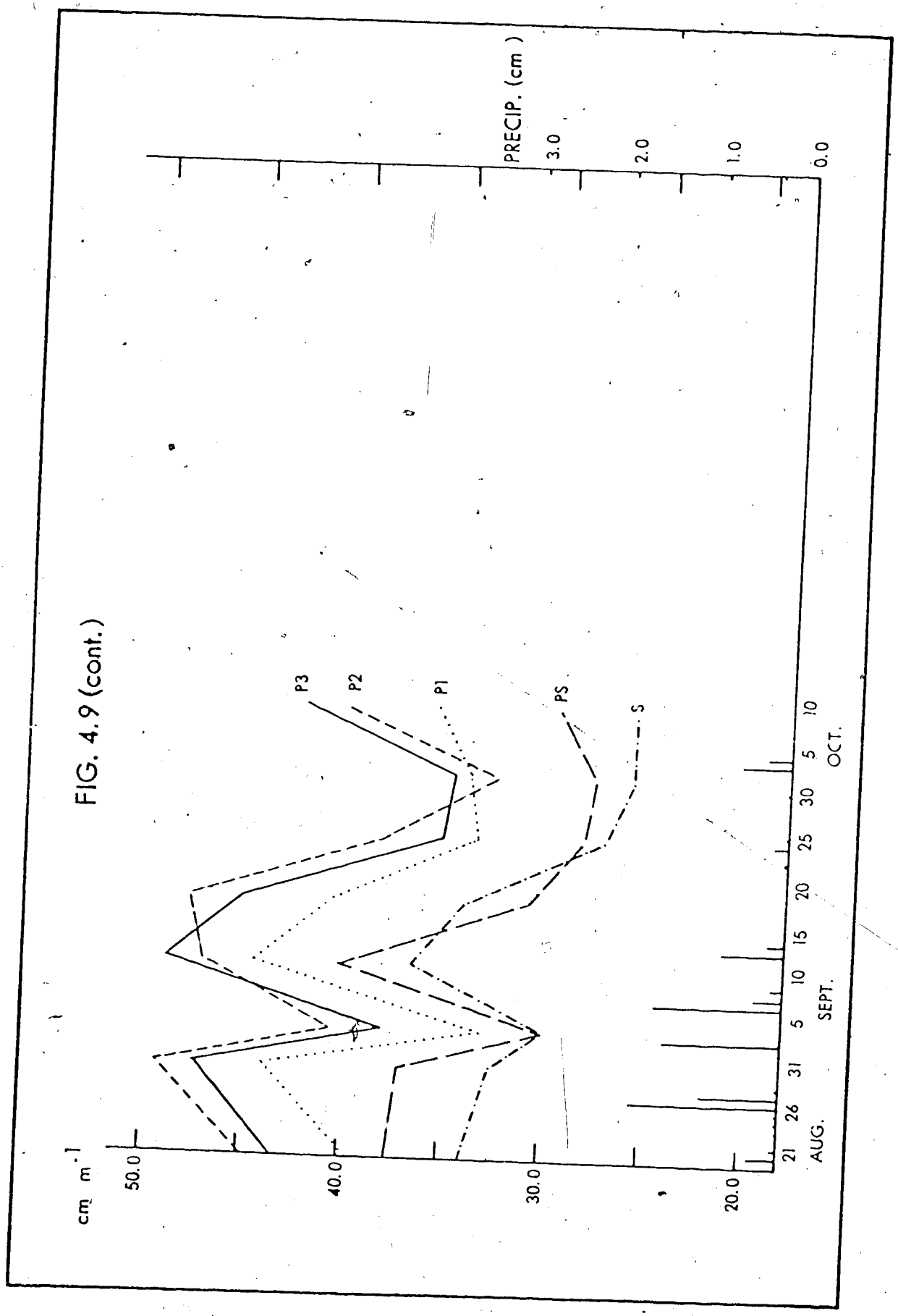
PRECIP. (cm)
3.0
2.0
1.0
0.0
P3
P2
P1
PS
S
cm m⁻¹
50.0
40.0
30.0
20.0
21
26
31
AUG.
5
10
15
SEPT.
20
25
30
5
10
OCT.

FIG. 4.9 (cont.)

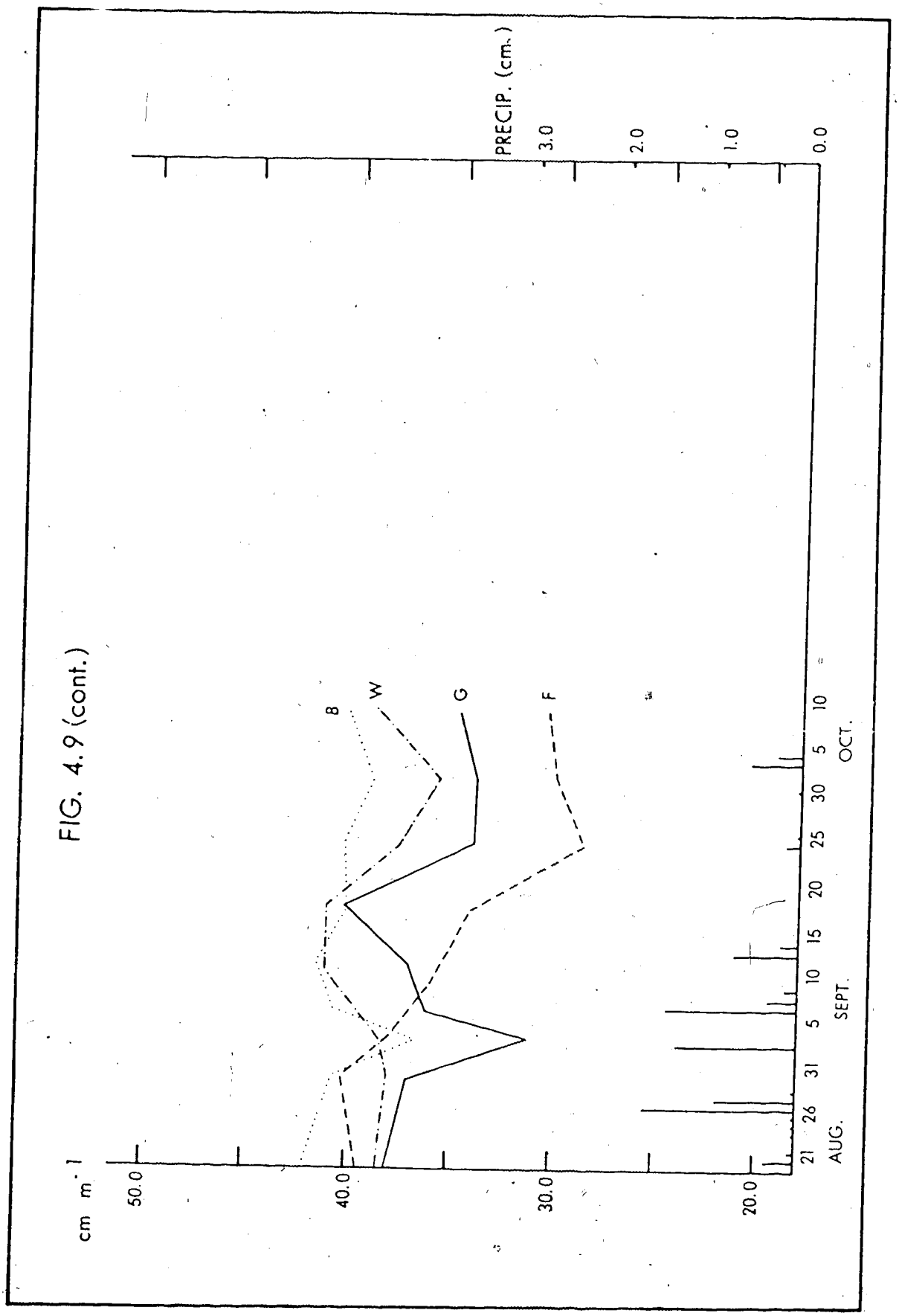
PRECIP. (cm.)
3.0
2.0
1.0
0.0
cm m⁻¹
50.0
40.0
30.0
20.0
B
W
G
F
21
26
31
AUG.
5
10
15
20
25
30
SEPT.
5
10
OCT.

FIG. 4.9 (cont.)

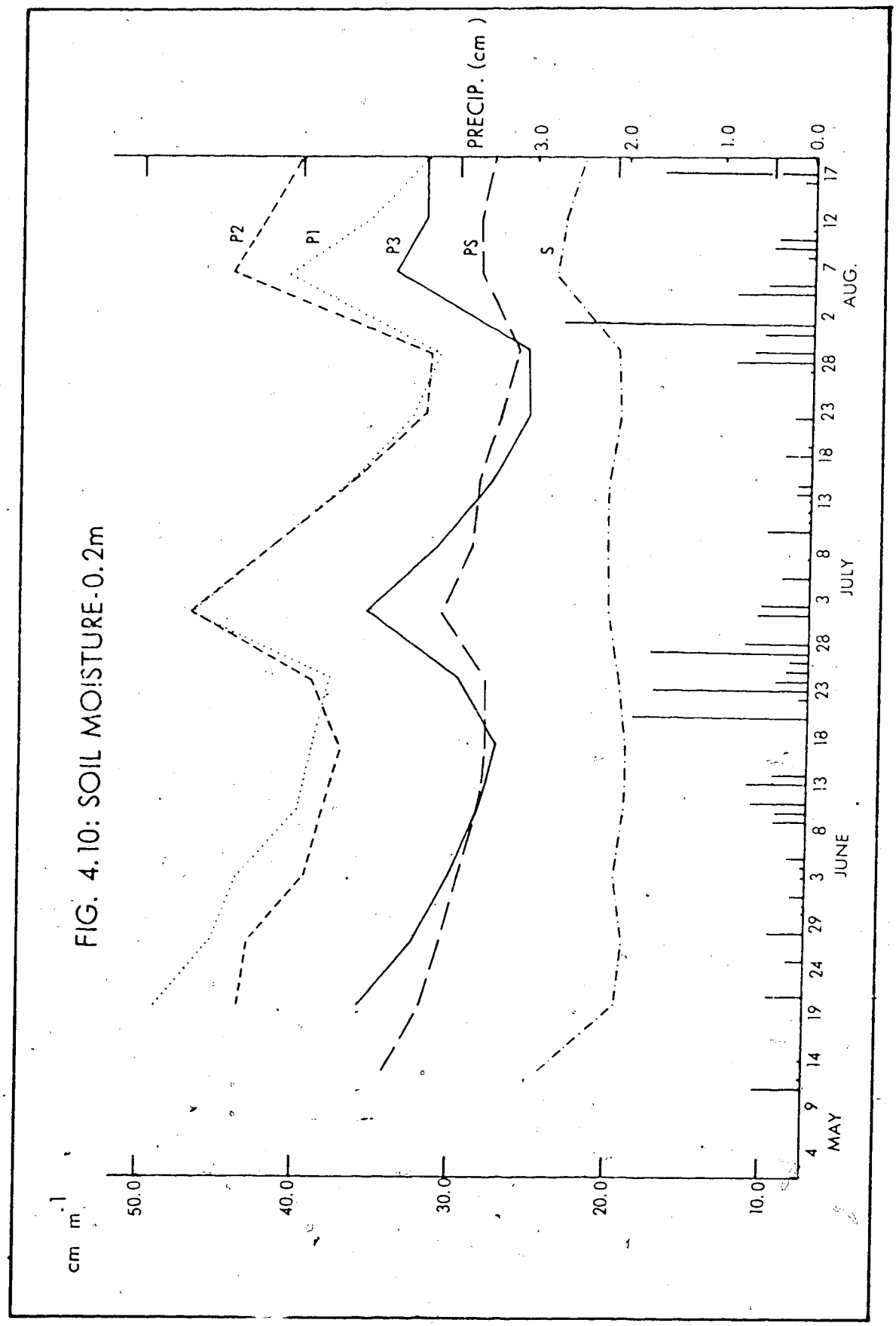

FIG. 4.10: SOIL MOISTURE-0.2m

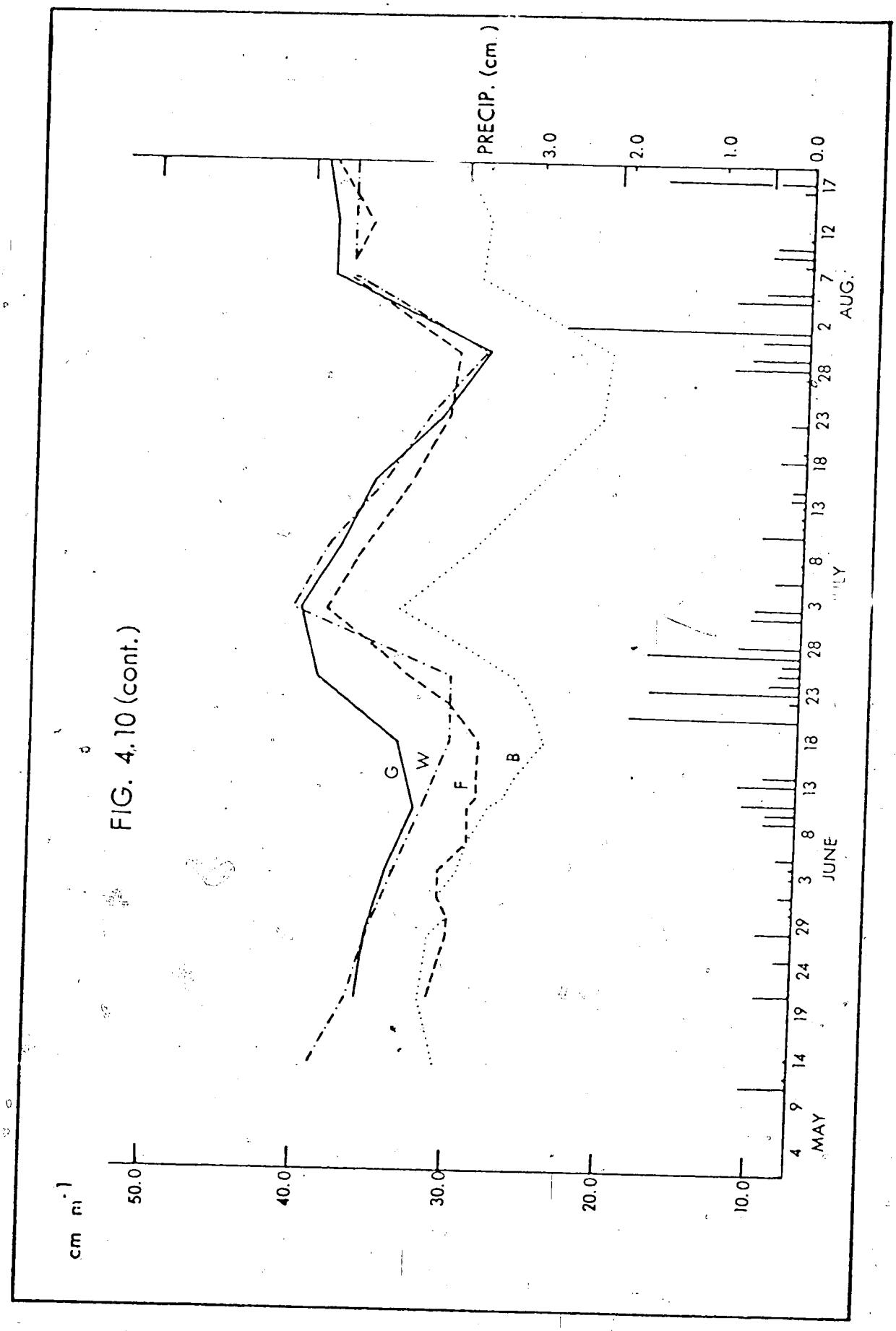
PRECIP. (cm)
3.0
2.0
1.0
0.0
cm ml⁻¹
50.0
40.0
30.0
20.0
10.0
G
W
F
B
4 9 14 19 24 29 3 8 13 18 23 28 3 8 13 18 23 28 2 7 12 17
MAY
JUNE
JULY
AUG.

FIG. 4.10 (cont.)

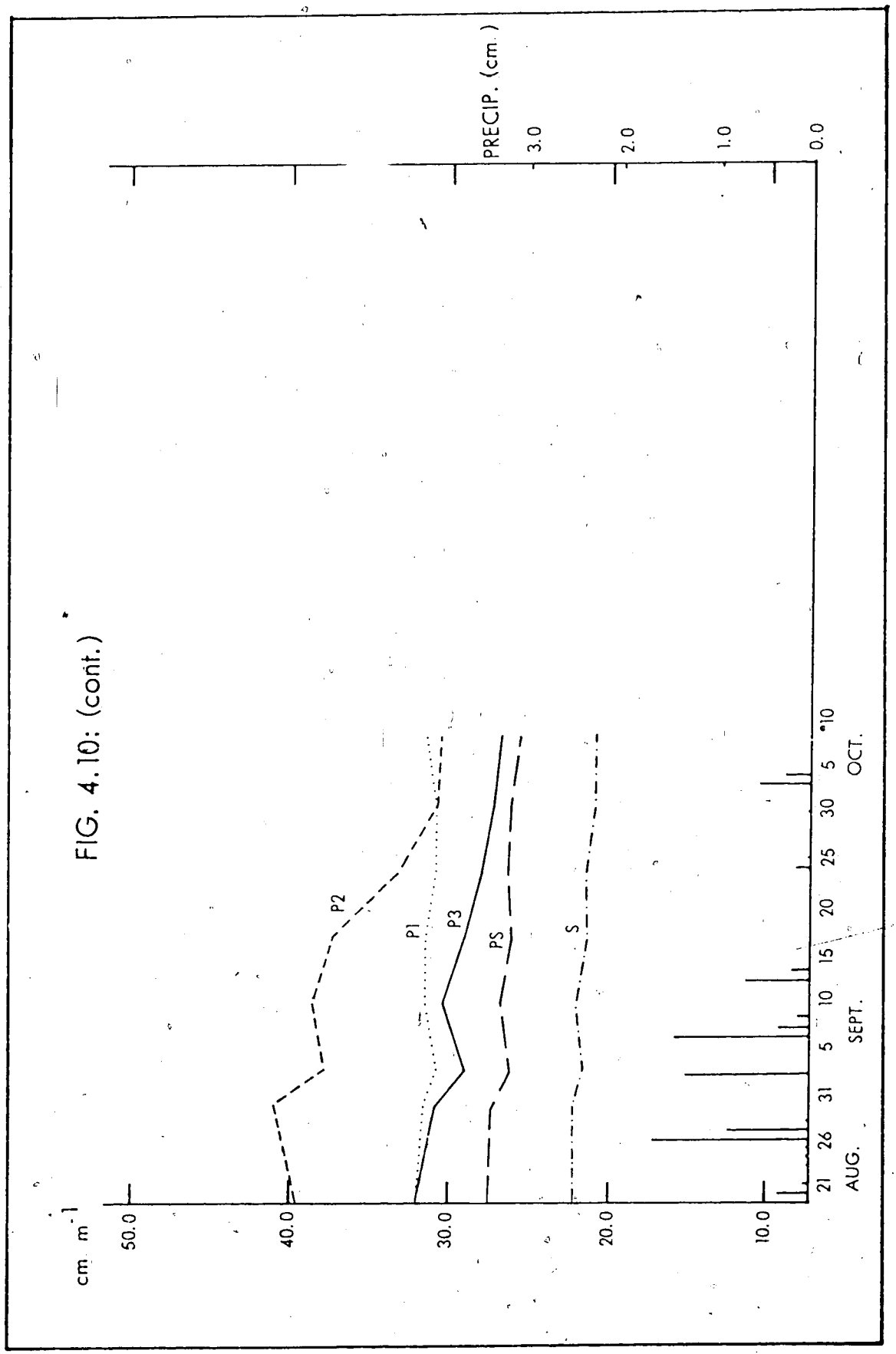
PRECIP. (cm.)
3.0
2.0
1.0
0.0
cm m⁻¹
50.0
40.0
30.0
20.0
10.0
P2
P1
P3
PS
S
21 26 31 5 10 15 20 25 30 5 10
AUG.
SEPT.
OCT.

FIG. 4.10: (cont.)

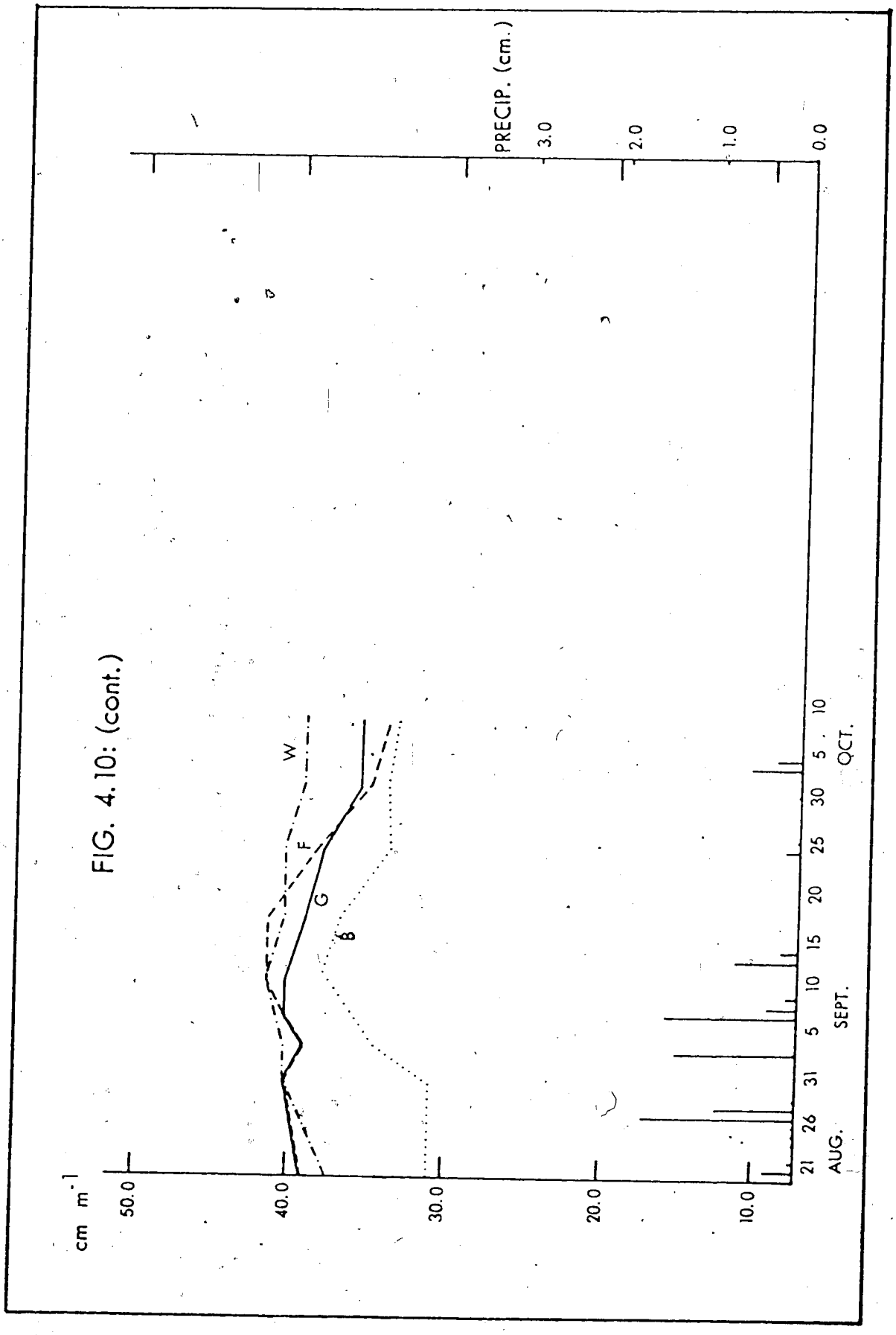
PRECIP. (cm.)
3.0
2.0
1.0
0.0
cm m⁻¹
50.0
40.0
30.0
20.0
10.0
W
F
G
B
21
26
31
AUG.
5
10
15
20
25
30
5
10
SEPT.
OCT.

FIG. 4.10: (cont.)

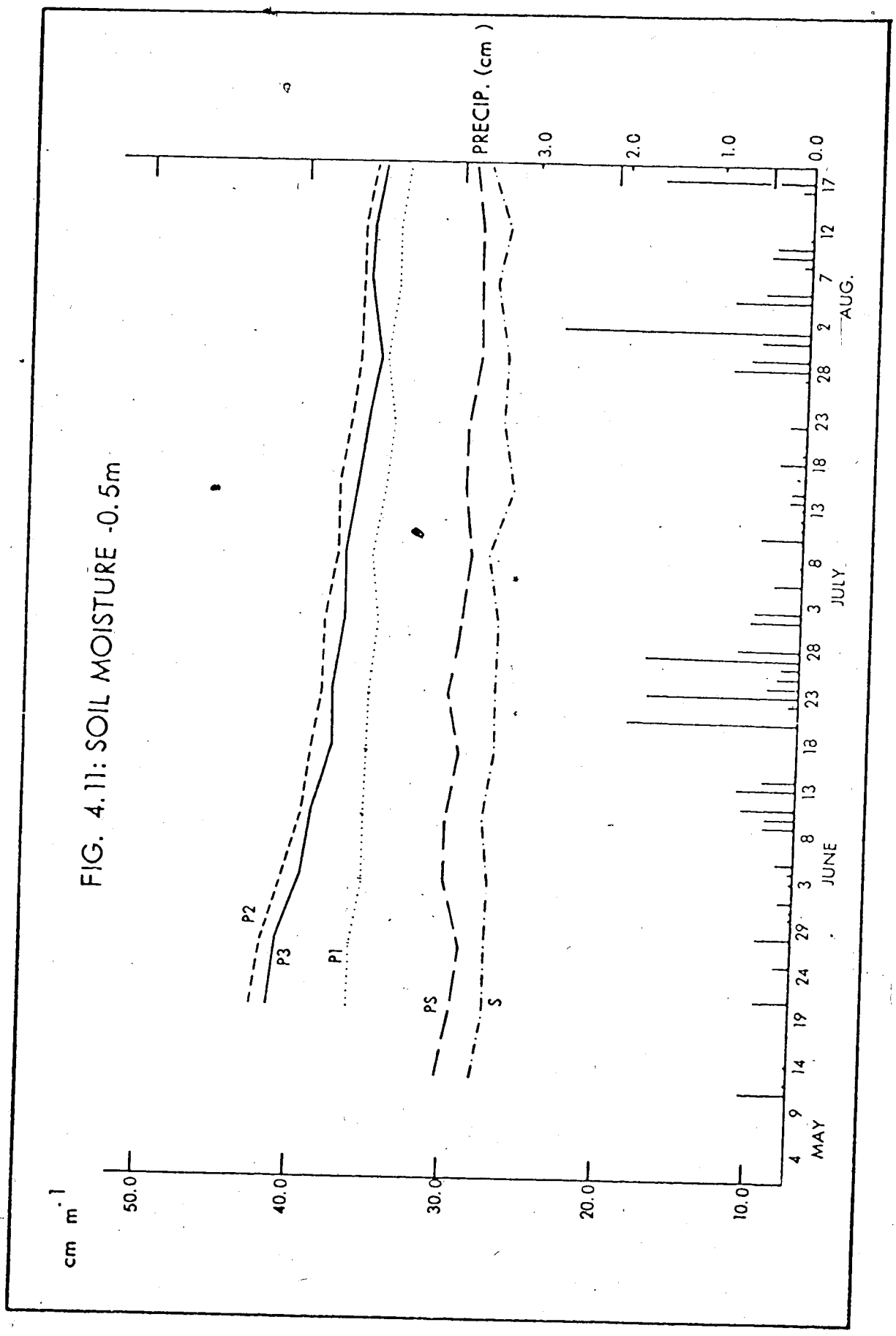
FIG. 4.11: SOIL MOISTURE -0.5m
cm m⁻¹
50.0
40.0
30.0
20.0
10.0
PRECIP. (cm)
3.0
2.0
1.0
0.0
P2
P3
P1
PS
S
4 9 14 19 24 29 3 8 13 18 23 28 3 8 13 18 23 28 2 7 12 17
MAY
JUNE
JULY
AUG.

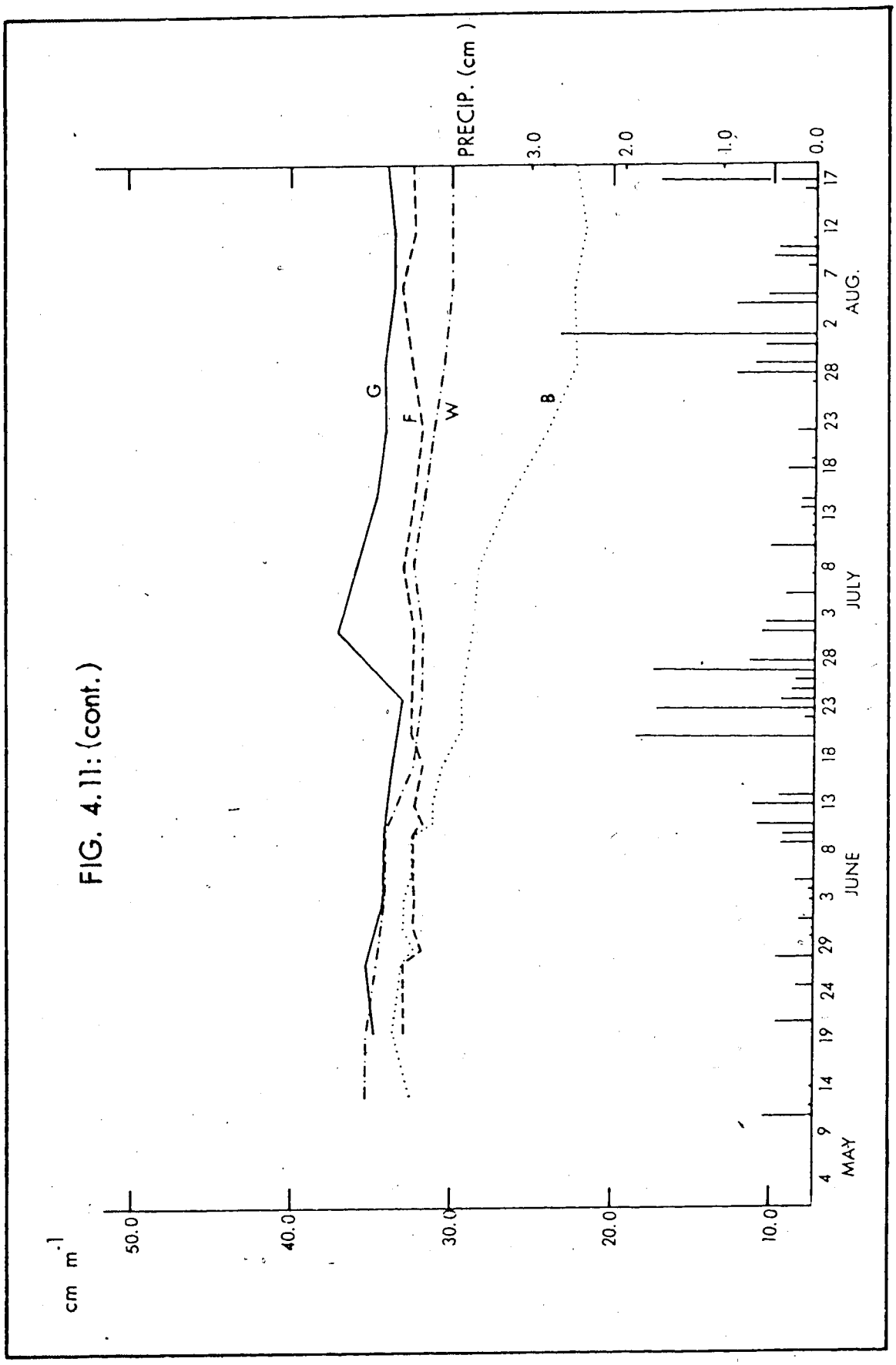
cm m⁻¹
50.0
40.0
30.0
20.0
10.0
PRECIP. (cm)
3.0
2.0
1.0
0.0
G
F
W
B
4 9 14 19 24 29 3 8 13 18 23 28 3 8 13 18 23 28 2 7 12 17
MAY
JUNE
JULY
AUG.

FIG. 4.11: (cont.)

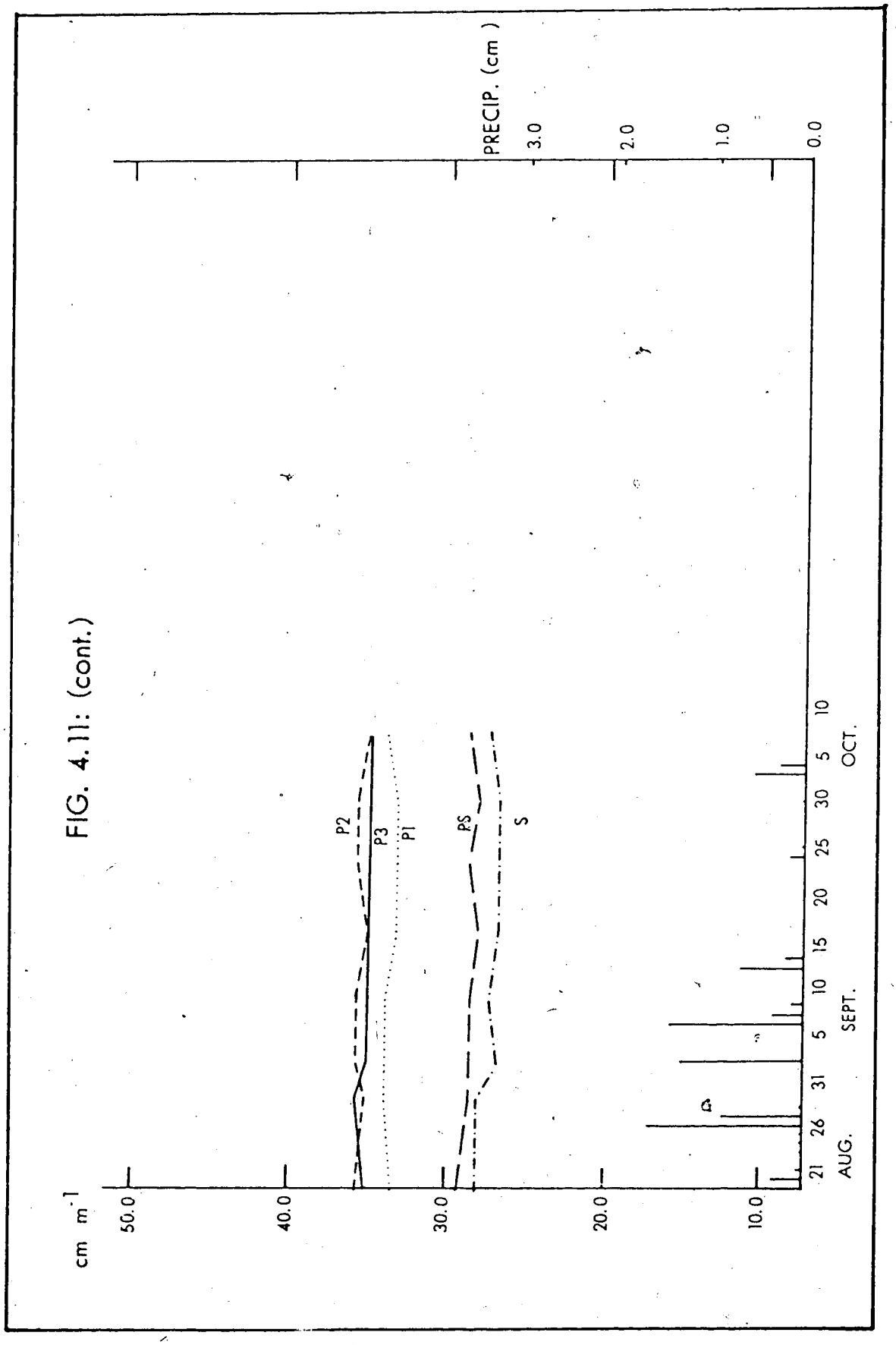
PRECIP. (cm)
3.0
2.0
1.0
0.0
cm m⁻¹
50.0
40.0
30.0
20.0
10.0
P2
P3
P1
PS
S
21 26 31 5 10 15 20 25 30 5 10
AUG.
SEPT.
OCT.

FIG. 4.11: (cont.)

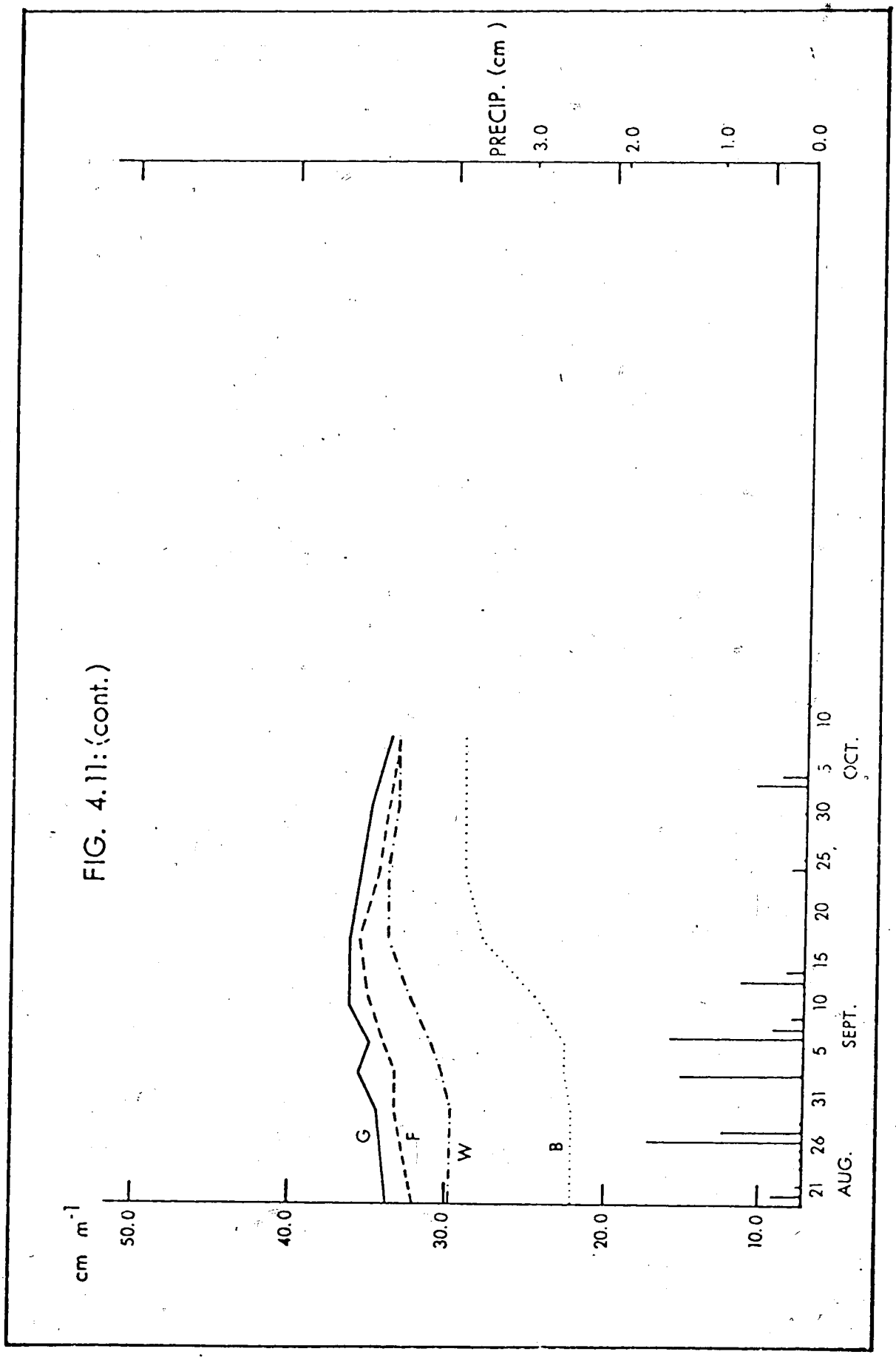
PRECIP. (cm)
3.0
2.0
1.0
0.0
cm m⁻¹
50.0
40.0
30.0
20.0
10.0
G
F
W
B
21
26
31
AUG.
5
10
15
20
25
30
SEPT.
5
10
OCT.

FIG. 4.11: (cont.)

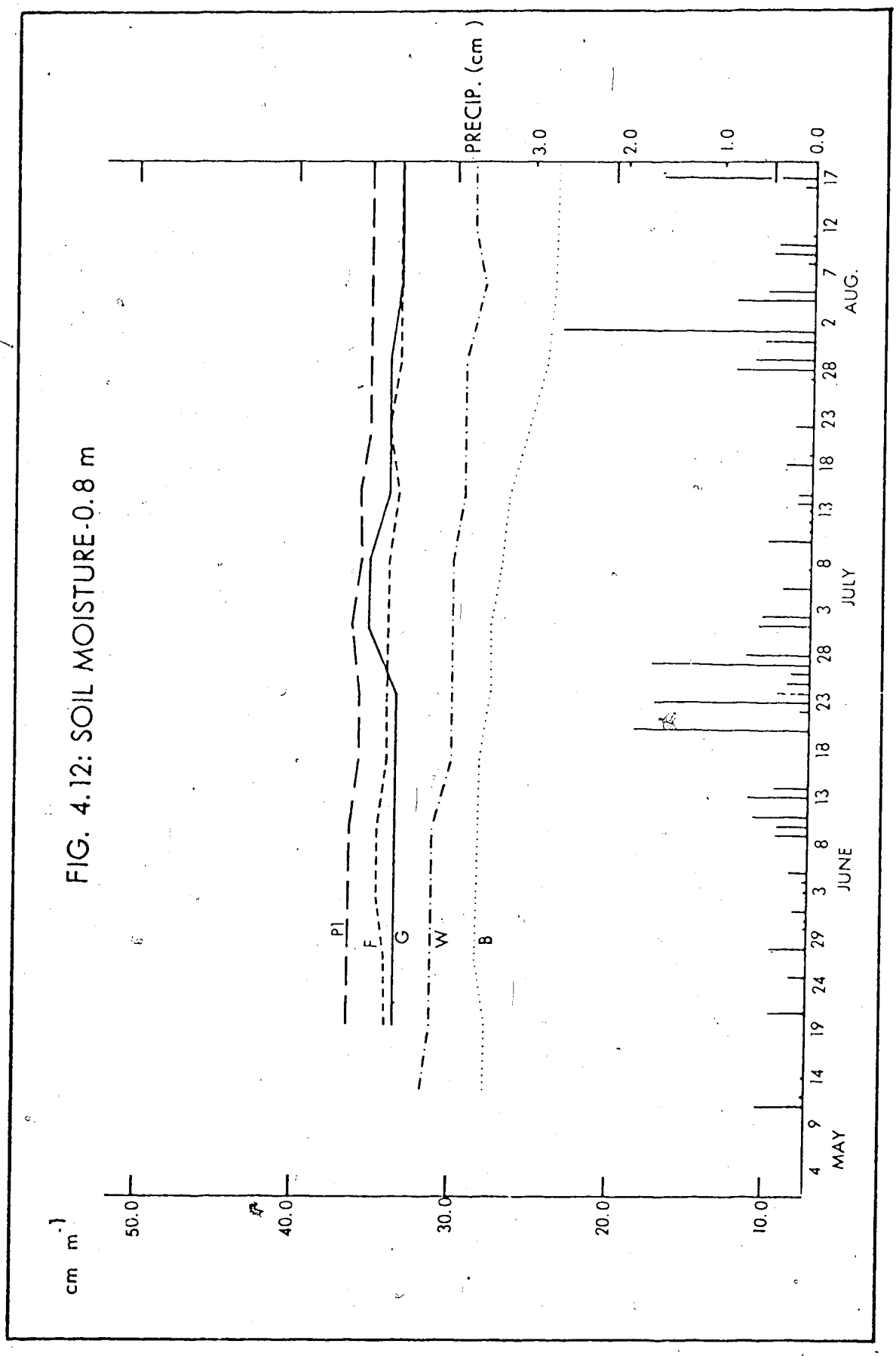

FIG. 4.12: SOIL MOISTURE-0.8 m

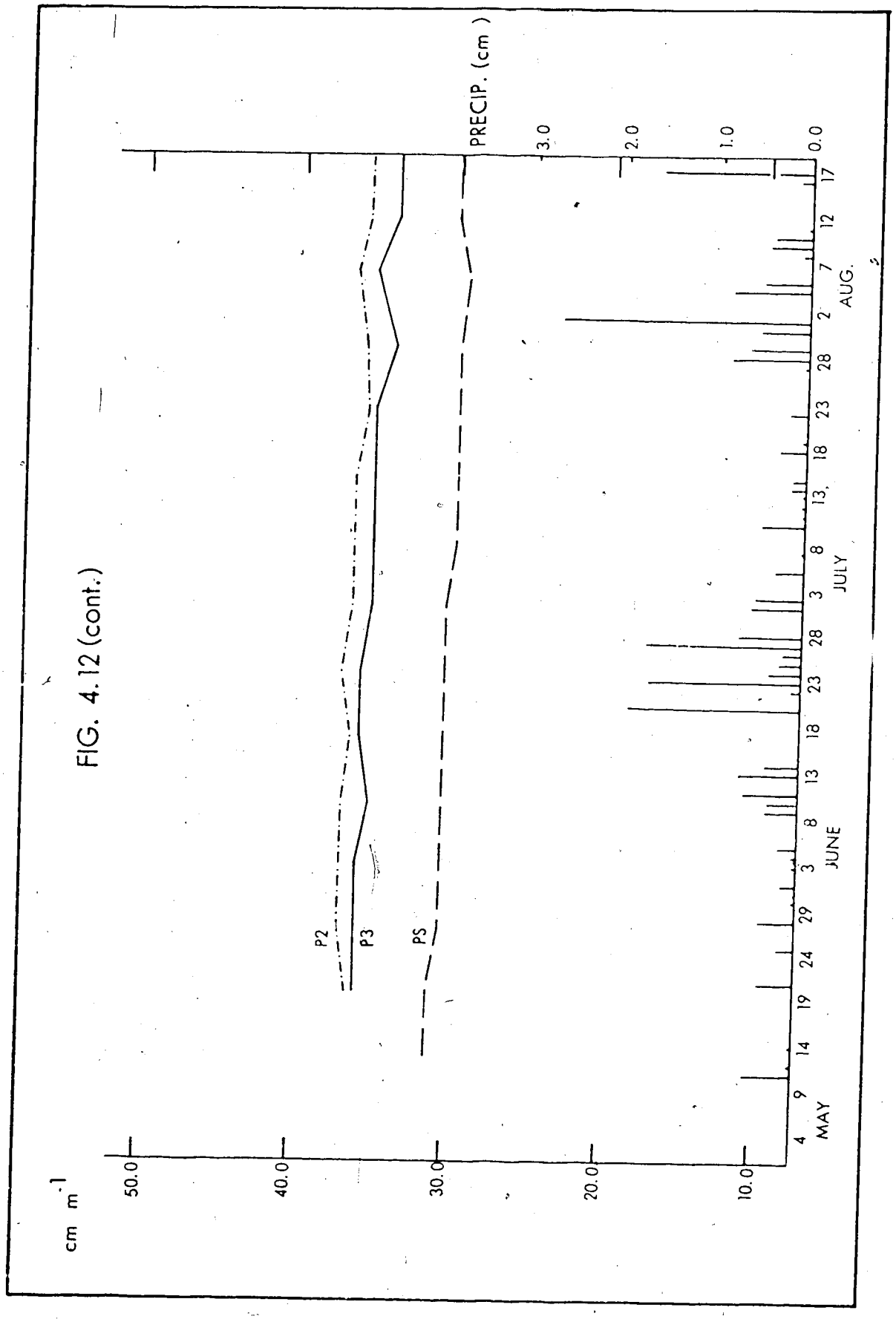
cm m⁻¹
50.0
40.0
30.0
20.0
10.0
P2
P3
PS
PRECIP. (cm)
3.0
2.0
1.0
0.0
4 9 14 19 24 29 3 8 13 18 23 28 3 8 13 18 23 28 2 7 12 17
MAY
JUNE
JULY
AUG.

FIG. 4.12 (cont.)

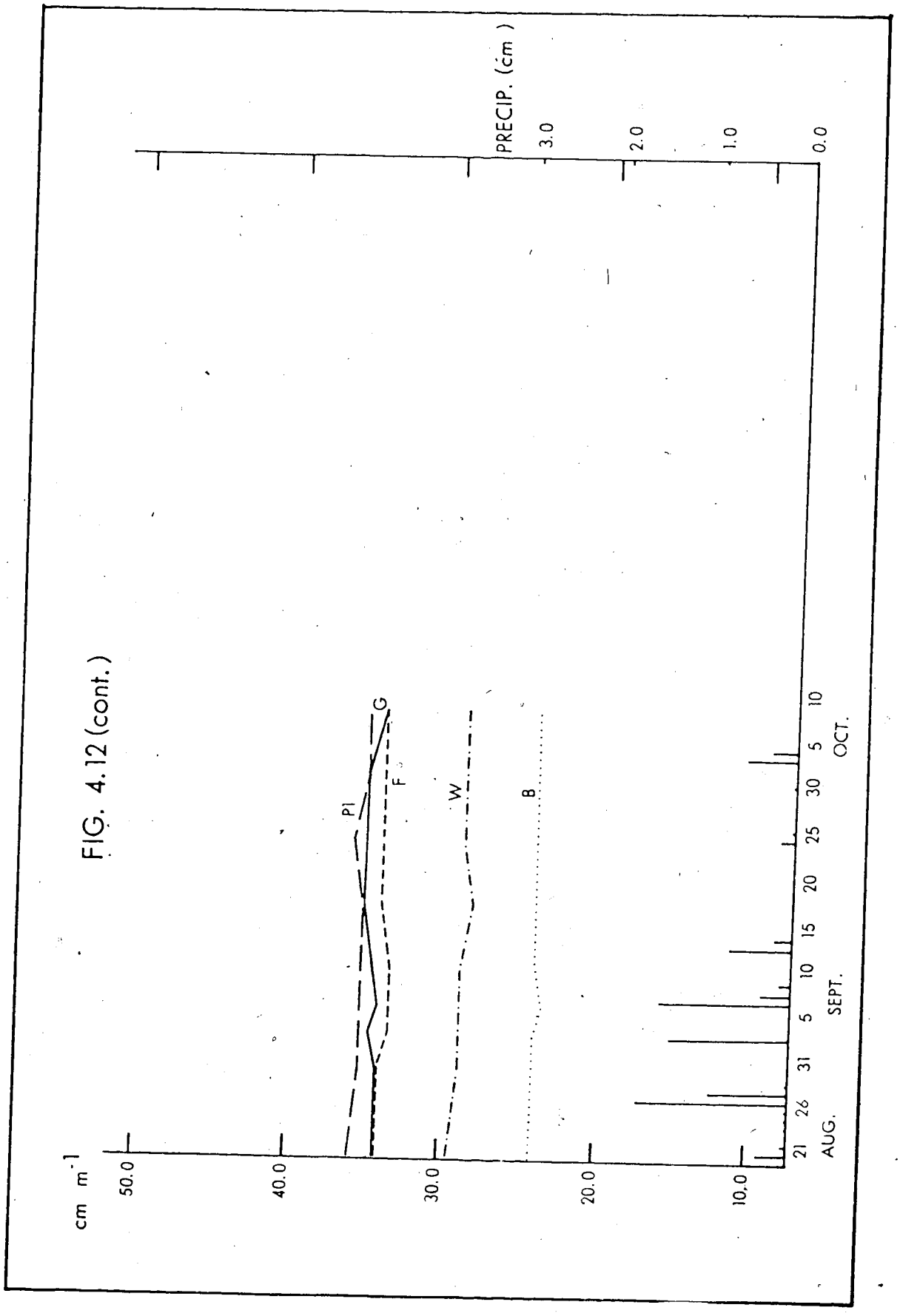
PRECIP. (cm)
3.0
2.0
1.0
0.0
cm m⁻¹
50.0
40.0
30.0
20.0
10.0
P1
G
F
W
B
21
26
31
5
10
15
20
25
30
5
10
AUG.
SEPT.
OCT.

FIG. 4.12 (cont.)

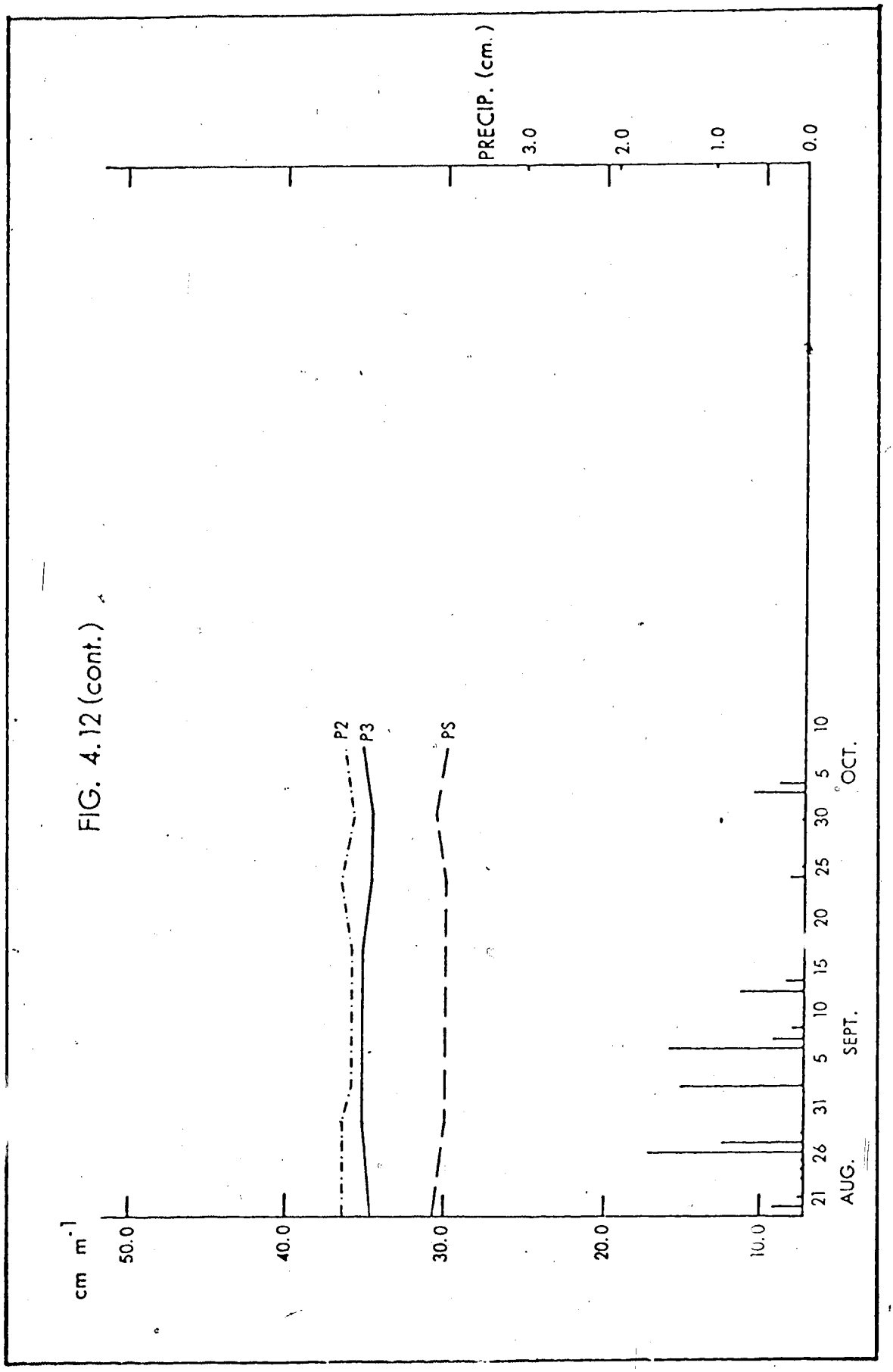
PRECIP. (cm.)
3.0
2.0
1.0
0.0
P2
P3
PS
cm m⁻¹
50.0
40.0
30.0
20.0
10.0
21 26 31 5 10 15 20 25 30 5 10
AUG.
SEPT.
OCT.

FIG. 4.12 (cont.)

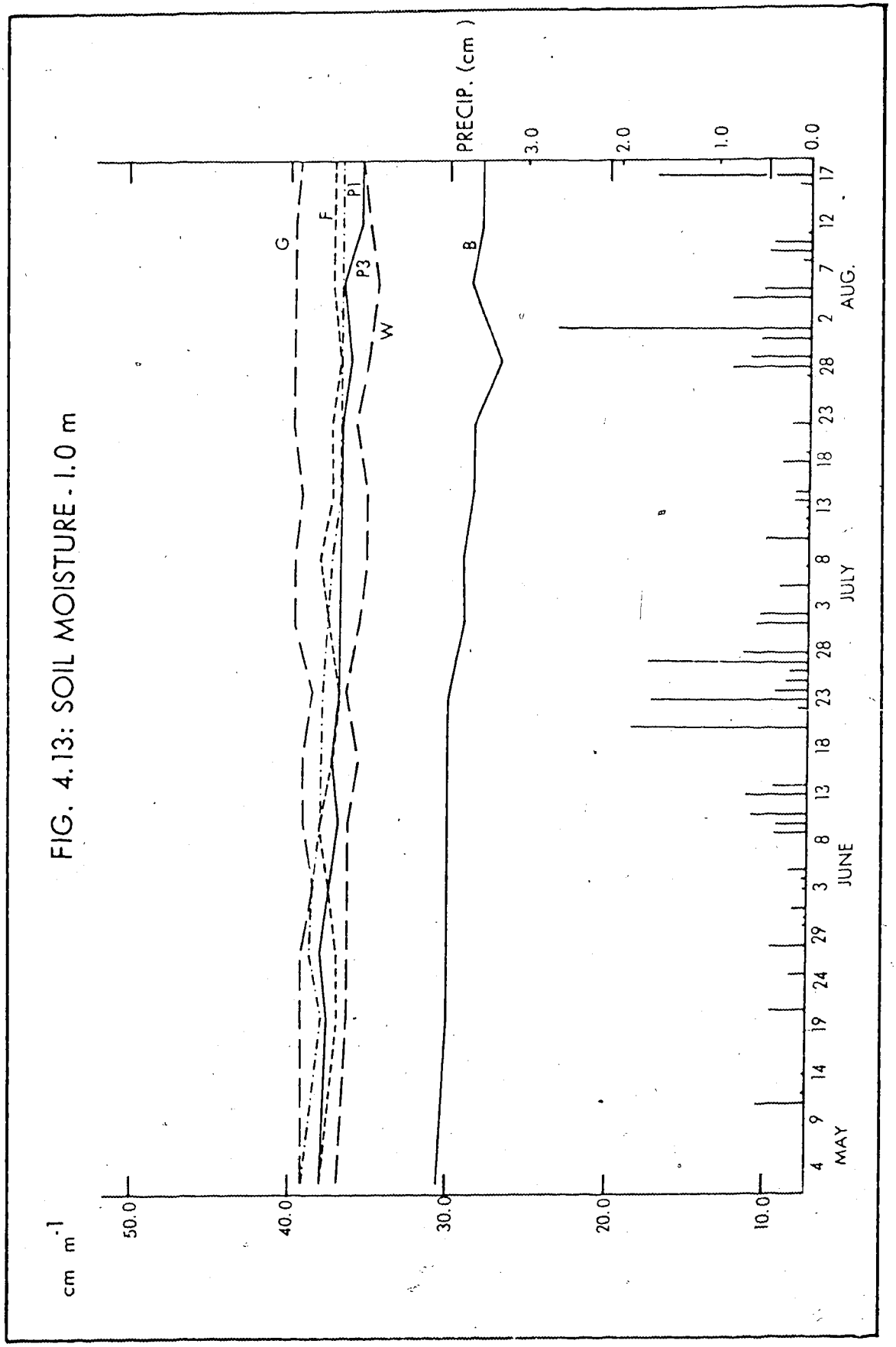

FIG. 4.13: SOIL MOISTURE - 1.0 m

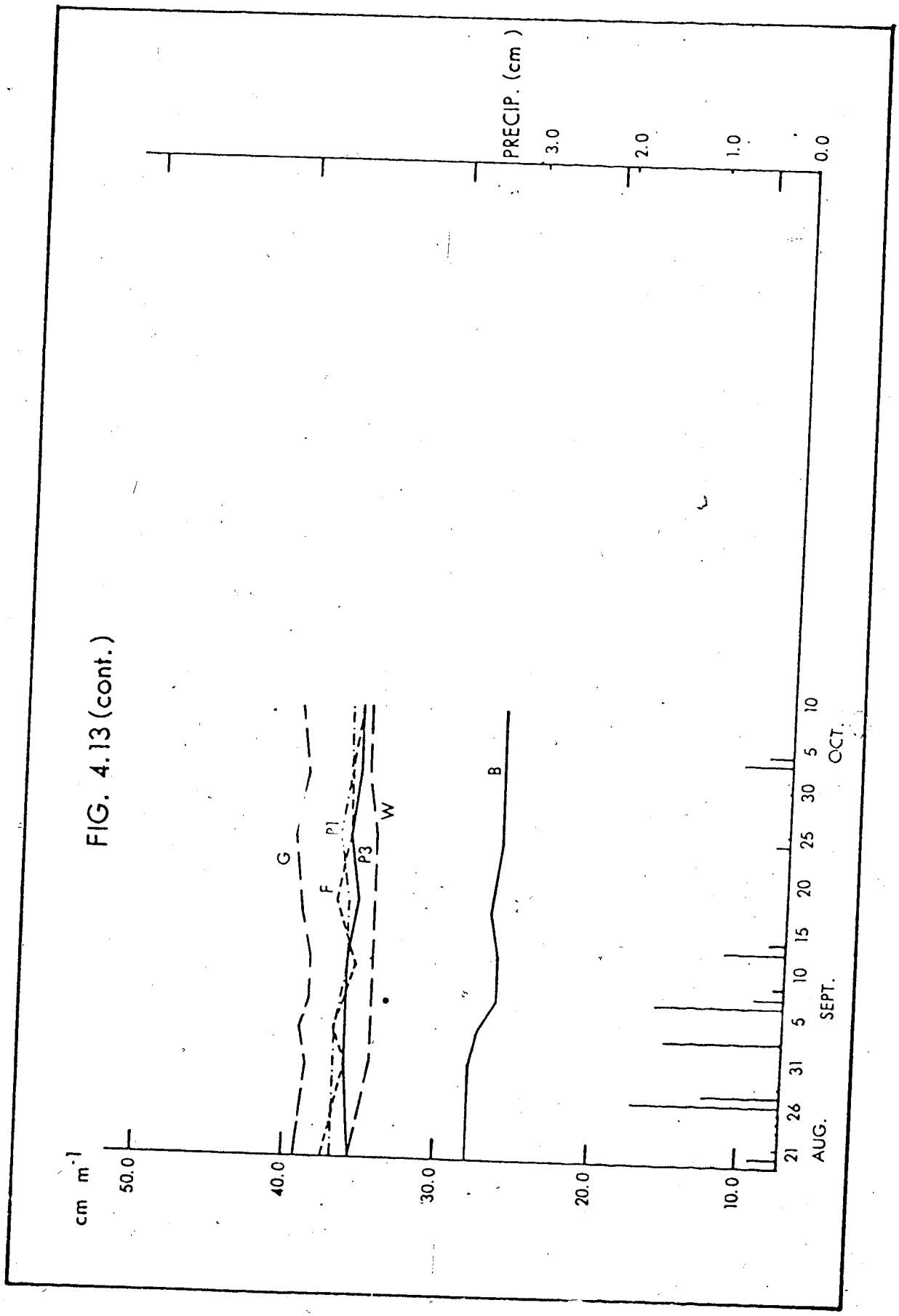
PRECIP. (cm)
3.0
2.0
1.0
0.0
cm m⁻¹
50.0
40.0
30.0
20.0
10.0
G
F
P1
P3
W
B
21
26
31
AUG.
5
10
15
20
25
30
SEPT.
5
10
OCT.

FIG. 4.13 (cont.)

contents were higher for most plots at this depth, S and F being the exceptions. At 0.5 m, PS was now one of the driest, though not as dry as S, while G and W were nearly equal. S, B, and P3 were wetter at this level than at shallower depths, while all others were drier. PS and F were the only plots wetter at 0.8 m than at 0.5 m, while all plots with data available at 1.0 m showed higher moisture contents. B was the driest plot at 0.8 m and 1.0 m with values of 28 cm m^{-1} and 30 cm m^{-1} respectively, while PS and W were fairly dry at 0.8 m, but were as wet as the other plots at 1.0 m.

4.4.2 June

Above mean precipitation and below mean temperatures, evaporation, and sunshine hours were recorded for this month. The first two weeks were fairly dry, with most of the precipitation falling in convective showers. The last two weeks were wet and cold, with daily precipitation exceeding 15 mm on three occasions. F saw a return of the stinkweed, as well as Canada thistle (Carduus arvensis) and other plant species. This condition persisted until the plot was weeded and tilled on the 15th. B and W also suffered weed invasions, B receiving small numbers of ball mustard plants (genus Brassica), and W getting hawk's beard (genus Hieracium). Moist conditions in P led to increased herbaceous cover, and poplar fluff was filling the air as the

trees released their seeds. By the end of the month, B sprouts had reached heights of up to 0.4 m.

Air temperatures for S plot became warmer than the other plots and maintained an advantage of slightly less than 1°C over PS, the coolest plot. G and P were fairly equal during the period, and maintained positions between S and PS. While S had warmer air, however, its soil temperatures were nearly 5°C colder than B, F, and W plots at both depths. PS was relatively cold as well, more than 1°C colder than the open plots.

Surface soil moisture showed general increases as a result of the late June rains. The P plots remained the wettest, while W was the wettest of the small plots, and S the driest. At 0.2 m depth, S became more than 10 cm m^{-1} drier than P, G, F, and W by the end of the month. Before the rains, PS had dropped to within 5 cm m^{-1} of S, but greater throughfall here allowed PS to gain 5 cm m^{-1}, while S was barely affected. At 0.5 m, G values showed a sharp increase on July 1, which may indicate that this was the only plot where infiltration of the previous week's rains could reach this depth. Slight increases one week later can also be seen at P2, F, W, and S and these may indicate a slower and substantially lower infiltration rate. Considering the very small change in its 0.2 m values, the increase at S is somewhat puzzling, but since

the increment was only 0.05 cm m^{-1} for all 4 plots, this little bump in the curve should not be considered significant. At greater depths, a slight downward trend was apparent at B and W towards the end of the month.

4.4.3 July

Mean temperatures and sunshine hours, near mean evaporation, and slightly below mean precipitation occurred during July. Between the 2nd and the 28th, no days had rainfall greater than 5 mm, and much of the precipitation fell during local convective storms. Heavier thunderstorms during the last week brought an additional 20 mm of rain to the area. Weeds gradually returned to F, and by the 15th, the plot was heavily covered with vigorous plant growth. Its surface was dry and crusty, with cracks evident throughout. The plot was tilled and weeded during the third week, but the dead plant material was left on the plot. Weeds had also returned to B, but were not as serious. The sprouts were still doing well, and by the end of the month had attained a maximum height of 0.9 m. Heads had formed by the 15th and these were large, promising a good yield. G and W also showed healthy growth and only a slight weed infestation.

Air temperatures for S were still the highest, exceeding [illegible] and P by 5°C and PS by more than 1°C during

the last 3 weeks. S however, continued to register the coldest soil temperatures at both depths. F and W were now about 2°C warmer than B, and G at 100 cm had also exceeded B's temperatures. PS was still cooler than the open plots, but maintained a 2°C advantage over S at 100 cm and a 1°C at 20 cm.

The dry weather produced a downward trend for surface soil moisture on all plots, but there were some changes in rank. B was now as moist as some of the P sites while PS declined rapidly. Toward the end of the month, W, F, and G were almost as dry as PS, while S was by far the driest at 25 cm m^{-1}, 3 - 5 cm m^{-1} lower than the open sites. The rains during the final week brought sharp increases to all the plots except P, B, and S. These did not react until greater precipitation fell during the first week of August.

At 0.2 m, a steady downward trend was evident for all sites except S, which was already too dry to lose much more water under these temperature conditions. By the 28th, B was nearly as dry as S, recording a value of 20 cm m^{-1}. PS and P3 were 6 cm m^{-1} wetter, while the other plots were clustered around the 29 - 31 cm m^{-1} range. At 0.5 m, S remained steady while B dropped far below 25 cm m^{-1}, and so became the driest at this depth. The growing barley was apparently beginning to tap the moisture reserves at lower levels by capillary action

extension of an active root system. This trend was detectable in small magnitudes at the 100 cm depth as well.

4.4.4 August

Above mean temperature and precipitation, near mean sunshine duration, and below mean evaporation, were the major features of August's weather. Heavy rains occurred during the first week, with 26.5 mm falling on the 1st. The other days recorded precipitation higher than 10 mm, but it was that first storm which seemed to have the greatest significance on soil moisture levels. Barley on B had started to turn colour during the last week of July, and was now ripening. However, by the third week, its condition had deteriorated. Weeds (mainly thistle) started to dominate, and the barley stand was suffering from the competition. Weeds had returned to F and W as well.

The early rains were accompanied by high temperatures, and the weekly temperature curve shows an increase over the end of July. G and S were now about equal, while PS started the month 1° C cooler. The range decreased during the middle of the month, but by the end, their values had diverged again. G was warmest at this point, while PS was more than 1° C cooler, having recorded a mean

temperature of 14.1°C. Soil temperatures showed increases for all plots at both depths, with the exception of F at 20 cm, which had a slight decline. Its status as the second warmest plot behind G remained unchanged, as did the ranks of the other plots. S was still 2°C colder than PS and 4°C colder than G and F at the 100 cm level. At 20 cm, S and PS were only 1°C apart, but G and F were still much warmer than both tree sites.

Surface moisture levels increased sharply during the first week because of the heavy rain. S now recorded values higher than F and W, and had the greatest weekly increase, which may be due to a lower surface evaporation rate than at the open sites. Values started to decline again, until the third and fourth weeks, when additional rain brought increases to P, F, PS, and B. Towards the end of the month, however, only the P plots reacted to the rain of the 26th. The smaller plots were declining and for S and G, the decline had been continuous since the first week. The 0.2 m level showed a similar trend, though S remained more than 5 - 20 cm m^{-1} drier than the other plots. B showed no decline after the initial week's rains, which may indicate the lack of water use by the now ripening crop. P maintained moister conditions, but G, F, and W were now as wet as P2, and wetter than all the other sites. B continued to be the driest at 0.5 m, while the 3 P plots held slight advantages over G and F. The wetter

plots showed a general downward trend while the dry plots remained steady, as did all the plots at lower depths.

4.4.5 September - October

The final five weeks of the observational program were warmer, sunnier, and wetter than mean conditions. Evaporation was slightly below the mean. The precipitation figures are somewhat misleading, because of the uneven distribution of rainfall during this period. Only 5% of the 44 mm recorded during September fell after the 13th, and rainfall during the first week of October was confined to the 3rd and 4th. Two days registered precipitation above 10 mm, and only 11 days out of 38 had measurable rainfall. However, another source of moisture entered the picture at this time--dew, which was observed 13 mornings during September (Table 4.6), and probably had some effect on surface moisture readings at the open plots. Dew does not regularly form in densely forested areas (Geiger, 1965), and indeed, that rule held true for Ellerslie. The sharp decline in temperatures, which is an important feature of September weather, led to higher values for relative humidity, as well as the frequent formation of dew, especially over long grass. Fungal growth increased as a result of the wet August weather, with moss growing in PS, and toadstools in S. F was once more infested with weeds after it

TABLE 4.6

DEW FORMATION IN SEPTEMBER

24 hr. period ending 0900 hrs. MST	Min (°C)	Dew Pt. (°C)	Dew (x)
1	10	10	-
2	10	9	-
3	3	5	-
4	7	9	x
5	9	10	x
6	7	6	-
7	5	3	-
8	2	4	-
9	5	7	-
10	6	7	-
11	8	6	-
12	6	5	-
13	4	8	x
14	5	7	x
15	5	9	x
16	5	8	-
17	5	9	-
18	3	9	x
19	8	7	-
20	3	7	x

TABLE 4.6 (con't.)

24 hr. period ending 0900 hrs. MST	Min (°C)	Dew Pt. (°C)	Dew (x)
21	5	9	x
22	6	8	x
23	6	8	x
24	8	11	-
25	8	9	-
26	4	9	x
27	5	5	-
28	2	8	x
29	6	8	-
30	4	1	-

had been tilled in August, and dew may have formed on the plant cover, which could have facilitated a rise in surface soil moisture late in the month, when the plant cover would be more extensive. This will be discussed later.

Leaves at W, PS, and P plots were turning colour, especially during the last two weeks, but leaf fall had not been completed before the field program was terminated on October 8. By this time, however, those leaves still on the branches were yellow or brown. The thistles on B plot were also turning brown as a result of some cold night conditions, when the temperature approached 0°C. G remained green, as did the weed cover on F.

PS was still the coolest plot, while the other sites had fairly similar air temperatures until the 15th when S cooled to the same level as PS, 11.0°C. G was now the warmest, but by the end of the program, all four plots had air temperatures within 0.5°C of each other. S had the coldest soil temperatures at both depths, 3°C below G and F. Rankings remained the same for this period as for August.

Surface moisture was affected by the first week's rains, as indicated by the increased levels during the first two weeks. An exception was F, which showed a continuous decrease until the third week, when the trend was reversed. G and P fluctuated quite strongly during

the month, while W and B were more stable, averaging 37 cm m^{-1} and 40 cm m^{-1} respectively. S, PS, and F were the driest while P, W, and B maintained levels up to 13 cm m^{-1} higher. It is difficult to quantitatively determine the effects of dew on these data, but it is possible that the increase registered during the third week at F, could have resulted from frequent dew formation on the weeds during this week. Another plot which might have been affected by dew was G plot, which suffered a moisture decrease that was less than anticipated, considering the week's light precipitation. Dew was observed at B as well, but the denser stubble cover could have prevented much of the dew from infiltrating into the soil before it could evaporate.

Although there may have been some surface effects, the 0.2 m level showed a downward trend after the first week's rains. B reacted very strongly to the rain, indicating the reduction in water use by the dying plant cover. B was now the fourth wettest behind W, G, and F, whereas 6 weeks earlier, only S was drier. S and PS continued to record the lowest moisture levels. At 0.5 m depth, B again showed a strong upward trend as a result of the late August and early September rains. By the second week, its moisture level had climbed from 22 cm m^{-1} to nearly 30 cm m^{-1}, surpassing both S and PS. The other plots maintained stable levels about 3 - 5 cm m^{-1} higher.

W had been somewhat drier during August, but showed an increase similar to B's, and was now at the same level as G, F, and P. At 0.8 m and 1.0 m depths, there was little change during the period, although B showed a slight decrease at 1.0 m. This may be a consequence of earlier water use by the previously healthy crop during early and middle summer.

4.4.6 Summary

General weather conditions for Ellerslie in 1976 (May - October) were slightly sunnier, warmer and wetter than mean conditions. Evaporation was sl htly lower. Seasonal change in vegetation characteristics was affected by a dry spring, which produced an early canopy at PS and P, and by a warm wet August, which may have influenced the demise of B before harvest time.[1] The warm dry conditions during September allowed PS to maintain its canopy until well after observations ceased.

Significant differences in air and soil temperatures were readily apparent throughout the growing season.

---

[1] Low soil moisture combined with high air temperature may be another factor. As the soil dries, the actual transpiration rate of the plant should fall below the potential rate. Since the potential rate is dependent on temperature, the plants' wilting point must also be related to temperature (Denmead and Shaw, 1962). Therefore, it is possible that the barley ceased to function before the August rains could influence plant growth.

Regression analysis (Table 4.3b) reveals that S plot's air temperatures were warmest during middle summer (when G plot registered a temperature of at least 15°C). PS and P were consistently cooler during this period. At lower temperatures, the temperature difference between the plots declined. S continued to have coolest soil temperatures, while other plots maintained their ranks (with some variations) during most of the summer. Soil moisture ranks were fairly consistent as well, except for B, which fluctuated according to its state of health. There were variations in response to rainfall, and this was due in large part to throughfall (e.g. S) and plant water use (e.g. B). Short term weather and plant growth effects did not influence the 0.8 m and 1.0 m levels, except during B's healthy growth period, which lasted until the second week of August. Frequent dew formation may have affected surface moisture levels at F and G, but it is difficult to determine its significance.

It is readily apparent that long term conditions greatly influenced soil temperature and soil moisture values, and the ranking of each plot in these two categories. Air temperature was more dependent on short term weather.

CHAPTER V

EXPERIMENTAL RESULTS AND ANALYSIS

5.1 Introduction

General climate and field conditions were examined in the previous chapter. Here, it is appropriate to consider the results of the radiation and energy balance measurements and derivations for the various plots. Albedo, global solar radiation, and net radiation are examined first, with special attention being given the prediction of Rn from (Q+q) using eq. (2.6). Having established the quantity of Rn available for the sensible, latent, and soil heat fluxes, one may now discuss the variations of these fluxes. This is followed by an analysis of the Bowen Ratios. Energy balances are calculated based on weekly values derived from regression equations of Rn and Gs, and on calculations of LE. Measurement and statistical errors are then accounted for in an effort to determine the reliability of the energy balance calculations, and consequently, the validity of the possible micro- and macro-scale climate effects caused by future land use changes in Central Alberta.

5.2 Radiation Balance

5.2.1 Albedo and Global Solar Radiation

Daily mean values for albedo and (Q+q) are listed

in Table 5.1. Values for June (Q+q) were slightly lower than for July despite a greater daylength. This is to be expected, since July had more hours of bright sunshine and lower rainfall. There was a sharp decline from July to August due to a decrease in bright sunshine hours, while September's values benefitted from a dry 3 week period with an abundance of clear days.

Mean albedo values ranged from 0.065 for F plot in June, to 0.250 for G plot in September. S plot was the most consistent, while W varied from 0.196 in July to 0.104 in September. Since there was little change in S plot's canopy structure during the summer season, lack of albedo variation is no surprise. Admittedly, the June data for W plot are based on just one 24-hour period, but July's values are only 1% higher than June's, and more than 9% above September's. The low September values for W, and PS, the other deciduous cover, were probably a consequence of leaf loss.

B plot's values seemed to fluctuate with the state of the crop's growth. In June and July, the plants were young, and green in colour, so albedo values were high. Towards the end of summer, however, the crop deteriorated, its colour changing to a dull brown, and dark green weeds had infested the plot. Meanwhile, the healthy large barley field had reached maturity, and its colour was golden brown. There were few weeds, and moist bare soil

TABLE 5.1

ALBEDO

(x 100%)

Dates	1000 Q+q($Wm^{-2}day^{-1}$)	PS	S	W	B	F	G
6/16 - 30	312.4	0.143	0.135	0.180*	0.237	0.065	0.175
7/ 1 - 31	340.6	0.130	0.128	0.196	0.243	0.135	0.230
8/ 1 - 31	240.5	0.125	0.133	0.177	0.225	0.225	-
9/ 1 - 10/7	218.1	0.110	0.132	0.104	0.175	0.148	0.250
					LB 0.150		

Albedo figures represent daily means calculated from a minimum of two 24 hour periods, unless marked with an asterisk (*), in which case, only one 24 hour period was available. LB represents data obtained from the larger barley field, September 5 - 9.

was visible between the stalks, thereby reducing reflectivity to a value 2.5% below B plot in summer.

F plot was affected by human activity. Higher albedo values at F indicated periods with substantial weed cover, and a dry crusty surface, while tillage and weeding resulted in albedo reduction. June albedo for G plot was affected by wet weather, which produced a low value of 0.14 on the 27th.

Overall, G plot and the young barley crop had the highest reflectivity, 3 - 5% greater than W with leaves, and 8 - 10% above S, leafy PS, and dry weed-infested F. They were 10 - 15% above leafless PS and W, and moist, weed-free F. Considering the magnitude of daily global solar radiation, this variation in reflectivity could amount to a difference of up to 40,000 $Wm^{-2}day^{-1}$ of Rn available for use by the various plots.

5.2.2 Net Radiation--Diurnal Variations

Diurnal variations of Rn for selected clear 24 hour periods are illustrated in this section. These periods were chosen to maximize the effect of the individual plots' albedos on their respective radiation balances, and to facilitate the detection of any measurement errors that may have occurred during the field study. Data for Gs and (Q+q) are included where available. Rn data for G plot are illustrated in all figures for comparative pur-

poses, since G was the base station. In addition, two of the figures contain data for Stony Plain (Q+q) and Rn. These will be discussed later.

The calendar date given represents the 24 hour period ending at 0900 hours MST on that date. Therefore, the data from 0900 - 2359 MST was actually measured one calendar day before the given date. This was done so as to synchronize the small plot measurements with the daily meteorological 0900 MST observations at the Ellerslie climate station.

A note of caution is given before discussing these data. The graphs represent individual 24 hour periods; this is important when considering their interpretation. It should not be assumed that similar diurnal variations have been occurring for any specified time period before or after the given date. The purpose of this research project is to examine gross energy balance differences over several months. Detailed analysis for much shorter time periods requires greater instrumentation, and is beyond the scope of this study.

Diurnal trends for PS plot are illustrated in Figs. 5.1 and 5.2. As might be expected, June 19 (Fig. 5.1) featured much higher midday (Q+q) values than October 2 (Fig. 5.2). Upon comparing the two graphs, certain major differences in longwave emissions can be seen. On June 19, nighttime Ln values for G and PS were fairly similar, while in October, emissions from PS were

FIGS. 5.1 - 5.12

DIURNAL VARIATIONS OF Rn AND Gs

5.1	June 19, 1976
5.2	October 2, 1976
5.3	June 30, 1976
5.4	September 26, 1976
5.5	May 31, 1976
5.6	July 24, 1976
5.7	May 27, 1976
5.8	July 4, 1976
5.9	September 17, 1976
5.10	June 2, 1976
5.11	July 18, 1976
5.12	July 18, 1976

FIG. 5.1:JUNE 19, 1976

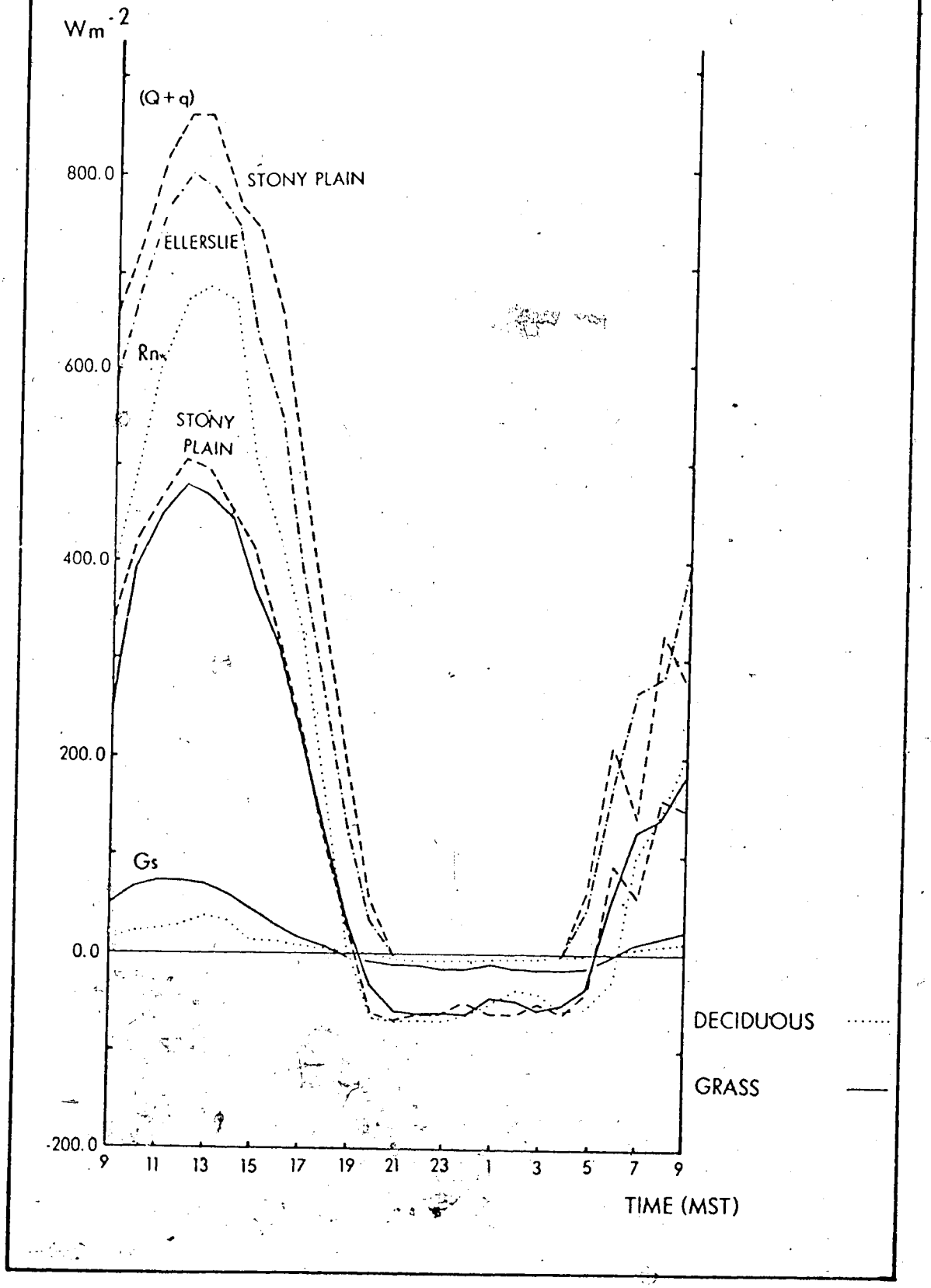

FIG. 5.2: OCT. 2, 1976

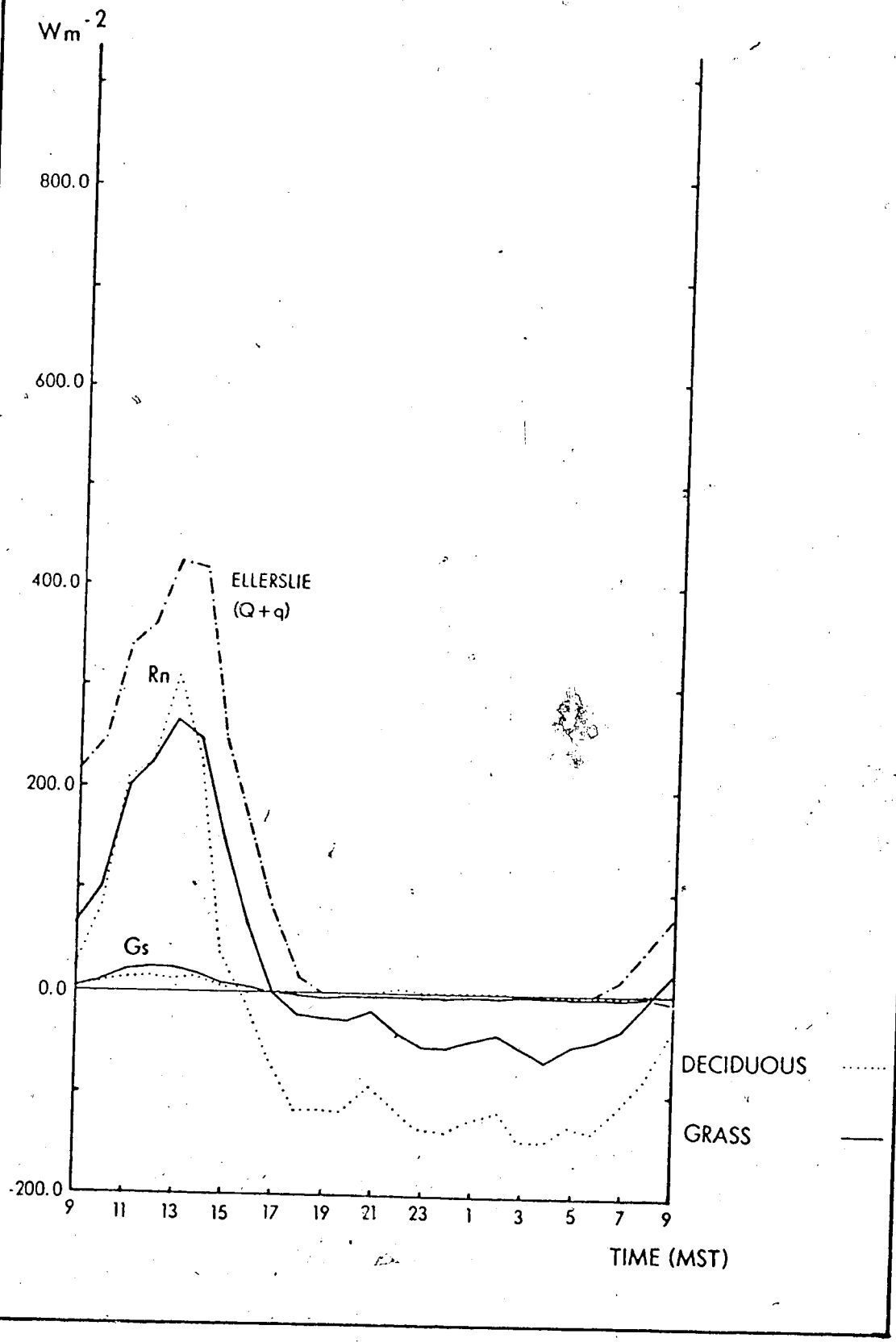

much greater, probably due to higher nighttime temperatures in the sparsely leafed tree canopy than in the open air.[1] This could have caused a lowering of daytime Rn values for PS, so that its peak was now the same as G plot's, and its morning and late afternoon values were lower. Considering the fact that G plot's albedo was twice that of PS in October, and that on June 19, PS exceeded G plot by more than 200 Wm^{-2} at 1300 MST, this change in rank is remarkable. Gs values at G plot exceeded values at PS during both days, while there were lower nighttime emissions at PS. Both occurrences illustrate the influence of the deciduous canopy in shading the ground during the day, and returning longwave energy to the soil surface at night.

S plot's diurnal trends for June 30 and September 26 are illustrated in Figs. 5.3 and 5.4 respectively. The results for June are similar to those of Fig. 5.1, although the midday Rn difference is smaller, and S plot's nighttime emissions are consistently greater than G plot's. However, the September situation is radically different from Fig. 5.2. Rn at S plot remains higher, and its Ln emissions are lower than G plot's. Considering the leaf loss on PS plot and the dense canopy of S plot, one may conclude that differences in canopy structure are probably

---

[1] Relative humidity may have been a factor, too. See Geiger (1965), p. 213.

FIG. 5.3: JUNE 30, 1976

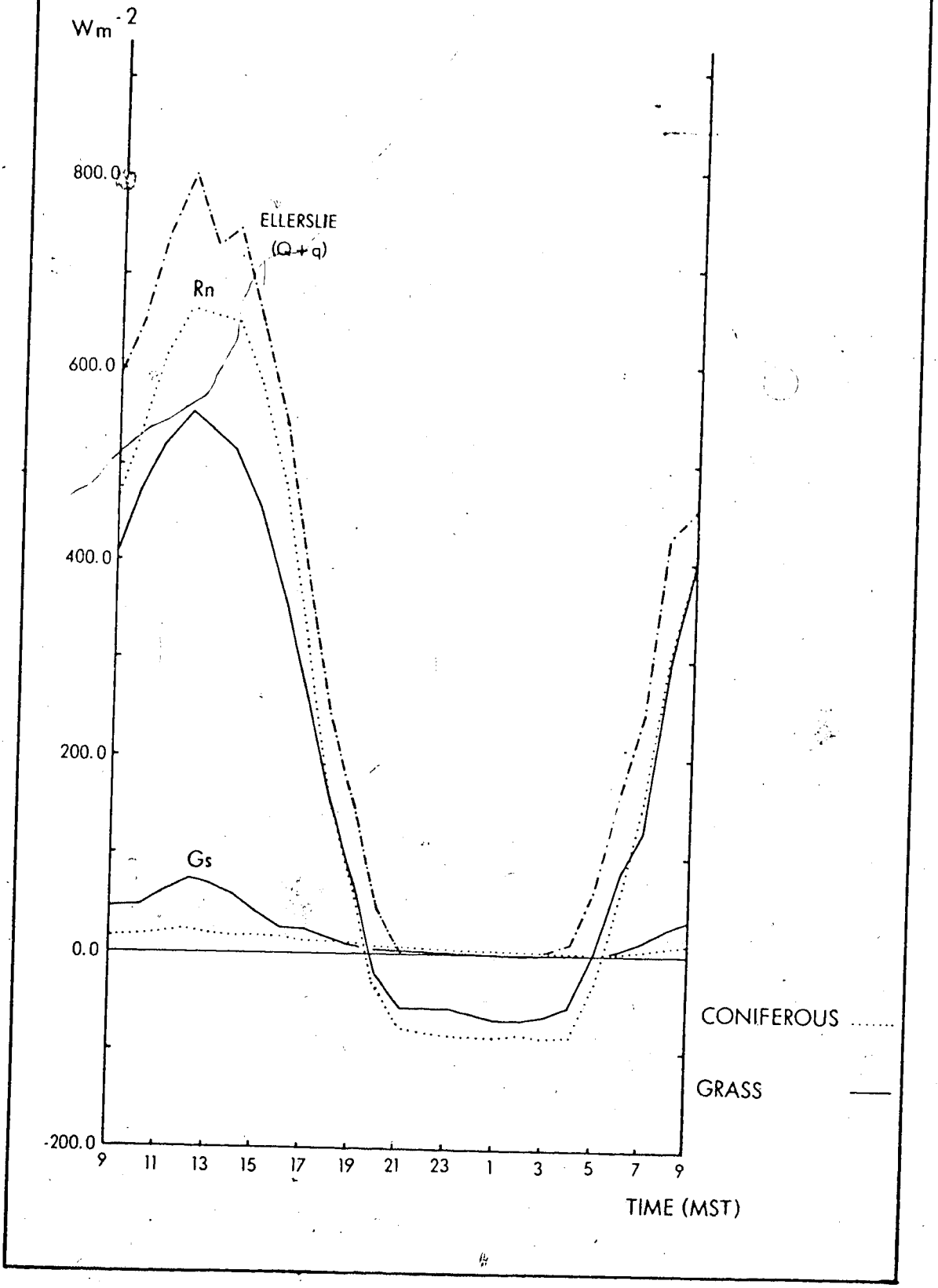

FIG. 5.4: SEPT. 26, 1976

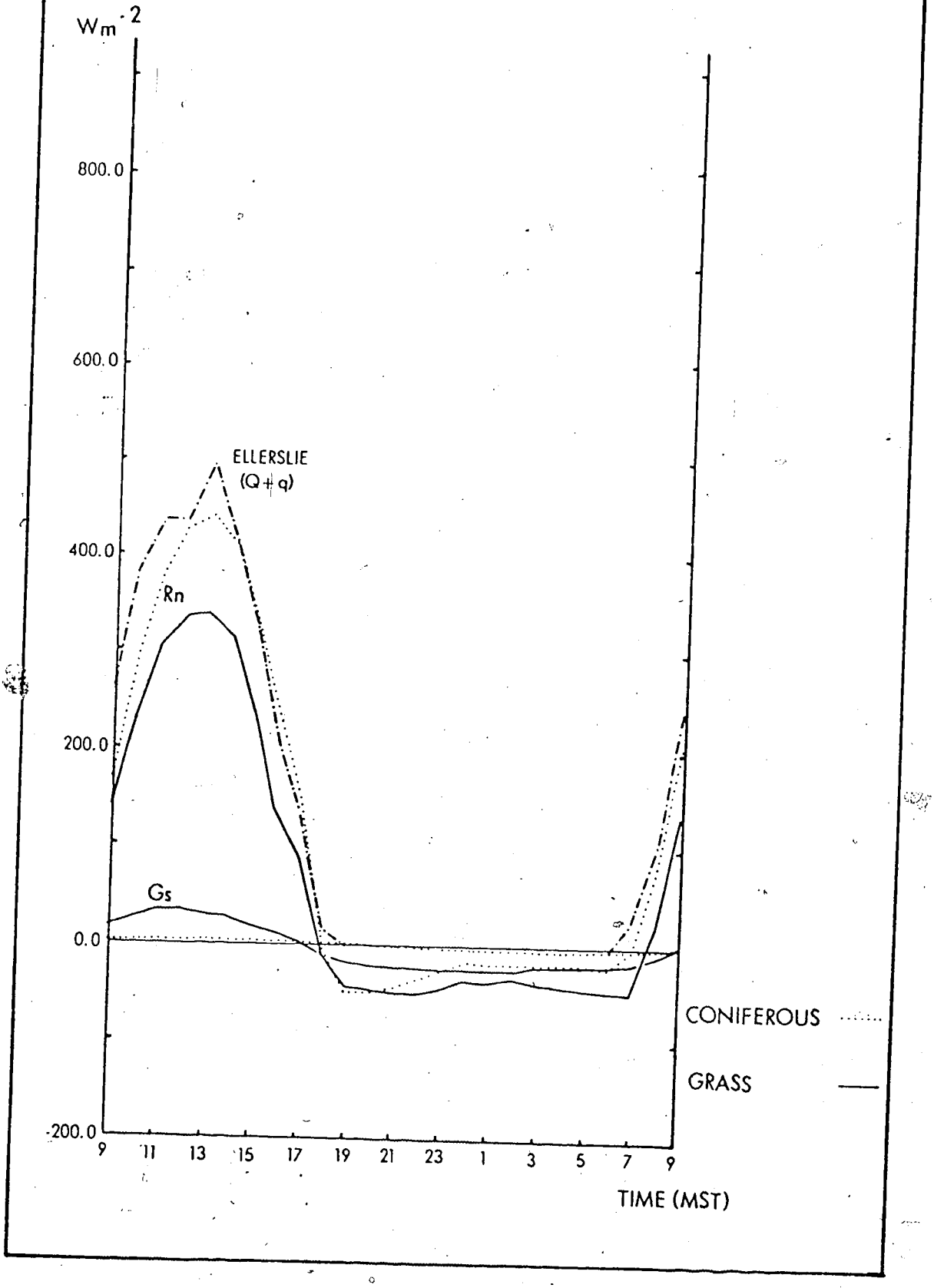

the major factor in this situation.

Rn slightly exceeds (Q+q) during the late afternoon of September 26. This could be due to a short period of positive Ln, or measurement error. Error possibilities are discussed in Section 5.2.5.

W plot data for May 31 and July 24 (Figs. 5.5 and 5.6 respectively) reveal that Ln emissions are similar to those of G plot. However, Rn values are higher during all daylight hours (as opposed to PS and S), thereby illustrating canopy structure differences. Its rough exposed surface allows greater absorption of low sun angle radiation than the relatively smooth G plot. Diurnal variations of Gs are similar to variations on PS plot.

B plot data for May 27, July 4, and September 17 (Figs. 5.7 - 5.9 respectively) show seasonal variations in Ln emissions, when compared to G plot. On May 27, Ln emissions were greater at B. On July 4, the difference between B and G was smaller, and on September 17, the two plots had similar Ln. Gs changed as well, with higher values being recorded for G pl in May and July, and for B plot in September. This illustrates the effect of changing plant cover and water use on B plot. In late May, surface moisture started to decline until heavy rain fell in late June. Heavy rain in late summer created wet surface conditions since plant water use had decreased. Moist soil has a higher thermal conductivity (K) than dry soil (Sellers, 1968, p. 128). According to the Gs equation:

FIG. 5.5: MAY 31, 1976

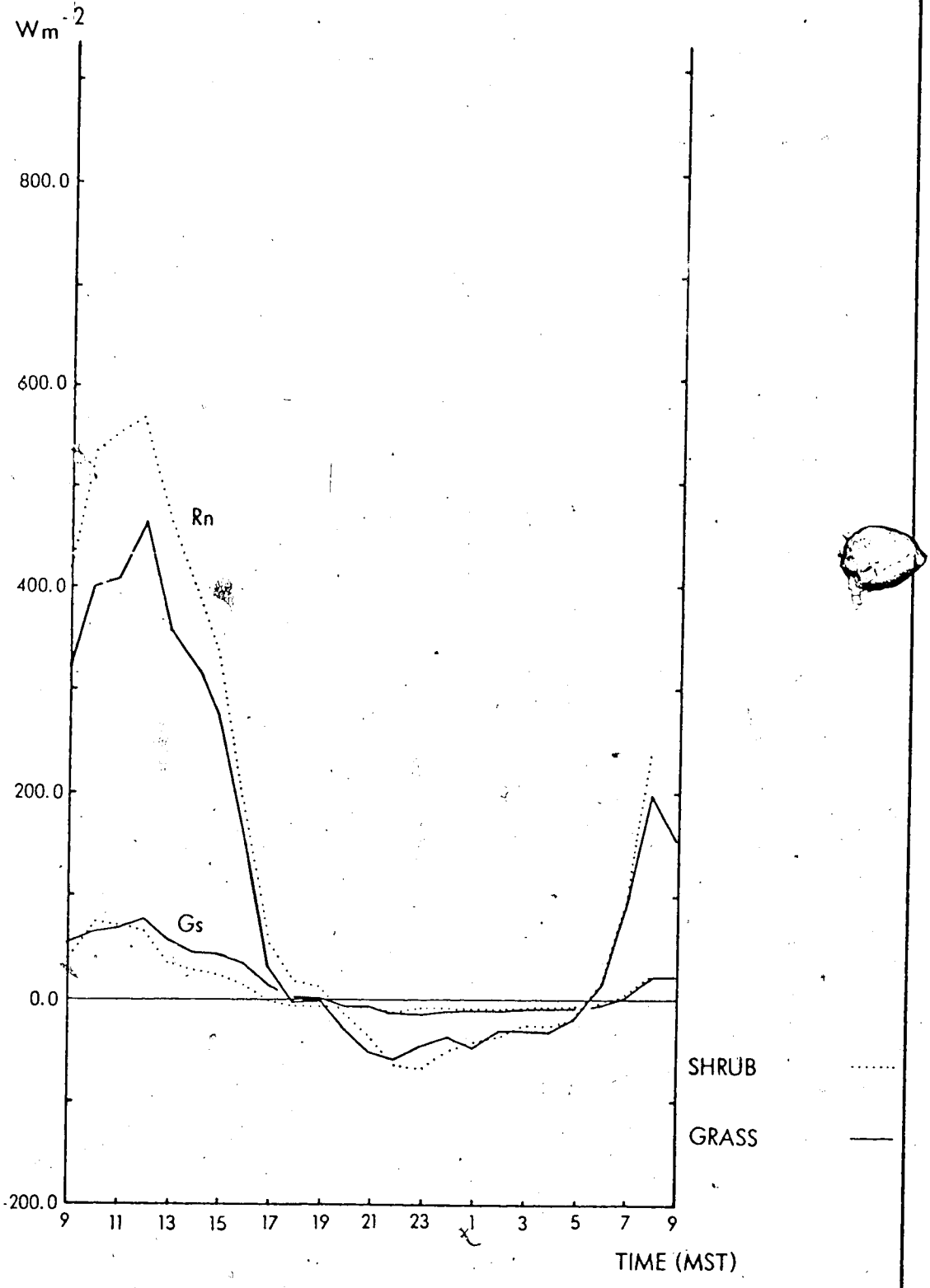

FIG. 5.6: JULY 24, 1976

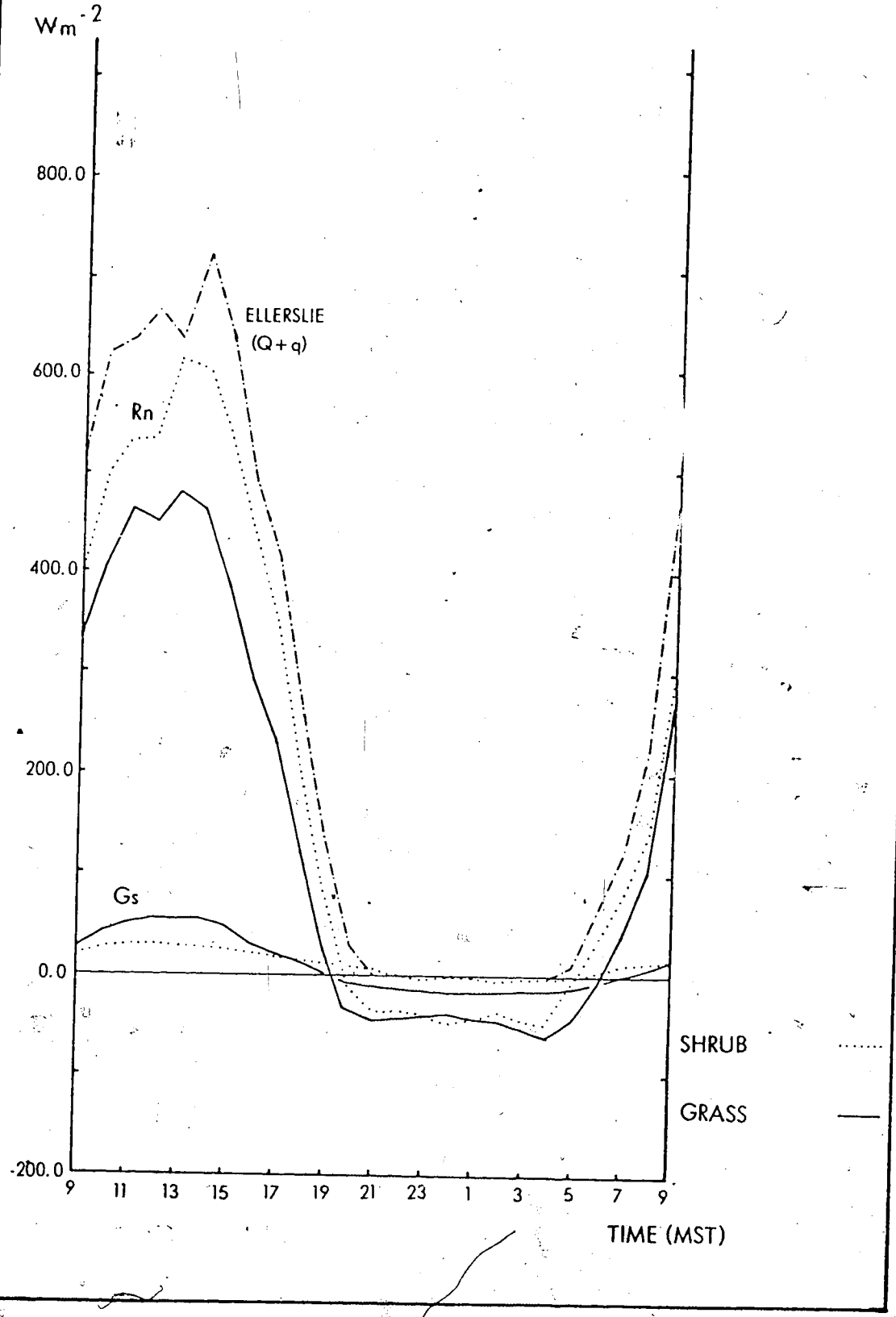

FIG. 5.7: MAY 27, 1976

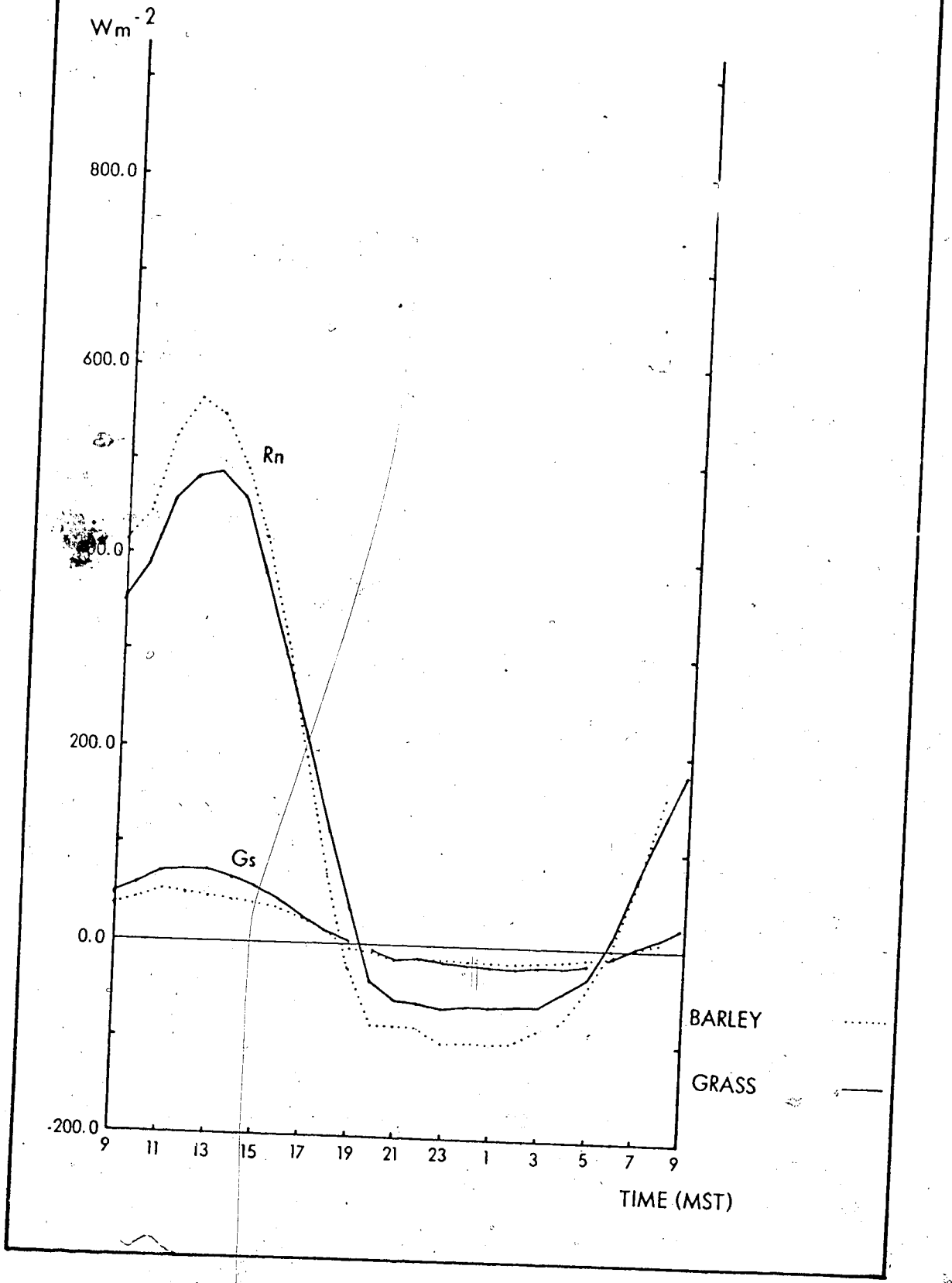

FIG. 5.8: JULY 4, 1976

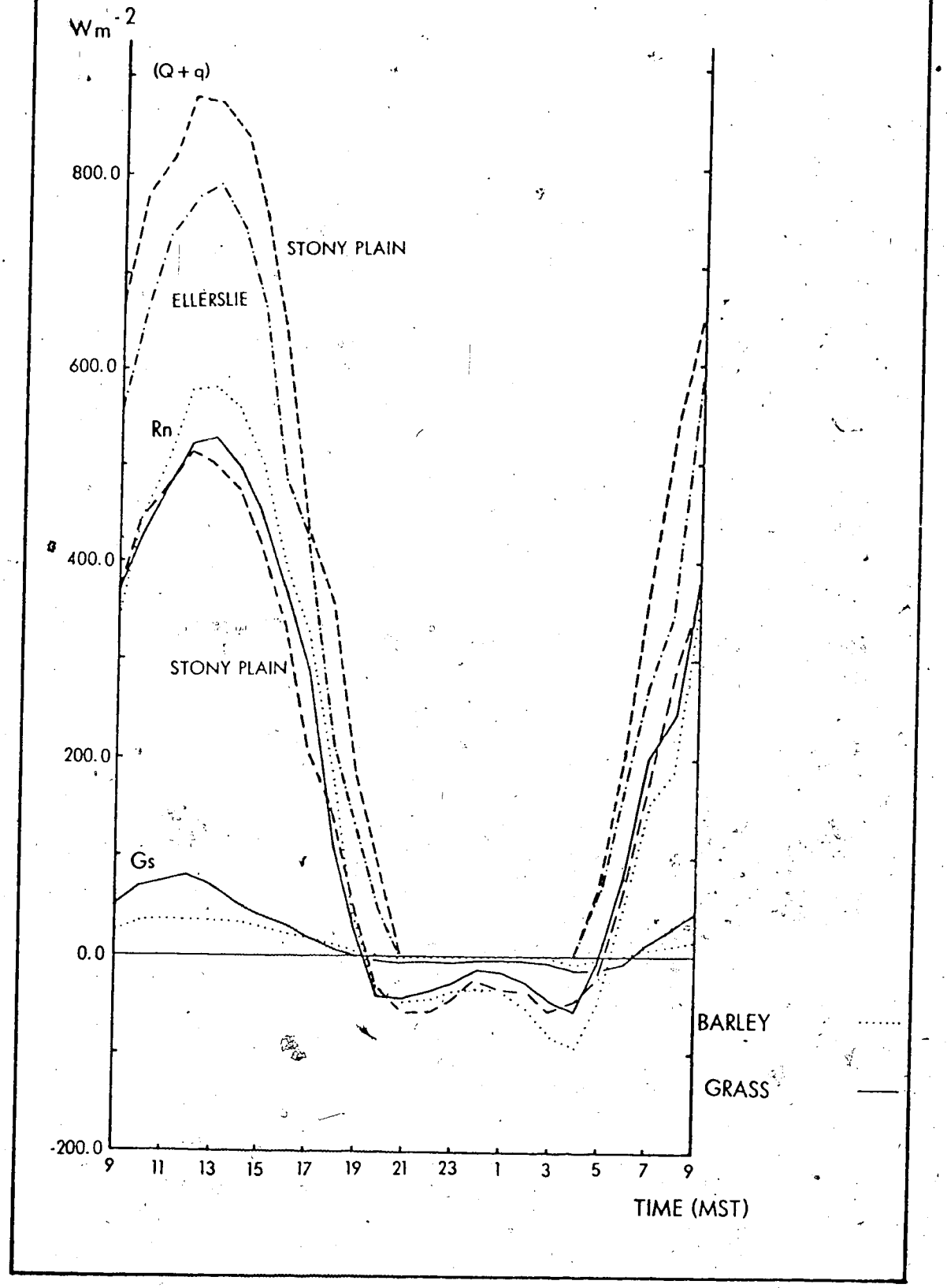

FIG. 5.9: SEPT. 17, 1976

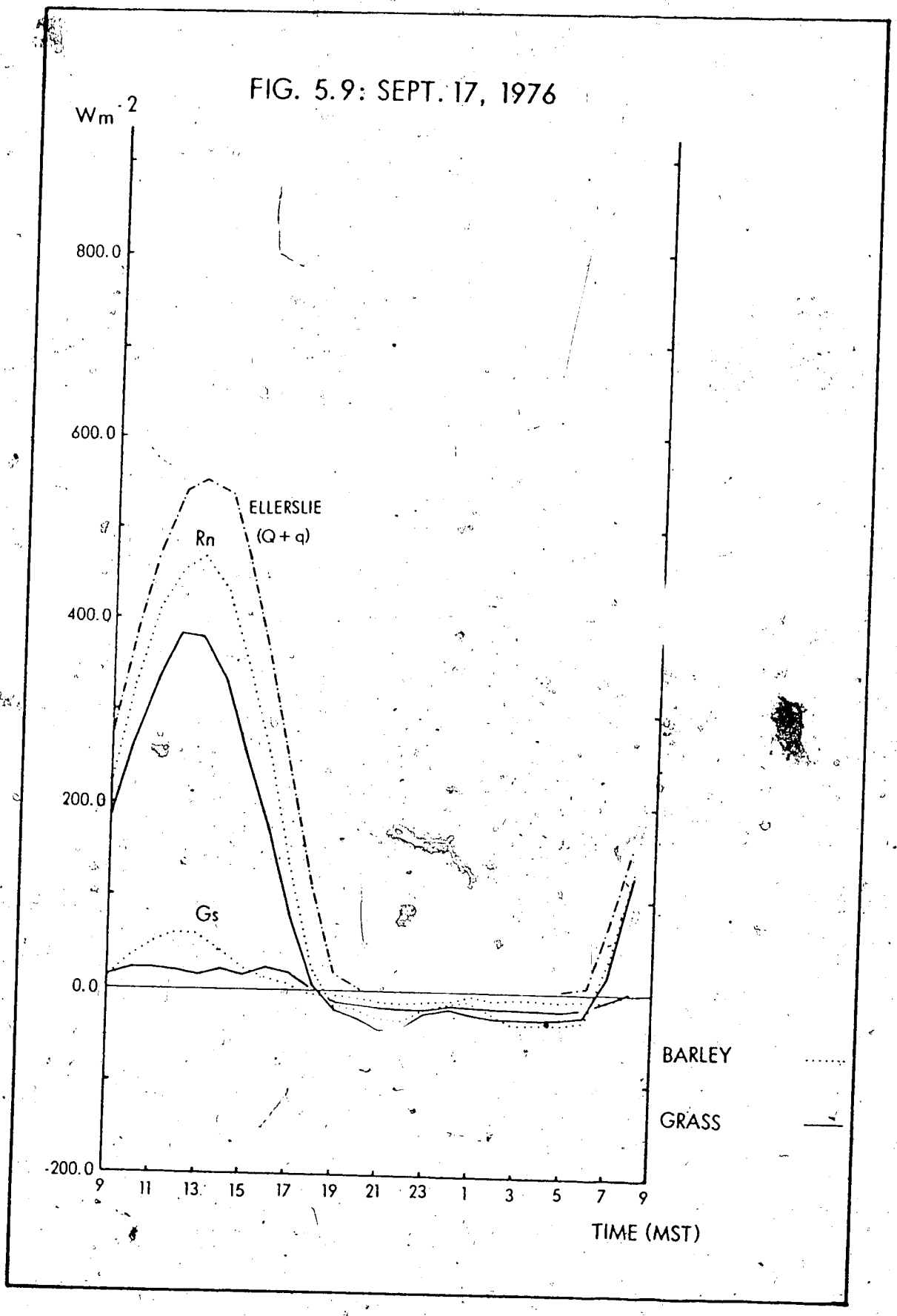

$$Gs = -K \frac{dT}{dZ} \qquad (5.1)$$ where $\frac{dT}{dZ}$ = temperature gradient

this should result in an increase in Gs in September since heat storage capacity is increased.[1] In July and late May, Gs values at B plot were reduced by the overlying plant cover, and low moisture levels, respectively. Nighttime soil heat losses were reduced somewhat due to the overlying plant cover.

F plot data for June 2, July 18, and September 18 (Figs. 5.10 - 5.12 respectively) illustrate the effect of F plot's variable weed cover on albedo, and consequently its Rn values. On June 2, maximum Rn values were as much as 150 Wm^{-2} higher than G plot's, while on September 18, the difference was only 50 Wm^{-2}. Ln emissions were generally greater at F plot, although on July 18, the heavy weed cover had an influence in equalizing the nighttime Ln on the two plots.

Certain other characteristics of the above diurnal variations can be noted. Many of the Rn curves show a peak at night. Time of occurrence varies with the plot, and with season. The seasonal variation is probably a consequence of prevailing weather, but the plot variations are interesting. F, PS and W recorded peaks 1 - 2 hours later than G plot (Figs. 5.10, 5.1 and 5.6) on June 2, June 19, and July 24 respectively. B and G recorded

---

[1] This is similar to energy transfer in a calm water body.

FIG. 5.10: JUNE 2, 1976

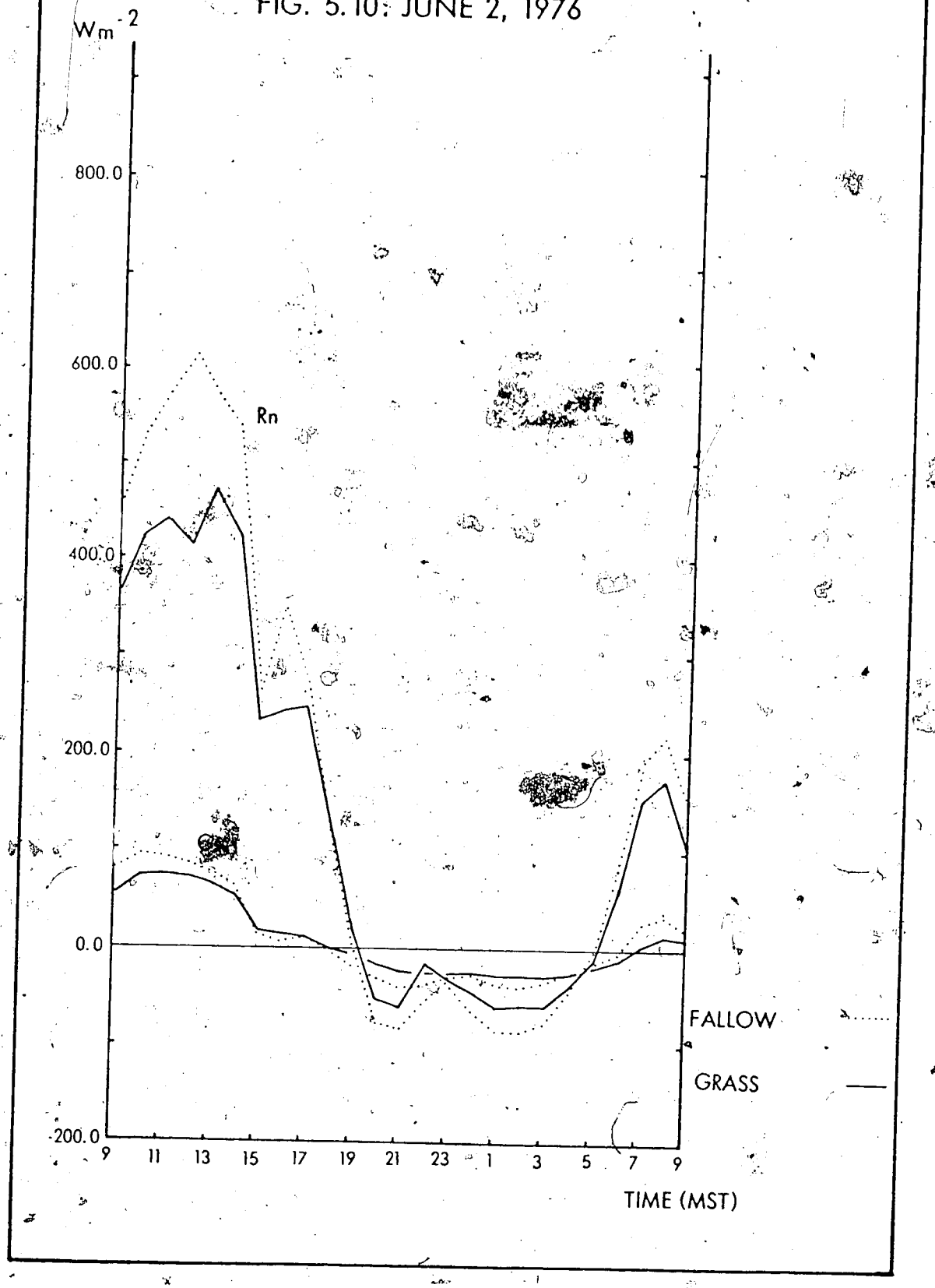

FIG. 5.11: JULY 18, 1976

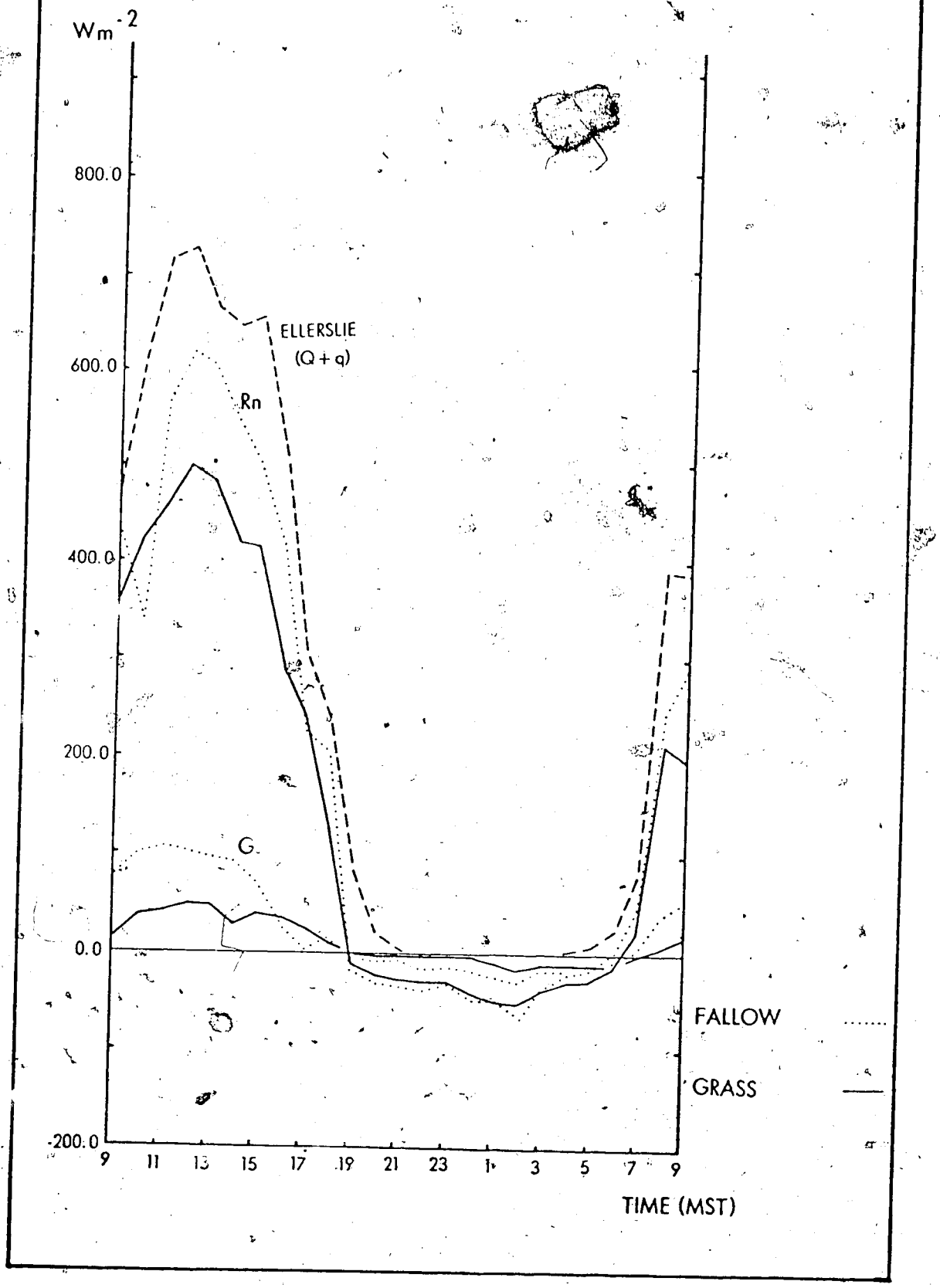

FIG. 5.12: SEPT. 18, 1976

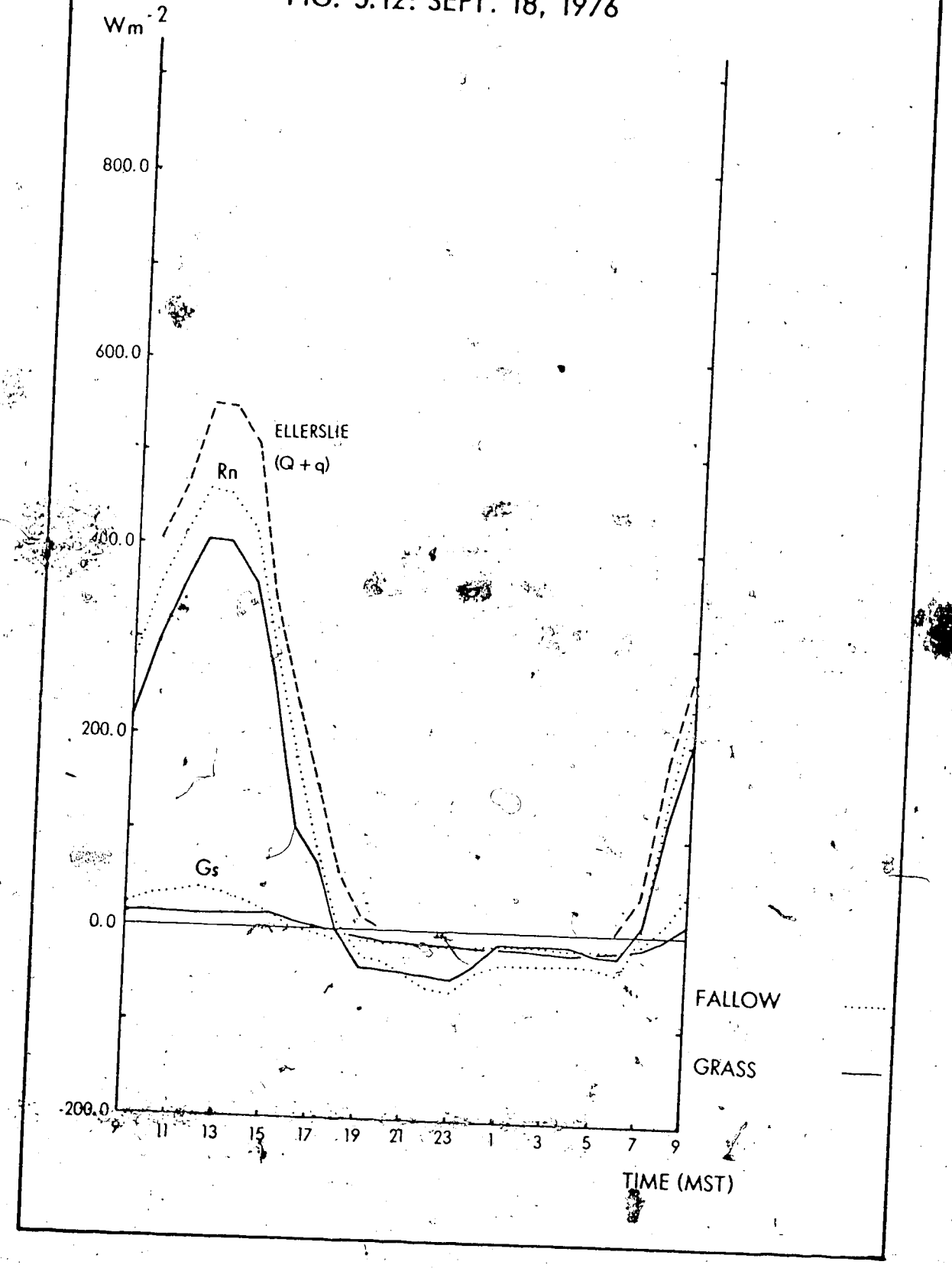

maximum Rn at similar times (Figs. 5.8 and 5.9). S plot showed little temporal variation with G. There does not appear to be a connection with nighttime Gs values, so this could be illustrating micro-scale differences in relative humidity. These differences are discussed in Section 5.2.4. Possible errors are examined in Section 5.2.5, including potential instrument calibration errors. Stony Plain (Q+q) and Rn data were inserted in Figs. 5.1 and 5.8 for that reason.

5.2.3 Net Radiation--Weekly Totals

Net radiation for G plot, the base station, was calculated from direct measurement during May 21 - August 3 and September 15 - October 7. During the intervening period from August 4 - September 14, Rn was derived from (Q+q) using eq. (2.6). Slope and intercept values are listed in Table 5.2, along with correlation (r), variance (r^2), standard error (S.E.), and level of significance (SIG). Slope and intercept fluctuations are in large part a result of variations in longwave emissions at night, and daytime albedo. Correlations and variance are very high, however, as are significance levels. Standard errors are less than 10% of average hourly values of). A reciprocal regression was computed as a check against unusual variations in the relationship between

TABLE [redacted]

Equation (2.6): Rn [redacted] q)+b

Date	Slope (a)	Intercept (b)	S.E.	r	r^2	SIG	N
7/20 - 22	0.74	-46.9	33.3	0.99	0.98	0.00001	72
7/26 - 29	0.70	-22.2	28.4	0.98	0.98	0.00001	110
7/31 - 8/2	0.76	-.8.6	33.0	0.98	0.95	0.00001	72
7/31 - 8/2*	1.25	+31.1	42.2	0.98	0.95	0.00001	72
9/15 - 17	0.76	-38.9	28.7	0.98	0.97	0.00001	72
9/18 - 21	0.77	-47.1	46.6	0.96	0.92	0.00001	[illegible]

N is number of hourly values used in the sample.
Asterisk (*) indicates reciprocal regression: $(Q+q) = a(Rn)+b$
Inverse of 0.76 = 1.31.

Rn and (Q+q). If the relationship is genuine, the slope should approximately equal the inverse of the slope using eq. (2.6). The inverse is listed in the table, and the slopes are within 0.06 of agreement.

A variation of eq. (2.6) was employed to predict Rn for the rotated plots, based on Rn data from G plot:

$$Rn\ (\text{rotated}) = a\{Rn(\text{G plot})\} + b \qquad (5.2)$$

Regression slopes and intercepts were computed at various times during the study period from paired data which consisted of simultaneous hourly measurements of Rn at G plot and at the rotated station. These were interpolated during intervening periods when the rotated set of instruments was measuring another plot.

Regression slopes and intercepts to be used in eq. (5.2) are listed in Table 5.3. With one exception, B plot on June 22 - 24, all correlations are greater than 0.90, and at least 80% of the variance is explained. The majority of standard errors range from 20.0 - 50.0 Wm^{-2}, with only four higher than 60.0 Wm^{-2} and one above 80.0 Wm^{-2}. On a percentage basis, most of the standard errors are similar to those calculated for eq. (2.6). An instrument malfunction during June 22 - 24 was the cause of the poor correlation and high standard errors calculated for this period. The slope and intercept were not used in subsequent calculations.

TABLE 5.3

REGRESSION SLOPES AND INTERCEPTS TO BE USED IN

Eq. (5.2): Rn(rotated) = a{Rn(G plot)}+b

Rotated Plot	Date	Slope (a)	Intercept (b)	S.E.	r	r^2	SIG*	N
PS	6/ 4 - 7	1.27	6.7 Wm^{-2}	44.1 Wm^{-2}	0.97	0.94	0.00001	96
	6/18 - 21	1.31	- 8.1	66.3	0.97	0.94		94
	7/ 9 - 12	1.18	-21.8	38.3	0.97	0.94		38
	8/ 4 - 8	1.42	- 7.0	89.3	0.93	0.87		46
	8/ 9 - 13	1.37	-29.8	59.9	0.97	0.94		84
	9/ 3 - 4	1.48	-23.9	44.7	0.98	0.96		47
	9/30 - 10/3	1.27	-65.3	58.2	0.93	0.86		76
	10/ 4 - 8	1.15	-24.6	67.4	0.91	0.82		59
S	6/11 - 14	1.14	0.6	50.1	0.97	0.95	0.00001	94
	6/29 - 7/1	1.24	- 1.8	39.8	0.99	0.98		66
	7/13 - 15	1.12	- 2.0	34.8	0.96	0.93		56

TABLE 5.3 (con't.)

Rotated Plot	Date	Slope (a)	Intercept (b)	S.E.	r	r^2	SIG*	N
S	7/27 - 30	1.26	- 7.0	31.7	0.98	0.97	0.00001	83
	7/31 - 8/2	1.16	- 6.7	24.4	0.99	0.98		72
	9/22 - 24	1.24	28.4	33.5	0.98	0.96		59
	9/25 - 27	1.21	25.9	16.9	1.00	0.99		72
W	5/28 - 31	1.24	- 5.1	36.7	0.99	0.97	0.00001	83
	6/15 - 17	1.13	19.0	64.3	0.96	0.92		45
	7/ 6 - 8	1.19	30.8	42.2	0.98	0.96		62
	7/23 - 26	1.23	17.3	[illegible]	0.99	0.99		95
	8/14 - 17	1.25	- 2.2	59.8	0.96	0.92		75
	9/10 - 11	1.30	- 0.7	34.6	0.99	0.98		17
B	5/22 - 24	1.20	- 1.1	39.3	0.98	0.96	0.00001	69
	5/25 - 27	1.18	- 7.9	26.1	0.99	0.98		72

TABLE 5.3 (con't.)

Rotated Plot	Date	Slope (a)	Intercept (b)	S.E.	r	r^2	SIG*	N
B	6/ 8 - 10	1.17	- 4.3	42.8	0.98	0.96	0.00001	70
	6/22 - 24	1.33	174.2	126.0	0.75	0.56	0.00043	16
	7/ 3 - 5	1.10	0.1	47.3	0.98	0.96		67
	7/20 - 22	1.12	18.9	24.4	1.00	0.99		71
	9/15 - 17	1.15	8.0	24.7	0.99	0.98		49
F	6/ 1 - 3	1.29	5.3	36.1	0.99	0.97	0.00001	70
	6/25 - 28	1.16	- 6.2	45.8	0.96	0.93		90
	7/16 - 19	1.21	4.8	36.8	0.99	0.98		87
	8/29 - 9/2	1.24	5.1	37.4	0.98	0.97		120
	9/18 - 21	1.14	15.2	34.8	0.98	0.97		89

* All SIG. levels at 0.00001 unless otherwise noted. Numbers are rounded.

Slopes ranged from 1.10 - 1.48. B plot registered the lowest ones, an indication that its albedo was the closest to G plot of all rotated stations. PS plot had the highest slopes, as well as high negative intercepts which slightly reduced Rn values. However, Rn values remained higher than those on S, W, and F plots since intercepts accounted for only 0.3 - 0.5% of Rn. Results for F plot were influenced by the same factors which affected its albedo; a dry crusty surface and extensive weed cover, both of which established themselves rapidly while the plot was undisturbed. Continuous tillage and weeding would probably have reduced the albedo, resulting in higher Rn values, and hence, higher regression slopes. Lower albedo values for W plot during September affected its slope, while S plot's slope was influenced more by changes in G plot's albedo rather than its own. PS plot represents a more complicated situation, due to the nature of its stand structure, and seasonal variations in leaf canopy density. Multiple reflection and absorption always reduce the albedo of a deep stand of vegetation. However, the albedo of an individual leaf is much higher, so leaf angle, sun angle, and foliage arrangement can temper the albedo reduction.

Calculated mean daily Rn for 5 - 9 day periods, using eq. (5.2), are listed in Table 5.4 and illustrated in Fig. 5.13. F plot had the highest values in late

TABLE 5.4

MEAN DAILY Rn

(1000 [illegible] day^{-1})

Date Period Ending	PS	S	W	B	F	G
5/27	168.3	164.3	177.7	163.9	183.6	138.1
6/3	174.8	164.7	172.9	164.6	180.2	139.6
10	188.3	171.8	176.4	173.2	18[illegible]7	148.1
17	240.6	212.7	211.2	214.4	229.4	186.5
24	218.7	198.8	192.7	187.1	198.8	167.1
7/1	209.5	204.8	194.0	181.8	191.5	165.2
8	259.0	250.9	253.8	234.1	250.9	212.7
15	214.1	200.8	215.8	199.4	215.2	179.3
22	254.8	236.8	247.6	227.3	245.1	202.5
29	233.3	212.6	214.9	195.7	211.1	174.4
8/6	178.4	152.0	155.0	141.3	153.6	125.8
12	235.2	208.3	213.6	193.2	210.2	172.2

TABLE 5.4 (con't.)

Date Period Ending	PS	S	W	B	F	G
8/19	211.8	183.7	188.1	171.9	186.8	151.8
28	237.0	202.6	209.1	189.1	205.9	167.3
9/2	269.5	227.6	234.7	212.4	231.1	186.3
9	215.9	178.8	187.2	-	177.1	-
10	-	-	-	168.1	-	145.0
16	150.6	129.6	137.5	114.5	124.1	99.4
23	144.0	130.5	139.5	123.7	121.8	106.5
30	111.4	106.9	115.8	101.2	98.0	87.1
10/7	72.9	74.7	81.3	71.1	67.2	60.6
20 week mean	198.4	179.9	185.2	171.1	182.6	150.6

Numbers are rounded.
Means calculated from 5 - 9 day totals.

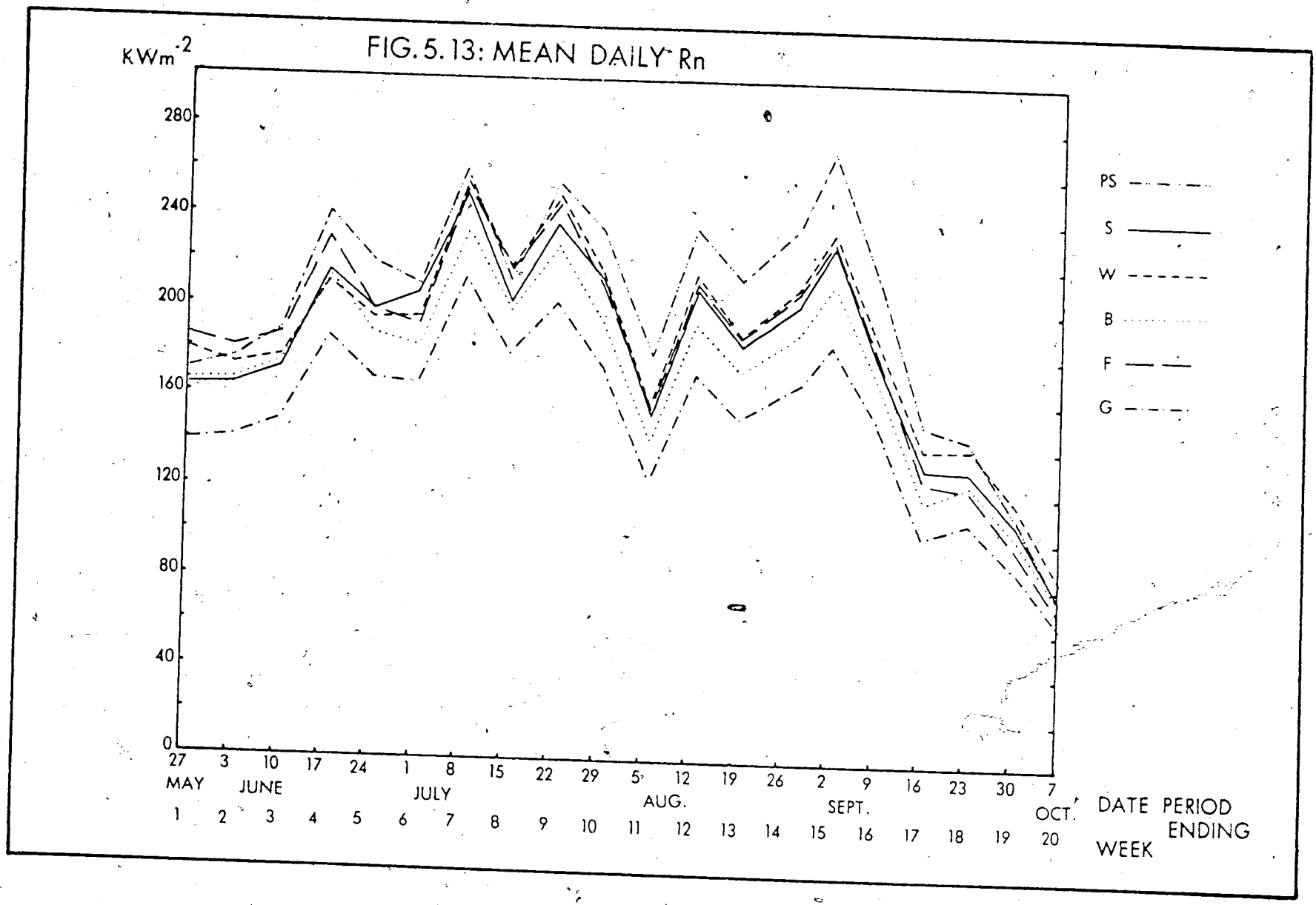
FIG. 5.13: MEAN DAILY Rn
KWm-2
280
240
200
160
120
80
40
0
PS
S
W
B
F
G
27 3 10 17 24 1 8 15 22 29 5 12 19 26 2 9 16 23 30 7
MAY JUNE JULY AUG. SEPT. OCT.
1 2 3 4 5 6 7 8 9 10 11 12 13 14 15 16 17 18 19 20
DATE PERIOD ENDING
WEEK

May and early June, but PS plot took the top rank on June 10, and maintained this position throughout much of the season. G plot had the lowest values during the entire period. The difference between G and PS ranged from a low of 12,000 $Wm^{-2}day^{-1}$ at the beginning of October to 60,000 $Wm^{-2}day^{-1}$ during the first week of September. Significant differences occurred during much of August, as PS absorbed 20,000 - 40,000 $Wm^{-2}day^{-1}$ more energy than W, F, and S plots, which were themselves 20,000 - 30,000 $Wm^{-2}day^{-1}$ higher than B and G plots. Again, the factors which must have had an influence were plant structure and surface conditions which affected the plots' albedo values. F plot's ranking during the first two weeks of the study period illustrates the potential this surface has for absorbing radiant energy if weeding and tillage are maintained. Although this increase in energy might have increased evaporation, the weeds could very easily consume as much if not more soil water, and their roots would be able to draw water from greater depths than would evaporation alone over a short time period. At this point, the idea is purely speculative. However, a detailed examination of Rn differences between the plots, and the partitioning of Rn into its various components, especially LE, will go a long way towards settling this and other issues.

5.2.4 Radiation Balance

Radiation balance was calculated for all plots on the basis of albedo, global solar radiation, and net radiation data presented in previous sections. Results are listed in Table 5.5.

Differences in the prevailing weather of each selected period are apparent in the results. Ln values were close to 0 in August, illustrating the influence of this period's humid conditions. Comparatively drier conditions during the other 3 periods allowed greater emissions of longwave radiation from the various surfaces.

Significant variation between the plots is apparent as well. G and F plots emitted the greatest amount of longwave radiation in June and August. They had to share top rank in July with S plot, while most plots had similar longwave emissions in September. The plots with the lowest emissions were B and PS in June, W and B in July, and PS in August and September.

Upon closer examination of the calculations, it is readily apparent that the main factors which are influencing these emission differences are stand structure and growth characteristics. PS plot's canopy, which allowed greater radiation absorption to take place, is also reducing longwave emissions. The various leaf layers

TABLE 5.5

RADIATION BALANCE (1000 $Wm^{-2}day^{-1}$)

RESULTS OF Eq. (2.4): $Rn = (Q+q)(1-\alpha)\pm Ln$

DATE	PS	S	W
6/16 - 30	214 = 342(1-0.14)-80	202 = 342(1-0.14)-92	193 = 342(1-0.18)-87
7/ 1 - 31	235 = 341(1-0.13)-62	220 = 341(1-0.13)-77	227 = 341(1-0.20)-46
8/ 1 - 31	223 = 241(1-0.13)+13	192 = 241(1-0.13)-18	198 = 241(1-0.18)-0
9/ 1 - 10/7	146 = 212(1-0.11)-43	130 = 212(1-0.13)-54	138 = 212(1-0.10)-53

TABLE 5.5 (con't.)

DATE	B	F	G
6/16 - 30	184 = 342(1-0.24)-76	200 = 342(1-0.07)-118	166 = 342(1-0.18)-114
7/ 1 - 31	208 = 341(1-0.24)-51	224 = 341(1-0.14)-69	187 = 341(1-0.23)-76
8/ 1 - 31	179 = 241(1-0.23)-7	195 = 241(1-0.12)-17	159 = 241(1-0.24*)-24
9/ 1 - 10/7	122 = 212(1-0.18)-52	124 = 212(1-0.15)-56	106 = 212(1-0.25)-53

Asterisk (*) indicates assumed albedo value.
Numbers are rounded.
Negative Ln indicates outgoing longwave radiation. Positive values indicate incoming

readily absorb these emissions and reradiate them to the cooler surface below. This effectively reduces vertical temperature gradients above the canopy, while a temperature inversion develops below, especially during clear daytime periods. The positive value calculated for August is probably a result of the combination of prevailing humid weather and the above structural effects. Had air temperature data been available for the canopy layer itself (rather than the plot's floor), temperatures warmer than the other plots would have been recorded this month. Previous studies in larger deciduous forests have shown the crown to be as much as 6°C warmer than the floor, depending on time of day, species, and stand age and density (Geiger, 1965). Although this large magnitude of temperature gradient would not happen in PS plot (since the stand is small and young), the radiation balance results indicate that if the plot was a larger stand, substantial temperature increases in the crown area would result. This is definitely a topic for further study at Ellerslie.

Similarly, S plot's canopy structure is influencing its longwave emissions and subsequent air temperature. However, stand height is lower, and density is greater than at PS plot. The air temperatures here were actually measured in the lower part of the crown. Consequently, these were consistently higher than PS plot's temperatures. The greater longwave emissions are an indication of the

comparative dryness of the air above S plot, as opposed to PS. This is not surprising considering the fact that PS is probably transpiring at a greater rate than S. Soil moisture utilization is illustrated in Section 5.3.1.

B plot's changing state of health is well illustrated in these results. In June and July, the actively transpiring crop had one of the lowest emission rates. By September, longwave emission was similar to the other plots, indicating a sharp reduction in water use.

W plot, the other deciduous cover, had lower emissions than PS plot during July, but ranks were reversed in June, August and September. This indicates a difference in length of active growth period. While PS remained active until well into the autumn, W started to lose its leaves during the first week of September, and its soil moisture levels showed a large increase during the last week of August.

G and F plots showed similar emissions throughout the study period. G plot's emissions during July and August were higher due to F plot's heavy weed cover and lower albedo, which combined to produce higher water losses due to transpiration and evaporation. The weed cover also reduced F plot's emissivity. At wavelengths shorter than 2.4 microns, many plants have lower emissivities than moist bare ground (Sellers, 1965, p. 41).

5.2.5 Errors and Analysis

Several sources of potential error exist when measuring and deriving radiation balance components. These include instrument placement, recorder reference points, calibrations, data extraction, and calculation errors.

Accurate data require that the instrumentation be properly maintained, and that the radiation sensor should have an unobstructed field of view. The height of the sensor varies with the size of the plot, and if the plot is small, this height must be reduced so that the instrument senses only the desired area. The only plot which posed certain difficulties in instrument placement was PS, since the instrument tower did not have sufficient height to completely clear the canopy. The instruments generally had unobstructed views of the sun during all periods but those with very low sun angles. Since radiation intensity during low sun angle periods is small compared to total incoming radiation, this error is not considered significant when calculating daily and weekly totals. In fact, a reduction in incoming radiation to the sensor should have decreased Rn values, and results show that PS had the highest Rn of the six plots, for most of the study period. The October diurnal graph (Fig. 5.2) shows Rn at PS to be

lower than at G. However, Table 5.3 reveals that the slope of the regression line is still greater than 1.0. As previously mentioned, the diurnal variations should not be considered as representative of much longer time periods, especially in autumn when PS is undergoing rapid leaf loss.

Albedo measurements at F plot posed a different problem, since F was affected by human activity such as weeding and tillage. As explained in Section 5.2.1, this factor is important to the plot's albedo, thereby making the date of measurement equally important. This will affect the results of eq. (2.4), specifically Ln, but the exact magnitude is unknown. A measurement error greater than $\pm 5\%$ is not expected. Thus, the maximum potential error would be found in June's Ln values, since (Q+q) - Rn is greatest. However, the seasonal total of this error should be small, since measurements were effected on widely separated dates (see Table 5.3) and over various surface conditions.

All instruments were factory or laboratory calibrated, and these should have been fairly consistent throughout the measurement period. In fact, the Eppley pyranometer measuring albedo was brand new. The digital counter being utilized to monitor (Q+q) was abandoned in favour of data extraction from the strip charts when it was suspected that the digital was not functioning

properly on days with low incoming (Q+q). The digital error is illustrated in Appendix 2.

Potential calibration errors were checked by comparing (Q+q) and Rn over G plot with published data obtained from Stony Plain (lat. 53° 33'N, long. 114° 06'W). While planning the field program, the idea of using Stony Plain data directly was discussed, but discarded in favour of direct measurement at Ellerslie because of potential differences in prevailing weather and its associated cloud cover. Table 5.6 illustrates the data difference between the two stations. The Rn differences could be indicating a combination of variations in prevailing weather and station surface albedo and Ln, as well as instrument calibration error. The surface effects would not be a factor in the (Q+q) differences. The significance of the error on this difference is hard to determine. It is quite likely that there is a calibration error, but it would appear that this is within acceptable limits, considering the fact that instrument errors of 5 - 15% are common. Subsequent detailed analysis will employ 2 week totals so that random variation can be reduced, and since the same data are employed for all rotated plots, this will not affect any differences calculated between them. Interestingly enough, if the Ellerslie (Q+q) were to be raised by 11%, albedos would be lowered 2 - 3% since the denominator of the fraction would be increased, and this change could create

TABLE 5.6

G PLOT, ELLERSLIE VS STONY PLAIN

Rn (1000 $Wm^{-2}day^{-1}$)

Date	Ellerslie	Stony Plain	Difference
6/1 - 30	177.0	168.7	+ 5%
7/1 - 31	186.2	170.8	+ 9%
8/1 - 31	159.4	136.0	+17%
Sum	522.6	476.5	+10%

(Q+q) (1000 $Wm^{-2}day^{-1}$)

6/1 - 30	311.4	339.6	- 8%
7/1 - 31	340.6	369.2	- 8%
8/1 - 31	240.5	291.0	-18%
Sum	892.5	999.8	-11%

Monthly totals adjusted for missing days.
Stony Plain Data Source: Monthly Radiation Summaries, Environment Canada.

somewhat questionable results, especially for PS and C plots.

The Rustrak strip chart recorders also presented a problem. Their calibrations and reference points were periodically checked while the recorders were operating in the field, but since these are battery powered, the reference points may vary with the strength of the battery. Battery power was continuously monitored, however, and recorder reference points were checked so as to ensure proper strip chart analysis.

Other errors in strip chart analysis are human in origin. Random error is expected, but if it is random, the sum total of the error over daily or weekly periods should approximately equal 0. Comparisons of strip chart analysis for the same 9 day period, completed on separate occasions by the author and Dr. Hage of the Geography Department, reveal a difference of 0.118 chart units on a chart scale of 100 units. The error is thus considered to be random.

Calculation errors are also human in origin, but these should be random as well. Major errors would reveal themselves upon comparison of measurement results against known norms.

Having considered the error possibilities, one may explain the radiation balance data for each plot, at least on a comparative basis, with those data obtained from other

plots. Equal amounts of global solar radiation were available for each surface cover at the same time. But Table 5.5 reveals marked differences as to how much of this energy was stored for later use by the various surfaces. PS plot consistently recorded the highest Rn values and the lowest outgoing longwave radiation emissions except for the first and last two weeks of the study. F and G plots had the highest emissions. Rn differences were quite large, and in some cases exceeded 60,000 $Wm^{-2}day^{-1}$. An imbalance has now been created, and this could affect water use and the other components of the energy balance. Therefore, it is anticipated that major differences in energy balance will be calculated for the various plots, and these may contribute to the differences in air and soil temperature and soil moisture which were observed during the study.

5.3 Energy Balance

5.3.1 LE

ΔPW and cumulative ΔPW are illustrated in Figs. 5.14 and 5.15 respectively. Results of eq. (2.12) are listed in Table 5.7 and illustrated in Fig. 5.16. Included in the figures are weekly rainfall data, and in Fig. 5.16, dates of human activity on F plot.

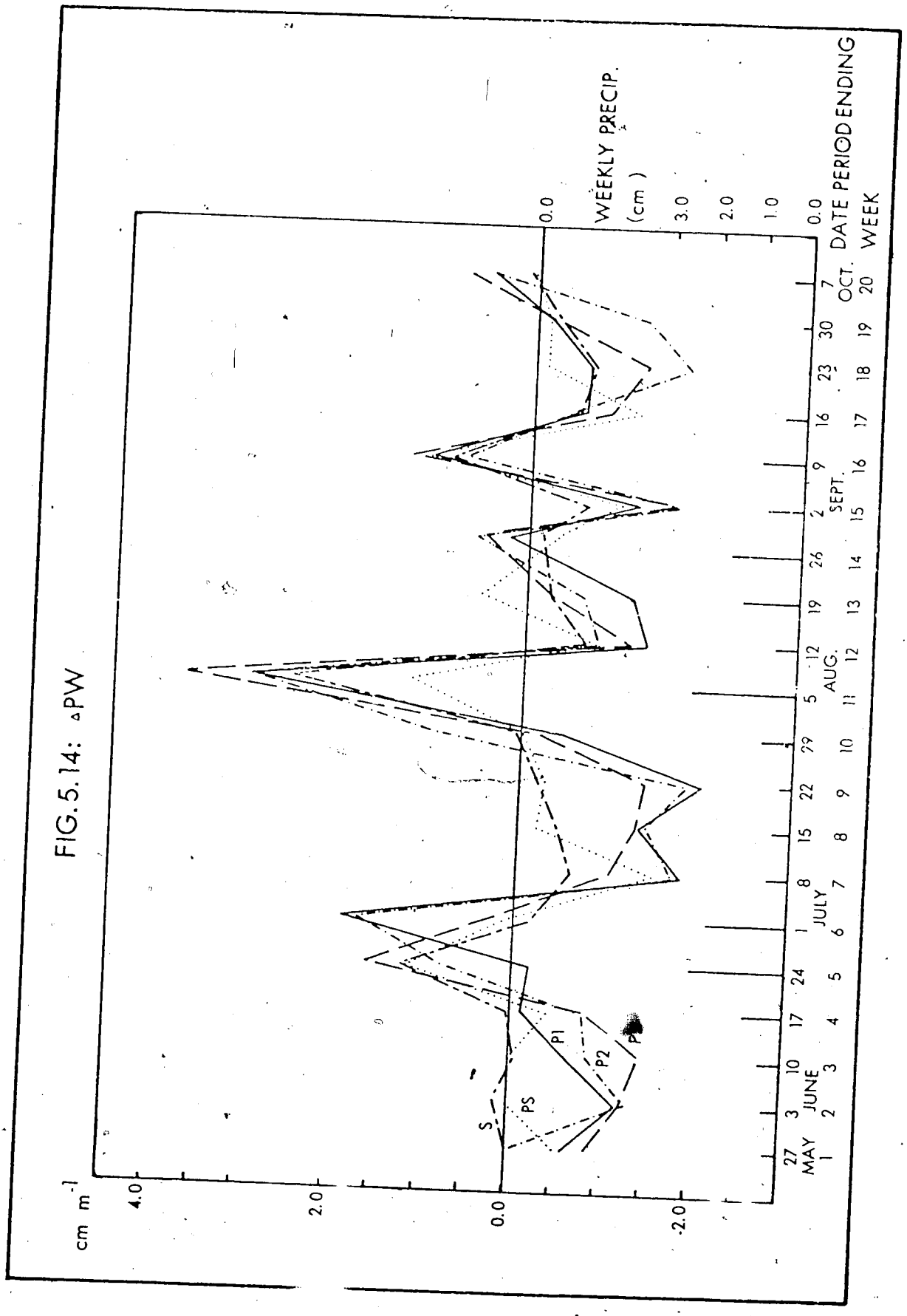
cm m⁻¹
4.0
2.0
0.0
-2.0
S
PS
P1
P2
P3
27 MAY
1 2 3 10 17 24
JUNE
1 8 15 22 29
JULY
5 12 19 26
AUG.
2 9 16 23 30
SEPT.
7 14 21 28
OCT.
DATE PERIOD ENDING
WEEK
1 2 3 4 5 6 7 8 9 10 11 12 13 14 15 16 17 18 19 20
WEEKLY PRECIP. (cm)
0.0
1.0
2.0
3.0
0.0

FIG. 5.14: ΔPW

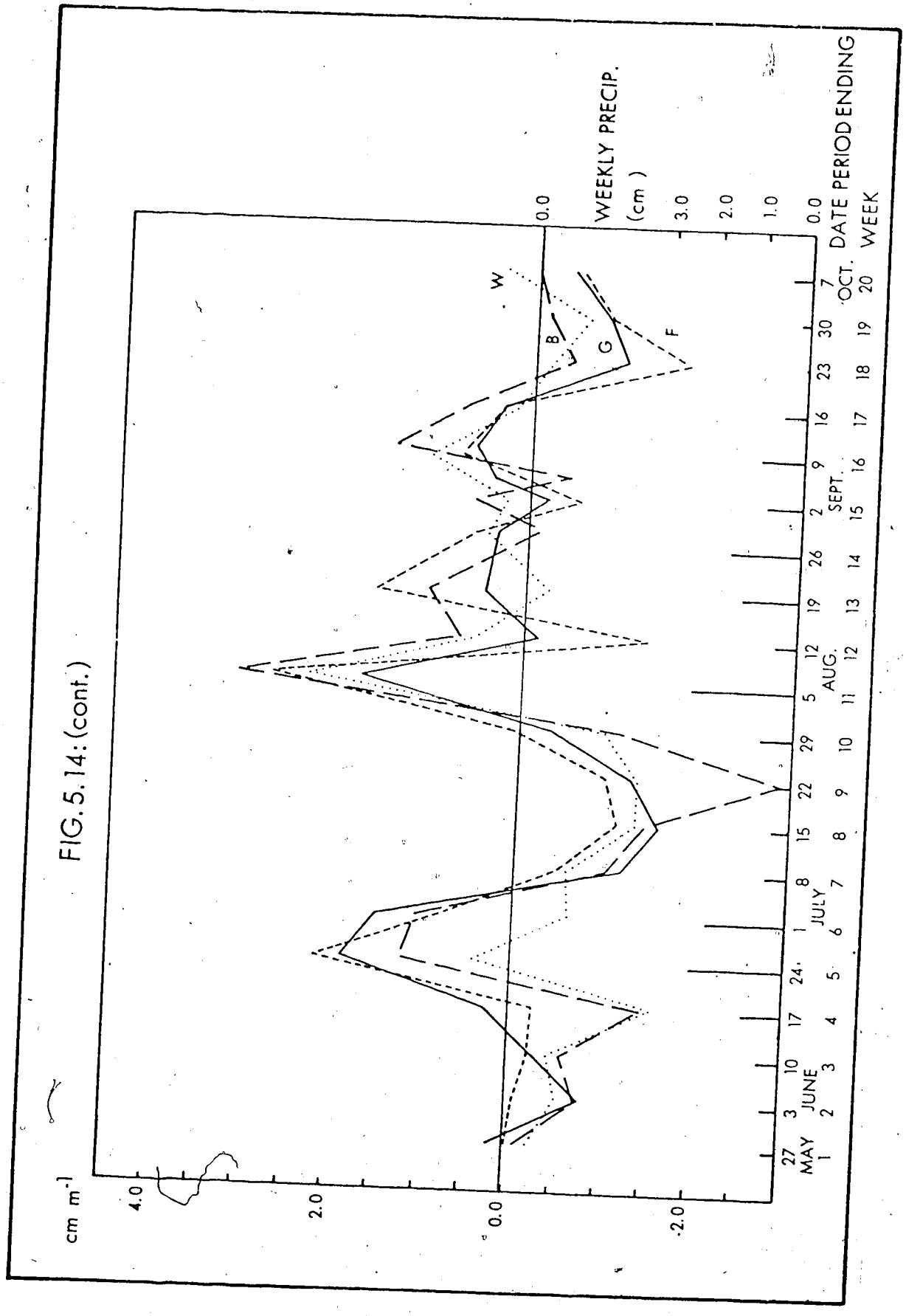
cm m⁻¹
4.0
2.0
0.0
-2.0
27 MAY
3 JUNE
10
17
24
1 JULY
8
15
22
29
5 AUG.
12
19
26
2 SEPT.
9
16
23
30
7 OCT.
DATE PERIOD ENDING
WEEK
1 2 3 4 5 6 7 8 9 10 11 12 13 14 15 16 17 18 19 20
WEEKLY PRECIP. (cm)
0.0
1.0
2.0
3.0
W
B
G
F

FIG. 5.14: (cont.)

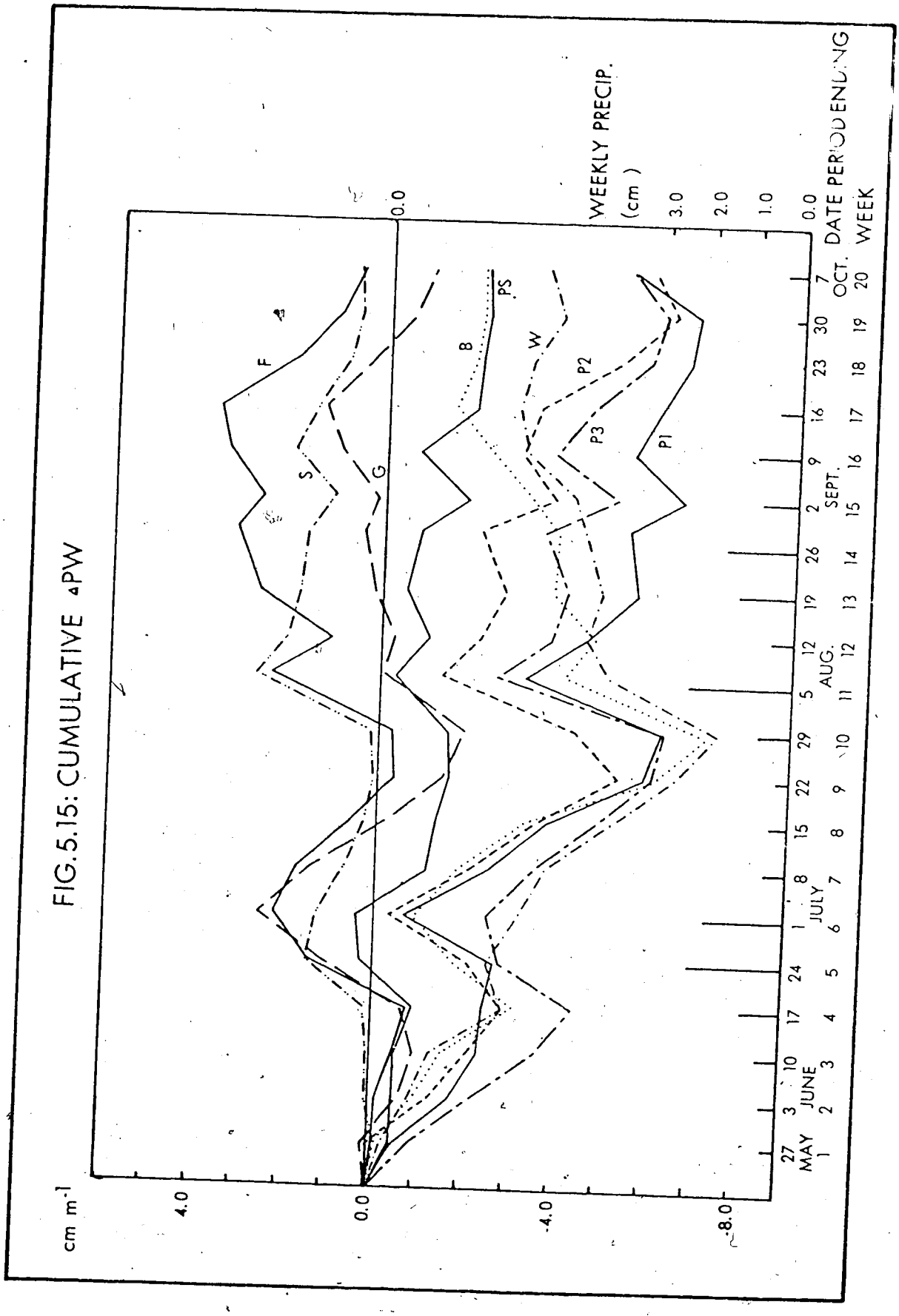
FIG.5.15: CUMULATIVE ΔPW
cm m⁻¹
4.0
0.0
-4.0
-8.0
F
S
G
B
PS
W
P2
P3
P1
WEEKLY PRECIP. (cm)
3.0
2.0
1.0
0.0
27 MAY 1 2 3 JUNE 3 10 17 24 1 JULY 6 7 8 15 22 29 5 AUG. 11 12 12 19 26 2 SEPT. 9 16 15 16 17 18 23 30 7 OCT. 19 20
WEEK
DATE PERIOD ENDING

TABLE 5.7

MEAN DAILY LE (1000 $Wm^{-2}day^{-1}$)

Date Period Ending	PS	S	W	B	F	G	P
5/27	65.3	36.3	50.9	41.6	39.8	26.3	62.8
6/3	40.6	32.9	76.5	91.2	48.2	91.7	114.5
10	53.5	55.6	80.8	89.0	70.3	70.3	110.8
17	119.4	94.3	189.1	183.8	113.6	80.8	130.4
24	173.9	169.2	217.8	168.6	115.3	134.7	198.9
7/1	196.7	209.0	241.8	142.3	155.7	115.9	124.5
8	140.5	86.6	87.8	113.0	83.1	124.1	139.3
15	59.1	72.0	128.8	131.7	113.6	142.3	125.9
22	43.9	42.5	110.1	202.0	86.1	104.8	130.3
29	90.2	86.6	114.6	153.4	85.5	111.8	84.9
8/6	169.6	98.4	109.1	68.8	91.3	139.7	65.7
12	108.6	104.0	23.8	104.0	150.2	70.0	132.3

TABLE 5.7 (con't.)

Date Period Ending	PS	S	W	B	F	G	P
8/19	116.5	162.0	163.7	86.8	53.6	123.5	186.1
28	155.3	146.6	120.2	147.1	115.2	127.5	121.0
9/2	195.1	162.3	95.9	64.7	159.8	134.4	228.7
9	46.5	59.4	48.2	-	68.8	-	49.0
10	-	-	-	44.8	-	49.4	-
16	122.3	81.7	42.3	12.4	35.3	44.6	86.5
23	5.9	38.8	14.1	25.2	98.9	63.2	69.0
30	22.2	28.1	50.3	22.2	67.3	63.2	47.0
10/7	45.5	44.3	31.3	50.2	79.2	75.6	14.6
20 week mean	94.9	90.3	102.3	98.3	89.6	95.1	109.1

Numbers are rounded.
Means calculated from 5 - 9 day totals.
Mean values for P were calculated from P1, P2, and P3 data.

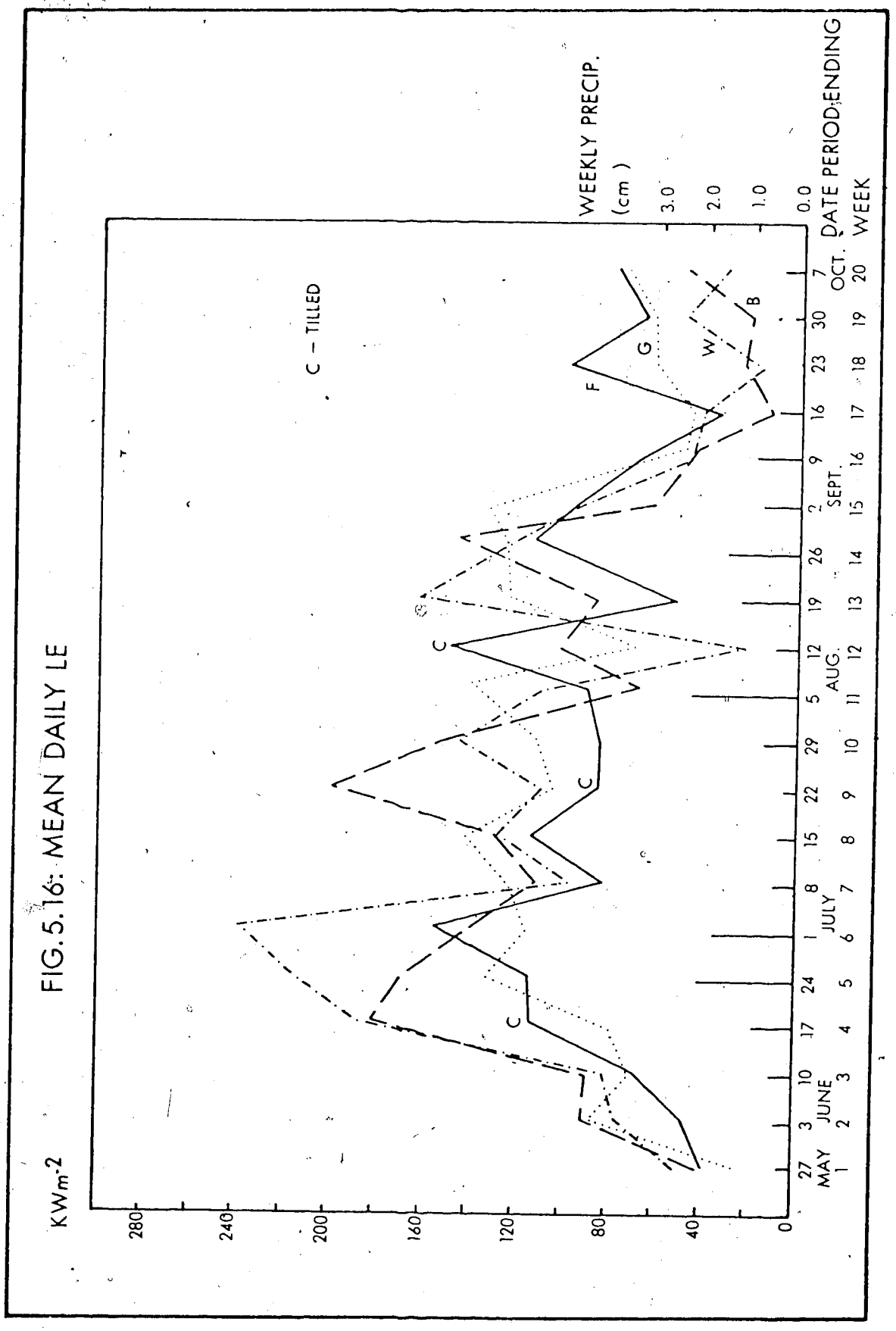

FIG. 5.16: MEAN DAILY LE

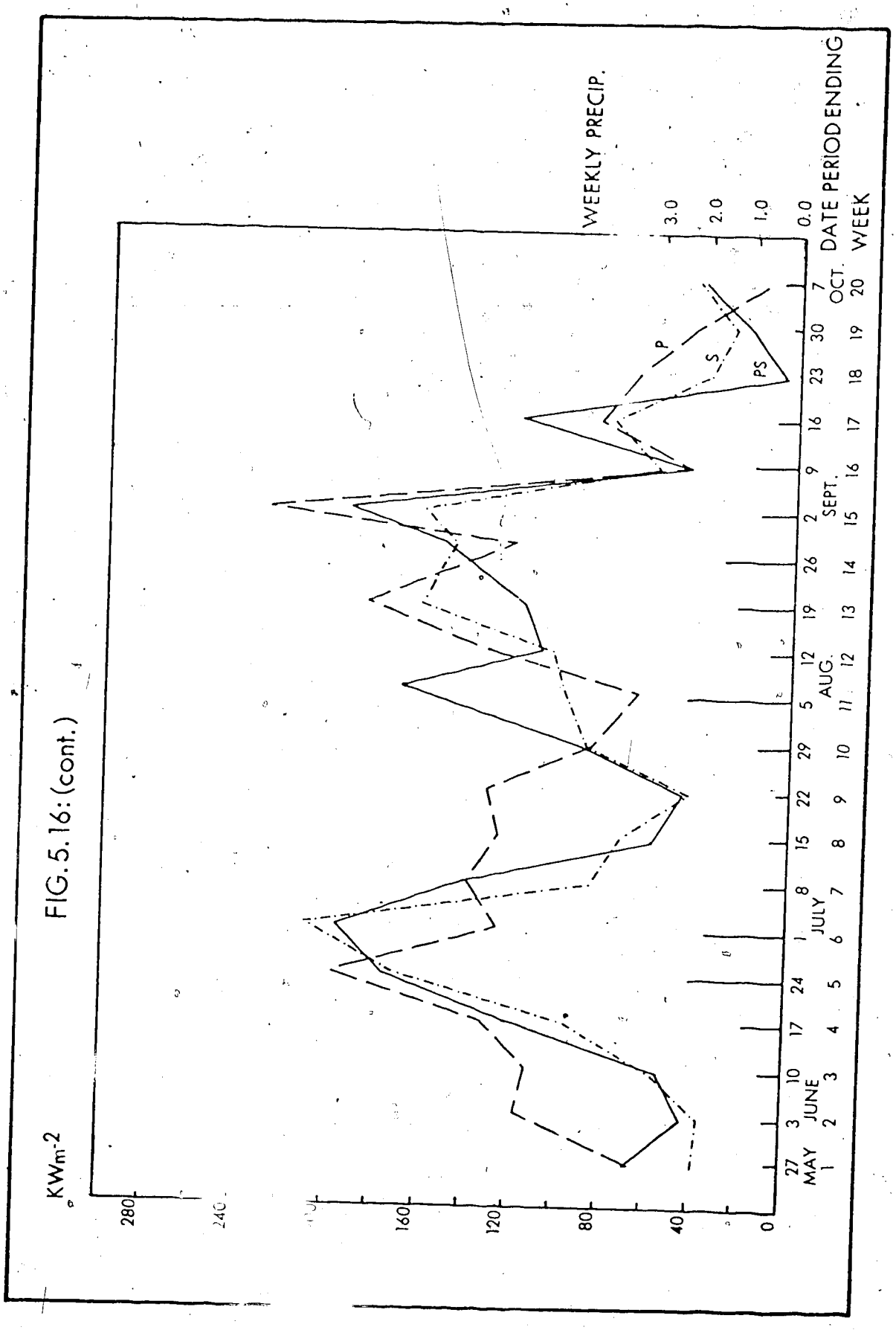
KWm-2
280
240
160
120
80
40
0
WEEKLY PRECIP.
3.0
2.0
1.0
0.0
P
S
PS
27 3 10 17 24 1 8 15 22 29 5 12 19 26 2 9 16 23 30 7 14 21 28
MAY JUNE JULY AUG. SEPT. OCT.
1 2 3 4 5 6 7 8 9 10 11 12 13 14 15 16 17 18 19 20
DATE PERIOD ENDING WEEK

FIG. 5.16: (cont.)

In general, all plots had reasonably similar LE values at the commencement of data collection. Most plots reached a peak at the end of June. However, subsequent calculations show the plot results diverging as the summer progressed. Although large scale divergence is not readily apparent in the ΔPW curves (except in mid-July), the cumulative curves reveal large variations between the plots at the start of the study. At this point, it is interesting to note the similarity in trends that most of the curves appear to follow after June 17, although it must be remembered that the plots started the growing season with different amounts of soil moisture, which would affect both ΔPW and cumulative ΔPW. However, the same cannot be said for the LE curves. Reactions to weather events were inconsistent, and overall trends are difficult to see, except for a general downward trend from September 2 until October. Similar fluctuations exist in the LE/Rn curves (Fig. 5.17).

Regression analysis revealed few significant linear relationships between the various plots' LE and LE/Rn values (Table 5.8). Correlations were fair for PS vs S and PS vs W, but it would be difficult to arrive at any conclusions based on these results, especially when one considers that the magnitude of the standard errors in the LE relationships often exceed 30% of the 20 week mean, and

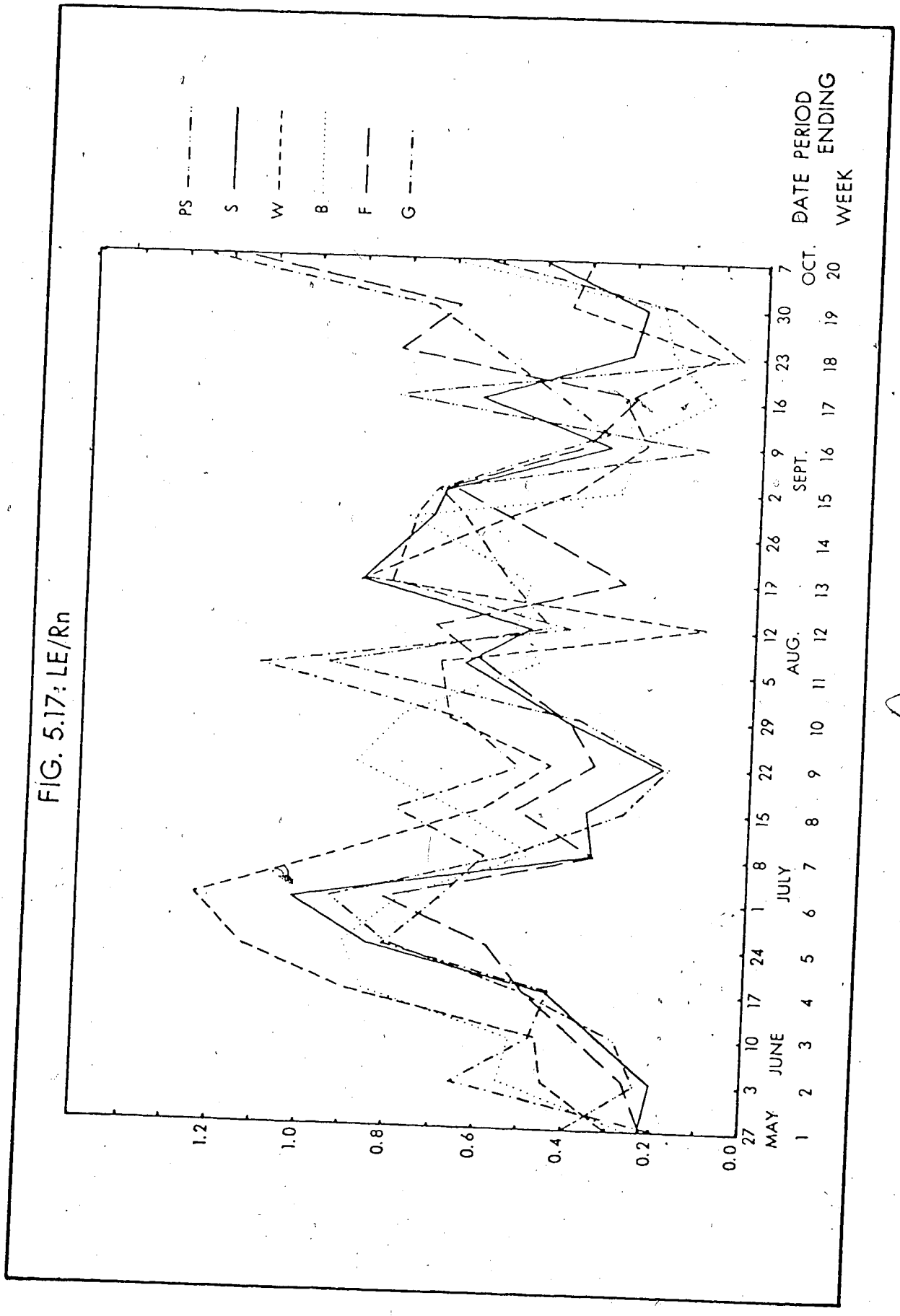
PS
S
W
B
F
G
1.2
1.0
0.8
0.6
0.4
0.2
0.0
MAY
JUNE
JULY
AUG.
SEPT.
OCT.
DATE PERIOD ENDING
WEEK

FIG. 5.17: LE/Rn

TABLE 5.8

REGRESSION OF LE AND LE/Rn

Parameter	x	y	Slope	Inter.	r	r^2	S.E.	SIG
LE	PS	S	0.80	13403.9	0.89	0.80	25354	0.00001
	PS	W	0.68	39236.7	0.63	0.40	52485	0.00245
	G	B			0.44	0.19	50355	0.03508
	G	F			0.36	0.13	35457	0.07352
	G	W	1.35	-30232.3	0.61	0.37	53862	0.00384
LE/Rn	PS	S	0.82	0.1	0.84	0.71	0.1	0.00001
	PS	W	0.73	0.2	0.61	0.37	0.3	0.00371
	G	B			0.17	0.03	0.2	0.25040
	G	F			0.56	0.32	0.2	0.00764
	G	W			0.27	0.07	0.3	0.13820

Regression analysis based on Table 5.7 and Fig. 5.17. Periods ending on September 9, 10, and 16 were not used since there were temporal inequalities between the plots.

LE intercepts and standard errors are in $Wm^{-2}day^{-1}$.

Slopes and intercepts listed only for relationships with $r>0.6$.

less than 50% of the variance is explained for all but the PS vs S case.

It is apparent that no simple relationship exists between the plots' LE values, nor can LE be linearly related to the plots' respective Rn values. This is in agreement with Davies (1972), who states that LE/Rn is not a general indicator of soil moisture. Therefore, more detailed analysis is required before any conclusions regarding soil water use can be reached.

5.3.2 Gs

Soil heat flux for G plot was calculated from direct measurement during May 21 - August 12 and September 17 - October 7. During the intervening period from August 13 - September 17, Gs at G plot was estimated by employing Gs/Rn ratios calculated before and after this period.[1] Data calculations followed a procedure similar to eq. (5.2) using regression slopes and intercepts:

$$Gs\ (\text{rotated}) = a\{Gs(\text{G plot})\} + b \qquad (5.3)$$

Although daily totals had to be estimated during the intervening period, hourly data were available at certain times, and regression slopes were calculated from these.

---

[1] These ratios are listed in a later section.

Regression slopes and intercepts are listed in Table 5.9. Correlations are generally lower than those listed in Table 5.3, but most of them are acceptable. Several individual periods, such as PS on September 3 - 4 and F on August 29 - September 2 were hampered by recorder problems, so their sample sizes were small, consequently affecting significance levels. S plot had two correlation values below 0.8, but these were probably due to physical factors rather than instrument error. The coniferous canopy's influence should vary only slightly, while Gs values at G plot fluctuate. This variance is magnified because the magnitude of Gs is so small. Therefore, large prediction errors are not anticipated, but to improve accuracy, the results for July 27 - 30 will not be used in subsequent calculations.

F plot, as expected, had the highest slopes because of greater soil exposure. S plot had the lowest ones for the opposite reason. Most of the intercepts are within 5 Wm^{-2} of 0.0 Wm^{-2}, indicating that there are no major temporal variations between the plots diurnal trends. W and PS plots showed large slope increases towards the end of the study period, and this was probably due to leaf loss, which increased surface exposure. F plot's slopes were probably affected by weed cover density and soil wetness The latter point is more important for F plot than for any other cover, since there is little or no overlying

TABLE 5.9

REGRESSION SLOPES AND INTERCEPTS TO BE USED IN

Eq. (5.3): Gs (rotated) = a{Gs (G plot)}+b

Rotated Plot	Date	Slope (a)	Intercept (b)	S.E.	r	r^2	SIG*	N
PS	6/15 - 17	0.33	5.2 Wm^{-2}	2.1 Wm^{-2}	0.97	0.93	0.00001	53
	6/18 - 21	0.40	0.2	5.5	0.93	0.86		94
	7/ 9 - 12	0.44	1.1	5.0	0.92	0.84		96
	7/13 - 15	0.51	0.8	4.8	0.90	0.80		71
	8/ 4 - 8	0.46	3.7	5.6	0.89	0.79		119
	8/ 9 - 13	0.36	4.9	5.1	0.88	0.77		104
	9/ 3 - 4	-0.13	13.0	2.4	-0.38	0.15	0.19819	7
	9/30 - 10/3	0.42	2.7	2.3	0.91	0.83		86
	10/ 4 - 8	0.67	1.7	6.9	0.74	0.54		117
S	6/29 - 7/1	0.25	3.7	2.9	0.89	0.79	0.00001	66
	7/27 - 30	0.22	2.9	4.0	0.57	0.33		93
	7/31 - 8/2	0.41	2.1	6.6	0.77	0.59		70

TABLE 5.9 (cont.)

Rotated Plot	Date	Slope (a)	Intercept (b)	S.E.	r	r^2	SIG*	N
S	9/22 - 24	0.15	0.1	1.7	0.88	0.77	0.00001	70
	9/25 - 27	0.13	2.7	1.9	0.82	0.67		72
W	5/28 - 31	0.80	- 0.7	5.6	0.96	0.93	0.00001	83
	7/23 - 26	0.42	6.1	3.3	0.95	0.91		94
	8/14 - 17	0.62	- 1.6	12.3	0.77	0.59		28
	9/10 - 11	1.00	3.3	7.8	0.98	0.97		23
B	5/22 - 24	0.78	- 3.3	3.4	0.99	0.97	0.00001	69
	5/25 - 27	0.72	- 3.0	3.2	0.99	0.97		72
	6/ 8 - 10	0.76	2.1	7.8	0.95	0.90		70
	6/11 - 14	0.82	5.3	9.6	0.91	0.82		94
	7/ 3 - 5	0.44	0.2	6.2	0.93	0.87		71
	7/ 6 - 8	0.47	4.6	6.2	0.92	0.85		72
	9/15 - 17	0.85	7.5	11.4	0.86	0.74		71

TABLE 5.9 (con't.)

Rotated Plot	Date	Slope (a)	Intercept (b)	S.E.	r	r^2	SIG*	N
F	6/ 1 - 3	1.37	1.7	13.0	0.95	0.91	0.00001	70
	6/ 4 - 7	1.58	3.9	13.5	0.94	0.88		96
	6/22 - 24	1.06	3.2	11.2	0.88	0.77		53
	6/25 - 28	0.77	0.3	8.9	0.91	0.83		38
	7/16 - 19	1.64	4.8	21.5	0.89	0.80		34
	7/20 - 22	1.81	8.7	16.2	0.94	0.89		72
	8/29 - 9/2	2.60	-41.7	7.1	0.90	0.81	0.00052	9
	9/18 - 21	1.21	9.3	12.4	0.92	0.84		65

*All SIG levels at 0.00001 unless otherwise noted.
Numbers are rounded.

vegetation that can intercept precipitation and reduce direct throughfall. B plot was also affected by surface wetness, but this varied with plant density and water use rather than precipitation frequency. During the summer, the healthy plant cover shaded the surface. Towards autumn, much of the plant cover was removed, thereby exposing the surface to solar radiation and wind. These events must have affected soil thermal conductivity at both B and F plots. Further discussion on this topic will continue in a later section.

Soil heat flux data are listed in Table 5.10 and illustrated in Fig. 5.18. While its magnitude is quite small compared to the other components of the energy balance, significant Gs differences between the plots may, in large part, account for differences in their respective soil temperatures, which are illustrated in Figs. 4.6 and 4.7.

Upon examining Fig. 5.18, one notices certain consistent patterns. F plot's values are the highest (except for one week in June) and G plot's are the second highest from May 27 - September 16. At that time, significant differences disappear, and the daily soil "energy balance" hovers fairly close to 0.0 Wm^{-2} as the winter seas approaches. Another interesting point is that in May and June, differences can be discerned between the remaining open plots (W and B) and the two wooded plots.

TABLE 5.10

MEAN DAILY Gs (1000 $Wm^{-2}day^{-1}$)

Date Period Ending	PS	S	W	B	F	G
5/27	5.8	4.9	13.5	13.5	21.3	18.0
6/3	2.2	2.2	6.1	5.9	10.4	7.6
10	3.3	3.8	9.4	9.5	19.5	12.5
17	3.1	2.7	6.7	6.4	12.4	9.5
24	5.0	3.4	8.3	7.6	13.4	12.6
7/1	7.0	4.2	10.2	9.1	12.9	16.8
8	9.2	5.9	11.9	9.6	22.8	20.9
15	5.3	3.3	5.4	4.8	14.5	10.3
22	7.3	5.2	7.0	7.0	25.7	15.0
29	3.9	3.1	3.4	4.0	15.1	8.1
8/6	5.2	4.6	5.5	6.0	22.6	11.3
12	3.2	3.4	5.0	5.2	19.4	9.0

TABLE 5.10 (con't.)

Date Period Ending	PS	S	W	B	F	G
8/19	5.3	3.7	5.1	2.6	19.6	6.8
28	5.9	4.1	5.6	2.8	17.1	6.0
9/2	4.0	2.5	4.7	2.8	13.9	5.2
9	1.1	0.4	2.2	-	6.6	-
10	-	-	-	1.7	-	2.9
16	0.7	0.3	1.7	1.1	1.9	1.2
23	0.2	0.1	0.5	0.4	0.6	0.5
30	1.2	0.3	2.7	2.1	2.6	2.4
10/7	0.2	0.0	0.4	0.3	0.3	0.3
20 week mean	4.1	3.0	5.7	5.2	13.8	8.9

Numbers are rounded.
Means calculated from 5 - 9 day totals.

FIG. 5.18: MEAN DAILY G_s

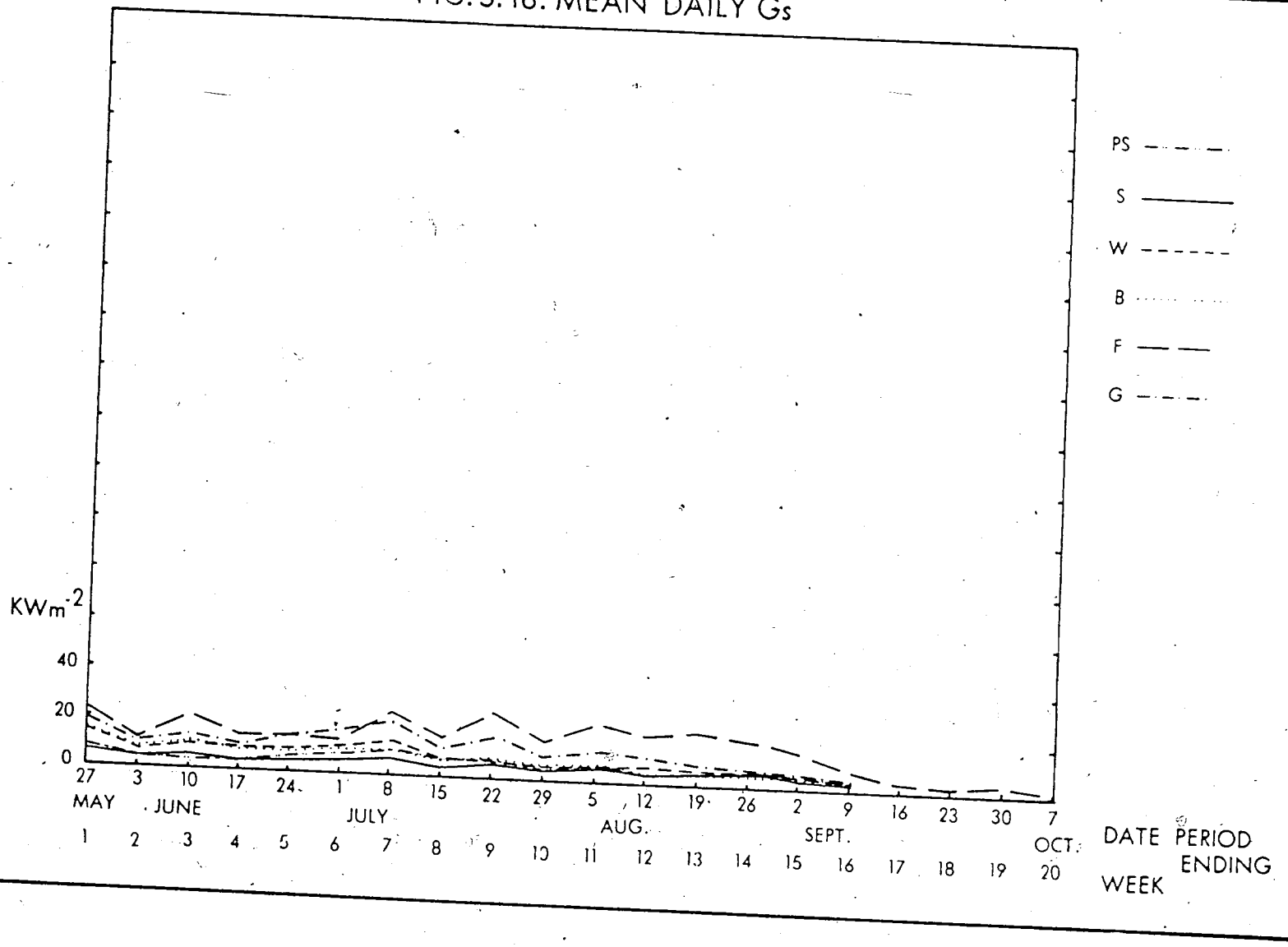

By July 22, the difference is reduced to a very small quantity.

Although the above trend description may have to be qualified somewhat due to possible interpolation errors (see Section 5.3.5), there can be little doubt that F and G plots recorded higher Gs values than the remaining four. Figs. 4.6 and 4.7 reveal that from June to September 1975 and 1976, F and G had the warmest 20 cm and 100 cm soil temperatures, while the two wooded plots were the coldest. Preliminary indications point to Gs differences as an important factor in the plots' soil temperature differences. However, further analysis is required in order to quantitatively determine the significance of the Gs differences.

5.3.3 H

Sensible heat flux data are listed in Table 5.11 and illustrated in Fig. 5.19. H is the residual term in the energy balance calculations, since it was the only parameter that was not directly measured. Hence, its results are dependent upon measurements of Rn and LE, and to a lesser degree on Gs.

Although there are large differences in mean values, with PS and S being the highest, and G the lowest, rankings for individual weeks varied. As with the LE results, trends in H are hard to see, but it appears that there is slightly

TABLE 5.11

MEAN DAILY H (1000 $Wm^{-2}day^{-1}$)

Date Period Ending	PS	S	W	B	F	G
5/27	98.1	123.1	113.6	109.2	122.6	93.7
6/3	131.7	129.6	90.5	67.7	121.4	40.2
10	131.3	112.4	86.1	74.8	96.9	65.4
17	118.1	115.6	15.0	24.2	103.5	96.3
24	40.0	26.3	- 33.9	11.0	70.2	19.8
7/1	6.1	- 8.3	- 58.7	30.4	23.0	32.5
8	109.7	158.4	153.3	111.3	145.0	67.6
15	147.2	125.5	81.0	62.6	87.1	26.7
22	203.9	189.2	130.0	17.8	133.2	82.8
29	139.6	123.0	66.5	37.9	110.4	54.4
8/6	3.9	49.2	40.1	66.1	39.6	- 25.2
12	124.0	100.9	185.4	83.6	40.4	93.2
19	90.4	18.0	19.3	82.5	113.5	21.4

TABLE 5.11 (con't.)

Date Period Ending	PS	S	W	B	F	G
8/28	75.9	51.9	83.2	39.1	75.8	33.8
9/2	70.2	62.8	133.9	144.8	57.2	46.5
9	168.6	119.2	136.4	-	102.0	-
10	-	-	-	121.9	-	93.8
16	27.5	47.6	93.5	100.9	87.1	53.5
23	138.7	91.1	125.0	98.0	21.9	42.8
30	88.9	77.9	62.8	76.7	27.6	21.5
10/7	28.3	29.7	49.6	20.5	- 12.8	- 15.3
20 week mean	99.5	86.6	77.1	67.6	79.3	46.5

Numbers are rounded.
Means calculated from 5 - 9 day totals.

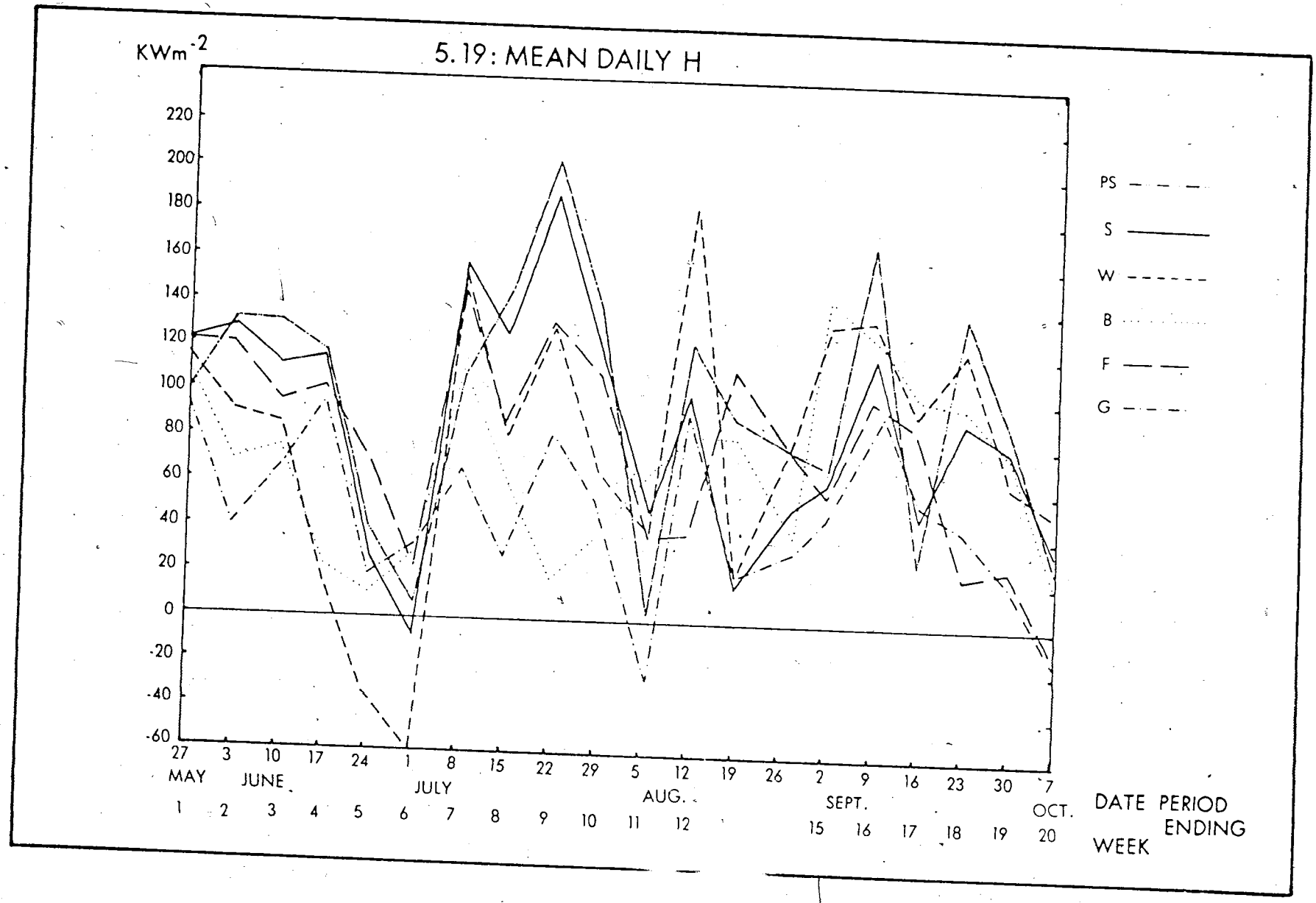
5.19: MEAN DAILY H
KWm-2
220
200
180
160
140
120
100
80
60
40
20
0
-20
-40
-60
PS
S
W
B
F
G
27 3 10 17 24 1 8 15 22 29 5 12 19 26 2 9 16 23 30 7
MAY JUNE JULY AUG. SEPT. OCT.
1 2 3 4 5 6 7 8 9 10 11 12 15 16 17 18 19 20
DATE PERIOD ENDING
WEEK

less chaos in the H curves so that certain patterns can be noted. In June, there is a general decline in values, followed by a sharp increase in July. A secondary minimum occurs on August 5, followed by another increase towards early September, and a decline of values at the end of the study period. However, certain individual plots do not appear to be following this trend at all times. G plot's values increase in mid-June, while the other plots showed a decline, and during late July and early August, B plot's curve slopes upward, contrary to the other five. The LE curve (Fig. 5.16) reveals that G plot's values for mid-June were fairly constant, so the increase in H was due to an increase in Rn alone. The situation in July represents a different story though, as LE values for B plot increased sharply, thereby accounting for the decline in H.

Other outstanding features include the large negative values for W at the end of June, and for G during the first week in August. Also, H values greatly fluctuate during mid-July and early August. The low values for W correspond to a period of very high LE values. The wide gap in H values on July 22 and August 12 were similarly caused. On the other hand, G plot registered only a 30,000 $Wm^{-2}day^{-1}$ increase in LE from July 29 - August 6, while H values declined by more than 70,000 $Wm^{-2}day^{-1}$. A decline in Rn accounted for the remaining 40,000 $Wm^{-2}day^{-1}$.

In general, PS and S ranked high for most of the study period. W, F, and B exceeded the tree plots' values on several occasions, but were usually ranked between the tree plots and G, which had the lowest or near lowest values, except during late June and weekly periods ending August 12 and September 16. As with the other parameters, further analysis is required to determine the significance of these rankings before conclusions can be reached.

5.3.4 Bowen Ratio

Bowen Ratio calculations are listed in Table 5.12 and illustrated in Fig. 5.20. The general trend during the first six weeks resembles the H curve, but instead of divergence, β values for all plots were quite similar at the end of June, despite large absolute differences in H. The tree plots separate themselves from the others during mid-July, while W does so on August 12 and F on August 19. There is incredible scatter of β values in September, but this is probably due to the decrease in magnitude of the energy balance components, which would facilitate enormous but unrealistic short-term changes in β. Another possible explanation is the large temperature difference between the warm surface and the fresh cold air mass that typically arrives in autumn. H (and consequently β) would be greater than normal in this

TABLE 5.12

BOWEN RATIO $\beta = \frac{H}{LE}$

Date Period Ending	PS	S	W	B	F	G
5/27	1.513	-3.389	2.220	2.614	3.074	3.555
6/3	3.246	3.931	1.183	0.741	2.519	0.438
10	2.452	2.021	1.068	0.839	1.378	0.930
17	0.988	1.226	0.081	0.131	0.910	1.192
24	0.229	0.155	-0.154	0.065	0.607	0.147
7/1	0.029	-0.040	-0.240	0.214	0.147	0.281
8	0.778	1.827	1.753	0.986	1.742	0.545
15	2.481	1.742	0.633	0.477	0.767	0.188
22	4.634	4.444	1.184	0.090	1.548	0.790
29	1.544	1.417	0.461	0.250	1.292	0.487
8/6	0.021	0.498	0.369	0.965	0.437	-0.180
12	1.139	0.970	7.793	0.809	0.269	1.329

TABLE 5.12 (con't.)

Date Period Ending	PS	S	W	B	F	G
8/19	0.776	0.111	0.118	0.950	2.118	0.173
28	0.489	0.354	0.692	0.266	0.658	0.265
9/2	0.360	0.387	1.396	2.236	0.358	0.346
9	3.628	2.006	2.829	-	1.482	-
10	-	-	-	2.722	-	1.899
16	0.225	0.582	2.208	8.167	2.468	1.200
23	23.442	2.359	8.888	3.891	0.223	0.677
30	3.951	2.792	1.245	3.445	0.412	0.340
10/7	0.598	0.684	1.579	0.406	-0.161	-0.202

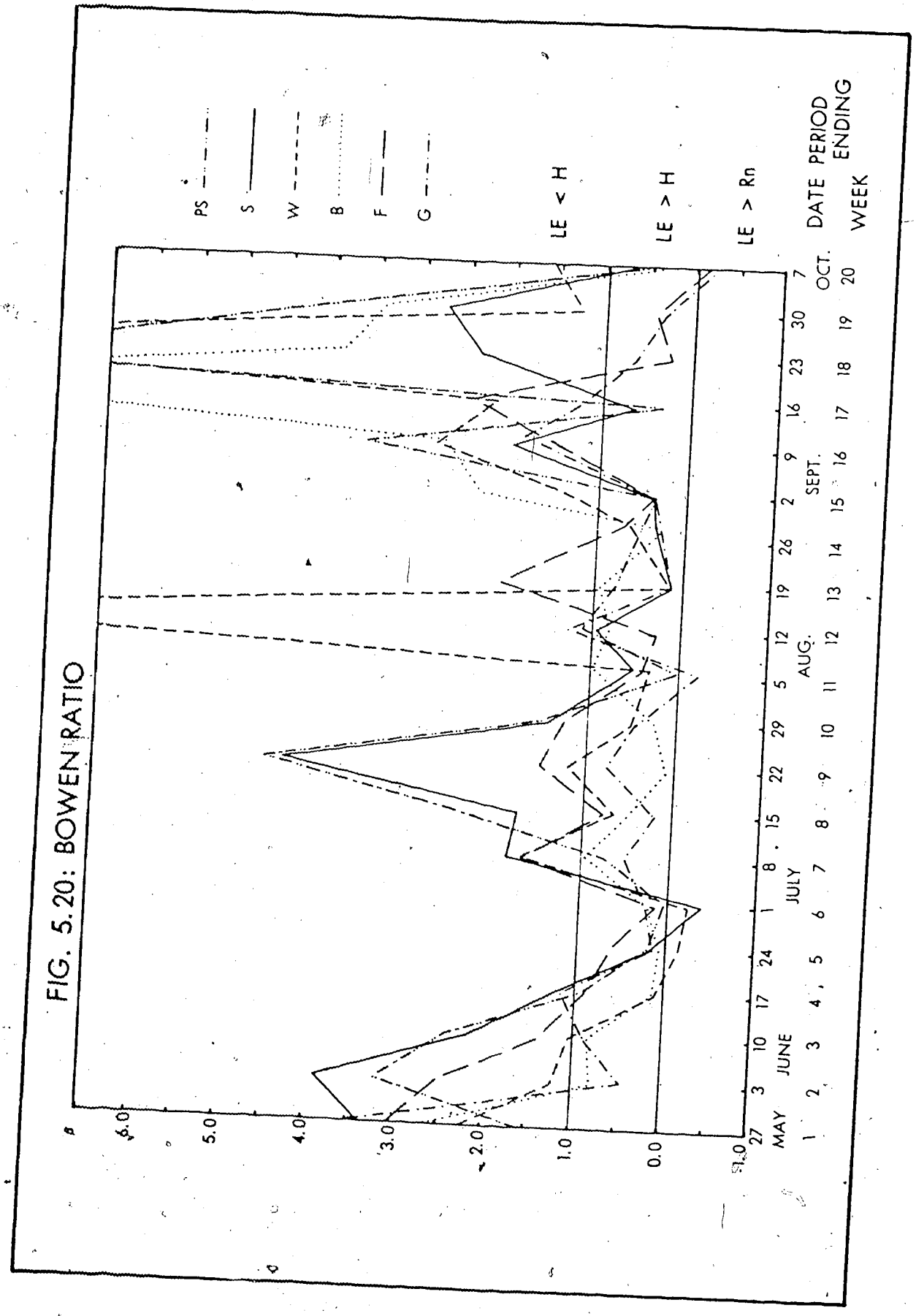

FIG. 5.20: BOWEN RATIO

situation (Denmead, 1969). Subsequent calculations of mean β values should not be affected by this, in any case.

In general, it can be noted that the early portion of the study period was dry, with more humid conditions prevailing at the end of June, and continuing towards early September. The exceptional values previously mentioned can be related to low LE values for these individual weeks. Low rainfall during much of July probably accounted for high β values at PS and S, since light precipitation would have been almost completely intercepted by the tree canopies. More intense precipitation, such as that provided by storms experienced at the end of June and the beginning of August, are required before soil moisture levels benefit substantially. Since the first priority of energy use involves water use, more of the available energy could be utilized for transpiration and evaporation rather than sensible heat.

While the above may explain high β values for PS and S, the cause behind W plot's high β value in August remains a mystery. It is possible that there was an error in soil moisture calculations for this individual measurement. However, the detailed analysis that follows uses mean values compiled over the entire study (a period of 20 weeks), which should effectively reduce the influence of this anomaly. Meanwhile, the high β value for F plot in August could be related to weeding and tillage,

which was done the previous week, and so temporarily reduced transpiration demands on Rn, thereby lowering LE.

5.3.5 Errors and Preliminary Analysis

Errors in energy balance calculations are basically the same as those in radiation balance calculations, but with two major additions. The first involves errors in soil moisture calculations, and the second concerns interpolation of regression slopes for Rn and Gs.

The neutron scattering equipment was calibrated during the study period, so large calibration errors are not anticipated. The most likely source for measurement error was the placement of the surface probe. This created some difficulty, especially at W plot, because the shrubs themselves were fairly close together. Since the August 12 measurement at W plot cannot be easily explained by physical factors, it may be assumed that the surface probe was not positioned properly on the plot surface. ΔPW calculations were based on soil moisture totals which were weighted according to the measurement depth. For example, if data were available for a 1 metre depth, the calculation procedure would be as outlined in Table 5.13. The surface calculation thus has a 10% influence on the final sum if data are available for 1 metre, and a some-

TABLE 5.13

PROCEDURE FOR SOIL MOISTURE CALCULATIONS

1) List all data by depth; e.g. 0.1 m -- x1
0.2 m -- x2
0.5 m -- x3
0.8 m -- x4
1.0 m -- x5

2) Calculate mean values for each layer; e.g. $\frac{x1 + x2}{2}$

3) Weight each value according to width of soil layer;
e.g. $\frac{x1 + x2}{2} \times 0.2$; $\frac{x2 + x3}{2} \times 0.3$

4) Sum all values to produce weighted mean; units are m^{-1} soil

5) ΔPW = data for time (t + 1 week) - data for time (t)

6) Convert from cm m^{-1} to gm m^{-1} for use in LE calculations.

what greater influence if only shallower depths can be monitored (as was the case with PS and S plots). This appears to be an isolated case, however, as the various soil moisture curves (including Fig. 5.15) show W following trends similar to several other plots both before and after this date. Final analysis is based on 20 week mean values, and it is anticipated that an individual error such as this one will not significantly affect the final results.

Regression equations have already been discussed in this chapter. Several large time gaps exist between periods of direct measurement, so there may be errors in interpolation of regression slopes during these periods. Due to the high correlations and significance levels recorded for all regression equations used, the magnitude of this error should be small, although this would be difficult to verify. Similarly, the usage of eq. (2.6) and assumed values for Gs/Rn poses additional problems on late August and early September results. However, as with the aforementioned situation, the regression equations utilized show high correlations and significance levels, and since Gs is a very small quantity, absolute errors should be small for both estimates. As previously mentioned, the final analysis is based on 20 week mean values. Also, shorter period mean values are calculated for 2 week periods to facilitate the equalization of time intervals for all measurements at all plots during the entire study

period. In other words, where there had previously been periods of 5 - 9 days, the final analysis will use only 14 day intervals. This should also serve to reduce the effect of random fluctuation errors.

Energy balance percentages for each period are shown in Table 5.14. Dates where data were estimated are included. Besides those previously mentioned, there were days when individual hours were missing from the base station data, but these were few in number, and should not affect mean values. The assumed Gs/Rn values are very small in magnitude, except for F plot, but large errors are not expected for this case either, since 15 weeks of data are available upon which Gs/Rn estimates can be made with some confidence.

The data presented in this study have been shown to be reasonably accurate, and representative of actual field conditions. Having considered the various error possibilities, it can be concluded that the data can be analyzed at least on a comparative basis. The purpose of the statistical analysis to follow is to determine the significance of the differences in energy balance between the plots. Upon examining mean energy balance ratios (Table 5.15), differences as large as 0.2 are noted for H/Rn, and 0.5 for β. It is hoped that when these differences are examined, the picture given by this table will be made clearer.

TABLE 5.14

ENERGY BALANCE (x100%)

Date Period Ending		PS			S			W		
		$\frac{H}{Rn}$	$\frac{LE}{Rn}$	$\frac{Gs}{Rn}$	$\frac{H}{Rn}$	$\frac{LE}{Rn}$	$\frac{Gs}{Rn}$	$\frac{H}{Rn}$	$\frac{LE}{Rn}$	$\frac{Gs}{Rn}$
5/27	A	0.580	0.386	0.034	0.749	0.221	0.030	0.637	0.287	0.076
6/3	A	0.754	0.232	0.014	0.786	0.200	0.014	0.523	0.442	0.035
10	-	0.697	0.284	0.019	0.654	0.324	0.022	0.489	0.458	0.053
17	A	0.490	0.496	0.013	0.544	0.443	0.013	0.073	0.895	0.032
24	J	0.182	0.795	0.023	0.132	0.851	0.018	-.173	1.130	0.043
7/1	AJ	0.028	0.939	0.034	-.041	1.020	0.021	-.300	1.247	0.053
8	-	0.422	0.542	0.036	0.631	0.345	0.024	0.607	0.346	0.047
15	-	0.695	0.280	0.025	0.625	0.359	0.017	0.378	0.597	0.025
22	-	0.799	0.172	0.029	0.798	0.180	0.022	0.527	0.445	0.029
29	A	0.597	0.386	0.017	0.578	0.408	0.015	0.311	0.673	0.017
8/6	-	0.020	0.950	0.030	0.322	0.647	0.031	0.260	0.704	0.036

TABLE 5.14 (con't.)

Date Period Ending		PS $\frac{H}{Rn}$	PS $\frac{LE}{Rn}$	PS $\frac{Gs}{Rn}$	S $\frac{H}{Rn}$	S $\frac{LE}{Rn}$	S $\frac{Gs}{Rn}$	W $\frac{H}{Rn}$	W $\frac{LE}{Rn}$	W $\frac{Gs}{Rn}$
8/12	C	0.525	0.461	0.014	0.484	0.499	0.016	0.865	0.111	0.024
19	CD	0.426	0.549	(0.025)	0.098	0.882	(0.020)	0.103	0.870	(0.027)
28	CD	0.320	0.655	(0.025)	0.256	0.724	(0.020)	0.398	0.575	(0.027)
9/2	CD	0.261	0.724	(0.015)	0.276	0.713	(0.011)	0.571	0.409	(0.020)
9	CD	0.780	0.215	(0.005)	0.666	0.332	(0.002)	0.730	0.258	(0.012)
10	CD	-	-	-	-	-	-	-	-	-
16	CD	0.183	0.812	(0.005)	0.367	0.631	(0.002)	0.680	0.308	(0.012)
23	A	0.957	0.041	0.002	0.702	0.297	0.001	0.895	0.101	0.004
30	-	0.789	0.200	0.011	0.734	0.263	0.003	0.541	0.435	0.025
10/7	A	0.373	0.624	0.003	0.406	0.593	0.001	0.608	0.385	0.006

A - Rn (plot G) includes 2 or more days with estimated hourly data.
J - Gs (plot G) as above.
C - Rn (plot G) calculated using eq. (2.6).
D - $\frac{Gs}{Rn}$ assumed . . . values in parentheses.

TABLE 5.14 (con't.)

Date Period Ending		B			F			G		
		$\frac{H}{Rn}$	$\frac{LE}{Rn}$	$\frac{Gs}{Rn}$	$\frac{H}{Rn}$	$\frac{LE}{Rn}$	$\frac{Gs}{Rn}$	$\frac{H}{Rn}$	$\frac{LE}{Rn}$	$\frac{Gs}{Rn}$
5/27	A	0.664	0.254	0.082	0.667	0.217	0.116	0.679	0.191	0.131
6/3	A	0.411	0.554	0.036	0.674	0.268	0.058	0.288	0.657	0.054
10	-	0.431	0.514	0.055	0.519	0.376	0.105	0.441	0.474	0.084
17	A	0.112	0.857	0.030	0.451	0.495	0.054	0.516	0.433	0.051
24	J	0.058	0.901	0.041	0.352	0.580	0.068	0.119	0.806	0.075
7/1	AJ	0.167	0.783	0.050	0.119	0.813	0.067	0.197	0.702	0.102
8	-	0.476	0.483	0.041	0.557	0.331	0.091	0.318	0.584	0.099
15	-	0.315	0.661	0.024	0.405	0.528	0.068	0.149	0.793	0.058
22	-	0.080	0.889	0.031	0.543	0.351	0.106	0.409	0.517	0.074
29	A	0.196	0.784	0.021	0.523	0.405	0.072	0.312	0.641	0.046
8/6	-	0.470	0.487	0.043	0.260	0.594	0.146	-.200	1.111	0.090

TABLE 5.14 (con't.)

Date Period Ending		B			F			G		
		$\frac{H}{Rn}$	$\frac{LE}{Rn}$	$\frac{Gs}{Rn}$	$\frac{H}{Rn}$	$\frac{LE}{Rn}$	$\frac{Gs}{Rn}$	$\frac{H}{Rn}$	$\frac{LE}{Rn}$	$\frac{Gs}{Rn}$
8/12	C	0.435	0.538	0.027	0.192	0.715	0.092	0.541	0.407	0.052
19	CD	0.480	0.505	(0.015)	0.608	0.287	(0.105)	0.141	0.814	(0.045)
28	CD	0.207	0.778	(0.015)	0.368	0.559	(0.083)	0.202	0.762	(0.036)
9/2	CD	0.682	0.305	(0.013)	0.248	0.692	(0.060)	0.250	0.722	(0.028)
9	CD	-	-	-	0.575	0.388	(0.037)	-	-	-
10	CD	0.724	0.266	(0.010)	-	-	-	0.642	0.338	(0.020)
16	CD	0.882	0.108	(0.010)	0.701	0.284	(0.015)	0.539	0.449	(0.012)
23	A	0.792	0.203	0.005	0.181	0.812	0.006	0.402	0.594	0.004
30	-	0.757	0.220	0.023	0.283	0.687	0.030	0.247	0.726	0.027
10/7	A	0.286	0.706	0.007	-.189	1.178	0.012	-.252	1.247	0.005

A - Rn (plot G) includes 2 or more days with estimated hourly data.
J - Gs (plot G) as above.
C - Rn (plot G) calculated using eq. (2.6)
D - $\frac{Gs}{Rn}$ assumed . . . values in parentheses.

TABLE 5.15

ENERGY BALANCE

	PS	S	W	B	F	G
H/Rn	0.501	0.482	0.416	0.395	0.434	0.309
LE/Rn	0.478	0.502	0.553	0.574	0.490	0.632
Gs/Rn	0.020	0.017	0.031	0.030	0.075	0.059
$\beta\left(\frac{H}{LE}\right)$	1.048	0.960	0.754	0.688	0.885	0.489

Numbers are rounded.
All calculations based on 20 week means.

5.4 Statistical Analysis of Energy Balance

5.4.1 Analysis Procedure

The purpose of this analysis is to determine trends and evaluate the statistical significance of the differences between mean values of the energy balance components for each plot. Having established that the data reasonably represent field conditions, the Paired t test can be used to provide an index, t, which is the ratio of the difference between the means to the standard error of the difference. This procedure examines sample means to see if the differences between them were a result of random variation, or significant differences between the individual cases that constitute the mean. This assumes that the individual differences are normally distributed. Several histograms illustrating the distribution of these differences are illustrated in Fig. 5.21. In a normal distribution, 95% of the individual cases are found within 2 standard deviations (SD) of the mean. This condition is satisfied in 7 of the 8 distributions shown. When dealing with small samples of data, certain inaccuracies can result from skewed distributions, and these must be taken into account.

The individual cases are 2 week totals of Rn, H, —, and Gs, for each plot. This was chosen to equalize the cases' time intervals. The t test is a rigorous

FIG. 5.21: HISTOGRAMS

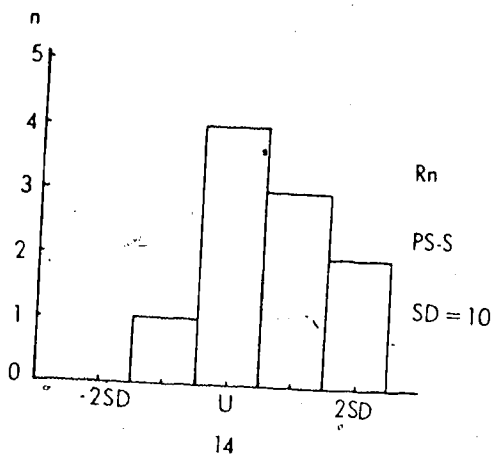

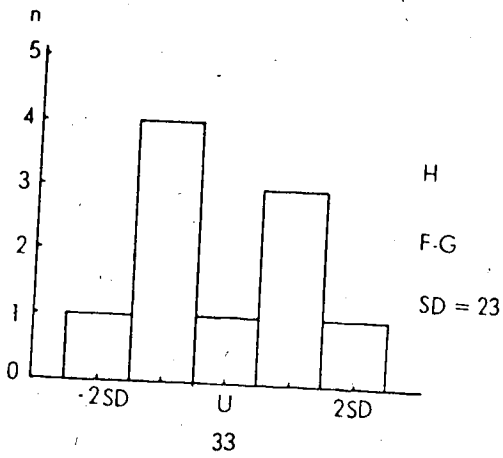

ALL UNITS IN $1000 \times Wm^{-2}$

U = MEAN
SD = STANDARD DEVIATION
n = NO. OF CASES

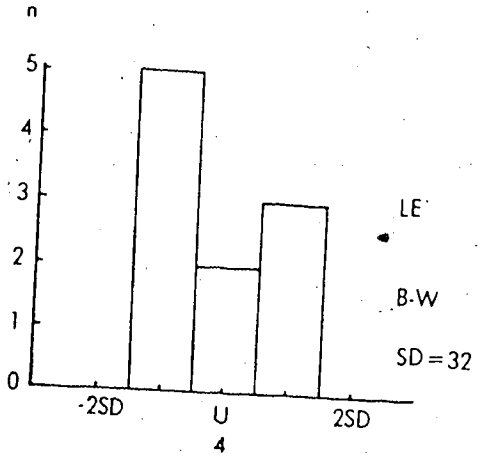

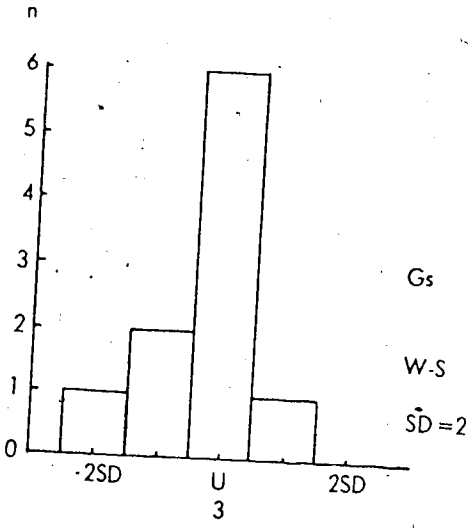

FIG. 5.21: (cont.)

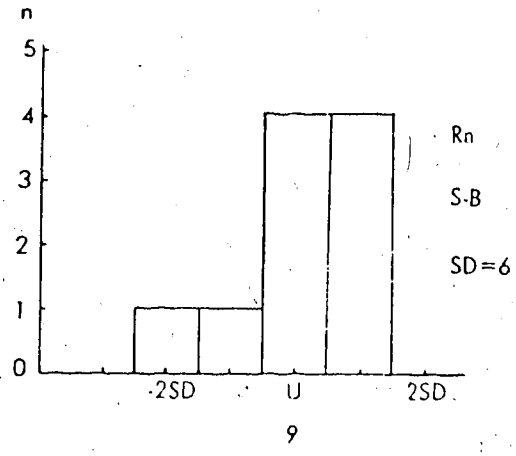

9

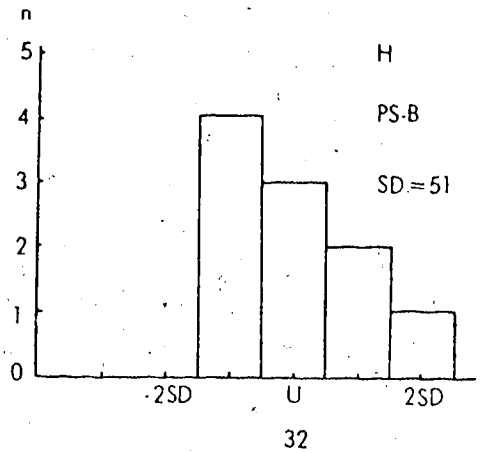

32

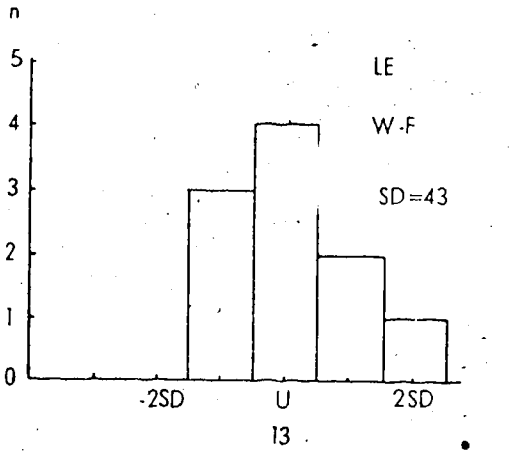

13

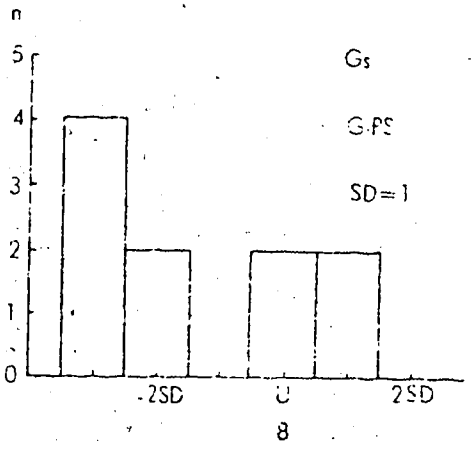

8

technique, and can be used for sample sizes as small as 3 cases (N = 3), if the concept of "degrees of freedom" is employed, rather than the actual number of cases. Degrees of freedom are the number of values that can be assigned arbitrarily, assuming that the sample total and mean remain unchanged. Although N-1 is often used for determining degrees of freedom, N-2 is used here since the standard error is also assumed to be unchanged. This increases the difficulty in proving significance, since a higher t value must be attained before the critical value is reached. For the purpose of this analysis, the 95% confidence limit is chosen as the minimum for rejection of the null hypothesis (there is no significant difference between the samples) and acceptance of the alternative hypothesis (there is a difference).

Simultaneously, the data are analyzed for correlation (r). This test determines the degree of relationship between the trends of a pair of samples. High correlations imply a strong statistical relationship, with a perfect correlation being r = 1.0. Note that it is possible to have high correlations and insignificant t values, and vice versa, for the same pair of samples, since the tests are independent of each other.

Before examining the test results, it is important to point out the limits of what a statistical test can say. Although it is possible to prove that the means are signifi-

cantly different, or that a strong correlation exists between two samples, the interpretation of these results is essentially based on human judgement and experience. These tests provide a mathematical basis for decision making, but they are not an end in themselves. Human judgement requires examination of many factors besides the test results, including physical, climatological, and biological factors, before conclusions can be reached.

5.4.2 Results

Paired t test results for Rn, H, LE, and Gs, are listed in Table 5.16. Analysis was done for the entire 20 week period, and for the first and second 10 week periods separately. Those results significant at the 99% confidence limit, as well as those at the 95% and below 95% (not significant) levels are included.

The numbers in the matrices are differences between the means of the two samples indicated. The difference is calculated by subtracting the row sample from the column sample. Negative numbers indicate that the row sample had the higher mean value of the two.

The rows and columns of each matrix are ranked by the magnitude of their sample mean daily Rn values. This parameter was selected because it is dependent on all other energy and radiation balance factors. It was

found that PS had the highest value, followed by W, F, S, B, and G, in that order. Since this ranking is used in every matrix, the negative values indicate that the ranking of that parameter for that time period does not agree with the 20 week (or total period) mean daily Rn rankings.

Correlation test results are listed in Table 5.17. The arrangement of these matrices is identical to Table 5.16, as are the indicated confidence limits. As previously mentioned, the distribution of significant t and r relationships are not necessarily the same.

At first glance, it can be noted that for the total period, significant differences exist between the plots' Rn and Gs values. In addition, strong degrees of relationship exist between the plots. However, if the period is split into halves, the first half shows poor correlations for Gs, while most of the second half differences are found to be not significant. Upon examining H, it appears that G plot is significantly different from the rest during the total and second half periods, while certain other plots, notably W and F, show significant differences from the trees and the remaining open plots respectively. Differences in the plots' LE values are found to be not significant over the total period, while some differences are computed between W and the trees during the first period, and B and several plots during

KEY FOR

TABLES 5.16, 5.17

TOTAL	5/21 - 10/7
1st	5/21 - 7/29
2nd	7/30 - 10/7

ø	not significant
*	significant at .05 level
**	significant at .01 level

TABLE 5.16

T TEST RESULTS (1000 $Wm^{-2}day^{-1}$)

Rn

TOTAL

	PS	W	F	S	B	G
PS	-					
W	13**	-				
F	15**	ø	-			
S	18**	5*	ø	-		
B	27**	14**	12**	9**	-	
G	47**	34**	32**	29**	20**	-

H

TOTAL

	PS	W	F	S	B	G
	-					
W	ø	-				
F	ø	ø	-			
S	12*	ø	ø	-		
B	ø	ø	ø	ø	-	
G	52**	ø	32**	40**	ø	-

TABLE 5.16 (con't)

LE

TOTAL

	PS	W	F	S	B	G	P
PS	-						
W	ø	-					
F	ø	ø	-				
S	ø	ø	ø	-			
B	ø	ø	ø	ø	-		
G	ø	ø	ø	ø	ø	-	
P	ø	ø	-19*	ø	ø	ø	-

Gs

TOTAL

	PS	W	F	S	B	G
PS	-					
W	-2*	-				
F	-10**	- 8**	-			
S	1**	3**	11**	-		
B	ø	ø	9**	-2*	-	
G	- 5**	- 3**	5**	-6**	-4**	-

TABLE 5.16 (con't,)

Rn

lst	PS	W	F	S	B	G
PS	-					
W	ø	-				
F	ø	ø	-			
S	14*	ø	ø	-		
B	22**	12*	15**	ø	-	
G	45**	35**	38**	31**	23**	-

H

lst	PS	W	F	S	B	G
PS	-					
W	54*	-				
F	ø	ø	-			
S	ø	-44*	ø	-		
B	ø	ø	46*	ø	-	
G	ø	ø	43*	ø	ø	-

TABLE 5.16 (con't.)

LE

lst

	PS	W	F	S	B	G	P
PS	-						
W	-42*	-					
F	ø	ø	-				
S	ø	44*	ø	-			
B	ø	ø	ø	ø	-		
G	ø	ø	ø	ø	ø	-	
P	ø	ø	-31**	ø	ø	ø	-

Gs

lst

	PS	W	F	S	B	G
PS	-					
W	-2*	-				
F	-10**	-8**	-			
S	1**	3**	11**	-		
B	ø	ø	9**	-2*	-	
G	-5**	-3**	5**	-6**	-4**	-

TABLE 5.16 (con't.)

Rn

2nd	PS	W	F	S	B	G
PS	-					
W	ø	-				
F	25**	9*	-			
S	23*	7**	ø	-		
B	33**	17**	ø	10**	-	
G	51**	35**	26**	28**	18**	-

H

2nd	PS	W	F	S	B	G
PS	-					
W	ø	-				
F	ø	ø	-			
S	ø	25*	ø	-		
B	ø	ø	ø	ø	-	
G	45*	54**	ø	29*	45**	-

TABLE 5.16 (con't.)

LE

2nd	PS	W	F	S	B	G	P
PS	-						
W	ø	-					
F	ø	ø	-				
S	ø	ø	ø	-			
B	ø	ø	ø	-27*	-		
G	ø	ø	ø	ø	-27*		
P	ø	-24*	ø	ø	-31*	ø	-

Gs

2nd	PS	W	F	S	B	G
PS	-					
W	ø	-				
F	ø	ø	-			
S	1*	1**	ø	-		
B	ø	ø	ø	ø	-	
G	ø	ø	ø	ø	ø	-

TABLE 5.17

CORRELATION TEST RESULTS (r)

Rn

TOTAL

	PS	W	F	S	B	G
PS	-					
W	.96**	-				
F	.95**	.98**	-			
S	.97**	.99**	.98**	-		
B	.95**	.98**	1.00**	.99**	-	
G	.96**	.99**	.99**	1.00**	1.00**	-

H

TOTAL

	PS	W	F	S	B	G
PS	-					
W	ø	-				
F	.72*	ø	-			
S	.95**	.67*	.77**	-		
B	ø	.74*	ø	ø	-	
G	.64*	ø	.77**	.72**	ø	-

TABLE 5.17 (con't.)

LE

TOTAL

	PS	W	F	S	B	G	P
PS	-						
W	.69*	-					
F	.74*	.65*	-				
S	.93**	.76*	.73*	-			
B	ø	.83**	ø	ø	-		
G	ø	ø	ø	.69*	.68*	-	
P	.74*	.84**	.73*	.81**	.77**	.81**	-

Gs

TOTAL

	PS	W	F	S	B	G
PS	-					
W	.77**	-				
F	.82**	.66*	-			
S	.94**	.82**	.95**	-		
B	ø	.95**	.64*	.75*	-	
G	.85**	.94**	.77**	.89**	.92**	-

TABLE 5.17 (con't.)

Rn

lst

	PS	W	F	S	B	G
PS	-					
W	.91*	-				
F	.92*	.97*	-			
S	.98**	.96*	.93*	-		
B	.95*	.97**	.99**	.95*	-	
G	.96**	.97**	.97**	.98**	.99**	-

H

lst

	PS	W	F	S	B	G
PS	-					
W	.92*	-				
F	.92*	.98**	-			
S	.98**	.96**	.98**	-		
B	ø	ø	ø	ø	-	
G	ø	ø	ø	ø	ø	-

TABLE 5.17 (con't.)

LE

lst

	PS	W	F	S	B	G	P
PS	-						
W	.96*	-					
F	ø	.93*	-				
S	.98**	.96**	.92*	-			
B	ø	ø	ø	ø	-		
G	ø	ø	ø	ø	ø	-	
P	ø	.89*	.97**	.94*	ø	ø	-

Gs

lst

	PS	W	F	S	B	G
PS	-					
W	ø	-				
F	ø	ø	-			
S	.94*	ø	ø	-		
B	ø	ø	ø	ø	-	
G	ø	ø	ø	ø	ø	-

TABLE 5.17 (con't.)

Rn

2nd	PS	W	F	S	B	G
PS	-					
W	1.00**	-				
F	1.00**	1.00**	-			
S	1.00**	1.00**	1.00**	-		
B	1.00**	1.00**	1.00**	1.00**	-	
G	1.00**	1.00**	1.00**	1.00**	1.00**	-

H

2nd	PS	W	F	S	B	G
PS	-					
W	ø	-				
F	ø	ø	-			
S	ø	ø	ø	-		
B	ø	ø	ø	ø	-	
G	ø	ø	ø	ø	.97**	-

TABLE 5.17 (con't.)

LE

2nd	PS	W	F	S	B	G	P
PS	-						
W	ø	-					
F	ø	ø	-				
S	.91*	.95*	ø	-			
B	.90*	.91*	ø	.96**	-		
G	ø	.89*	ø	.69*	.96**	-	
P	ø	.92*	ø	.96**	.95*	.88*	-

Gs

2nd	PS	W	F	S		G
PS	-					
W	.97**	-				
F	.93*	.96**	-			
S	.97**	.98**	.99**	-		
B	ø	ø	.88*	ø	-	
G	ø	.90*	.96**	.93*	.97**	-

the second. Both H and LE values show large numbers of significant correlations over the total period, but there are almost none for H during the second half.

Another general observation that can be made concerns the distribution of negative differences. Rn and H have few, but LE and Gs have many, indicating that their rankings are considerably different from the total period mean daily Rn rankings. Having based the plot rankings on total period mean daily Rn values, it is appropriate to concentrate the analysis on this particular matrix. The other matrices can provide additional inputs as to the factors behind the establishment of this particular ranking, and the implications of these results on microclimate.

According to the test results, PS has significantly higher Rn values than any other plot. There appears to be little difference between W, F, and S, so they may be grouped between PS and B. G plot is significantly lower than B in the Rn ranks.

Why is the PS plot ranked first? It was found to have relatively low albedo values, but S and F plots' albedos were comparable. However, PS had lower longwave losses than S and F, higher first period H values than F, and higher total period H and Gs values than S. Its second period Rn values were considerably higher than F and S plots' values. F was not significantly lower during

the first period since its low weed cover allowed greater soil exposure, thereby reducing albedo. Meanwhile, what [illegible] W? This plot's higher albedos were compensated by lower longwave emissions, while its low September albedo allowed greater radiation absorption during the second period. Non-significant differences were found for the two half periods, yet the situation is different for the entire period as a whole. The only source for this difference is first period H, where PS is higher by 54,000 $Wm^{-2}da[illegible]^{-1}$. This is partially offset by significantly higher values for first period LE at W plot. Both relationships have strong correlations, as do the Rn differences. A re-examination of first half field data reveals that W had much greater soil moisture content, and LE demands were higher than the Rn available, thereby necessitating additional input of advected energy from elsewhere. Consequently, H became negative. Had W plot's albedo been lower, Rn might have been raised sufficiently to meet LE demands and so reduce the Rn difference. Hence, the key factors behind PS outranking W are probably lower soil moisture content and lower albedo during periods of high LE demand.

It is important to note that PS plot's LE values did not differ significantly from P, and during the total period, a fairly strong correlation was computed. This indicates that despite differences in age, size, and soil moisture availability, PS and P plots' seasonal evapotranspiration rates are similar. However, when P was compared

to W, the other deciduous plot, it was found that P plot's LE values were significantly higher than W plot's during the second period. P is older and larger than the other two, and this should reduce its ability to draw in heat and energy from the outside, in which case its LE values would be reduced somewhat.[1] Differences in species, age, plot size, and soil moisture availability, are all factors in LE differences. However, in this case, these factors have combined to reduce the LE differences between PS, P, and W over the total period. Otherwise, it is likely that PS, with adequate soil moisture, would have far exceeded the other plots' LE values, and its H values would have been reduced. It is doubtful that the Rn rankings would be significantly changed, however, because of the radiation balance differences, especially the albedo component.

The next question concerns W, F, and S plots' similar Rn rankings. A significant difference was found between W and S during the total period, and W and F during the second half. No significant differences were computed for the first half. Correlations were highly significant in all cases.

---

[1]This is the "oasis" effect (see Rauner, 1976), which was previously discussed in Section 2.4.1. The effect becomes weaker as woodlot sizes increase.

Why should these plots have fairly similar rankings? W plot's albedo is much higher than the other two while it has a leaf canopy. However, longwave losses are lower, so W plot's Rn values are raised. The source of the difference between W and S appears to be total period Gs, but nothing seems to explain the 9,000 $Wm^{-2}day^{-1}$ advantage calculated for W over F during the second period, since all other components show non-significant differences and poorly correlated relationships. The total period result shows no significant difference between W and F, so the second period's difference was not large enough to affect it. There is probably a trade-off between F plot's advantage in Gs, and smaller less significant advantages in H and LE for W and S. It would appear that W plot's higher albedo is compensated by greater evapotranspiration rates and lower longwave emissions. The latter is probably a result of the former, since W plot could have had a higher relative humidity on a micro-scale, which would tend to reduce longwave losses. On the other hand, trees are known to reflect longwave radiation more strongly than solid ground (Geiger, 1965; Jarvis et al., 1976). Therefore, differences in canopy structure, bare soil exposure, and foliage characteristics (e.g. leaf orientation) must be taken into consideration when examining Ln losses, as well as for the Gs advantage enjoyed by W because of its stand structure, which is lower and less dense than S.

The two lowest ranks are occupied by B and G plots. The magnitudes of the Rn differences between B vs G and B vs S are 20,000 $Wm^{-2}day^{-1}$ and 9,000 $Wm^{-2}day^{-1}$ respectively. Both values were found to be significant, and the relationships well correlated.

B plot undergoes rapid structural changes during the growing season, as it advances from seedling to mature plant in four months or less. Consequently, two important parameters are affected; albedo, and soil water use. Albedo varies with plant height and bare ground exposure (Fritschen, 1966), so reflectivity was higher for July's taller plant cover, than for June's shorter one. As the plants matured and changed colour, reflectivity was reduced substantially. LE values were high from June to August, but declined markedly in early September, due to reduced plant activity. In fact, second period LE was shown to be significantly lower than G plot's, while its H values were higher. Second period H appears to be one main factor behind B plot's higher rank, since G plot had higher total period Gs, as well as second period LE. Another factor that must be considered is longwave loss, which is greater for G plot from June to August.

Meanwhile, what about the plots ranked above B? It appears that albedo is the main factor separating B from W, F, and S. The difference between B and F is augmented by F plot's greater Gs values. W had lower longwave

losses than B, especially in June, perhaps indicating lower micro-scale relative humidity and higher surface temperature at B. The smaller Rn difference between B and S is due to albedo differences alone, and this is slightly offset by a 2,000 $Wm^{-2}day^{-1}$ advantage for B plot's Gs values. Previous studies in Canberra, Australia (Denmead, 1969) indicated that Rn and LE should be higher for coniferous species, while H and Gs are lower. The discrepency in the Ellerslie study's H and LE results must therefore be caused by S plot's limiting soil moisture supply.

G plot was ranked sixth, due to its high albedo and longwave losses, and significantly lower H values. These were slightly offset by high Gs values. LE values did not differ significantly from other plots.

5.5 Implications of Results on Central Alberta Climate

5.5.1 Basis for Conclusions

Previous sections have included discussions on raw field data, calculated energy balances, computed statistical results and the reasons behind them. Various errors have been considered and interpretations presented within the limits set by the quantity and accuracy of the data and the power of regressions, t tests, and correlations. As a result of these factors, there are no attempts at utilizing absolute values of energy balance parameters

for the purpose of mathematical or statistical modelling similar to Table 2.3 or otherwise. However, there exists a statistical basis for comparing the gross energy balances of the various plots at Ellerslie. That was the purpose of the field program. It is now possible to discuss the implications of these results on Central Alberta climate, keeping in mind the potential influence of horizontal advection.

5.5.2 Potential Micro-Scale Effects

Significant differences in Rn and Gs have been calculated for all six experimental plots. Certain plots also exhibited differences in H. No significant differences were calculated for total period LE although some were found for shorter periods. Since all field investigations were done on relatively flat terrain, any statements made herein will apply strictly to flat areas. Large topographic variations have a profound influence on energy and water balances but exposure and slope aspect were constants in this experiment, and are not considered in the following discussion.

PS has the highest Rn values, so one would expect that its surface temperature would be relatively high as well, yet its longwave emissions were the lowest of all, despite what should have been a high longwave albedo. Deciduous trees are efficient water users, so even though

soil moisture levels were low, the trees survived the summer with no apparent damage. However, its high H and β values are interesting, especially since LE should normally be dominating its energy balance (Rauner, 1976). Since H increases if surface temperatures are warmer than the air, it is possible that H is most significant at night, when air temperature and evaporation rates are lower. Consequently, a land use change from farmland to deciduous forest would probably cause an increase in nighttime minimum temperatures at canopy level. If soil moisture is not limiting, daytime LE should increase to the point where it approaches, or maybe exceeds Rn. In that case, daytime maximum temperatures would be reduced while relative humidity would rise. This effect would be increased if there were numerous woodlots of small size (less than 1 km^2) in fairly close proximity to each other. Unfortunately, soil moisture is frequently limiting, so chances of this occurring in Central Alberta are low, unless several successive wet years occur. In either case, soil temperatures will remain lower than the more open surfaces due to significantly lower Gs values.

Coniferous woodlots should have slightly cooler soil temperatures than deciduous areas, since Gs is lower. However, other conclusions involving coniferous areas are not as easy to make.

Longwave losses are higher, implying either a higher longwave albedo or higher surface temperatures. H and Rn are significantly lower for the total period and these relationships are highly correlated so the trend is consistent. Since lower H and Rn values imply cooler surface temperatures relative to the overlying air, longwave albedo would ordinarily be the most likely cause of high Ln losses. Although energy balance results would seem to indicate that coniferous areas should be cooler than deciduous areas, screen level temperatures were warmer at S plot due to canopy structural differences. On the other hand, lower H values may be due to an increase in overlying air temperature, rather than a decrease in surface temperature. The situation is further complicated by its extremely low soil moisture levels, which affected LE.

There is one factor that has not yet been discussed; Rn variations with surface wetness. Wilson's (1976) study of irrigation effects on micro-scale climatic parameters at Ellerslie showed that Rn was lower over dry grass than wet grass. He attributed this to an increase in surface temperature, which would increase longwave emissions thereby reducing Rn. Therefore, it seems likely that S plot has higher surface temperatures than PS, so if its soil conditions continue to be drier, coniferous area air temperatures will be warmer than deciduous. Since H values are lower, these must be attributed to lower Rn, and in an indirect

way, to low soil moisture levels. β does not differ significantly from PS plot's results (Table 5.14) so small coniferous woodlots will have an effect similar to small deciduous woodlots if soil moisture is enhanced. As long as the prevailing weather remains dry, its "oasis" influence will be reduced. Unlike the deciduous areas, coniferous areas would probably exhibit higher daytime and lower nighttime air temperatures, and a lower relative humidity than both deciduous and open areas. It would be interesting to compare S and PS under identical soil moisture conditions.

The shrub plot ranked second in mean daily Rn, primarily due to low longwave losses. Although it is a deciduous cover, its unique canopy structure is responsible for creating its own micro-climate, which is different from a deciduous forest. Soil moisture levels were much higher at W than at PS, because of its superior ability to retain winter snows. This additional snow cover was instrumental in maintaining higher winter soil temperatures. However, the high moisture content probably raised the soil's thermal conductivity, since water replaced air in the soil pore spaces. In addition, there was less organic matter than at the other open plots.[1] Consequently, W had lower summer soil temperatures than B and G plots, despite a lower albedo and comparable Gs values. Therefore, shrubs should maintain

---

[1] See Sellers (1965), p. 127.

warmer winter and cooler summer soil temperatures than fallow, grass, and barley covers. Its soil moisture levels should continue to be higher as well, although its advantage could be reduced after several dry winters and wet summers.

It is somewhat difficult to state any firm opinions about air temperature over shrub covers. No direct air temperature measurements were made, as these were assumed to be similar to G plot's. Due to the small size of the plots, this assumption was valid for the experimental conditions, but what about for larger surface areas? Results indicate that Ln is lowest and Rn is highly ranked but total period H does not significantly differ from any plot. Since its soil moisture levels were consistently higher, its surface temperature was probably cooler than PS, S, and F plots, while a full leaf canopy existed. Lower albedo, similar or higher Ln losses, and higher H values, indicate that autumn surface temperatures may be as high as or higher than these plots.

β was higher at W plot than at B and G plots, but statistical analysis reveals that total period H and LE differences are not significant. Therefore, W plot's surface temperatures are probably cooler than these plots as well, when it has a full leaf canopy. During autumn, the situation is similar to that previously described. These statements raise questions about differences in time of leaf fall between PS and W, and the changes in late summer

and early autumn energy balances that this causes.

The present soil moisture regime is the main factor behind these differences. Higher albedo contributes to the difference between W and PS, S, and F plots during full canopy conditions. Since shrub's albedo is lower than ... and G plots' throughout the growing season, soil ... isture's influence increases in this situation. Another factor that may be considered in the latter cases is lower wind speeds over shrub than over barley or grass. This is a likely event, considering shrub's taller woody canopy structure, which would offer stiffer resistance to surface winds. The idea is speculative, and a comparison of screen level wind speeds and roughness length calculations would be useful in determining its accuracy.

F plot ranked very close to W plot in Rn, but its radiation and energy balances were quite different. Higher longwave losses were evident despite lower albedo values during the first period. Gs was much higher than at all other plots due to greater exposure of the dark soil surface to incoming radiant energy, so higher soil temperatures should be expected under fallow fields during summer. Winter temperatures will vary with depth of snow cover, and under existing conditions, lower temperatures are expected unless there is a heavy weed cover or inducement of snow drifting by human intervention (e.g. snow fences).

Despite its advantages in Rn, F plot's H values were not significantly higher than barley's, except during the first period when barley was actively transpiring. G plot's H values were lower for the total period, while no significant difference was calculated betwee. F and PS, S or W.

Having concluded that F plot's summer soil temperatures are highest, it must now be determined whether this, as a surface temperature, is higher than the other plots' surface temperatures. It appears that the answer is yes, since PS, W, and B plots have lower Ln emissions. However, this is not obvious when comparing F to S and G plots.

S plot recorded comparable longwave losses because Rn and albedo were not very different, and on occasion, its losses were actually greater. Overall, their surface temperatures are probably similar, although this relationship is certain to be affected by weed cover density and rface wetness at fallow fields.

Similar longwave losses were also calculated for G plot, but Rn is much lower, and albedo much higher. Meanwhile, soil temperatures under grass were higher from July to September despite lower Gs values (see Fig. 4.6). G plot had greater water use, but F plot had lower soil moisture levels at the start of the study period, which may have reduced LE differences. It is suggested that F has a higher daytime surface temperature than G because of lower

albedo and soil moisture levels (which ultimately lead to lower evaporation rates). At night, these higher moisture levels, combined with the overlying plant cover, should allow G to maintain warmer soil temperatures, but the air layer in contact with the surface would still be cooler than at F plot since release of heat is more gradual. As a result of higher daytime evaporation and transpiration, relative humidity of air over grass is greater, and when combined with cooler nighttime surface temperatures in September, dew occurred more frequently over grass. Since maximum dew usually occurs 1 - 2 metres above ground in non-forest areas (Geiger, 1965), the taller grass plants would have an added advantage in attracting dew.

Thus, the overlying air is cooler over grass than over fallow fields, and this temperature difference should increase if the fields are larger in size (as opposed to the reduced "oasis" effect should woodlot sizes increase). Relative humidity will be lower for fallow field a[illegible] except during immediate post-rainfall periods, in which case surface evaporation would be higher and β would decrease. Subsequently, air temperatures would be lower, and relative humidity would be higher.

One question that remains is whether G plot's surface temperature is cooler than all other plots besides F and S. PS and W have previously been examined. I was concluded that PS would have higher nighttime minimum

temperatures, and possibly lower daytime temperatures, depending on LE. W would be cooler when its canopy is full, but might be warmer after leaf loss occurs.

B plot had higher Rn, lower Ln, and lower Gs values than grass. Second period H was much higher while second period LE was lower. Overall β was higher, but this result was still below PS, S, W, and F plots. Since LE appeared to dominate B plot's energy balance from June to early August, its surface temperatures were probably cooler. Second period results indicate reduced water use, so more energy was utilized as sensible heat. Therefore, barley surface temperatures during second period were probably higher than grass temperatures, and the overlying air's relative humidity was probably lower, which reduced the frequency of dew formation. However, it would not exceed temperatures at the fallow and tree plots. This does not agree with Denmead's (1969) findings, which showed (Pinus radiata) to have lower surface temperatures (mean for the canopy) than wheat, since LE was higher. At Ellerslie, however soil moisture is extremely limiting at S plot, so LE is reduced and H increases.

5.5.3 Potential Macro-Scale Effects

Rural land use in Central Alberta is dominated by cropland. Census figures indicate that this dominance is

increasing, as is the use of land for fallow rotations. Natural pasture and woodlots are declining. It is beyond the scope of this discussion to speculate on future rural land use trends. Some hypothetical possibilities can be mentioned, however, and their associated effects on climate described.

If woodlot acreages continue to decline in favour of cropland and fallow fields, albedo levels in former wooded areas will show an increase in general. Surface level temperatures should increase, while at former canopy (tree-top) levels, temperatures may decline slightly. Soil moisture shall be enhanced since interception of winter snows will be reduced, but surface wind will increase, and unless shelterbelts are present, much of this snow will be blown away. There will be other horizontal effects as well, including an increase in open area horizontal heat transport. Surface temperatures will depend on the extent of fallow acreage, but winter and summer soil temperatures will certainly increase. If soil moisture conditions are improved, LE will increase, but a continuation of present conditions will lead to increased H values, higher surface and air temperatures, and wind erosion will become more prominent. Vertical effects include increased temperature gradients, which could lead to greater local convective activity.

On the other hand, should woodlot acreages increase, surface winds will be reduced, albedo will decline, and soil moisture and soil temperature will decline. β will increase in woodlot areas, but their horizontal "oasis" effects could be profound, if, as previously described, numerous small woodlots are established in the region. However, this depends on availability of adequate soil moisture and it is anticipated that under present conditions, soil moisture will not be adequate under flatland woodlots. Shelterbelts, however, are a different matter. Rows of trees oriented perpendicular to the wind can act as snow fences so that snow can accumulate. Open shrub woodlots would also be useful in this regard.

---

1. Besides interception, woodlots may prevent the accumulation of snow at the soil surface by enhancing snowmelt and evaporation. This would be a consequence of high radiation absorption at the woodlot's edge (Hage, personal communication).

CHAPTER VI

SUMMARY AND CONCLUSIONS

6.1 Summary of Findings

The gross energy balances of six different landscape surfaces typical of Central Alberta have been examined. Analysis included measurements and derivations of albedo, net radiation, sensible heat flux, latent heat flux, soil heat flux, and other parameters such as soil temperature, soil moisture, and air temperature. Incoming global solar radiation, precipitation, and topographic exposure were constant for all plots.

Results have been given for each of these parameters, and comparisons made between the different plot surfaces. The plots have been ranked according to total period mean daily net radiation. The small poplar plot ranked highest, followed by shrub, fallow, spruce, barley and grass plots in that order. The shrub, fallow, and spruce plots were found to have fairly similar net radiation values, while significant differences were calculated between the remaining surfaces. Therefore, a more appropriate ranking would be:

highest . . . poplar

shrub, fallow, spruce

barley

lowest . . . grass

The major factors behind this ranking appear to be differences in albedo, canopy structure, relative humidity, soil moisture, and longwave emissions, but these had varying influences on each of the net radiation results. No significant differences have been calculated for total period latent heat flux, indicating similarities in total period water use brought about by limitations in soil moisture. Grass had the lowest sensible heat flux values over the total period. Fallow was found to have the highest soil heat flux values, with grass ranked second. Upon partitioning the study period into halves, significant sensible heat flux and latent heat flux differences were calculated between several plot pairs. Therefore, it is not surprising to find that hypothetical rankings of surface temperatures would probably vary with time:

midsummer		late summer, early autumn	
highest . . .	fallow, spruce	highest . . .	fallow, spruce, shrub
	poplar		poplar
	barley		barley
	grass	lowest . . .	grass
lowest . . .	shrub		

Experimental results are not in complete agreement with published findings from other locations. Areas of discrepancies include energy balance results for the two

wooded plots. Specifically, latent heat flux values are below expected levels, while sensible heat flux values are above. It is concluded that limiting soil moisture is the main factor behind these changes in energy balance.

6.2 Conclusions and Recommendations

The purpose of this study was to examine the gross energy balances of six different vegetation surfaces, and the manner in which each surface responded to equal amounts of incoming solar energy and precipitation. Despite the small size of each plot, significant differences were identified within their respective energy balances, and these were linked to several unique factors found in the various vegetation covers.

Solar radiation is not a purely atmospheric factor. Its magnitude may be strongly affected by surface properties such as albedo, canopy structure, and soil moisture availability. Evapotranspiration is similarly dependent on canopy characteristics, as well as macro-scale atmospheric events. Consequently, both factors have to be considered before applying published energy balance data from other locations to local conditions.

Differences between external published energy balance data and local data are also indicative of the adaptability of certain vegetation covers to environments that may be

outside their normal ranges (or habitats). Ellerslie is located in an aspen transition zone bordering natural prairie grasslands. The two tree plots, especially the coniferous, have unusually low soil mositure contents and high Bowen Ratios. They are absorbing too much energy, and this is probably affecting their surface temperatures. Normally, local deciduous and coniferous woodlands are restricted to stream valleys and depressions where there is some shade, and moisture can accumulate. Large scale tree planting on open flat lands will not be very successful unless additional moisture is provided, and tree densities are restricted to fairly low levels. The coniferous plot at Ellerslie is too dense for the local environment to adequately support it. It is likely that the spruce trees here will not survive much longer, unless several wet summers occur. Individual trees and shelterbelts are more suitable than square woodlots.

Many questions arise out of this study. If net radiation differences can be traced to differences in surface temperature between wet and dry surfaces, does duration of surface wetness vary between the plots? Is the deciduous canopy warmer or colder than the coniferous canopy? Would their albedos and air temperature profiles be similar if soil moisture is unlimiting? Would greater soil moisture levels affect their soil temperatures? What are the radiation and wind profiles of the tree and shrub plots?

Do these plots affect micro-scale wind patterns? Would changes in wind patterns and the differences in canopy structures influence snow accumulation? Are there significant "edge effects" at the tree plots which could be partly responsible for reducing their soil moisture levels? Would their effects be different if the plot sizes were larger? Does tilled fallow use more water than weed infested fallow? Are the screen level air temperatures at the shrub, barley, and fallow plots different from the grass plot? Would they be different if the plots were larger, and if so, would this affect evaporation, and consequently, plant growth and soil moisture levels? Would energy balance results be significantly different at other locations within the area, such as Stony Plain, St. Albert, or Wetaskiwin? Research on these and other topics are required before land use influences can be more adequately predicted.

This study, despite its size, has merely scratched the surface. The Ellerslie facility is unique, and should be utilized to its fullest capacity. In fact, it should be expanded if possible, to include plots of different crop types, and additional tree plots, since mean values could then be calculated from several plots rather than just one. This would improve data accuracy immensely so that absolute values of net radiation, latent heat flux, soil heat flux, and other parameters could be utilized

directly for the purpose of developing a statistical model that could predict changes in energy balance from changes in land use. Facilities of this kind should also be established at other locations if possible.

Geiger (1965) quotes the late German researcher A. Schmauss, who said that "everything fits in with everything else." This is particularly true when the living processes of plants are involved, since there is always feedback between plants and environment, and this feedback may affect the physical relationship that is being examined. The adaptive ability of plants must be considered when attempting to assess land use effects on climate. But plants have limits to their ranges, and human intervention is often necessary to maintain these plants outside their natural habitats. The present dilemma that many North Americans are facing this year is partially a result of inadequate consideration of local climatological and hydrological resources, and the limits they impose on local agriculture. No extensive alteration of the landscape should ever be undertaken without first accepting the responsibility for any side effects this alteration may cause, whether or not a problem might arise "only" once in twenty years. Since these side effects are not yet adequately documented, for Central Alberta at least, such action should not be blindly undertaken or should be adequately documented when action has already been undertaken.

BIBLIOGRAPHY

ANDERSON, M. C. 1970. Interpreting the fraction of solar radiation available in forest. Agric. Meteorol., 7, 19 - 28.

ANGSTRÖM, A. 1925. The albedo of various surfaces of ground. Geog. Annal., 7, 339 - 342.

BAUMGARTNER, A. 1965. Energetic bases for differential vaporization from forest and agricultural stands. Paper presented at the Inter. Sym. on For. Hydro., Aug. 29 - Sept. 10, 1965, at Penn. State U., State College, Penn.

BLAD, B. L. and N. J. ROSENBERG. 1974. Lysimetric calibration of the Bowen Ratio-Energy Balance Method for evapotranspiration estimation in the Central Great Plains. J. Appl. Meteorol., 13, 227 - 236.

BRENDER, E. V. 1974. Impact of past land use on the lower Piedmont forest. J. of For., 72, 34 - 36.

BUDYKO, M. I. 1958. The heat balance at the earth's surface. Trans. by Nina Stepanova, U. S. Weather Bureau, Dept. of Commerce.

BUDYKO, M. I. 1974. Climate and Life. English edition cited by David H. Miller. Inter. Geophysics Series, 18. Academic Press Inc., New York, 508 p.

CHANGNON, S. A. 1972. Atmospheric alterations from man-made biospheric changes. In W. R. D. Sewell (ed.), Modifying the Weather. Western Geog. Series, 9. Dept. of Geog. U. of Victoria, Victoria, B. C. 135 - 184.

COHEN, S. J. 1975. Radiation prediction in a deciduous forest. Unpub. B.Sc. Thesis, Dept. of Geog., McGill U.

DAVIES J. A. 1972. Actual, potential, and equilibrium evaporation for a beanfield in southern Ontario. Agric. Meteorol., 10, 331 - 348.

DAVIES, J. A. and P. H. BUTTIMOR. 1969. Net radiation, heating, and reflection coefficients at Simcoe. Agric. Meteorol., 6, 373 - 386.

DENMEAD, O. T. 1969. Comparative micrometeorology of a wheat field and a forest of Pinus radiata. Agric. Meteorol., 6, 357 - 371.

DENMEAD, O. T. and I. C. McILROY. 1970. Measurements of non-potential evaporation from wheat. Agric. Meteorol., 7, 285 - 302.

DILLEY, A. C. and W. SHEPHERD. 1972. Potential evaporation from pasture and potatoes at Aspendale. Agric. Meteorol., 10, 283 - 300.

FEDERER, C. A. 1968. Spatial variation of net radiation, albedo, and surface temperature of forests. J. Appl. Met., 7, 789 - 795.

FEDERER, C. A. 1971. Solar radiation by leafless hardwood forests. Agric. Meteorol., 9, 3 - 20.

FREMLIN, G. (ed.) 1974. The National Atlas of Canada. Dept. of Energy, Mines, and Resources, Ottawa. 254 illus.

FRITSCHEN, L. J. 1966. Evapotranspiration rates of field crops determined by the Bowen Ratio Method. Agron. J., 58, 339 - 342.

FUCHS, M. and C. B. TANNER. 1968. Calibration and field test of soil heat flux plates. Soil Sci. Soc. Amer. Proc., 32, 326 - 328.

FUCHS, M. and C. B. TANNER. 1970. Error analysis of Bowen Ratios measured by differential psychrometry. Agric. Meteorol., 7, 329 - 334.

GAY, L. W. 1971. The regression of net radiation upon solar radiation. Arch. Meteor. Geophys. Biobl., Ser B., 19, 1 - 14.

GEIGER, R. 1965. The Climate Near the Ground. Harvard U. Press, Cambridge, Mass. 611 p.

GLOVER, J. 1972. Net radiation over tall and short grasses. Agric. Meteorol., 10, 455 - 459

IDSO S. B. 1969. An analysis of the heating coefficient concept. J. Appl. Met., 7, 716 - 717.

IMPENS, J., R. LEMEUR and R MOERMANS. 1970. Spatial and temporal variation of net radiation in crop canopies. Agric. Meteorol., 7, 335 - 337.

JARVIS, P. G., G. B. JAMES, and J. J. LANDSBERG. 1976. Coniferous Forest. In Monteith ed. (1976), 171 - 240.

JEFFREY, W. W. 1964. Vegetation, water, and climate: needs and problems in wildland hydrology and watershed research. Reprint from the Proc. of the Water Studies Institute Sym. held at the U. of Sask., 13 Nov., 1964.

KALMA J. D. 1972. The radiation balance of a tropical pasture, II. Net all-wave radiation. Agric. Meteorol., 10, 261 - 275.

KALMA J. D. and R BADHAM 1972. The radiation balance of a tropical pasture, I. The reflection of short-wave radiation. Agric. Meteorol., 10, 251 - 259.

KUNG, E. C. R. A. BRYSON, and D H. LENSCHOW. 1964. Study of continental surface albedo on basis of flight measurements and structure of earth's surface cover over North America. Monthly Weather Review, 92, 543 - 546.

LEAF, C. F. 1975. Watershed management in the Rocky Mountain Subalpine Zone. The status of our knowledge. USDA Forest Service Res. Paper RM - 137, 31 p.

[redacted] A. 1968. An investigation of turbulence within the forest. J. Appl. Met., 7, 410 - 416.

MONTEITH, J. L. 1959. Reflection of shortwave radiation by vegetation. Quart. J. Roy. Meteor. Soc., 85, 386 - 392.

MONTEITH, J. L. (ed.) 1976. Vegetation and the Atmosphere, Volume 2. Academic Press, London, 439 p.

MONTEITH, J. L. and G. SZEICZ. 1961. Radiation balance of bare soil and vegetation. Quart. J. Roy. Meteor. Soc., 87, 159 - 170.

MONTEITH, J. L. and G. SZEICZ. 1962. Radiative temperature in the heat balance of natural surfaces. Quart. J. Roy. Meteor. Soc., 88, 496 - 507.

MULLER, R. A. 1966. The effects of reforestation on water yield: A case study using energy and water balance models for the Allegheny Plateau, New York. Publ. Climatol., Laboratory of Climatology, 19, no. 3, 251 - 304.

MULLER, R. A. 1971. Transmission components of solar radiation in pine stands in relation to climatic and stand variables. USDA Forest Service Res. Paper. PSW-71/1971, 13 p.

PAWLUK, S. 1964. Description of soils at the Ellerslie farm. Unpub. manuscript, Dept. of Soil Sci., U. of Alberta.

POLAVARAPU, R. J. 1970. A comparative study of global and net radiation measurements at Guelph, Ottawa, and Toronto. J. Appl. Meteor., 9, 809 - 813.

PRIESTLY, C. H. B. and R. J. TAYLOR. 1972. On the assessment of surface heat flux and evaporation using large scale parameters. Mon. Wea. Rev., 100(2), 81 - 92.

RAUNER, J. L. 1976. Deciduous forest. In Monteith ed. (1976), 241 - 264.

REIFSNYDER, W. E., G. M. FURNIVAL and J. L. HOROWITZ. 1971. Spatial and temporal distribution of solar radiation beneath forest canopies. Agric. Meteorol., 9, 21 - 37.

RIPLEY, E. A. and R. E. REDMANN. 1976. In Monteith ed. (1976), 351 - 398.

ROACH, W. T. 1955. Measurements of atmospheric radiation and the heat balance at the ground at Kew, May 1953 - May 1954. Air Ministry Meteor. Res. Committee, M.R.P., no. 936, Great Britain.

ROSE, C. W. J. E. BEGG, G. F. BYRNE, J. H. CONCZ, and B. W. R. TORSSELL. 1972. Energy exchanges between a pasture and the atmosphere under steady and non-steady state conditions. Agric. Meteorol., 9, 385 - 403.

ROSENBERG, N. J. 1969a. Evaporation and condensation on bare soil under irrigation in the East Central Great Plains. Agron. J., 61, 557 - 561.

ROSENBERG, N. J. 1969b. Seasonal patterns in evapotranspiration by irrigated alfalfa in the Central Great Plains. Agron. J., 61, 879 - 886.

ROSENBERG, N. J. 1974. Micro-Climate: The Biological Environment. John Wiley & Sons, New York, 315 p.

ROUSE, W. R. 1965. Aspects of a forest microclimate. Unpub. Ph.D. Thesis, Dept. of Geog., McGill U.

ROUSE, W. R. and R. G. WILSON. 1972. A test of the potential accuracy of the water-budget approach to estimating evapotranspiration. Agric. Meteorol., 9, 421 - 446.

SATTERLUND, D. R. 1972. Wildland Watershed Management. The Ronald Press Co., New York. 370 p.

SELLERS, W. 1965. Physical Climatology. Univ. of Chicago Press, Chicago, Ill. 272 p.

SEWELL, W. R. D. (ed.) 1972. Modifying the Weather. A Social Assessment. Western Geog. Series, 9. Dept. of Geog., U. of Victoria, Victoria, B. C. 349 p.

STANHILL, G., G. J. HOFSTEDE, and J. D. KALMA. 1966. Radiation balance of natural and agricultural vegetation. Quart. J. Roy. Meteor. Soc., 92, 128 - 140.

STUDY OF MAN'S IMPACT ON CLIMATE (SMIC). 1971. Inadvertant Climate Modification. The M.I.T. Press, Cambridge, Mass. 308 p.

TIMMONS, D. R., R. F. HOLT, and J. T. MORAGHAN. 1966. Effect of corn population on yield, evapotranspiration, and water use efficiency in the Northwest Corn Belt. Agron. J., 58, 429 - 432.

VERMA, T. R. 1968. Moisture balance in soils of the Edmonton area. Unpub. Ph.D. Thesis, Dept. of Soil Science, U. of Alberta.

WEIR, I. R. (ed.) 1971. Atlas of the Prairie Provinces. Oxford U. Press, Toronto. 31 illus.

WHITE, J. 1975. Water demands of the agriculture economy in Manitoba. Unpub. essay.

WILSON, C. V. 1975. The Climate of Quebec: Energy Considerations. Environment Canada, Ottawa. Climatological Studies no. 23. 120 p.

WILSON, J. D. 1976. Local advection arising from a change in surface temperature. Unpub. M.Sc. Thesis, Dept. of Geog., U. of Alberta

APPENDIX I

CALIBRATIONS

Instrument	Calibration ($Wm^{-2}mv^{-1}$)	Comment
Net pyrradiometer (base)	11.15	Factory
Net pyrradiometer (rotated)	11.10	Factory
Pyranometer (global)	109.29	Factory
Pyranometer (albedo)	98.35	Factory (March, 1976)
Soil heat flux plate (base)	58.82	Hage and Honsaker (May, 1976)
Soil heat flux plate (rotated)	178.57	Factory
Surface moisture probe	Probe ratio = 2.246 (% od*) -0.312	Cohen (June, 1976) $r^2 = 0.87$
Depth moisture probe	Probe ratio = 0.0017 ($Kg\ m^{-3}$) -0.026	$r^2 = 0.98$
Thermohygrograph Temp. Poplar (PS)	Chart reading +2°C	Weatherburn (Nov. 1976)
Thermohygrograph Temp. Spruce (S)	Chart reading 0°C	Weatherburn (Nov. 1976)

APPENDIX I (con't.)

Instrument			Calibration	Comment
Thermohygrograph	Temp.	Poplar Forest (P)	Chart reading -2°C	Weatherburn (Nov. 1976)
Thermohygrograph	RH.	(PS)	Chart reading 5%	Weatherburn (Nov. 1976)
Thermohygrograph	RH.	(S)	Chart reading -5%	Weatherburn (Nov. 1976)
Thermohygrograph	RH.	(P)	Chart reading -15%	Weatherburn (Nov. 1976)

NOTE: Thermohygrograph Temp. data only used to estimate missing data from individual days.

* % od = % oven dry weight
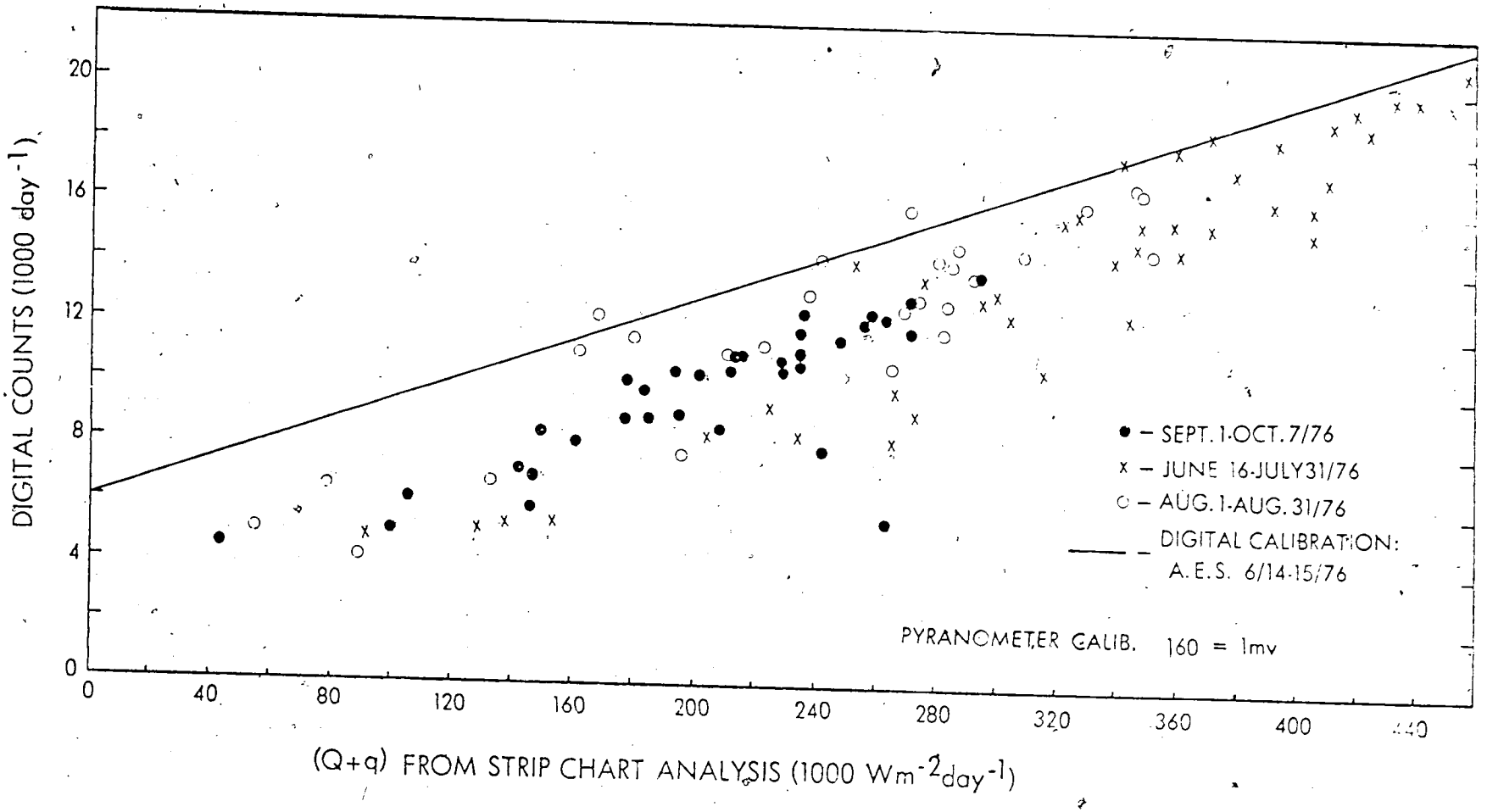
APPENDIX 2: ELLERSLIE (Q+q)MEASUREMENTS; DIGITAL COUNTS vs STRIP CHART ANALYSIS